Reinforcement of Timber Dowel-Type Connections Using Self-Tapping Screws

Zhang, Cong

Award date:
2018

Awarding institution:
University of Bath

Reinforcement of Timber Dowel-Type Connections Using Self-Tapping Screws

Cong Zhang

A thesis submitted for the degree of Doctor of Philosophy

University of Bath

Department of Architecture and Civil Engineering

September 2018

Acknowledgements

First and foremost, I want to thank Dr Wen-Shao Chang. Under his supervision and support, I gained invaluable experimental experience. More importantly, I am one step closer to being an independent researcher. Having a sharp mind, Dr Chang's advice has always been creative, shaping my research with interesting objectives. In autumn 2017, Dr Chang moved to Sheffield with a promotion, but continued to act as my external supervisor. His critical opinions are very useful to my future published papers. Apart from research, Dr Chang also shared with me his experience and positive ideas which are now deeply embedded in my head. *'When you fall to the ground, be sure to search for gold'*. This may not be the most accurate translation, but it tells me that, when facing failures, be fearless and learn from them, and failures are also invaluable.

Thanks to Professor Richard Harris who is my second supervisor. Professor Harris has always been encouraging, especially for my first presentation at INTER 2015, Sibenik, Croatia. Professor Harris is very well experienced in timber engineering design and construction. He has offered very insightful recommendations on my research topic. I am very proud to be one of his students and learn from a great engineer.

In September 2017, Dr Bhavna Sharma was appointed as my lead supervisor. Dr Sharma has patiently helped me with constructing the structure of my thesis. I would like to thank Dr Sharma for her great contribution of time and effort. I received a lot of encouragement and advice when I was preparing for the Three Minute Thesis competition as a finalist.

I also want to thank associate Professor Kiho Jung, from Shizuoka University in Japan. Jung started his one-year visit to Bath in 2017, a year that was crucial for me with regard to intensive experiments. Benefiting from his huge knowledge of timber engineering and practical experience, I have improved my skills in performing a good experiment.

As experimental based research, the completion of my work could never have been achieved without the assistance of the team of technicians, especially from Will Bazeley and David Williams.

Now, to my dear friends and colleagues, you have made my days in the office more colourful and my life in Bath full of joy.

Finally, I would like to thank my parents and family members who have always been supporting and caring for the entire period of my PhD study. Sentences carrying my love for you are never enough.

Abstract

The study investigates the mechanical performance of dowel-type timber connections reinforced by partially threaded self-tapping screws. The literature review emphasises that, with a lack of a design code for using self-tapping screws as reinforcement, there are concerns over using fully threaded screws, which may have difficulties during the installation.

The study first confirmed that, comparing with partially threaded screws, fully threaded screws require higher drive-in torque and are more vulnerable to torsional damage, especially under the circumstance when a pre-drilled hole is not provided and with the presence of wood defects, such as knots. This brought about the ideas of using partially threaded screws in order to reduce the drive-in torque and investigating the relationship between thread configuration and the effectiveness of screw reinforcement.

The results of embedment tests in this study indicated that partially threaded screws achieved similar improvement in the mechanical properties of wood as screws with complete thread. Using digital image correlation (DIC), this study revealed that the withdrawal capacity from the point end of the screw and the pull-through resistance from the screw head are utilised to control wood splitting, which is similar to the 'rope effect' in connections. Test results also confirmed that, within a certain range of crack width, partially threaded screws are as effective as fully threaded screws in enhancing the mechanical performance of specimens with artificial cracks.

This study then extended the investigation to a larger scale, from tensile connections to moment-resisting connections, and confirmed the improvement of mechanical performance of connections when reinforced by partially threaded self-tapping screws.

A portal frame reinforced by partially threaded screws was tested under static load. It showed significant improvement in the ultimate moment-resisting capacity and rotation angle compared to an unreinforced portal frame. A theoretical prediction method of the moment-resisting capacity of screw-reinforced connections is proposed and conservative predicted values are obtained.

The experimental results demonstrate the effectiveness of using partially threaded self-tapping screws, in strengthening connections and ensuring a more ductile failure mode in the connections. In addition, partially threaded self-tapping screws are easier to install than fully threaded screws.

Contents

List of Tables

List of Figures

List of Symbols

Latin upper-case letters

D_u	Ductility of the connection
$F_{ax,Rd}$	Design value of axial withdrawal capacity of the fastener
$F_{ax,Rk}$	Characteristic axial withdrawal capacity of the fastener
F	Force
$F_{m,d,max}$	Maximum load normal to its distance to the centre of rotation due the moment
$F_{v,Rk}$	Characteristic load-carrying capacity per shear plane per fastener
K_{ser}	Slip modulus
M_d	Design moment-resisting capacity of the connection
M_k	Characteristic moment-resisting capacity of the connection
$M_{y,Rk}$	Characteristic yield moment of fastener

Latin lower-case letters

b	Width
d	Diameter; Outer thread diameter
$f_{ax,k}$	Characteristic withdrawal strength perpendicular to the grain
$f_{c,90,d}$	Design compressive strength perpendicular to the grain
$f_{h,k}$	Embedment strength
$f_{head,k}$	Characteristic pull through parameter for fasteners
h	Depth
h_e	Loaded edge distance
k_{def}	Deformation factor
k_u	Rotational stiffness of the connections per shear plane
l_{ef}	Effective length of the load distribution; Penetration length of the threaded part
n	Number of fasteners
n_{ef}	Effective number of fasteners
n_{sp}	Number of shear planes
r	Radius of curvature
r_{max}	Maximum distance between the dowel and the centre of rotation
r_i	Distance between the dowel and the centre of rotation
t	Thickness

Greek lower-case letters

α	Angle between a force and the direction of grain; Angle between the screw axis and the grain direction, with $\alpha \geq 30^\circ$
β	Angle between a force and the direction of grain
δ	Displacement
ρ_k	Characteristic density
ρ_m	Mean density
τ	Shear stress
ψ_2	Factor for quasi-permanent value of a variable action

Chapter 1 Introduction

1.1 Background and motivation

Compared to buildings made of steel and concrete, a timber structure has less embodied energy and higher carbon storage, emphasising the idea of a low-carbon society. These advantages have led to high-rise timber structures becoming popular around the world. With the completion of the 18-storey student residence, Brock Commons Tallwood House, see Figure 1-1, in 2017, the height of the tallest wood building has increased to 53 meters.

Figure 1-1: The Brock Commons Tallwood House at University of British Columbia, Vancouver (UBC, 2017).

However, in Brock Commons Tallwood House, the core of the building and the connections between the glulam columns are made of reinforced concrete and steel. In a high-rise timber building, massive dead loads and lateral loads must be transferred from beams to columns through connections and then reach the foundation. For a heavy timber structure, dowel-type connections are often used but they have a number of disadvantages compared to steel. Due to the low tensile strength perpendicular to the grain of wood, design codes have strict rules on the geometry of connections to prevent brittle failure. This means the connections occupy more interior space. Additionally, wood as a natural material is sensitive to moisture variation, which can cause damage to timber and reduce the capacity of the connections.

Due to the above disadvantages, research has focused on reinforcing the mechanical properties of timber members. The materials for reinforcement range from metals like steel and aluminium to fibre-reinforced polymer (FRP). Plates, fabrics and rods are the typical forms of such reinforcements. To bond these reinforcements, resins and metal fasteners are used, either externally or internally, based on aesthetic requirements and accessibility. Experimental studies have shown their superior performance in enhancing the mechanical properties of timber elements. However, their disadvantages are also acknowledged; for metal reinforcement, weight and corrosion resistance are in question; for FRP materials, the durability of the bond formed by epoxy resins, against ageing and moisture variation, are not yet fully understood. There have been investigations into pre-stressing the reinforcement so as to achieve better enhancement, the reinforcement is placed either inside or near the surface of the timber member and bonded firmly to the wood by resins. However, this requires careful preparation work with highly trained labour; the complex procedures also make it expensive in time.

With the recent development of self-tapping screws, much research has been dedicated to promoting their use to enhance the low tensile and compressive strength of timber perpendicular to the grain. Through high axial load-carrying capacity, self-tapping screws have shown the capability of controlling wood splitting, thus making the members more ductile. Furthermore, compared to other reinforcements, self-tapping screws have good concealment and are simpler, faster and easier to use.

However, the lack of knowledge of long-term performance of screw reinforcement subject to moisture variation and dynamic loading, such as vibration and seismic activities, indicates a long journey to the complete standardisation of screw reinforcement.

In addition, various forms of self-tapping screws are available on the market and the thread configuration on the screws varies with brand. As the screw is driven into the wood, the drive-in torque increases with the penetration depth of the threaded part. A large torsional force, especially for the cases of fully threaded screws, is imposed on the screw that tend to break it. Thus, extending knowledge of the influence of thread configuration on the effectiveness of screw reinforcement is essential in selecting screws with better workability (ease of installation). Furthermore, existing and new timber moment-resisting connections are prone to splitting due to moisture variation and limited knowledge is available for the performance of screw reinforcement. The current research on reinforcing the crack damaged connections are also limited.

1.2 Research aims and objectives

The primary aims of this research are:

- To understand the impact of thread configuration and screw to dowel distance on the effectiveness of reinforcement.
- To propose a suitable range of thread configurations not only to reduce the drive-in torque but also maintaining the effectiveness of screw reinforcement.
- To validate the effectiveness of screws with the proposed thread configurations as reinforcement on specimens with and without cracks, tensile connections, moment-resisting connections and portal frames.

The objectives of this research are:

- To provide key evidence that various thread lengths can result in a difference of drive-in torque.
- To identify the influence of thread length, thread location and screw to dowel distance on the enhancement of embedment strength.
    - Visualising their influence through the strain distribution on the surface of specimens.
    - Understanding the mechanism of self-tapping screws as reinforcement.
- To examine the effectiveness of the proposed thread configuration to reinforce specimens with different sizes of artificial cracks.
- To validate the effectiveness of self-tapping screws with the proposed thread configuration so as to enhance the mechanical performance of various dowel-type connections:
    - Tensile connections loaded parallel to the grain.
    - Undamaged and damaged moment-resisting connections.
    - Beam-to-column connections and portal frames.
- To establish an analytical model to predict the moment resisting capacity of screw-reinforced dowel-type connections.

The thesis is structured in accordance with the order of these objectives.

1.3 Thesis structure

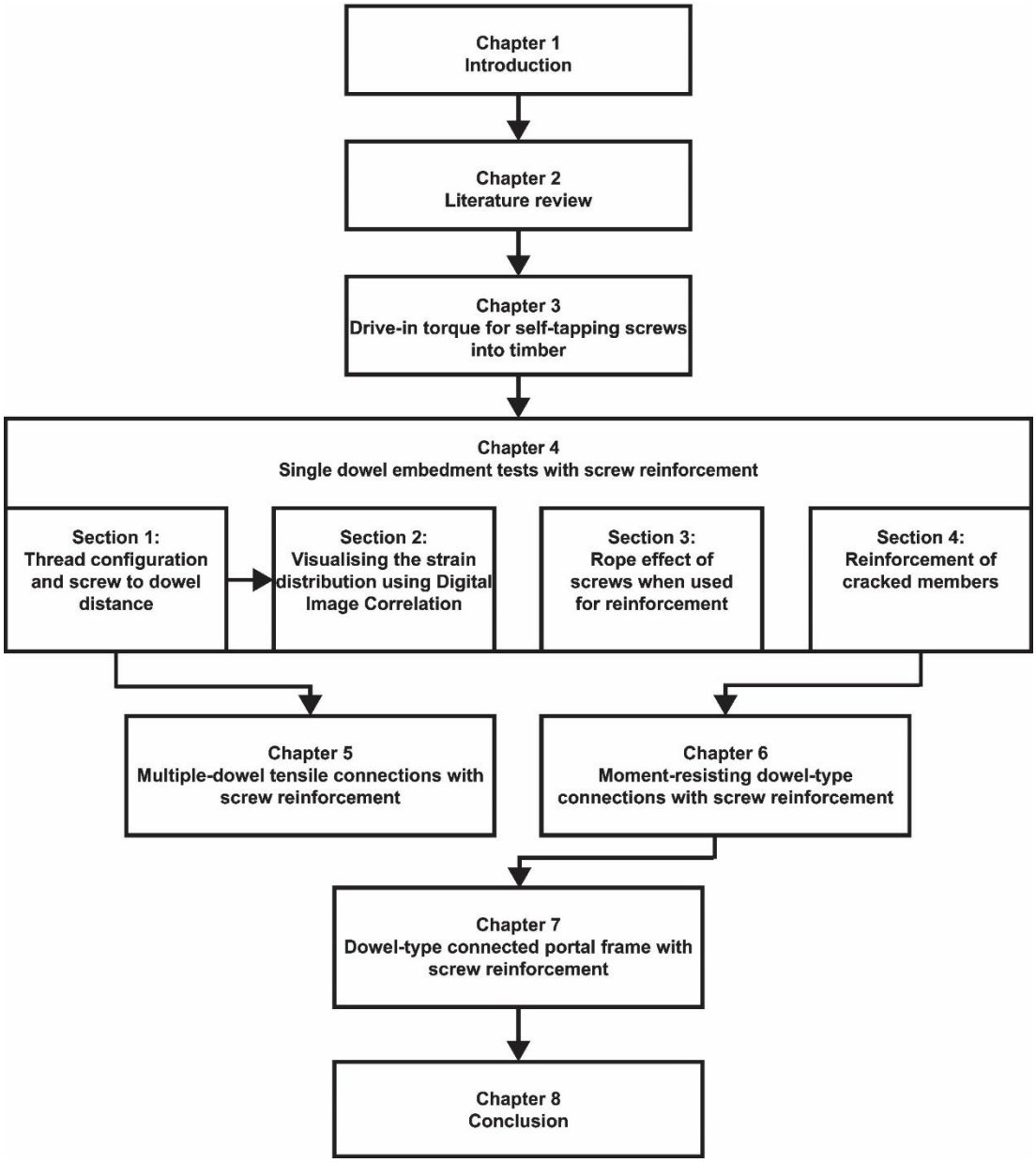

Figure 1-2: Flow chart displaying the structure of this thesis.

The structure of this thesis is demonstrated in the flow chart in Figure 1-2. After the brief introduction to the background of current research on the reinforcement of dowel-type timber connections, Chapter 2 reviews the available reinforcement on timber elements using metal, FRPs and self-tapping screws.

Chapter 3 provides experimental evidence of the influence of thread length on drive-in torque of self-tapping screws. In addition, Chapter 3 discusses the influence of thread profile (such as reamer) and screw diameter on the magnitude of drive-in torque. The implication of

knots is also investigated. The importance of having pre-drilled holes for self-tapping screws as reinforcement is highlighted.

With the knowledge from Chapter 3, typical thread configurations were introduced for embedment testing and this is presented in Chapter 4, which is subdivided into four sections. It starts by identifying the influence of thread configuration and screw to dowel distance on enhancing the embedment strength, ductility and stiffness of timber. Then, in the second section, their impact on strain distributions is visualised by DIC technique. The section identifies potential substitution to screws with complete thread by screws with partial thread on the point end through comparing their reinforcement performance in the experiment.

'Rope effect' is a term used to describe and quantify a positive influence of the initial failure of fasteners on the load-carrying capacity of dowel-type connections. For screws as reinforcement, similar actions to the rope effect is discussed in the third section of Chapter 4. The experiment in this study measured the splitting resistance provided by the screw in relation to thread length and location.

The last section of Chapter 4 demonstrates the effectiveness of using screw reinforcement to enhance the embedment strength and ductility of timber specimens with artificial cracks. The purpose of having artificial cracks is to simulate connections which have timber splitting due to moisture variation.

Chapter 5 describes the experimental work to examine the performance of screws with partial thread on the point end to reinforce dowel-type connections subject to static tensile load acting parallel to the grain.

Chapter 6 is an extension to the experimental work of Chapter 4, which used screws to reinforce moment resisting connections with artificial cracks which represents the damage due to moisture variation. Screws with various thread configurations were used to improve the mechanical properties of the connections. Tests on beam-to-column connections, reinforced by self-tapping screws, are also presented. A prediction method is proposed to estimate the characteristic moment-resisting capacity of the reinforced connections, based on the embedment strength obtained from Chapter 4.

Chapter 7 presents the experimental tests of reinforcing portal frames with partially threaded screws. Similar analytical models were used to predict the theoretical moment-resisting capacity of the unreinforced and reinforced frames.

The conclusions of the study and discussion of future works is presented in Chapter 8.

The thesis is in a portfolio style that contains several published papers and manuscripts which are under review. The report on the experimental work described in Chapter 3 has been submitted to the '*Proceedings of the Institution of Civil Engineers – Construction Materials*'. The first section of Chapter 4 was presented at the *INTER 2015* conference in Croatia. The second section of Chapter 4 has been submitted to the '*Journal of Materials in Civil Engineering*' and is under review. The third section of Chapter 4 has been submitted to the journal of '*Proceedings of the Institution of Civil Engineers – Construction Materials*' and is under review. The last section of Chapter 4 for crack reinforcement has been submitted to the '*Proceedings of the Institution of Civil Engineers - Structures and Buildings*' and is under review. The content of Chapter 5 was included in a paper presented at the *WCTE 2016* in Vienna. The study of the first part of Chapter 6 has been submitted to '*Construction and Building Materials*' and is currently under revision. The second part of Chapter 6 was presented at the *WCTE 2018* in Seoul, Republic of Korea. The content in Chapter 7 has been published in '*Engineering Structures*'.

Chapter 2 Literature Review

2.1 General reinforcement on timber elements

Timber as a natural material features anisotropic properties due to the arrangement of fibres in favour of the growth direction of the trunk. The material has a much lower compressive, tensile and shear strength perpendicular to the grain, compared to the strength parallel to the grain. To minimise the risk of brittle failure due to excessive load perpendicular to the grain, design codes often set limitations on the geometry of the timber members. This, however, increases the size of the timber elements as well as the budget of a project.

In addition, existing timber structures can lose their designed capacity due to mechanical and biological damage. According to the failure analysis of structures in Germany, Frese and Blaß (2007) found that cracks parallel to the grain accounted for about 75% of the failure cases. Cracks are mainly due to stress concentration (e.g. notches and beams with service hole) or moisture variation. Other major types of failure are shear failure, tension failure and decay due to fungi and insects.

Therefore, for both newly designed and existing timber elements, reinforcement can be applied either externally or internally to strengthen the mechanical properties of the timber element. In this section, various reinforcement methods are discussed in accordance to their purposes of application.

2.1.1 Replacement

Timber elements are prone to decay due to fungal and insect attack if the moisture content in the wood is suitable for their growth. The decayed part can lose strength, which may result in structural failure. In addition, timber members that are damaged by fire can lose their load-carrying capacity due to reduction of cross-section and strength.

Wheeler and Hutchinson (1998) catalogued the repair method of timber structures into three aspects: traditional repairs, mechanical methods and resin methods. Traditional repair involves using the exact kinds of timber and tools to fabricate a new timber member with authentic traditional methods and to replace the damaged one. This method maintains the authenticity of the elements, however, it is often difficult to obtain replacement timber and requires highly skilled labour to replicate the original member. In addition, design codes are not available for traditional repairs.

For mechanical methods, reinforcement, such as metal plates, were fixed to the damaged member by bolts (Davis and Mettem, 1997). The reinforcement is often visible and can be unattractive, which is not a preferred option for repairing historical buildings. While not a preferred method, there are calculation codes (e.g. Eurocode 5) available.

Figure 2-1: Replacing damaged timber part and using steel rods placed in existing beam to connect with new timber (top) (Wheeler and Hutchinson, 1998); Rotafix used CFRP plate to connect new timber and existing beam in a property dating to c1600 in St Albans, Hertfordshire (Rotafix, 2014) (bottom).

A more modern technique, often known as resin-bonded rod repair method, replaced the damaged parts with a new one that was connected to the existing beam by forming a scarf joint or connected using bonded in rods or plates (Pizzo and Schober (2008); Franke *et al.* (2015)). Commonly, steel rods or FRP plates are placed in the existing beam and then connected to the replacement part with epoxy resin-based adhesives. In the UK, a system named 'Resiwood' developed by Rotafix has been widely used on repairing historical timber buildings. Figure 2-1 demonstrates the use of steel and FRP elements in repairing existing beams.

The procedure for carrying out the resin-bonded repair method was described in Franke *et al.* (2015). The whole stage of repairing, from removing the decayed part to curing of resins, requires supporting props to ensure the structure stability. In addition, grooves or holes need to be prepared to place the steel or FRP elements. The advantage of this method is the low intervention to the original structural elements. However, as discussed by Wheeler and Hutchinson (1998), there are concerns over long-term performance and performance in high moisture content environment.

2.1.2 Flexural reinforcement

For a beam in bending, compressive and tensile stresses parallel to the grain are distributed on the top and bottom surface of the beam, respectively. The natural defects of wood, such as knots, can create a weak spot on the tension side and lead to a brittle failure of the beam.

For decades, much research has been focused on reinforcing the flexural strength of timber beams. The reinforcement methods can be catalogued by the material applied and sub-divided by the form and location of the reinforcement.

2.1.2.1 External metal reinforcement

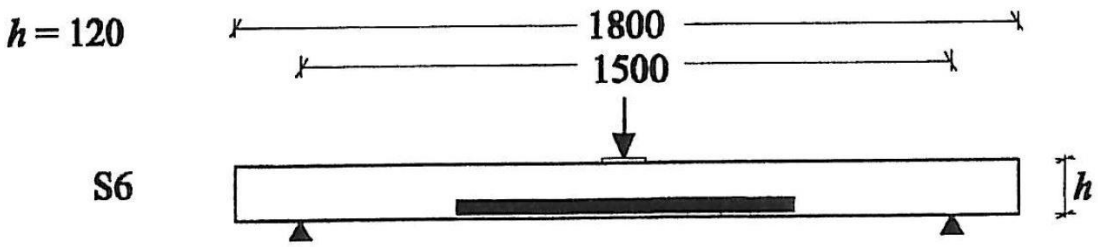

Figure 2-2: Details of the bending test of the beam reinforced with punched metal plates (represented by the black strip), (Nielsen and Ellegaard, 1999).

Nielsen and Ellegaard (1999) used punched metal plate fasteners to reinforce the timber beams, see Figure 2-2. Test results showed only limited enhancement by placing the punched metal plates near the tension side of the beam.

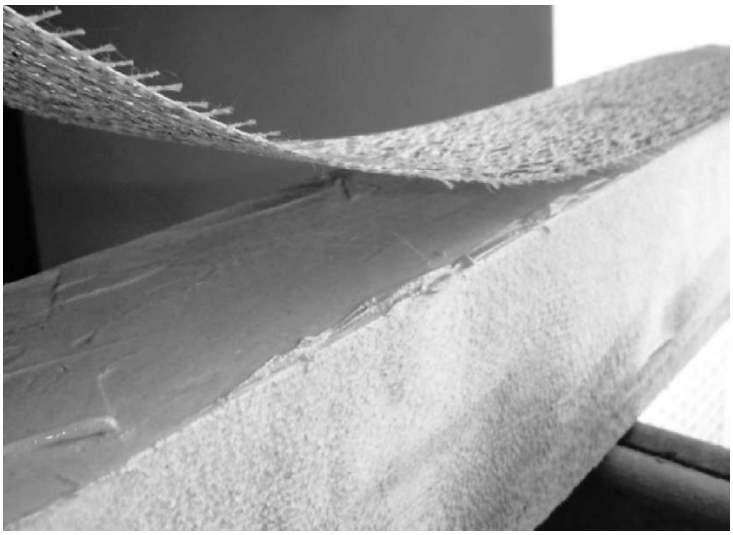

Figure 2-3: Applying the high strength steel cords on the tension side of the beam by Borri and Corradi (2011).

Borri and Corradi (2011) strengthened the flexural capacity of timber beams with high strength steel cords externally bonded to the tension area of beam using epoxy resins, as shown in Figure 2-3. Another attempt made by Jasieńko and Nowak (2014) was to place steel plates on the top, bottom or side surfaces, respectively, using epoxy adhesive, see Figure 2-4. The reinforcement in these studies greatly increased the flexural capacity of the beam compared to the unreinforced beams.

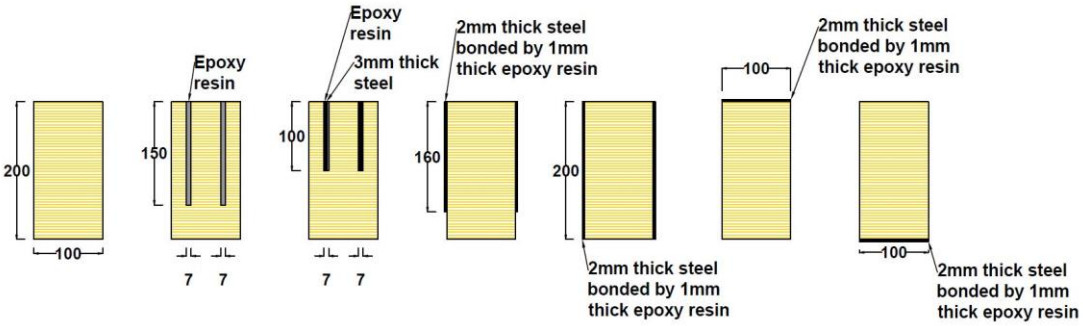

Figure 2-4: Locations of the steel reinforcement on the beams tested by Jasieńko and Nowak (2014).

However, as the bond strength may change with temperature and moisture variation, using adhesives to form the bonding between the metallic cords or plates and the wood was uncertain (Bulleit *et al.*, 1989). The challenges of using adhesives are discussed in Section 2.1.6.2.

In addition, external reinforcement using metal elements is not always aesthetically attractive and the accessibility to the external surface could be restricted. Therefore, research has also focused on using concealed internal metal reinforcement which is discussed in the following section.

2.1.2.2 Internal metal reinforcement

Early studies using steel bars in the 1950s have been summarised by Bulleit *et al.* (1989), the steel bars, either with square or circular cross-section, were placed in a notch which was cut into a lamination of the glulam beams. Bulleit *et al.* (1989) described this method to be effective in improving beam stiffness and strength but it was time-consuming and unusual to cut a notch into the lamination at that time. Triantafillou and Deskovic (1992) summarised the works which placed steel and aluminium plates between laminations, however, the concerns over using adhesive still exists.

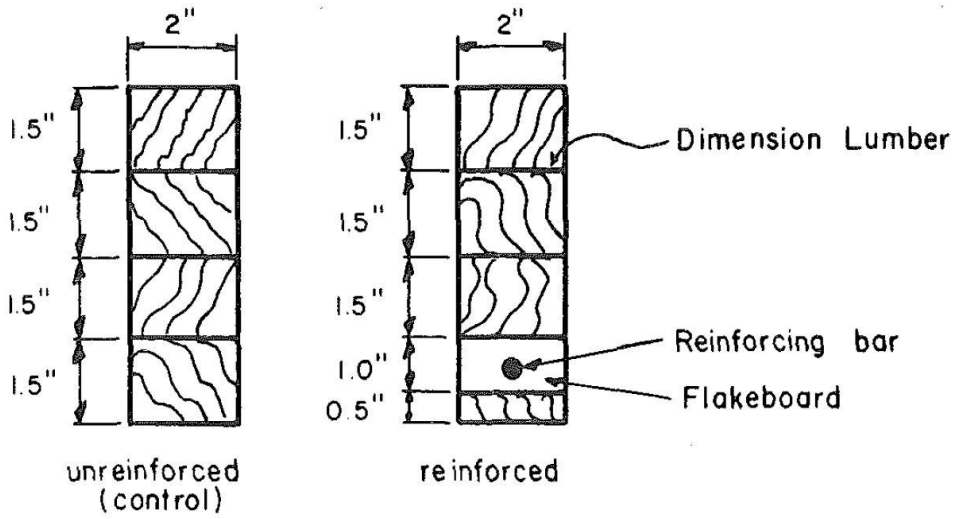

Figure 2-5: Steel reinforcement suggested by Bulleit et al. (1989).

Bulleit *et al.* (1989) proposed the use of steel bars embedded in Oriented Strand Board (OSB) or known as flakeboard that was placed in between laminations of the glulam beam. The configuration of the reinforcement is shown in Figure 2-5. The bottom lumber beneath the OSB can provide some fire protections for the reinforcement as well as reducing the chances of the steel bars splitting out of the beam. Tests on their proposed beam achieved a 30% increase in stiffness but no improvement in moment capacity is found. According to Bulleit *et al.* (1989), moisture increase could cause reduction of wood mechanical properties and the internal bonding strength of the OSB, thus, leading to a lack of reinforcing effect.

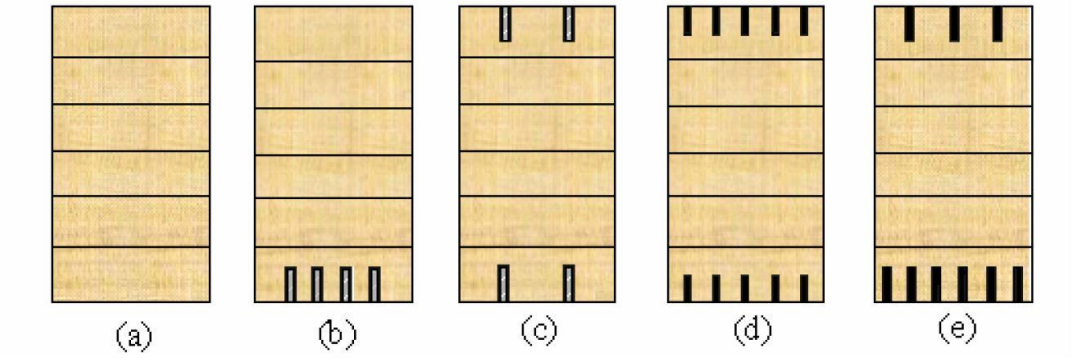

Figure 2-6: Arrangements of reinforcement in Kliger et al. (2007): (a) unreinforced, (b) reinforced by steel on tension side, (c) reinforced by steel on compression and tension side, (d) reinforced by CFRP on compression and tension side and (e) reinforced by CFRP with different arrangements on compression and tension side.

Recent studies (e.g. Alam *et al.* (2009), Kliger *et al.* (2007) and (2008)) placed steel bars in rectangular sections inside the compression and tension sides of the beam. The reinforcement was placed in grooves that were cut in the beam, and then bonded to the wood using epoxy resins. As suggested by Kliger *et al.* (2007), the steel reinforcement was placed vertically in the beam to increase the shear area between wood and steel as well as making the reinforcement less visible, see Figure 2-6. Their work showed that steel reinforcement was effective in improving flexural strength and stiffness. Kliger *et al.* (2008) also proposed an analytical model and found that greatest ductility can be achieved by placing all the reinforcement on the tension side, and, maximum strength can be achieved by having 25% of reinforcement on the compression side and 75% of reinforcement on the tension side. Furthermore, Kliger *et al.* (2008) found that all types of reinforcement can reduce the variability in mechanical properties compared to the unreinforced specimens. Jasieńko and Nowak (2014) reinforced timber beams with internal steel plate, which were vertically placed and bonded to the wood, as shown previously in Figure 2-4, and achieved a higher enhancement in load-carrying capacity compared with other reinforcement configurations.

An alternative method was suggested by González-Bravo *et al.* (2008, 2010), using steel plates with U-shape cross-section attached to the upper face of the beam by screws, as shown in Figure 2-7 below. The reinforcement increased the stiffness and load-capacity by at least 45% and 36%, respectively, compared to unreinforced glulam beams. One problem remaining for this solution is the screw fixation of the plate, which may restrain the dimensional change of the wood due to moisture variation. Cracks could develop and undermine the mechanical performance of the beam.

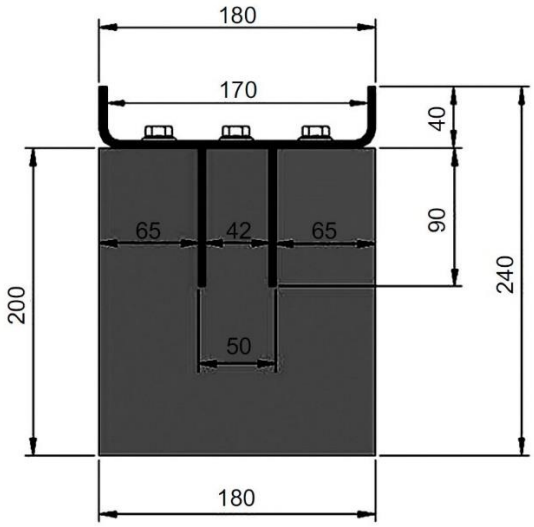

Figure 2-7: Cross-section of the beam reinforced by the steel reinforcement in González-Bravo et al. (2010).

De Luca and Marano (2012) and McConnell *et al.* (2014) put pre-stressed steel tendons near the tension side of glulam beams. The reinforcement arrangements of De Luca and Marano (2012) is shown in Figure 2-8.

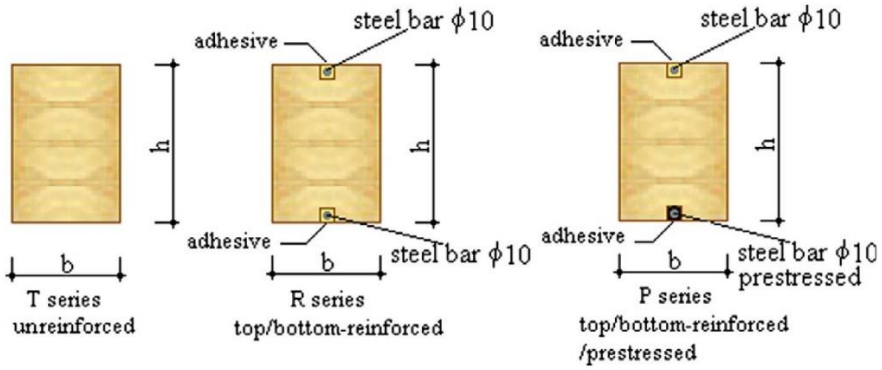

Figure 2-8: Arrangements of reinforcement shown in De Luca and Marano (2012).

Both works showed that glulam beams reinforced by pre-stressed steel bars, as well as those reinforced by steel bar simply bonded to the wood, achieved significant improvement in flexural properties. In McConnell *et al.* (2014), pre-stressed steel bars that were end anchored showed less improvement in the mechanical properties of glulam beams than those were bonded to wood using adhesives, with a reduction of 56% and 70% in ultimate capacity and stiffness, respectively.

According to De Luca and Marano (2012), the epoxy adhesive was allowed to set for 30 days. McConnell *et al.* (2014) stated that the slow setting nature of the epoxy adhesive can ensure a strong timber-steel bond by filling the voids thoroughly. However, in practice, this method is more suitable for pre-fabrication in a factory than in-situ, considering the time it

would take. In addition, the long-term performance of the reinforcement is unknown. The pre-stressing method is also more complex as it involves tensioning the steel tendons (Franke *et al.*, 2015) and also the safety risks should be well considered.

Steel reinforcements have demonstrated their excellent performance in enhancing timber elements. However, for decades, researchers have been seeking for alternative materials to raise the flexural performance of timber beams, as there is high risk of corrosion for metal reinforcement (Triantafillou and Deskovic, 1992).

2.1.2.3 External FRP reinforcement

FRP is a combination of fibres and polymeric resin. As described by Schober *et al.* (2015), the high strength fibres can provide load-bearing capacity and stiffness while the resin helps to transfer the loads and provides protection to the fibres. The various available FRPs can be catalogued by the type of the fibre: carbon (CFRP), aramid (AFRP), glass (GFRP), basalt (BFRP) and steel (SFRP) (Franke *et al.*, 2015). The typical forms of FRP reinforcement used for timber are fabrics, rods and plates, made by the pultrusion techniques.

Compared with steel, FRPs have several advantages, as mentioned in Schober *et al.* (2015). They have higher strength-to-weight ratio, better corrosion resistance and ease of handling on site.

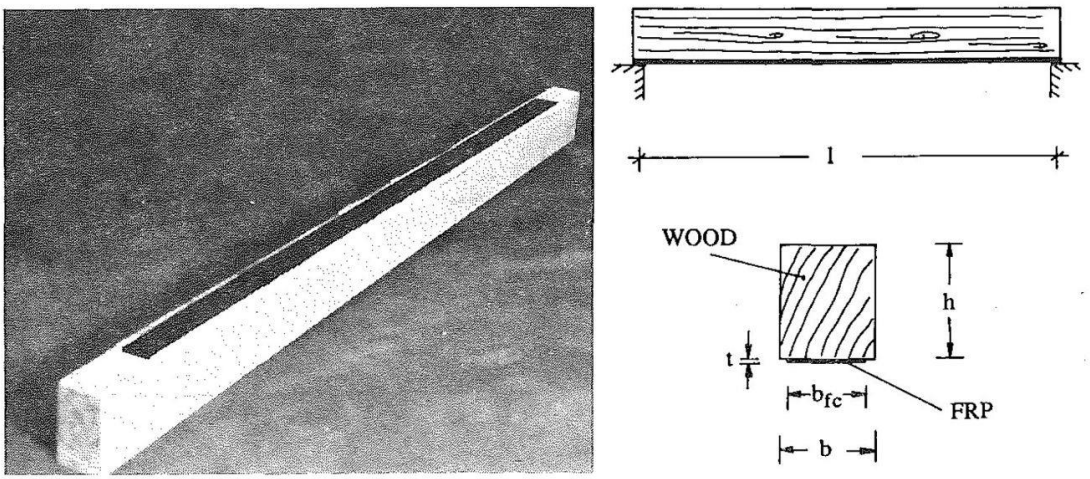

Figure 2-9: CFRP sheet bonded to the tension side of the beam (beam on the left was flipped over to observe the reinforcement) (Plevris and Triantafillou, 1992).

Early studies using external FRP reinforcement bonded to the tension side of the beam in the 1980s have been summarised by Plevris and Triantafillou (1992). Experimental tests in Plevris and Triantafillou (1992) showed that even thin CFRP bonded to the beam can enhance its flexural strength, stiffness and ductility. A demonstration of a FRP reinforced

beam is shown in Figure 2-9. Triantafillou and Deskovic (1992) proposed to prestress the CFRP sheets when bonding to the beam and found this technique achieved higher load-carrying capacity and stiffness than non-prestressed CFRP reinforced beam. As Triantafillou and Deskovic (1992) stated, the long-term performance of using this technique was uncertain and the pre-stressing force may reduce due to moisture change, creep and relaxation of the structure.

Kliger *et al.* (2016) summarised several pre-stressing techniques in the last decade, the benefit of pre-stressing is achieving a higher load-carrying capacity with less material requirement when compared to normal FRP reinforcement methods. However, a major problem with pre-stressing is the shear stress concentration developed at the ends of the FRP laminate. The shear stress can possibly exceed the bonding strength of the adhesive, leading to debonding of the FRP laminate. A demonstration of the shear stress concentration is shown in Figure 2-10.

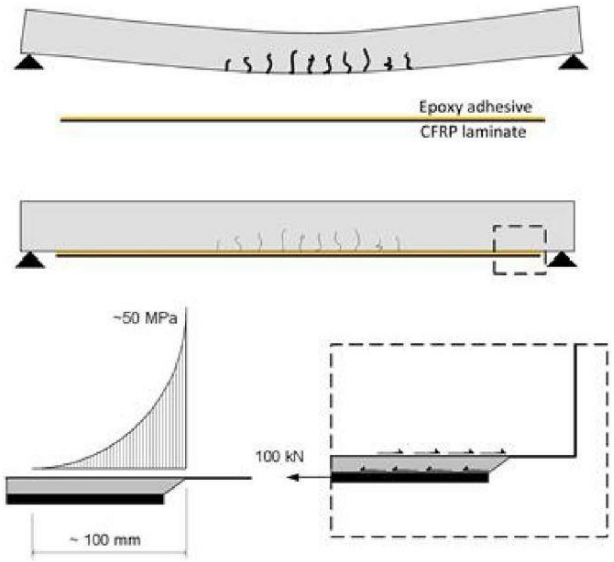

Figure 2-10: Shear stress concentration at the ends of FRP reinforcement (Kliger et al., 2016).

In the work done by Borri *et al.* (2005), the influence of the amount of external reinforcement was examined and results showed that by increasing the number of layers of CFRP sheets attached to the tension side of beam, a higher load-carrying capacity can be achieved. Li *et al.* (2009) conducted similar tests and confirmed the increase of flexural strength with increasing number of layers of CFRP sheets. The results in Li *et al.* (2009) showed that Chinese hemlock beams applied with three layers of CFRP sheets achieved 10% higher improvement than with only one layer of CFRP. However, only two or three beam tests were done for each reinforcement scheme in both sets of work.

Figure 2-11: H-type GFRP reinforcement applied on the compression side of the beam (Corradi and Borri, 2007).

For reinforcing existing beams, when the access to the tension zone is restricted, Corradi and Borri (2007) proposed the use of H-type GFRP pultruded elements bonded to the compression face of the beam, see Figure 2-11, and successfully increased the flexural stiffness, strength and ductility of the beams. Their proposed reinforcement was also applied in reinforcing the beams in Palazzo Collicola, built in the 18th century, where the tension side of the beams were restricted due to the presence of valuable decorations.

CFRP has been widely used as reinforcement in the above research, however, it also has very high cost compared to GFRP. Yang *et al.* (2013) proposed the use of hybrid fibre-reinforced polymer (HFRP) in which fibre with high modulus offers stiffness and load-carrying capacity while fibre with low modulus make the entire composite more durable and cheaper. Flexural testing of beams reinforced by HFRP, which consisted of CFRP and high strength GFRP, showed similar ultimate load-carrying capacity but a better ductility than those reinforced by CFRP (Yang *et al.*, 2013). The cost of HFRP used by Yang *et al.* (2013) was only half of that of the CFRP sheets.

With the experience from internal steel reinforcement, some researchers have realised that internal FRP reinforcement is more aesthetically appealing and better fire protection can be gained when embedded in the wood compared to external application. Therefore, various pieces of research have been conducted using internal FRP reinforcement and compared with external FRP reinforcement.

Schober and Rautenstrauch (2007) tested timber beams strengthened by either external (*Vh*) or internal (*Vs* or *Vv*) CFRP. Experimental tests showed that the arrangement of internal reinforcement (*Vv*) achieved higher load-carrying capacity but a larger number of tests are required for confirmation. All types of reinforcement had the same cross-sectional area, as shown in Figure 2-12. However, experimental tests done by Glišović *et al.* (2016), using

similar arrangements on glulam beams, showed that CFRP plates externally attached to the tension side of the beam achieved a better performance than internal reinforcement. Overall, both works have shown that external and internal FRP reinforcement can effectively improve the flexural stiffness and load-carrying capacity of timber beams.

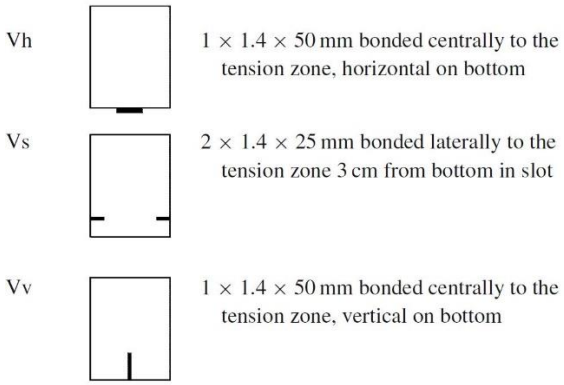

Figure 2-12: Arrangements of external reinforcement (Vh) and internal reinforcement (Vs and Vv) demonstrated in Schober and Rautenstrauch (2007).

Osmannezhad *et al.* (2014) compared the performance between external and internal GFRP reinforcement, see Figure 2-13. With the same layers of GFRP, beams with reinforcement placed at the tension side of glulam beam in Figure 2-13 (c) achieved slightly higher improvement in MOE (modulus of elasticity) and MOR (modulus of rapture) when compared to those with internal reinforcement Figure 2-13 (d). In addition, the use of four layers of reinforcement Figure 2-13 (e) achieved the highest improvement in mechanical properties of the beam and the reinforcement can be well protected. However, manufacturing glulam beams with such reinforcement is complex and time-consuming. Raftery and Harte (2011) and Raftery and Rodd (2015) placed GFRP plates on the tension face of the glulam beam and a sacrificial lamination beneath the GFRP reinforcement utilising the charring resistance from wood to protect the FRP from fire. Their experimental work showed that reinforcement can enhance the bending moment capacity of beam and found no premature delamination of the sacrificial lamination before the failure of the beam.

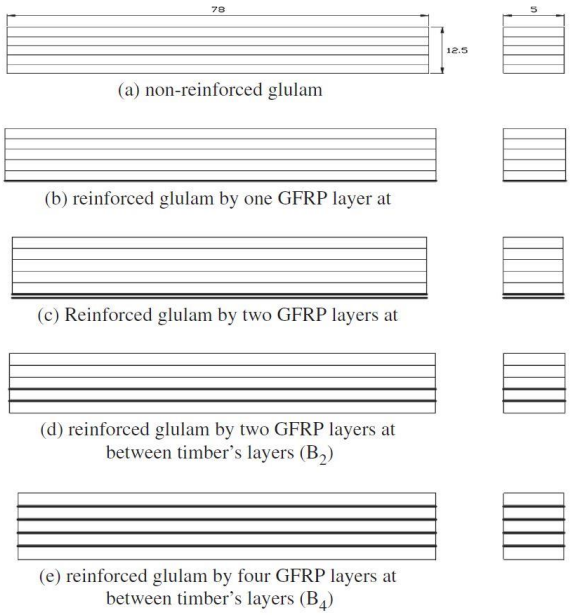

Figure 2-13: Arrangements of reinforcement in Osmannezhad et al. (2014).

Overall, the performance of internal reinforcement can be confirmed while, compared with external FRP reinforcement, they have less effect on the appearance of timber beams and are better protected against fire damage. According to Brunner and Schnüriger (2005), the delamination of the reinforcement was reduced when it was placed inside the beam. A more detailed discussion of current research using internal FRP reinforcement is presented in the next section.

2.1.2.4 Internal FRP reinforcement

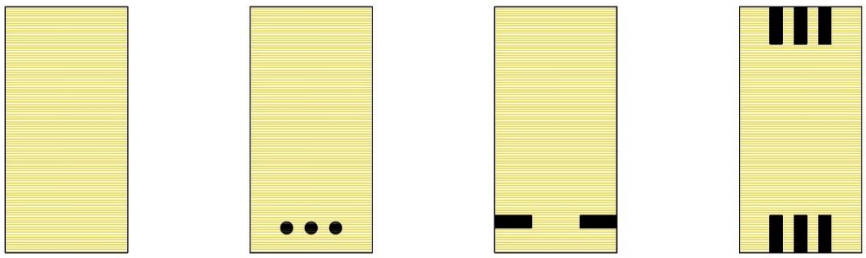

Figure 2-14: Common arrangements of internal FRP reinforcement on timber beam.

Numerous studies have been conducted on reinforcing timber beams with internal FRP elements. The typical reinforcement arrangements are demonstrated in Figure 2-14 while the forms and ratios of reinforcement on the compression and tension sides remain flexible, depending on the accessibility and purpose of reinforcement. This section discussed previous studies using internal FRP reinforcement by the type of FRP materials applied. Current research mainly focuses on GFRP, an inexpensive low strength material, and CFRP, which has a high strength but is twice as expensive as GFRP (Yang *et al.*, 2013).

GFRP reinforcement

Gentile *et al.* (2000, 2002) conducted experimental tests on sawn timber beams reinforced with GFRP bars. The reinforcement was bonded to the grooves cut near the tension side of the beam and different reinforcement ratios in the cross-section were applied. Results from Gentile *et al.* (2000, 2002) showed that the reinforcement transformed the failure mode from tension to compression failure and higher flexural strengths of up to 46% were observed. Gentile *et al.* (2000) also stated that higher-graded beams required less reinforcement than lower-graded beams. Alhayek and Svecova (2012) confirmed the improvement in strength of both higher-graded and lower-graded beams with the use of GFRP laminates. However, their work did not find significant improvement in stiffness by reinforcing the timber beams.

Raftery *et al.* (2012) and Raftery and Whelan (2014) researched the influence of the size of the GFRP rod reinforcement, the geometrical shape of the grooves and the amount of reinforcement on the mechanical properties of glulam beams, as shown in Figure 2-15. Their results showed that using smaller diameter of reinforcement did not have any advantages in improving the flexural properties of the beams, see Figure 2-15 (Phase B). In addition, circular grooves (Phase D) showed better reinforcement performance than that of the square ones (Phase C). A possible explanation given by Raftery and Whelan (2014) is that circular grooves can reduce the stress concentration, thus delaying the failure of the beam. Furthermore, by doubling the amount of reinforcement, the stiffness and ultimate moment capacity of the beam were increased two times as well.

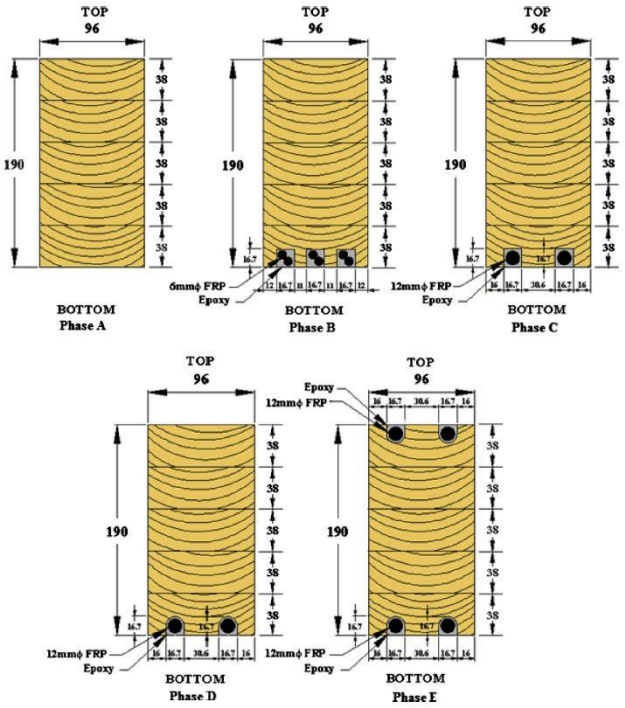

Figure 2-15: Arrangements of GFRP rod reinforcement in Raftery and Whelan (2014).

Alam *et al.* (2009) compared the performance between internal GFRP and CFRP reinforcement, GFRP was outperformed by CFRP in every aspect in terms of improving the mechanical properties of beams. However, GFRP still offers a great option to reinforce lower-grade timber beams.

CFRP reinforcement

CFRP as a high-strength FRP material has been considered as an alternative to steel reinforcement. Kliger *et al.* (2007), Kliger *et al.* (2008) compared the difference between internal steel and CFRP reinforcement, see Figure 2-6. Their experimental tests showed that CFRP achieved higher improvement in stiffness and slightly lower load-carrying capacity than steel. Nowak *et al.* (2013) and Lu *et al.* (2015) placed CFRP reinforcement in different arrangements and achieved significant enhancement in flexural strength and stiffness. Their proposed method is effective but with more grooves to be cut for installing the FRP reinforcement, which increases the complexity and duration of the work. In addition, the impact of variation of moisture content and the long-term performance of the reinforcement are not well-considered.

Other types of FRP materials as reinforcement

With the development of FRP, some researchers have also been reinforcing timber beams other than using GFRP and CFRP. André (2006) summarised the mechanical properties of natural fibres; compared with glass fibres, the natural fibres are cheaper, renewable and some of them have comparable mechanical properties to glass fibres. As André (2006) noted, natural fibres, such as flax and hemp, have high potential to be alternatives to GFRP to reinforce timber beams when proper chemical or mechanical treatments are applied. Furthermore, products made by BFRP have similar mechanical properties to GFRP and a coarse surface which is perfect for forming a strong bond with wood using adhesives (Raftery and Kelly, 2015).

Borri *et al.* (2013) bonded flax, bamboo, basalt and hemp fibres on the tension zone of beams to strengthen their mechanical properties. A picture of the fibres is shown in Figure 2-16. Test results showed that flax and basalt fibres improved the load-carrying capacity of lower-graded beams by at least 38% which was comparable to CFRP reinforcement. The improvement of using natural fibres on higher-graded beam was very limited, especially with bamboo fibres. However, as Borri *et al.* (2013) commented, natural fibres have the advantage of lower production cost and energy consumption and are biodegradable, compared to traditional FRP.

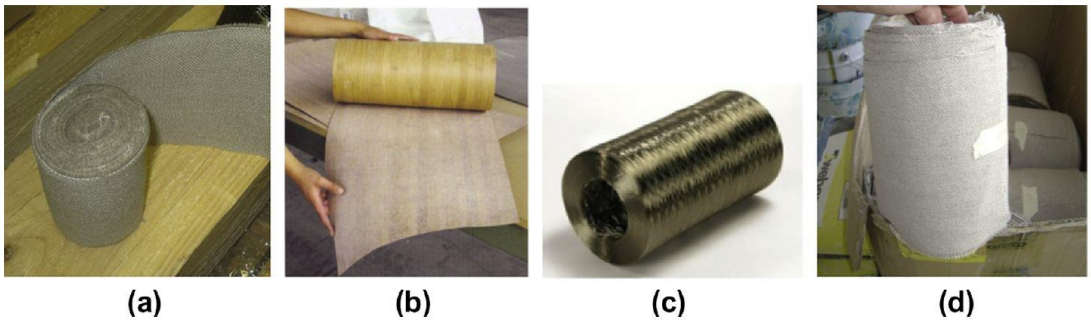

Figure 2-16: Natural fibres demonstrated in Borri et al. (2013): (a) flax fibre, (b) bamboo fibre, (c) basalt fibre and (d) hemp fibre.

Raftery and Kelly (2015) proposed the use of BFRP rods, a more environmentally friendly composite, to reinforce the tension zone of glulam beams. Their experimental work showed that BFRP reinforcement improved the global stiffness of beams by 8.4% and the ultimate moment capacity by 23%.

Overall, compared to natural fibres, traditional FRPs have less variation in material properties and can provide more stability in terms of dimensional change of wood due to the variation of moisture content. A sufficient knowledge base of natural fibres is required to fully exploit their potential.

2.1.3 Compressive reinforcement

Figure 2-17: Reinforcement scheme tested in Ed and Hasselqvist (2011): steel plates (left), threaded steel rods (middle) and wooden rods (right).

The locations where compressive reinforcement is required are mainly in the support and the loading regions of a timber element. Limited research has been conducted on reinforcing these areas, as beams are prone to fail in bending. Ed and Hasselqvist (2011) and Crocetti *et al.* (2012) presented a study to reinforce the beam support area using steel plates fixed to the sides of the beam by steel plates, glued-in threaded steel rods and wooden rods, as shown in Figure 2-17. Test results revealed all three reinforcements were effective while steel and wooden rods achieved better improvement in the load-carrying capacity of the beam than steel plates. Ed and Hasselqvist (2011) also reported that the variation of the depth in steel rods is more critical than for wooden rods, meaning the steel rods in the same beam are not

installed at the same level. This is due to difficulties in installation. As a result, some of the steel rods will be in bearing first leading to non-uniform loading on each steel rods and has an impact on the test results (tilting of the beam). As Franke *et al.* (2015) stated, installing glued-in rods and screws at these load concentrated areas can be difficult on existing structures.

2.1.4 Shear reinforcement

For a uniformly loaded timber beam, the highest shear stress parallel to the grain occurs at the neutral axis above the supports. Excessive stress can cause cracks parallel to the grain and brittle failure of the beam. Similar problems can also occur to notches and beams with service hole where stress concentration is generated.

To increase the shear resistance of the beam, CFRP fabrics were bonded to the sides of beams by Triantafillou (1997), as shown in Figure 2-18. The tested reinforcement successfully increased the load-carrying capacity of the timber beams.

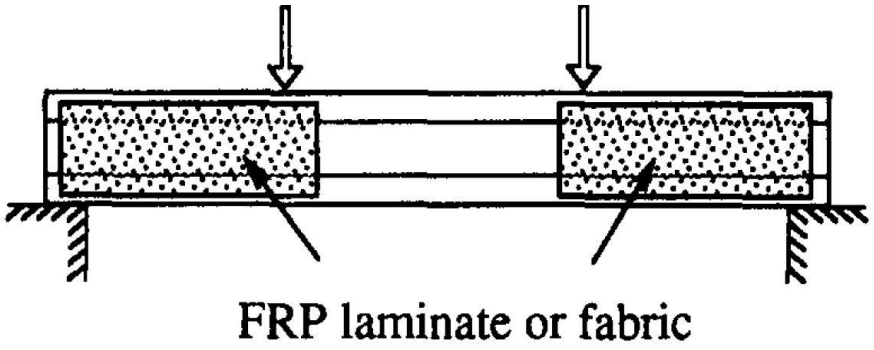

Figure 2-18: Demonstration of CFRP fabrics used as shear reinforcement (Triantafillou, 1997).

A similar experimental study was carried out by Akbiyik *et al.* (2007) which compared the use of hex bolts, lag screws, and plywood and GFRP side plates for shear repair of damaged beams. All arrangements of the reinforcement, shown in Figure 2-19, had effectively improved the load-carrying capacity of damaged beams compared to the undamaged ones. However, with a limited number of specimens, comparison among the arrangements is difficult.

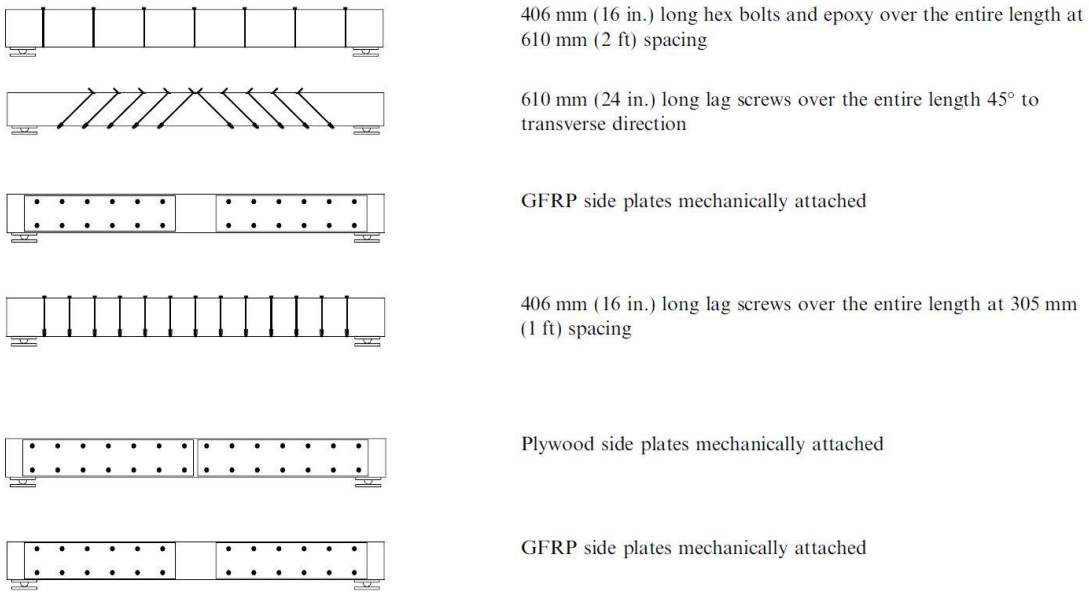

Figure 2-19: Arrangements of shear reinforcement in Akbiyik et al. (2007).

Similar to the bolts and lag screws, Radford *et al.* (2002) used bonded-in GFRP rods as 'shear spikes' to repair the shear capacity of beams with horizontal cracks. Apart from the restored flexural strength and stiffness, as commented by Radford *et al.* (2002), the shear repair using GFRP rods had less impact on the aesthetic perception, compared to external reinforcement, where only one surface was required for insertion of reinforcement.

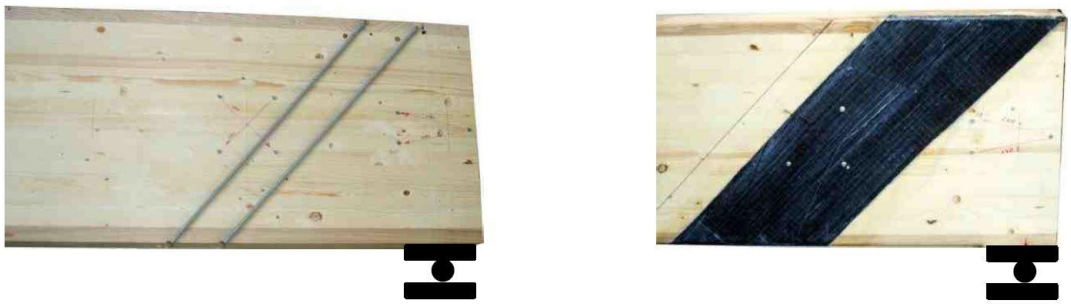

Figure 2-20: Orientation of self-tapping screws (left) and CFRP mesh (right) in the tests done by Widmann et al. (2012).

Widmann *et al.* (2012) used CFRP mesh and self-tapping screws to reinforce glulam beams (with the bonding of central lamella in poor quality) which had already failed in bending tests. The reinforcements are shown in Figure 2-20. Both types of reinforcement significantly increased the load-carrying capacity of the damaged beam.

2.1.5 Tensile reinforcement

Due to the low tensile strength of wood perpendicular to the grain, the literature reviewed is mainly focused on reinforcing two types of timber elements: beams and connections.

2.1.5.1 Reinforcement on beams

Tensile stresses are often concentrated in notches, curved beams and beams with service holes. Crack development in these beams is often rapid and can result in brittle failure. André *et al.* (2006) proposed the use of GFRP and flax fibre-reinforced polymer (FFRP) laminates bonded to the sides of glulam beams. The tensile tests confirmed that both types of FRP reinforcement can improve the tensile strength of beams perpendicular to the grain and their ductility while the use of natural fibres is lighter and greener than GFRP. However, more repetitions of the test are required to confirm the results. As André *et al.* (2006) commented, the performance of the reinforcement under cyclic moisture variation should be investigated, as swelling and shrinking of the wood is greater than for FRP materials, leading to internal stresses which can have negative impact on the wood-FRP bonding.

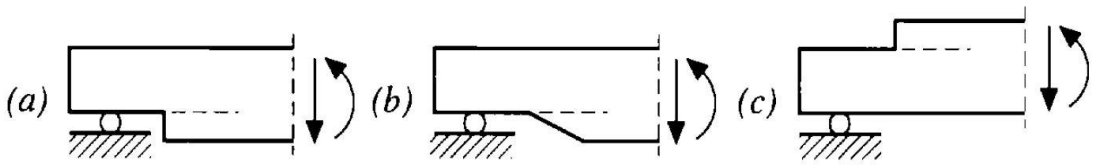

Figure 2-21: Typical shapes of notched beam, dashed lines indicate the path of timber splitting (Gustafsson, 1995).

Notches, as shown in Figure 2-21, are often avoided in design but maybe necessary to lift the floor level, provide clearance or a fit of the beam to the structure (Gustafsson, 1995). However, they are vulnerable to splitting due to excessive tensile stress perpendicular to the grain or due to high shear stress.

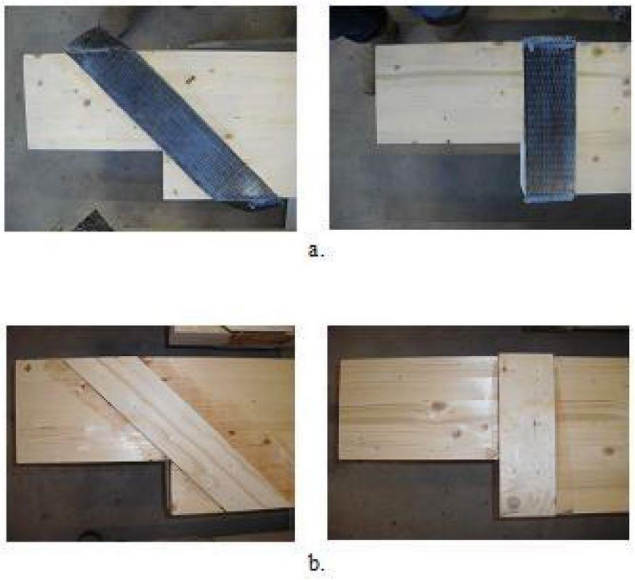

Figure 2-22: Arrangements of CFRP reinforcement (top row) and plywood panel (bottom row) applied in Fawwaz and Hanna (2012).

Fawwaz and Hanna (2012) conducted tests on notches reinforced by CFRP fabric and plywood panels, as shown in Figure 2-22. The reinforcements effectively enhanced the load-carrying capacity of the beams by 2.5 times when compared to the unreinforced beams.

As the current design approaches only consider the tensile stresses perpendicular to the grain in notches, the failure mode of reinforced beams often transferred to shear failure or a mixture of shear and tensile failure. Jockwer *et al.* (2013) and Jockwer (2014) proposed to increase the shear capacity of the beam by varying the orientation of reinforcement to reduce the chance of having shear failure, thus, further increased the load-carrying capacity of the beams. According to Jockwer (2014), reinforcement, in the form of inclined FRP sheets or self-tapping screws at 45˚, can effectively control both tensile and shear failure of the beam.

The reinforcement of beams with service holes is discussed in Section 2.2.4. For double tapered beams, curved beams, pitched cambered beams, there are high concentrations of tensile stress at the apex zone. Threaded rods and side plates can be used as reinforcement, see Figure 2-23.

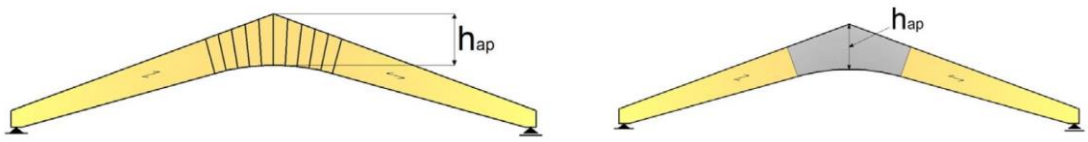

Figure 2-23: Reinforcement of pitched cambered beam using threaded rods (left) and side plates (right) (Franke et al., 2015).

Kasal and Heiduschke (2004) proposed the use of glued-in composite tubes containing GFRP and Kevlar fibre, a para-aramid fibre, on curved glulam timber beams as reinforcement. The FRP tubes placed vertically in the arch, as shown in Figure 2-24, significantly improved its load-carrying capacity.

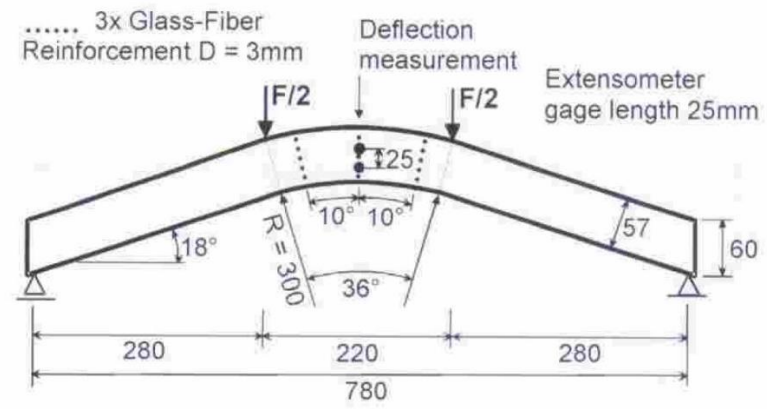

Figure 2-24: Curved glulam beam with FRP rods as reinforcement (Kasal and Heiduschke (2004).

2.1.5.2 Reinforcement on connections

There are various types of timber connections, an overview is given in Figure 2-25, and most of them use metal fasteners. There are also traditional timber joints which do not use steel, as it was expensive, but simply transfer the load by compression (Thelandersson and Larsen, 2003). For heavy timber structures, bolts and dowels are used and current research is mainly focused on reinforcing dowel-type connections.

The circular shape of the fastener in timber joints increases tensile stresses perpendicular to the grain, leading to crack initiation and propagation, thus, reducing the ductility of the joints.

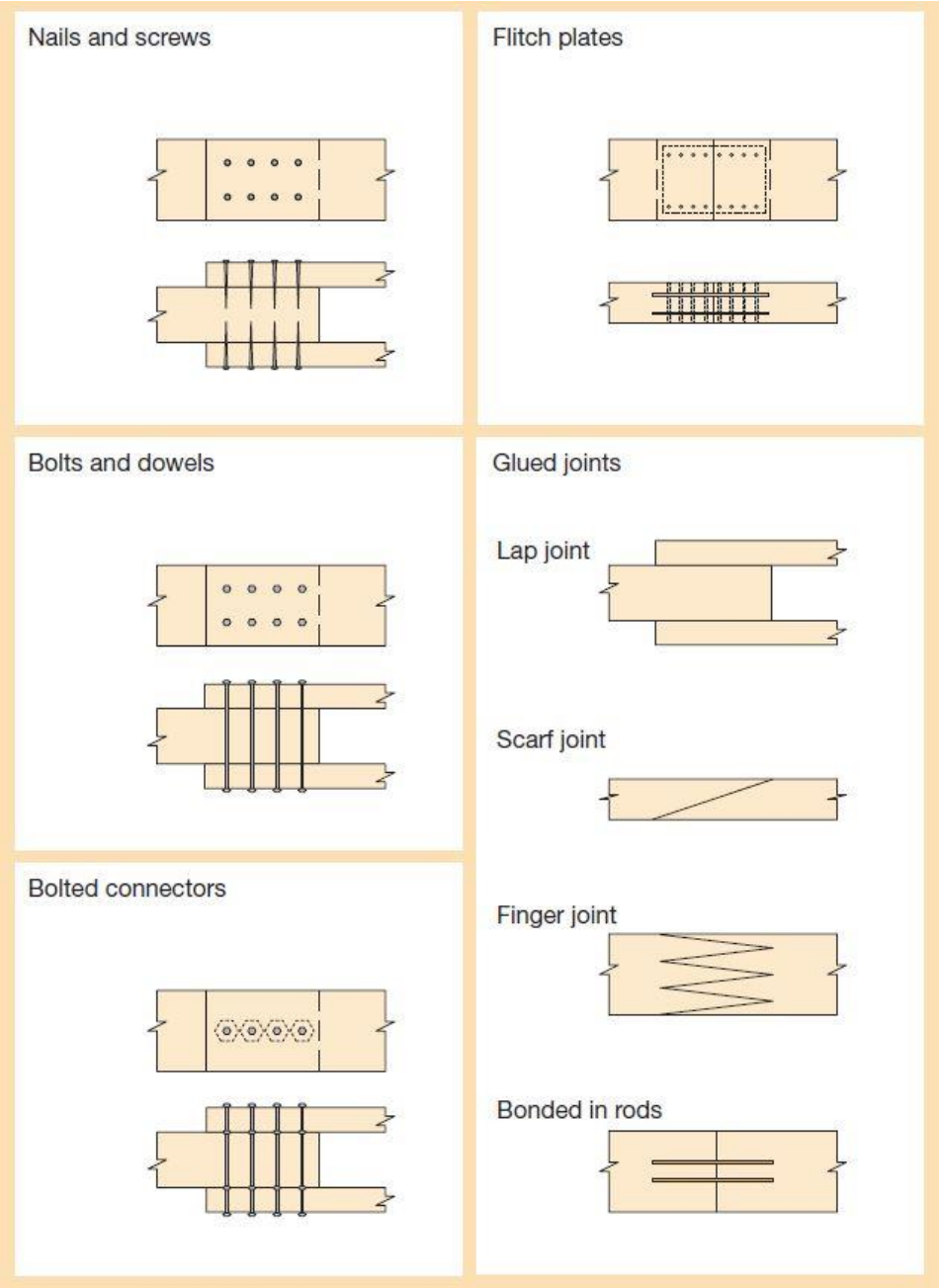

Figure 2-25: Examples of connections (IStructE, 2007).

Large numbers of experimental tests were done by Soltis *et al.* (1997), in which GFRP sheets were bonded onto the surface of timber connections. Test results showed that GFRP reinforcement significantly increased the load-carrying capacity and tensile strength perpendicular to the grain, when the connections were loaded either parallel to the grain or perpendicular to the grain. In addition, Soltis *et al.* (1997) found that additional layers of reinforcement can further increase the load-carrying capacity of the connections. Similar tests have also been done by Chen (1999) and Heiduschke and Haller (2008) where FRP materials improved the load-carrying capacity and ductility of connections.

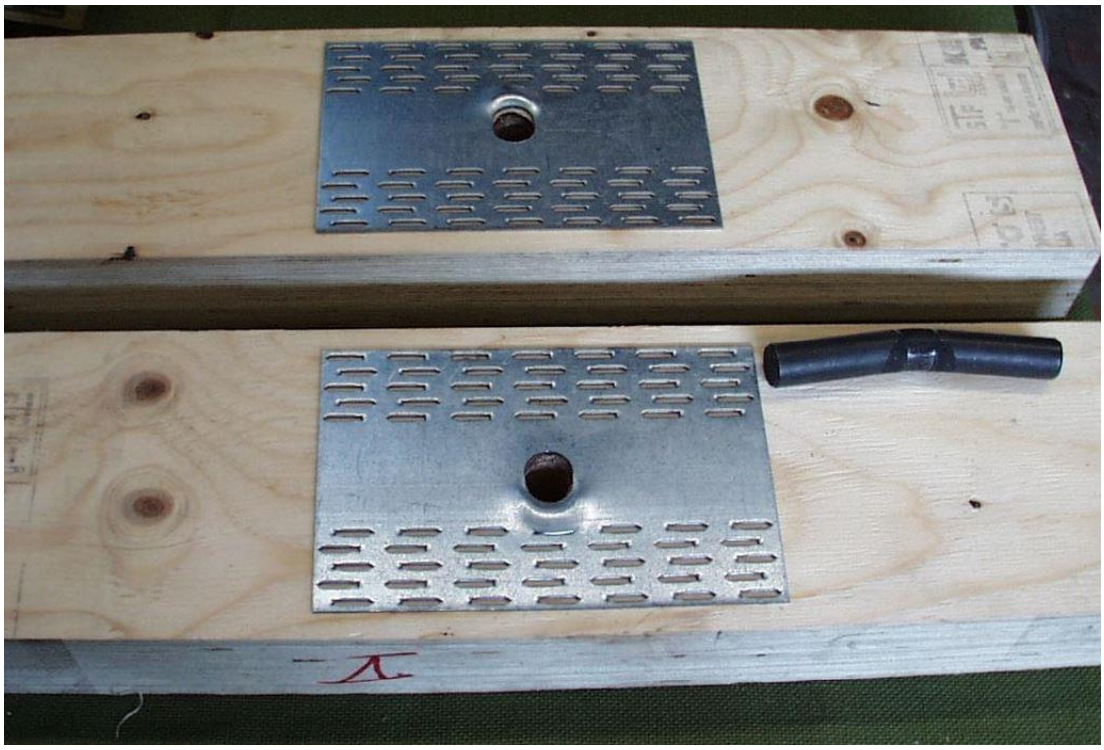

Figure 2-26: Dowel-type connections reinforced by steel nail plates (Blaß et al., 2000).

Apart from FRP reinforcement, numerous studies have used metal reinforcement. In the studies by Hockey *et al.* (2000) and Blaß *et al.* (2000), steel nail plates were pushed into the surface of the timber around the fastener group and a bond between the teeth of the truss plate and wood was formed. Both works showed effective improvement in the load-carrying capacity and ductility of the connections. An example of the reinforcement is shown in Figure 2-26.

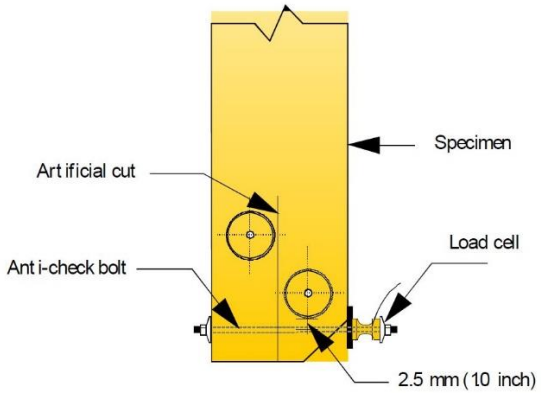

Figure 2-27: Anti-check bolt as reinforcement for split ring connection (Quenneville and Mohammad, 2000).

Quenneville and Mohammad (2000) used anti-check bolts to reinforce damaged split ring connections with cracks where the bolts were placed between the split rings or within the end distances, as shown in Figure 2-27. The reinforcement successfully restored the tensile

strength of the damaged connections and further enhanced its ductility, which is better than that of the undamaged connections.

For metal reinforcement, a major consideration is the corrosion resistance and long-term performance with moisture changes, however, limited research is available.

2.1.6 Considerations for current reinforcement methods

Different kinds of metal and FRP reinforcement and their improvement in the mechanical properties of timber members have been demonstrated and confirmed in the previous sections. The reinforcements are in various forms and can be applied to timber either externally or internally through mechanical or chemical bonding. However, questions over their long-term performance and durability remain.

Table 2-1: Comparison of metal and FRP reinforcement over engineering considerations.

Considerations	Metal		FRP	
	External	Internal	External	Internal
Aesthetical intervention	*High*	*Moderate*	*Moderate*	*Low*
Accessibility	*Moderate*	*Moderate*	*Moderate*	*Moderate*
Material weight	*High*	*High*	*Low*	*Low*
Material cost	*Low to moderate*	*Low to moderate*	*Moderate to high*	*Moderate to high*
Corrosion resistance	*Low*	*Low*	*High*	*High*
Fire resistance	*Low*	*Moderate*	*Low*	*Moderate*
Bond durability (adhesive)*	*Highly dependent on the quality during the bonding process and long-term performance in question*			
Reversibility	*Moderate to high*	*Low*	*Moderate to high*	*Low*
Installation complexity	*Moderate*	*High*	*Moderate*	*High*
Groove preparation	*N/A*	*Required*	*N/A*	*Required*
Surface preparation	*Required*	*Required*	*Required*	*Required*
Installation duration	*Moderate*	*High*	*Moderate*	*High*
Resin setting time	*Low*	*Moderate*	*Low*	*Moderate*

** Metal reinforcement can also be mechanically fixed by fasteners.*

2.1.6.1 Metal reinforcement

One of the major drawbacks of steel and aluminium reinforcement is their low corrosion resistance. Exposed metal elements will lose strength, making the reinforcement ineffective. Corrosion protection, such as anodic coating, can temporarily prevent the steel from reacting with oxygen but, as the anodic metal (e.g. zinc) is sacrificed, the reinforcement is at risk of corrosion eventually.

In addition, the size and weight of the reinforcement make it more difficult to handle on site. As proposed by previous studies, metal reinforcement can be bonded by structural adhesives. The long-term performance of the bonding between wood and steel is in question.

As for pre-stressing the steel element, complexity and duration of mounting the reinforcement can limit its application.

2.1.6.2 FRP reinforcement

According to Schober and Rautenstrauch (2007), the service life of structural adhesive has not been fully understood, as the oldest bonded joints are only around seventy years old and the current artificial ageing technique may not simulate greater age. It undermines the credibility of FRP reinforcement and most of the intervention methods lack reversibility. For instance, repairing a historical site with FRP reinforcement may be damaging to the appearance and sacrifice original material in exchange for structural stability; with a lack of knowledge of when and how the reinforcement will lose its efficiency, the risk of critical brittle failure of the structure increases. In addition, further repair of the FRP reinforced structural element could bring more severe intervention to the historic buildings.

As Schober and Rautenstrauch (2007) commented, the bonding process is a critical stage to ensure the utilisation of the strength of FRP material, however it is difficult to control its quality on-site. For example, Fossetti *et al.* (2015) conducted a comparison between GFRP and CFRP reinforcements. The reinforcements were internally bonded to grooves prepared near the tension side of the beam; unfortunately, poor soaking of the FRP material and excessive amount of resins compromised the effectiveness of reinforcement, which led to unsatisfactory results. The poor soaking of the reinforcement reduced the bond between the fibre and the resin. Schober *et al.* (2015) mentioned a few points of quality control for bonding on site, such as inspecting the gluing surface and testing of on-site samples. The listed quality checks demonstrated the level of complexity and difficulty of installing FRP reinforcement on timber elements. Currently, the standards for conducting the bonding process are still under development.

Tascioglu *et al.* (2003a, 2003b) found that the adhesives used in GFRP reinforcement was susceptible to fungal penetration and the chance of delamination of the FRP reinforcement was higher for pre-treatment than post-treatment. As wood treatments are necessary for the cases where fungal attacks, re-application of the chemicals over years may eventually bring problems to the bonding between wood and FRP.

Schober *et al.* (2015) described the research on the bond behaviour of FRP reinforcement as in its infancy. More research is required on the long-term performance of the wood-FRP bond and the influence of changing moisture content.

Table 2-1 above compares the common engineering aspects of both metal and FRP reinforcements. FRP reinforcements have better performance than steel with lower intervention to the aesthetic of the timber members, higher strength-to-weight ratio and they are easier to handle on-site. However, attaching reinforcement to wood using adhesives requires high bonding quality at the cost of construction time. Apart from investigating the bond durability and long-term performance of FRP reinforcement, researchers have been turning to the use of self-tapping screws as reinforcement which features a few more advantages than FRP materials, which will be discussed in the next section.

2.2 Screw reinforcement on timber elements

2.2.1 Self-tapping screws

With the development of technology, the manufacturing process of screws has moved from handmade thread cutting to mass production of screws with rolled on threads.

Figure 2-28: Traditional wood screws.

Most traditional wood screws are made by the thread cutting method. One feature of the traditional wood screw is the partly threaded and partly smooth shank; the threaded part is typically 60% of the total length of the screw (Dietsch and Brandner, 2015), as demonstrated in Figure 2-28. The threaded part is produced by cutting from the original blank rod. Thus,

the thread diameter of a traditional wood screw is often same as that of the smooth shank. According to Thelandersson and Larsen (2003), a wood screw would require a pre-drilled hole to prevent splitting of wood around it if the shank diameter was larger than 8mm. As traditional wood screws are not hardened during the manufacture process, they have low axial load-carrying capacity and bending capacity. Dietsch and Brandner (2015) also added that the use of washers to enhance the axial load-carrying capacity by increasing the pull through capacity of the screw. Moreover, the traditional wood screw can fail due to the excessive torque generated when driven into the wood.

The modern thread rolling technique has replaced the thread cutting method. Opposite to cutting of materials from a blank rod, the core concept of thread rolling is to press the rod with dies having thread-shaped ridges to form the threads, resulting in the outer thread diameter of the screw being larger than the shank diameter (Oberg *et al.*, 2016). The material loss is significantly reduced in this method. In addition, as the threads are cold formed by dies, work hardening also enhances the axial load-capacity, bending capacity and torsional capacity of the screw as well as its wear resistance. The modern self-tapping screws are mostly made from the thread rolling technique.

The term 'self-tapping' means that the screw can drill its own hole, often without a pre-drilled hole. Self-tapping screws can be classified into two groups: thread forming and thread cutting. Thread-forming screws are suitable for materials which allow sufficient plastic deformation to form the thread without removing any materials as the screw is drilled into them (BS 4171:1972) (BSI, 1972). The thread cutting screws cut the material and remove it from the substrate as the screw enters. To gain the tapping ability, the thread cutting screws are equipped with a flute on the point, so the chips can leave the hole without blocking or over-heating the screw.

Self-tapping screws are available in partially threaded and fully threaded products. In addition, the screw often has a diameter up to 14mm and a length up to 1000mm (Dietsch and Brandner, 2015). For diameters ranges from 12-20mm and lengths ranges from 1000-3000mm, threaded rods, without screw heads, are normally used. A picture of modern self-tapping screws is shown in Figure 2-29.

Figure 2-29: Modern self-tapping screws (the longest one in this picture is 400mm).

Currently, there is a large variety of self-tapping screws, with various screw configurations, available on the market. In terms of screw configuration, these can be generally divided into the variations of screw head, thread and screw point.

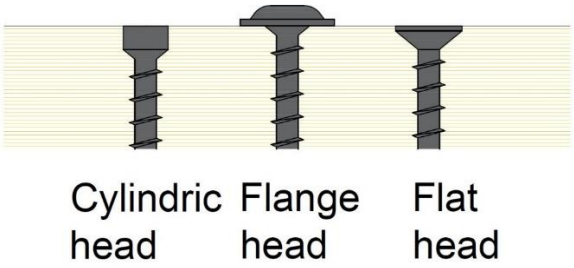

Figure 2-30: Typical types of screw head.

Some typical screw heads are: cylindric head, flange head and flat head (as shown in Figure 2-30). The cylindric head allows the head to sink into the wood thus being almost invisible. The flange head and flat head provide a larger head area, to increase the pull-through capacity, while the latter can sink into the wood to offer a smooth surface. The screw head can further be divided by the types of screw drive, however this is not including in the discussion here.

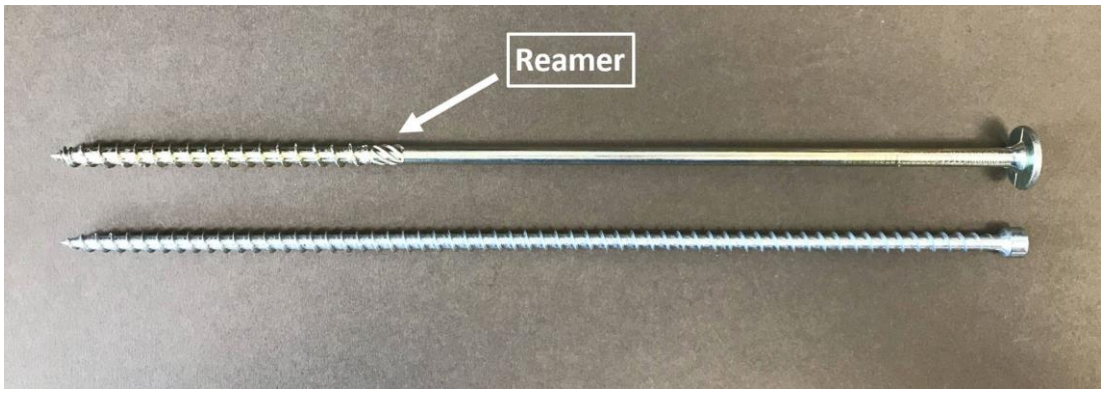

Figure 2-31: Partially threaded (top) and fully threaded (bottom) self-tapping screws.

The thread configurations, for instance, the pitch, depth, thread angle and thread length also vary with brand. Manufacturers have developed different kinds of self-tapping screws for different purposes: a partially threaded screw may have a reamer located at the end of the threaded part to clear the wood for an easier entrance of the smooth shank while a fully threaded screw is designed to take higher tensile and compressive load as well as further increase the pull-out strength. Figure 2-31 demonstrates the partially threaded and fully threaded modern self-tapping screws.

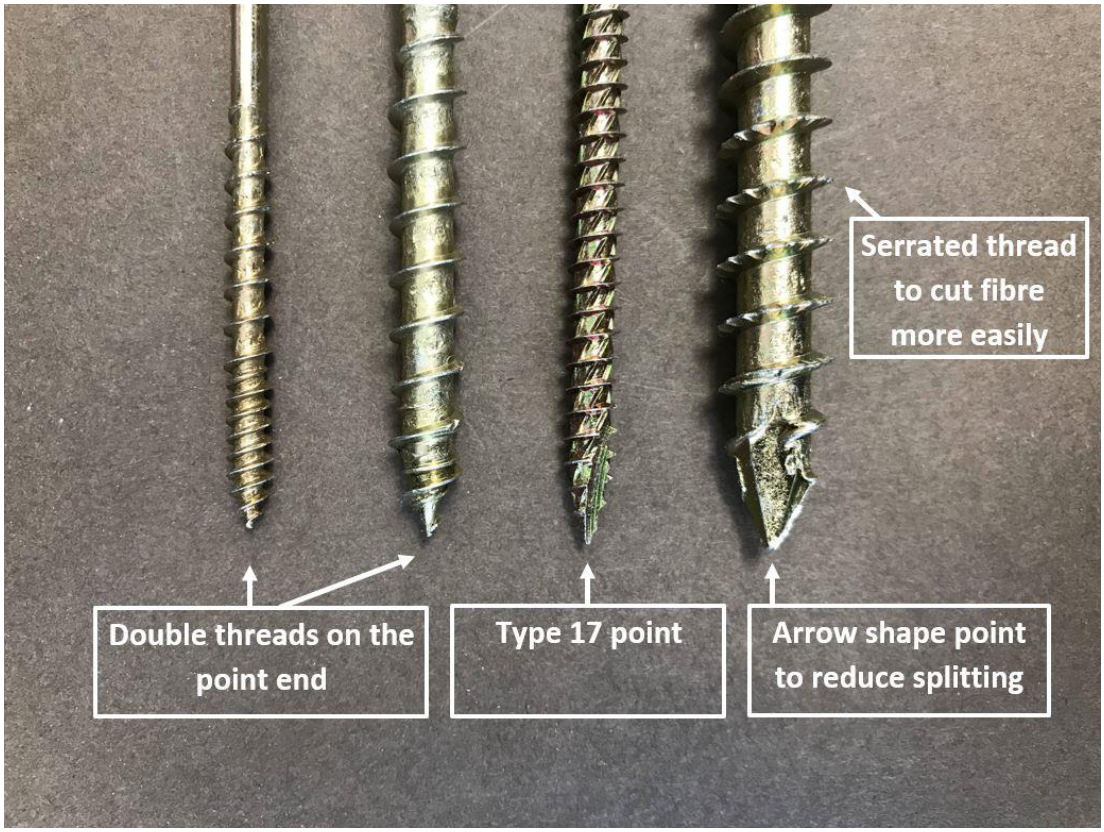

Figure 2-32: Demonstration of various points on modern self-tapping screws.

The screw points are also carefully designed. When applying on hard surfaces, a screw may require a long period of time to start drilling into the material, because the thread does not always exist on the very tip of the screw. Therefore, the screw has to penetrate the material deep enough for the thread to bite on the material for installation. Figure 2-32 shows the double threaded points on self-tapping screws which allow for an easier entering of the screw into timber, especially hardwood. A Type 17 point (see Figure 2-32) is also often used for application with timber where the small wood chips generated from drilling can accumulate and slow down the drilling process. The flute designed on the tip of Type 17 point can capture the chips and allow them to exit from the drilled hole.

The purpose of pre-drilled holes is to prevent the wood from splitting, while it can also benefit the screws to be installed accurately and reduce the driving resistance. Recent research proposed the use of inclined screw for various reasons, the application of pre-drilled holes can aid the installation process. The advanced design of self-tapping screws makes pre-drilling less necessary, compared to traditional wood screws. However, as stated by most of the technical approvals by screw manufacturers (e.g. ETA-11/0030 (ETA-Danmark, 2016) and ETA-13/0796 (OIB, 2017)), pre-drilled holes are allowed with a diameter not greater than the inner diameter of the screw. For the use of self-tapping screws in hardwood or wood with a density $\rho \geq 550 kg/m^3$, pre-drilled holes are advised (Dietsch and Brandner, 2015).

For screws used as fasteners in connections, the current design code EC5 (BSI, 2004) requires that screws (with a diameter greater than 6mm) have pre-drilled holes (with a diameter smaller than the diameter of the screws) in Clause 10.4.5 and need a control plan for ‘correct pre-drilling’ in Clause 10.7 but does not give any more specific instruction on performing a pre-drilled hole, such as methods and tools. One possible risk comes with the use of screws with high slenderness, as a knot can possibly bend the drill for the pre-drilling, it is difficult to ensure the pre-drilled hole is straight and the screw may be offset.

Overall, pre-drilling is an effective method to ensure the successful installation of self-tapping screws. However, it also adds extra time and budget in a project.

2.2.2 Compressive reinforcement

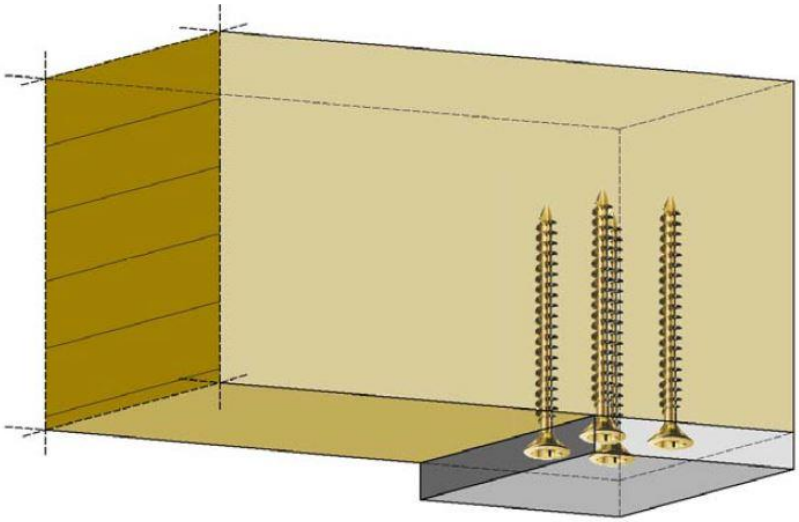

Figure 2-33: Demonstration of compressive reinforcement at beam support (Bejtka and Blaß, 2006).

Bejtka and Blaß (2006) proposed the use of self-tapping screw to reinforce beam supports, see Figure 2-33, and proposed calculation models to find the load-carrying capacity and stiffness of reinforced supports. The load-carrying capacity is expressed as:

$$F_{90,Rd} = min\begin{cases} k_{c,90} \cdot b \cdot l \cdot f_{c,90,d} + n_s \cdot F_{ax,Rd} \\ b \cdot l_{ef} \cdot f_{c,90,d} \end{cases} \quad (2\text{-}1)$$

where:

$F_{90, Rd}$ is the design load-carrying capacity perpendicular to the grain;

$k_{c,90}$ is a load distribution factor ranging from 1 to 1.75;

b is the width of the beam;

l is the length of the support;

$f_{c,90, d}$ is the design compressive strength perpendicular to the grain;

n_s is number of screws;

$F_{ax,Rd}$ is the withdrawal capacity of the screw;

l_{ef} is the effective length of the load distribution.

In their experimental tests, the reinforced supports showed significant increase in load-carrying capacity and stiffness. As mentioned in Section 1.3, the installation of screw reinforcement may be difficult to apply on existing heavy beams due to limited accessibility.

2.2.3 Shear reinforcement

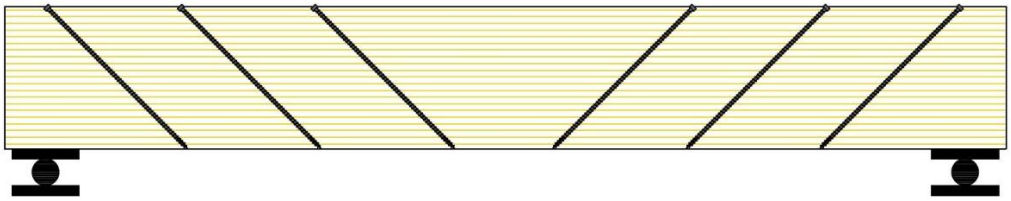

Figure 2-34: Arrangement of shear reinforcement of timber beam.

Shear reinforcement of timber beams is often in the diagonal arrangement shown in Figure 2-20 and Figure 2-34. Based on these arrangements, Trautz and Koj (2009) modified them and proposed a nested diagonal reinforcement which is shown in Figure 2-35. The diagonal screws can carry tension while the blue ones carry compression. The nested diagonal reinforcement achieved much better shear stiffness than diagonal reinforcement.

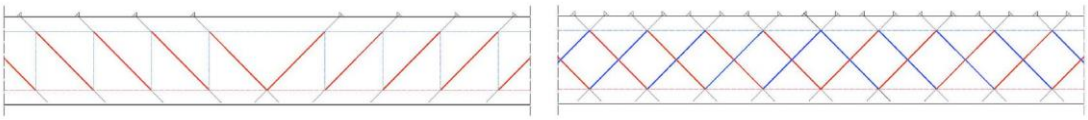

Figure 2-35: Arrangements of shear reinforcement proposed by Trautz and Koj (2009): diagonal reinforcement (left) and nested diagonal reinforcement (right).

A design model of shear reinforcement by self-tapping screws is proposed by Dietsch *et al.* (2013). Experimental work showed good agreement with the model and demonstrated that the shear strength and stiffness was improved in both undamaged and damaged glulam beams. According to Dietsch *et al.* (2013), for undamaged beams, an increase of shear capacity of 20% was possible through screw reinforcement. Furthermore, the tests conducted by Dietsch *et al.* (2013) and Widmann *et al.* (2012) both showed that increasing the number of self-tapping screws can increase the load-carrying capacity of glulam beams.

The above research reinforced the shear capacity parallel to the grain of glulam beams. For Cross Laminated Timber (CLT), the grain direction of each layer is perpendicular to the adjacent ones. As the rolling shear of timber is about three times lower than the shear capacity parallel to the grain (Dietsch and Brandner, 2015), the rolling shear capacity of CLT elements should be strengthened when excessive shear stresses occur.

Figure 2-36: Typical rolling shear failure of CLT element (Flores et al., 2016).

Mestek *et al.* (2011) enhanced the load-carrying capacity of CLT panels with inclined fully threaded self-tapping screws and proposed a design concept of screw-reinforced CLT elements. Mestek *et al.* (2011) recommended self-tapping screws as a simple and cost-effective reinforcement.

However, the influence of design parameters, such as the amount of self-tapping screws, reinforcement spacing and inclination, on the effectiveness of reinforcements still require further investigation.

2.2.4 Tensile reinforcement

Timber splitting due to excessive tensile stresses perpendicular to the grain is likely to occur in beams with service holes, notches and connections.

2.2.4.1 Reinforcement on beams

For beams with service holes, the stress flow is disturbed around the holes and causes excessive tensile stresses perpendicular to the grain. Reinforcement is required to prevent crack initiation and propagation, to maintain the load-carrying capacity and ductility of the beam. The design approach of using reinforcement has been standardised in Germany (DIN, 2013).

Aicher and Höfflin (2009) and Aicher (2011) conducted experimental tests on glulam beams with holes that were reinforced by fully threaded self-tapping screws, glued-in rods and external plywood panels. Based on a small sample size, all the reinforcements enhanced the mechanical properties of the beam with similar improvement.

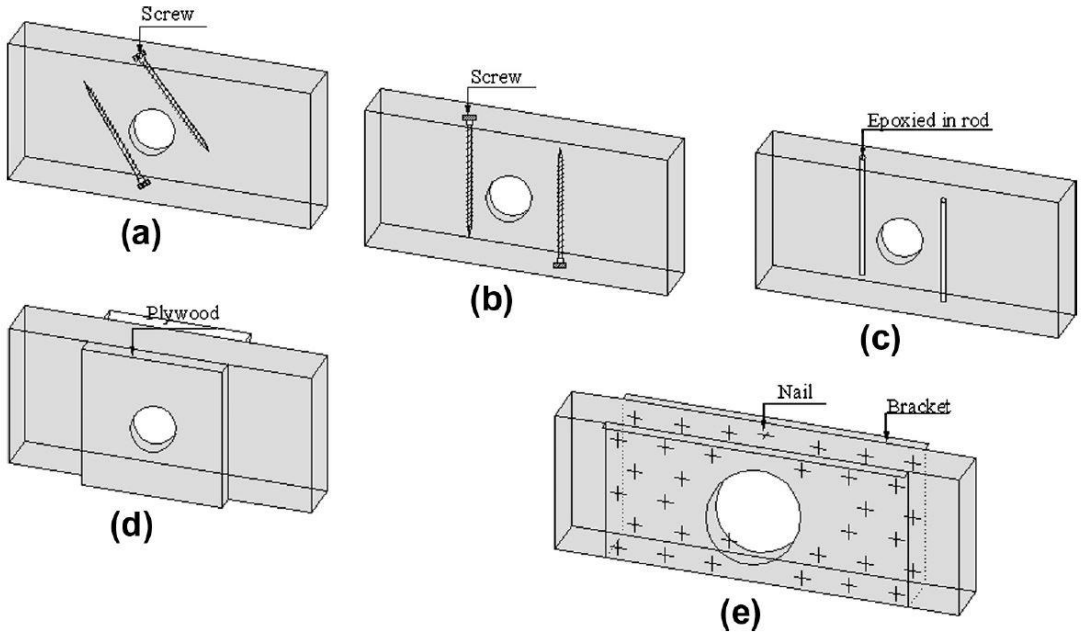

Figure 2-37: Various reinforcement arrangement tested in Ardalany et al. (2013a).

Ardalany *et al.* (2012, 2013a) reinforced LVL beams with holes using self-tapping screws, glued-in rods and bonded plywood panels as shown in Figure 2-37. According to Ardalany *et al.* (2013a), sizes of round holes ranging from 42-63% of the depth of the beam caused a reduction of load-carrying capacity from 30-52%. Their test results showed that self-tapping screws placed either vertically or inclined can effectively restore the flexural behaviour and load-carrying capacity of a beam with hole to that of a beam without hole. They expressed the difficulties in driving the screw at an inclined angle. Ardalany *et al.* (2013a) also found that screw reinforcement was more effective in preventing crack propagation than crack initiation. As for the glued-in rods, they recommended avoid preparing the vertical hole for the rod on the tension side, as it can undermine the mechanical properties of the beam, similar to the effect of knots located on the tension side. The nailed steel plates were ineffective when compared to other reinforcements, because the lack of continuous connection to the beam made the plate buckle (Ardalany *et al.* (2013a)) and the plate cannot follow the contour of the hole, which may also cause damage to anything passing the service hole. An analytical model for a reinforced LVL beam with a hole is proposed by Ardalany *et al.* (2013b), where tensile load induced by shear stress and bending moment are considered separately.

With detailed design information provided in EC5 clause 6.5 (BSI, 2004), design approaches of reinforcing notches are available in the German national annex (DIN, 2013). Reinforcement methods using FRP have been demonstrated in Figure 2-22. Jockwer *et al.* (2013) and Jockwer (2014) presented experimental tests using self-tapping screws to

reinforce notches and achieved significant improvement in load-carrying capacity. As mentioned in Section 2.1.5.1, their work also recommended enhancing the shear capacity of the beam to further enhance the performance of reinforcement, by orientating the inclination of the self-tapping screw. Notches reinforced by screws placed at 45˚ achieved higher load-carrying capacity than those with screws placed at 90˚. However, as Gustafsson (1995) wrote, when drying, the placement of rods or screws may limit the movement of the wood as it tended to shrink, which can cause cracking on the beam.

As for tapered, curved and pitched cambered beams, tensile reinforcement is required at the apex area. Jönsson (2005) reinforced curved glulam beams with self-tapping screws, as shown in Figure 2-38, and found that reinforcement not only restored the load-carrying capacity of failed beams but achieved 10-20% higher capacity than the original beams. The test results also showed that moistening of a beam can halve the capacity when the relative humidity is changed from 40 to 80%. However, cyclic drying and moistening of reinforced beams is not included in Jönsson (2005). The influence of screw reinforcement on timber members under moisture variation is still unanswered.

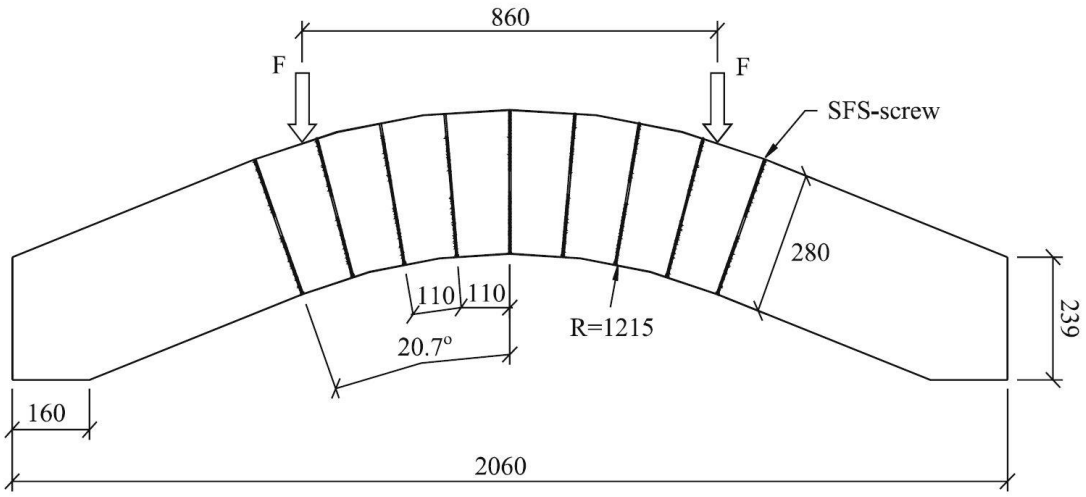

Figure 2-38: Arrangement of screw reinforcement on curved glulam beam tested by Jönsson (2005).

For such beams with extremely large dimensions, the length of available self-tapping screws is insufficient to use as reinforcement. Threaded rods with superior length have been used as reinforcement on these curved members, see Figure 2-23.

2.2.4.2 Reinforcement on dowel-type connections

In recent studies, screw reinforcement was used to enhance the mechanical properties of tensile connections, loaded parallel to the grain, and moment connections.

Tensile connections

Mastschuch (2000) investigated the influence of pitch lengths of screw on the effectiveness of reinforcement on bolted connections. Fully threaded rods and lag screws with pitch lengths of 1.8mm and 4mm, respectively, were used in the tests by Mastschuch (2000). The results showed that threaded rods with fine pitch cannot effectively control splitting in the connections, as the thread-wood anchorage was weak. For connections reinforced by lag screws with coarse pitch, they exhibited better ductility.

For screw reinforcement, as the timber tends to split, the pull-out and pull-through strength of the screw are utilised. According to Crook (1945), screws with a pitch length between 3.2mm to 6.4mm (equivalent to 4 to 8 pitches per inch) can provide adequate pull-out strength; screws with a pitch smaller than 3.2mm tend to break more fibres, when drilling into the wood, thus reducing the withdrawal capacity of the fastener and the restraint against splitting.

In addition, Mastschuch (2000) compared the results of connections reinforced by lag screws placed either at the mid-position between two bolts (half fastener spacing) or at distance of almost one fastener spacing (reinforcement is further away from the reinforced bolt but closer to the next bolt). It showed that lag screws placed further away from the bolt demonstrated better ductility, as Mastschuch (2000) explained, the wood between the bolt and reinforcement acted as a compressible material, providing a smoother load transfer mechanism. However, a larger number of tests is required for confirmation.

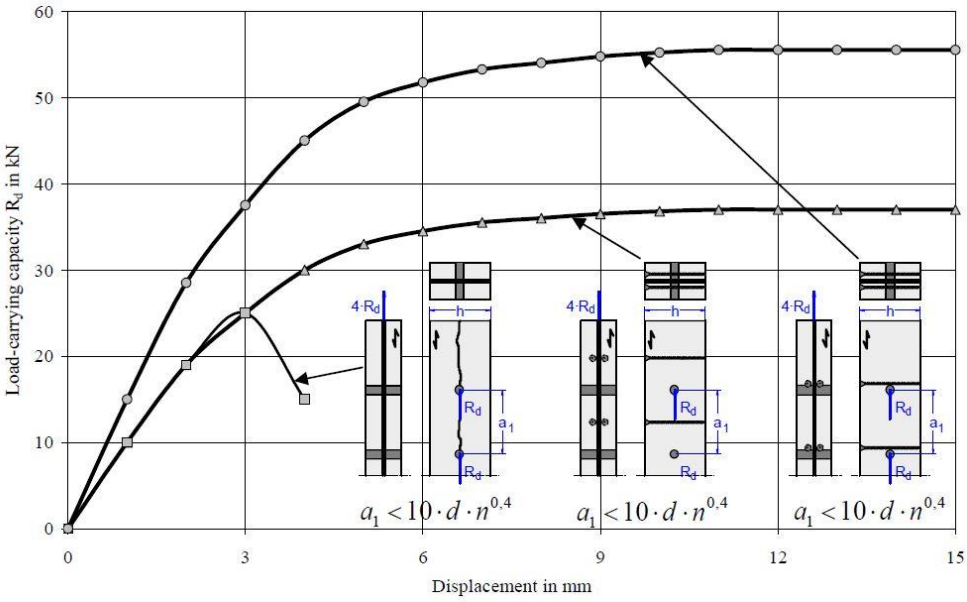

Figure 2-39: Typical load-displacement curves for unreinforced and reinforced connections (Bejtka and Blaß, 2005).

Blaß and Schmid (2001), Mohammad *et al.* (2006) placed the self-tapping screw at various distances from the fastener and found slight improvement in the mechanical properties. According to Bejtka and Blaß (2005), their experimental test results confirmed the increase of both load-carrying capacity and stiffness, by placing the screw closer to the dowel as indicated in Figure 2-39.

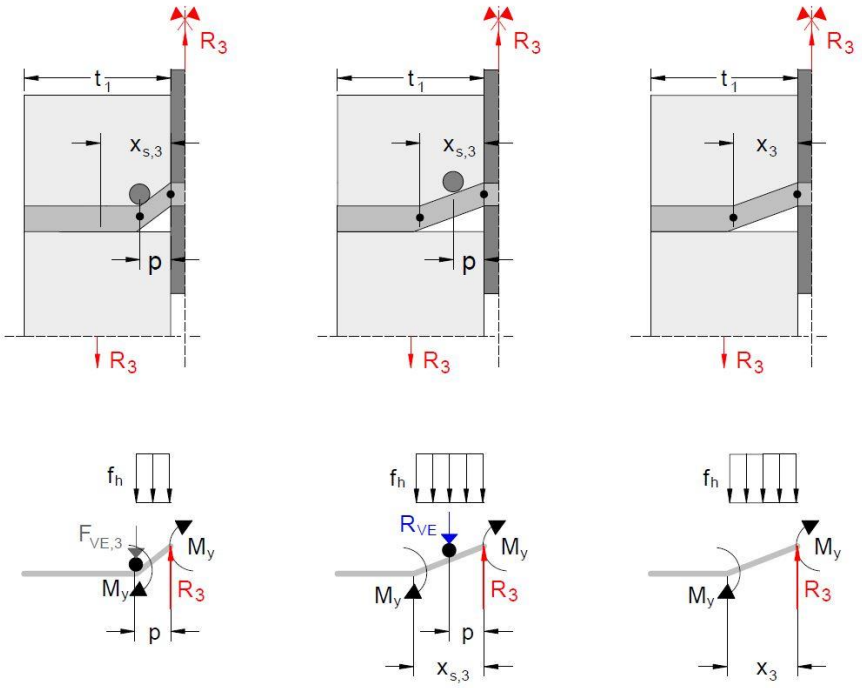

Figure 2-40: Example of reinforced steel-to-timber connection with a screw in rigid state (left), reinforced connection with a screw in 'soft' state (middle) and unreinforced connection (right) (Bejtka and Blaß, 2005).

Bejtka and Blaß (2005) also proposed a calculation model for screw-reinforced dowel-type connections based on the Johansen's yield theory. In their model, the reinforcing screw is assumed to display an ideal rigid-plastic behaviour, where the screw will not move if the imposed load on it, F_{VE}, is smaller than the load-carrying capacity, R_{VE}; however, if F_{VE} reaches R_{VE}, the screw can move and yield as a 'soft' support (Bejtka and Blaß (2005)). Figure 2-40 shows an example of failure mode 3 (a combination of embedment failure and fastener yielding) in unreinforced and reinforced steel-to-timber connections.

The load-carrying capacity R_3 can be found by using force and moment equilibrium. The important factor of the calculation model is the distance from the screw to the steel plate, p. According to Bejtka and Blaß (2005), if p is smaller than the x_3, which is the distance from the hinge to the steel plate, the reinforcement can increase the load-carrying capacity of the connections; otherwise, the reinforcement is ineffective. A series of calculation models regarding timber-to-timber and steel-to-timber, with different failure modes, are published in Bejtka and Blaß (2005) and guidance to the Johansen's yield model can be found in STEP

1995 (Blaß, 1995). The proposed calculation models are also verified by experimental tests in Bejtka and Blaß (2005).

The idea of the relationship between the screw to plate distance, *p*, and hinge to plate distance x_3 is a good criterion of the enhancement of load-carrying capacity but screws placed beyond the hinge point may still have an influence on splitting.

As suggested by Dietsch and Brandner (2015), the screw should be placed with a minimum edge distance, $a_{4,c}$, as guided by the EC5 for screws as connectors. However, the screw reinforcement tested in Bejtka and Blaß (2005) was placed at 15mm away from the steel plate, which is too close to the edge and may damage the member due to the reinforcement. Therefore, the impact of screw position to the edge should be evaluated.

Echavarría (2007) investigated the influence of screw reinforcement on single dowel connections with reduced edge distance. The tensile test results showed that for connections with a reduced edge distance of *2d*, self-tapping screws placed at *1d* distance to the fastener significantly increased the load-carrying capacity by more than two times when compared to the unreinforced connections. However, for other reduced edge distances of *3d*, *4d* and *5d*, the improvement in capacity was limited.

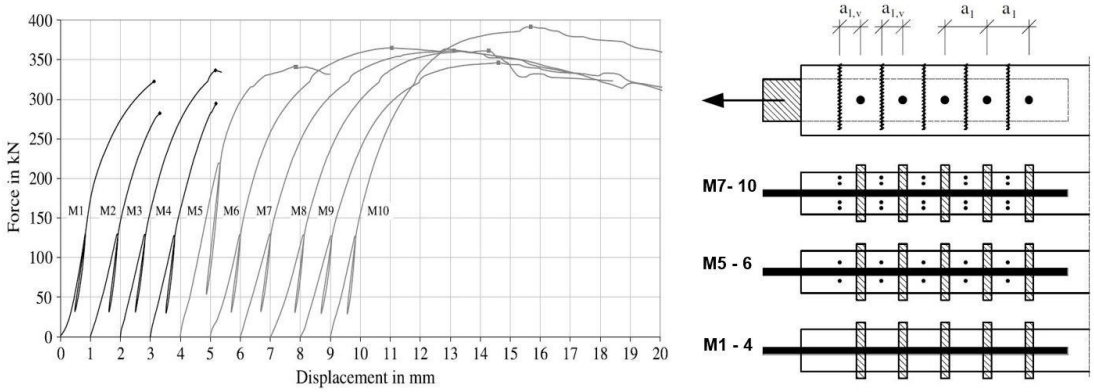

Figure 2-41: Load-displacement curves of screw-reinforced connections and reinforcement configurations (Blaß and Schädle, 2011).

Blaß and Schädle (2011) presented work on reinforcing tensile connections with different amounts of screw reinforcement. The load-displacement graph and reinforcement configurations are shown in Figure 2-41. It was found that reinforcement improved the load-carrying capacity and ductility of the connections and doubling the amount of reinforcement showed further enhancement. However, in practice, increasing the number of screws means additional time and cost. Therefore, optimising the reinforcement is a preferable option to simply doubling the amount of reinforcement.

Apart from reinforcing connections made by sawn timber and glulam, Lokaj and Klajmonová (2014) also investigated the mechanical performance of round timber bolted joints strengthened by various types of reinforcement, see Figure 2-42. The static tests showed that modified washers using steel plates and BOVA steel plates (plates providing holes for nails), achieved best improvement in load-carrying capacity, while the connections reinforced by screws reduced the variation in capacity, indicating greater reliability. Lokaj and Klajmonová (2014) suggested using two screws rather than other reinforcement, because of their simplicity and good performance in enhancing the capacity of the connections.

Figure 2-42: From left to right: modified washers, BOVA steel plate, one screw, two screws and steel band as reinforcement (Lokaj and Klajmonová, 2014).

In terms of repairing damaged connections due to moisture fluctuation, experimental work done by Delahunty *et al.* (2014) has shown the potential for self-tapping screws as reinforcement. In their tests, a self-tapping screw with two thread segments was installed to reinforce bolted connections with artificial cracks, as demonstrated in Figure 2-43.

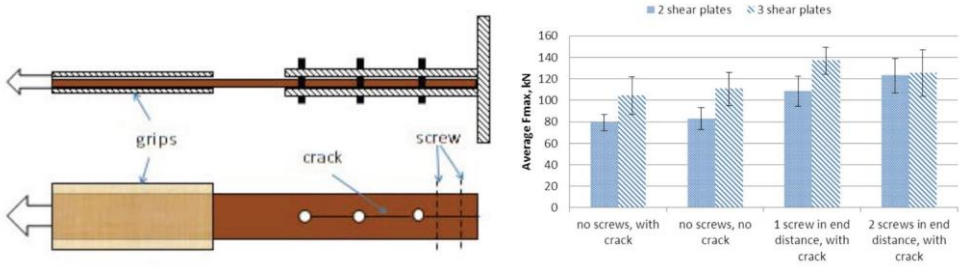

Figure 2-43: Specimen configuration and test results (Delahunty et al., 2014).

For connections having either two or three shear plates, reinforced by self-tapping screws, the load-carrying capacity of the damaged connections was significantly higher than the undamaged ones. However, Delahunty *et al.* (2014) did not explain the reason that the connections with three shear plates reinforced by two screws showed less capacity than that of the same type of connections reinforced by only one screw. In addition, the work done by

Delahunty *et al.* (2014) only considered a single size of crack. However, in practice, the size of the crack normally grows as it develops; thus, the effectiveness of screw reinforcement, to restore the mechanical properties of connections with larger cracks, remains to be answered.

Palma *et al.* (2013) examined the mechanical and fire performance of screw-reinforced dowel-type connections, the installation procedure of the screw is demonstrated in Figure 2-44. The experimental tests confirmed that the durability of connections in fire was improved by screw reinforcement.

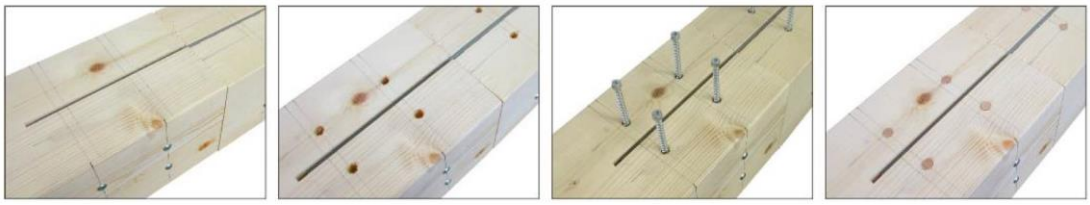

Figure 2-44: Installation of the screw reinforcement with wooden plugs to provide fire protection for the screws (Palma et al., 2013).

Moment-resisting connections

In large timber structures, dowel-type connections are preferred due to their simplicity and elegance, however, their moment-resisting capacity is limited by the tensile strength of timber perpendicular to the grain.

When subject to high lateral load, such as in a seismic event, the moment-resisting capacity of the connections should be sufficient. In exchange for higher capacity, this often leads to additional cost as designers need to increase the number or the size of the fasteners and subsequently enlarge the dimensions of the timber elements with increased spacing, end and edge distance as requested by design codes. Furthermore, the moment-resisting capacity of the connections can be reduced due to moisture fluctuations. The change of relative humidity in the surrounding environment leads to the moisture exchange in the wood for equilibrium. Dimensional change of the timber member is inevitable as wood intakes moisture (causing swelling) or releases moisture (causing shrinking). As the wood around the fasteners is restrained in movement, stress concentration in these areas leads to splitting of the wood and reduces the moment-resisting capacity of the connections. Therefore, researchers have been trying to use self-tapping screws to reinforce the connections and enhance their mechanical properties.

Table 2-2: Summary of test results (Lam et al., 2008).

	Static			Dynamic		
	MU	MR	MD	CU	CR	CD
Description	*Unreinforced*	*Reinforced*	*Reinforced 'MU' group after failure*	*Unreinforced*	*Reinforced*	*Reinforced 'CU' group after failure*
Maximum moment (kNm)	*31.49*	*65.88*	*58.85*	*35.70*	*62.54*	*54.54*
Rotation (˚)	*2.97*	*16.59*	*13.29*	*4.01*	*15.90*	*12.65*

Lam *et al.* (2008) reinforced bolted timber connections with self-tapping screws placed 40mm (over *2d* distance) away from the bolts and their test results are shown in Table 2-2. As can be seen, in both static and dynamic loading condition, self-tapping screws significantly improved the moment-resisting capacity and ductility of the connections. In addition, the reinforcement effectively enhanced the mechanical properties of failed connections to a state even higher than the original intact connections.

Lam *et al.* (2010) and Gehloff *et al.* (2010) examined the performance of screw-reinforced, bolted connections, with reduced edge distance under dynamic loading. The configurations of their tests are shown in Figure 2-45. The bolts in the connections were placed close to the edge which in turn increases the moment capacity as the distance from the bolt to the centre of rotation is increased. With the aid of the self-tapping screw to prevent splitting failure of the wood at reduced edge distances, the moment-resisting capacity of the connection was increased by approximately 3 times when compared to the unreinforced connections (Lam *et al.* (2010)). However, their work did not find any significant improvement in the mechanical properties of the connections by placing the self-tapping screws closer to the bolts. According to Gehloff *et al.* (2010), placing the screws closer reduced the variation in test results and may have positive impact on the energy dissipation.

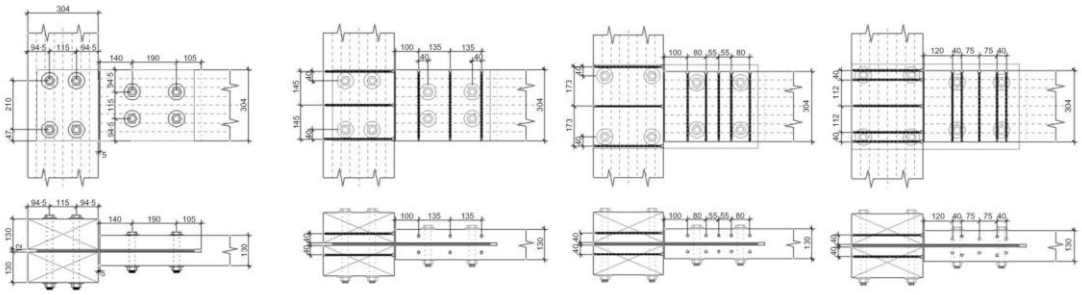

Figure 2-45: Configurations of tested specimens (left to right): unreinforced connection, screw-reinforced connection, screw-reinforced connection with reduced edge distance and screw-reinforced (screws were placed closer to the bolts) connections with reduced edge distance (Lam et al. 2010).

2.3 Advantages and research gaps for screw reinforcement

Research presented in the previous sections have shown the potential of using self-tapping screws to enhance the mechanical properties of timber elements. Compared to metal and FRP reinforcement, the advantages of screw reinforcement can be summarised into the following points:

- Fewer concerns about appearance
- Lower requirements for accessibility
- Simple installation
- Quick installation
- Reversible (can be retrieved easily)

However, as a recently developed reinforcement method, there are a large number of remaining questions regarding to the performance and reliability of self-tapping screws.

Firstly, the understanding of the performance of screw reinforcement under moisture variation is limited. Angst and Malo (2012) measured the moisture induced stresses in unreinforced and reinforced glulam specimens in both drying and wetting phase. Their experimental tests found that self-tapping screws restrained the movement of the glulam specimen in swelling or shrinking when compared to unreinforced specimens. However, they also discovered that self-tapping screws may increase the stress in the wood that is close to the edge of the beam during the drying phase. Further research on the durability of thread-wood anchorage in extreme environments is required.

Furthermore, current research focuses on the static performance of screw reinforcement on timber members. The understanding of the performance of screw-reinforced beams,

connections and panels under dynamic loading is not fully established. Other parameters of screw reinforcement, such as screw spacing, end and edge distance, are also paramount for the development of a standardised design approach.

2.3.1 Drive-in torque and thread configurations

Currently, the self-tapping screws available on the market have various forms of thread configuration. As the screw is driven into the wood, friction between the wood and the screw increases with the penetrated depth of the threaded part. The drive-in torque subsequently rises and can potentially damage the screw. Therefore, ensuring adequate thread-wood anchorage for reinforcement purpose and avoiding damage to the screw during installation are the main criteria in choosing the suitable forms of self-tapping screws as reinforcement.

The limited knowledge about the influence of thread configuration (thread length and location) on the effectiveness of screw reinforcement becomes the major drive of this study. The impact of screw to dowel distance on the performance of reinforcement is also included in this research.

The above research questions lead to an investigation of the relationship between the drive-in torque and thread configuration of self-tapping screws, which is presented in the next chapter. Other factors, such as knots and pre-drilled holes, that could affect the performance of screw reinforcement are also discussed.

Chapter 3 Drive-In Torque for Self-Tapping Screws into Timber

The content of this chapter has been submitted to the *Proceedings of the Institution of Civil Engineers - Construction Materials* and is under review.

3.1 Introduction

Self-tapping screws are becoming increasingly popular in the construction industry. With their advanced manufacture techniques, they feature higher load-carrying capacity than traditional wood screws. Currently, they can be used as connectors or for reinforcement in timber structures. Examples of the use of self-tapping screws on continuous purlin and connections are demonstrated in Figure 3-1. In a continuous purlin, the screws are under compression and tension respectively when the load is parallel to the surface of the member, or both under tension when the load is perpendicular to the surface (Thelandersson and Larsen, 2003). The inclined screws enable the use of the high axial strength of a screw. Thelandersson and Larsen (2003) also reported that connections using inclined screws achieve an increase of 50% in the load-carrying capacity when compared to those with screws installed perpendicular to the grain.

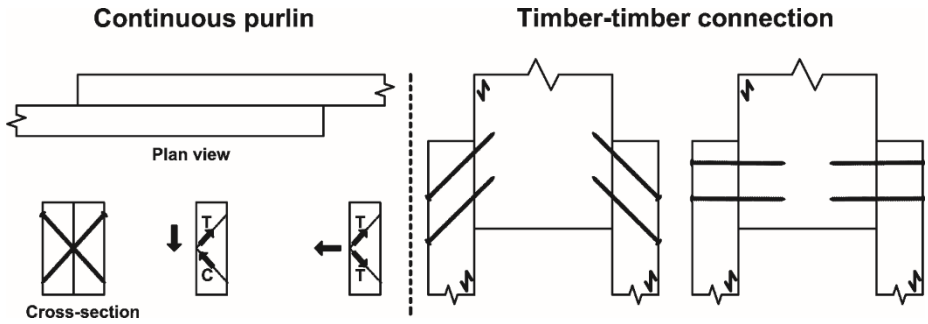

Figure 3-1: Examples of self-tapping screws as connectors for beam (left) and connections (right).

For reinforcement purposes, self-tapping screws can be used in various situations. Studies by Blaß and Schmid (2001), Bejtka and Blaß (2005) and Blaß and Schädle (2011) demonstrate the improvement of load-carrying capacity and ductility of dowel-type connections reinforced by self-tapping screws which can control timber splitting due to excessive tensile load perpendicular to the grain. Ardalany *et al.* (2013a) used self-tapping screws to effectively reinforce beams with holes having concentration of tensile stress around them.

For beam supports, the load-carrying capacity is limited by the compressive strength of timber perpendicular to the grain. Bejtka and Blaß (2006) used self-tapping screws with high axial strength to reinforce the support region and achieved 3 times higher load-carrying capacity and 5 times greater stiffness than with unreinforced ones. Mestek *et al.* (2011) experimentally tested and confirmed the shear capacity of CLT elements improved by self-tapping screws. This brief overview of research shows the great potential of self-tapping screws for use in timber structures.

With an increasing market for self-tapping screws, more and more types of screws are available, and the thread profile of screw varies with brand. When the screw is being installed, friction appears as the thread is in contact with the wood. This driving resistance grows with increased contact area between wood and thread as the screw drills further into the wood. A fundamental question arises as to how the thread configurations of screws differ in terms of workability (how easily the screws can be installed). For a long self-tapping screw with full thread, a high torque for installation is often required, especially when passing through the knots. The requirement of a high torque may lead to the use of more powerful machines as well as requiring additional personnel, tools and time.

Currently, the approach to reinforcing connections using self-tapping screws is included in the national annex of countries like Germany (DIN, 2013). However, the difference between using fully threaded and partially threaded self-tapping screws is not known. In the works in Chapter 4 and Chapter 5, self-tapping screws with 33% thread on the point end, achieved similar improvement in embedment strength to the screws with 100% thread.

Furthermore, the concept widely advertised by screw manufacturers is that it can penetrate either wood or metal and drill a path for itself without a pre-drilled hole. One critical issue is the problem caused by knots which inevitably exist in timber. A knot is the remaining part of a branch in the trunk of a tree and it normally has higher density than the surrounding wood (Nardin *et al.*, 2000). It can damage the self-tapping screws by creating a surge of friction and slowing down the installation process. More importantly, as the screw always tries to find the easiest path, a knot may offset the drilling direction of the screw thus making the positioning of screws more difficult than expected. Unfortunately, the current knowledge for self-tapping screws to overcoming the mentioned issues is limited and the methods to correctly prepare pre-drilled holes require specification.

As the drive-in torque is related to thread length, this study aims to find the influence of screw configuration from a perspective of required installation torque. In addition, the effects from knots and the presence of pre-drilled holes are also investigated. Two kinds of screw

involving three different types of thread configurations were tested. The drive-in torques of screws with and without pre-drilled holes were also compared.

3.2 Materials and methods

3.2.1 Material preparation

Gl24c glulam beams have a moderate price and are commonly used in practice. Therefore, a 300mm deep by 140mm wide GL24c glulam beam, made from European Whitewood (can be either silver fir (*Abies alba*) or Norway spruce (*Picea abies*)), was chosen to conduct the torque test. The purpose of using only one beam is to ensure consistency of the timber density. The beam had a density of 421kg/m^3 and an average moisture content (hereafter M.C.) of 8.5% (CoV= 7.1%). The moisture content for each face (except the two cross-sections) was measured three times using a moisture meter. The beams were stored and prepared indoor at 18.5°C and 63.4% relative humidity (RH).

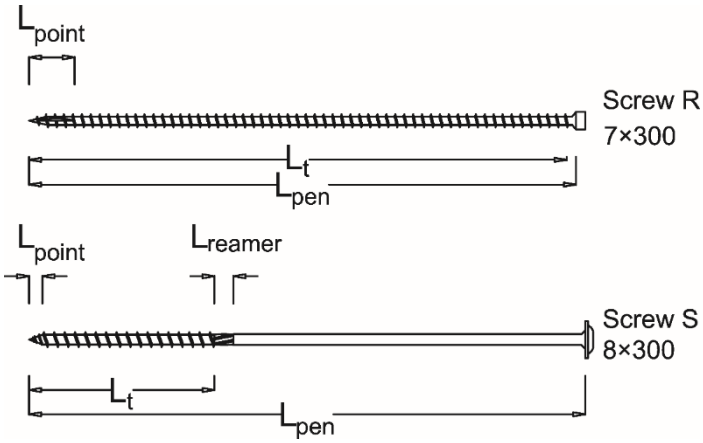

Figure 3-2: The two types of screws used in this study.

Two different self-tapping screws, R and S, were used in the test, as shown in Figure 3-2. The two types of screw were selected as they are exactly 300mm in length meaning they can fit into the 300mm deep beam that were also used in the connection tests in Chapter 6 and Chapter 7. In addition, the Screw S has approximately one third of thread of the Screw R. This ratio was frequently used in the embedment tests in Chapter 4. Table 3-1 summarises the properties of screws used in this project. The thread configurations of the screws are shown in Figure 3-3. Screw R had a cylindrical head and its penetration length, L_{pen}, was 295m. It also had a Type 17 point (contains a flute to capture chips) which helps to penetrate wood more quickly. Screw S was partially threaded and had a double threaded point (for a faster insertion of the screw). A reamer was located next to the threaded part for preparing a smooth driving for the screw shank.

Table 3-1: Specifications for the self-tapping screws.

Screw type	L_{pen} (mm)	L_t (mm)	L_{point} (mm)	L_{reamer} (mm)	Outer Ø (mm)	Inner Ø (mm)	Pitch (mm)
R	*295*	*290*	*25*	*N/A*	*7*	*4.6*	*4.8*
S	*300*	*100*	*13*	*10*	*8*	*5.3*	*5.6*

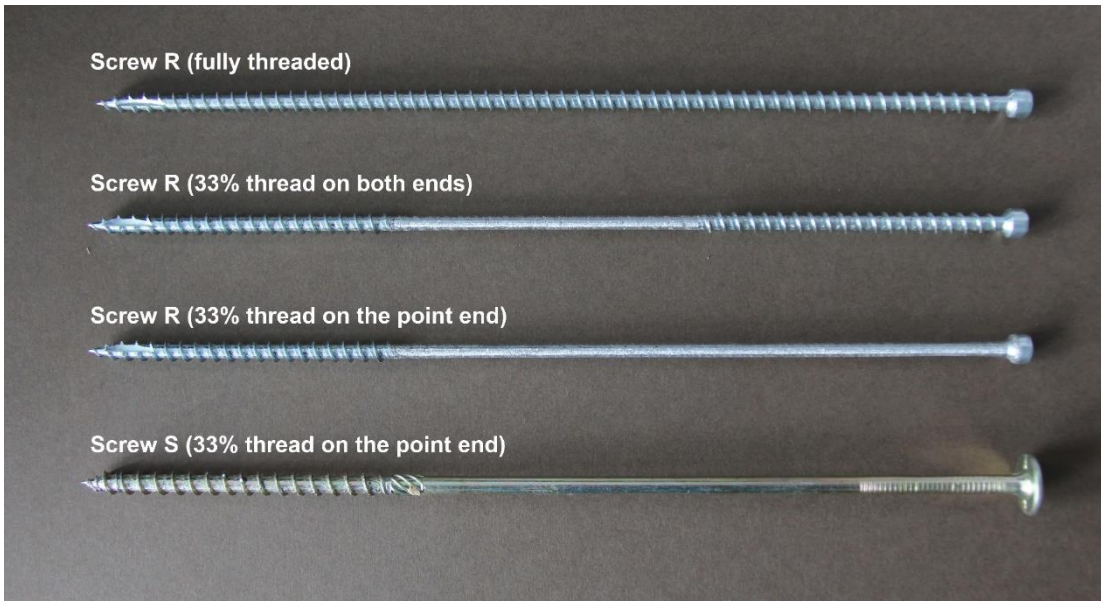

Figure 3-3: Prepared self-tapping screws in this test.

In the experimental works in Chapter 4 and Chapter 5, screws with 100% thread, screws with 33% thread on both ends and screws with 33% thread on the point end achieved similar performance as reinforcement. It is therefore worth comparing the torque required to install Screw R with different thread configurations. In addition, as there are a vast number of self-tapping screws available on the market, screws with a different diameter can also influence the required torque, so that a comparison between Screw R with 33% thread on the point end and Screw S is necessary. Furthermore, as self-tapping screws are designed to penetrate the wood without any pre-drilling holes, a comparison is made of the torque required to install screws with and without pre-drilled holes. This test can lead to a deeper understanding of the influence of having pre-drilled holes. The details of each testing group are given in Table 3-2 according to the technical approvals from the screw manufacturers (ETA-11/0030 (ETA-Danmark, 2016) and ETA-13/0796 (OIB, 2017)). Groups A, B, C and G used pre-drilled holes and groups D, E, F and H used self-tapping screws without pre-drilled holes.

Table 3-2: Summary of each group.

	Group	A	B	C	G
With pre-drilled hole	Screw type	*R*	*R*	*R*	*S*
	Characteristic torsional strength (N·m)	*18*	*18*	*18*	*25.6*
	Threaded length (mm)	*290*	*200*	*100*	*100*
	Thread location	*Fully threaded*	*100mm on both ends*	*Point end*	*Point end*
	Screw inner diameter (mm)	*4.6*	*4.6*	*4.6*	*5.3*
	Pre-drilled hole to screw inner diameter ratio	*0.87*	*0.87*	*0.87*	*0.90*
	Diameter of the drill (mm)	*4*	*4*	*4*	*4.76*
	Pre-drilled hole depth (mm)	*180*	*180*	*180*	*180*
	Repetitions	*5*	*5*	*5*	*5*
	Group	D	E	F	H
Without pre-drilled hole	Screw type	*R*	*R*	*R*	*S*
	Characteristic torsional strength (N·m)	*18*	*18*	*18*	*25.6*
	Threaded length (mm)	*290*	*200*	*100*	*100*
	Thread location	*Fully threaded*	*100mm on both ends*	*Point end*	*Point end*
	Repetitions	*5*	*5*	*5*	*5*

A grinder was used to remove the unwanted parts of threads, and sandpaper was then applied to polish the surface so as to minimise the friction, see Figure 3-3.

According to Clause 10.4.5 in EC5 (BSI, 2004), the pre-drilled holes for screw shank should have the same diameter and depth of the screw shank and the diameter of pre-drilled hole for the threaded part should be 70% of the screw shank diameter. The requirements for the pre-drilled hole was difficult to achieve owing to the height limit of the specimen for the pillar drill machine and the available drill sizes at that time. As the pre-drilled holes did not fully met the requirements of EC5 due to the mentioned limitations, the screws were expected to experience a higher torque when compared to the ideal condition (full compliance with EC5). This is because the installation of screws for the last 120mm length in the wood was

not covered by pre-drilling. In addition, the slightly large pre-drilled hole for the threaded part of the screw may reduce the drive-in torque as less amount of wood was expected to be in contact with the screw to generate friction. Overall, the influence of the depth of the pre-drill is considered as the dominant factor and the reduction of the drive-in torque is expected to be greater when full requirements of the pre-drilled hole are met.

In this study, the pre-drilled hole was set to be 180mm deep. For the groups with pre-drilled holes, a ratio of approximately 0.9 of pre-drilled hole size to screw inner diameter was applied to both types of screw.

The glulam beam was marked for the location of the screws and pre-drilled holes. The end and edge distances of the screws followed BS EN 15737:2009 (BSI, 2009b) and the spacing for screws followed the guidance from EC5 (BSI, 2004) on designing screws as connection fasteners. The arrangement of screws is shown in Figure 3-4. The beam was divided into five test sections with one section reserved for additional tests. The spacing arrangement was repeated for all sections. Tests from the same group were distinguished by assigning the section number to the group name and this is used later for analysing results. A total of 40 tests were conducted on one glulam beams.

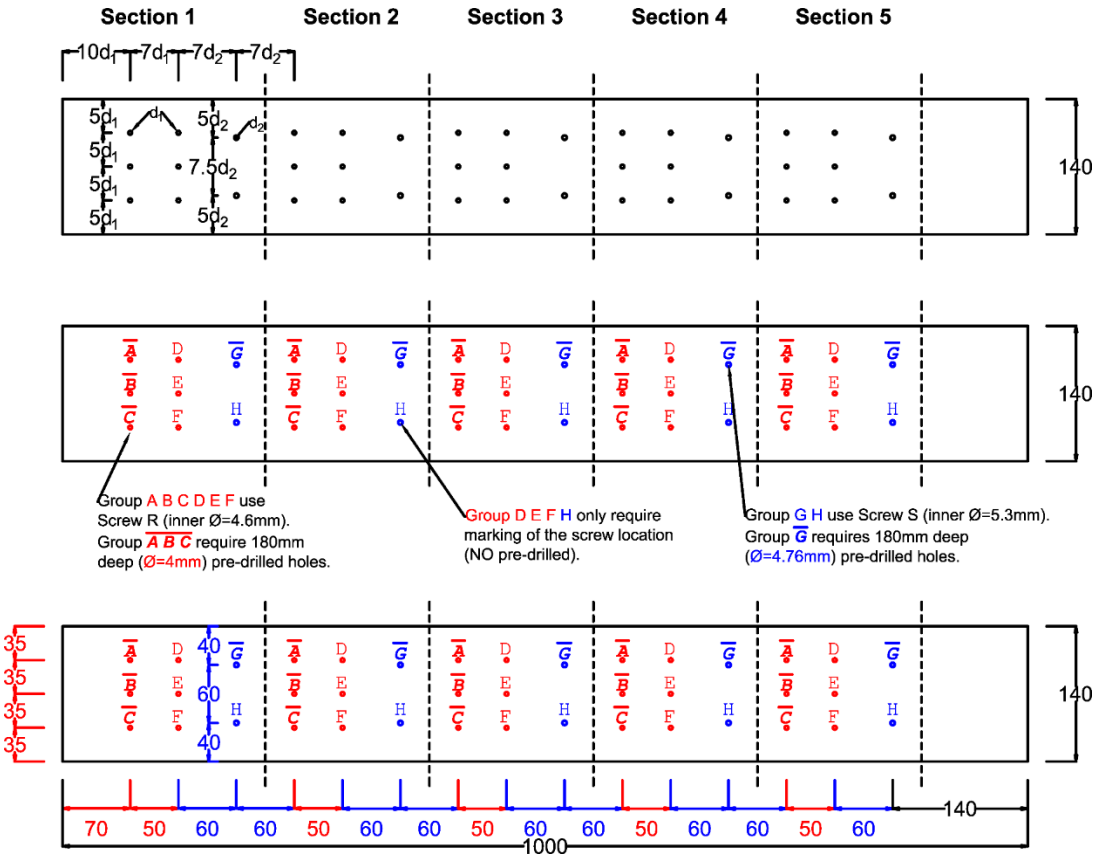

Figure 3-4: Screw arrangement for the torque test. The spacing satisfies the minimum requirement of design geometries.

3.2.2 Test set-up

The glulam beam was tightly fixed using instant clamps to ensure that the movement of the entire beam was minimised when installing the screw. To measure the torque to install the self-tapping screws, a Bacho TAM1430 digital torque analyser (1.5-30Nm) was used. To successfully connect the analyser to the screw, one end of an extension bar was clamped into the slot of the hand drill and the other end fitted into the socket on the analyser. Then, a drive socket was connected to the lower part of the analyser and the Torx screw driver bit was fitted into the drive socket. The hand drill could then drive the screw in, while the analyser gave the current torque reading, see Figure 3-5. The test started from section 1 to section 5 and followed the alphabetical order, from screw A to H, for each section. The influence of installed screws on the drive-in torque of the screw being installed is not considered in this study.

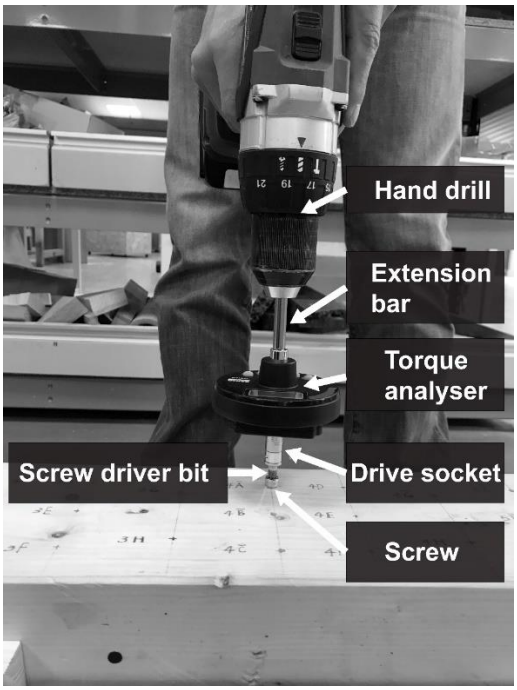

Figure 3-5: Setting up the analyser.

During the test, a video recording device was used to film the readings on the analyser. As the analyser gives an instant reading, the speed of the hand drill was controlled to be at a slow rate. This was to avoid capturing blurred readings when the torque analyser spun too fast.

3.3 Results and discussion

During the test, some screws experienced a surge of torque, possibly as a result of knots inside the glulam beam. As for those groups without pre-drilled holes, a higher peak torque can be observed while visual observation did not find significant inclination of the screw.

Table 3-3 gives an overview of the maximum torque measured for each test. The coefficient of variation (CoV) displays the variability of values in each group to the mean value. As can be seen, the values of CoV in groups D, E, G and H are higher than 20% and it is very likely that the data were disturbed by outliers with high torques measured by the analyser. In fact, those groups with lower values of CoV were found to be less influenced by knots. The reason for the surge of torque in these tests could be due to knots hidden inside the beam. To validate this assumption, the glulam specimen was cut open using a band saw at the location of the screws.

Table 3-3: Maximum torque for each test in this study.

		Group A	Group B	Group C	Group G
With pre-drilled hole	1	*5.48*	*5.09*	*5.59*	*9.95*
	2	*7.53*	*5.23*	*5.53*	*8.60*
	3	*6.43*	*5.95*	*5.13*	*7.40*
	4	*6.59*	*5.73*	*5.17*	*8.19*
	5	*8.25*	*7.33*	*5.59*	*12.56*
	Average max torque	*6.86*	*5.87*	*5.40*	*9.34*
	CoV	*16%*	*15%*	*4%*	*20%*
		Group D	Group E	Group F	Group H
Without pre-drilled hole	1	*10.49*	*14.39*	*8.33*	*9.79*
	2	*8.29*	*8.93*	*6.49*	*14.39*
	3	*8.23*	*10.03*	*6.25*	*9.33*
	4	*8.39*	*8.55*	*6.07*	*10.05*
	5	*15.2*	*8.39*	*6.73*	*10.93*
	Average max torque	*10.12*	*10.06*	*6.77*	*10.90*
	CoV	*30%*	*25%*	*13%*	*19%*

3.3.1 Knots inspection

In total, 15 cuts in the transverse direction were made and the pieces were labelled for inspection, as shown in Figure 3-6. A detailed survey of each test after inspection is summarised in Table 3-4.

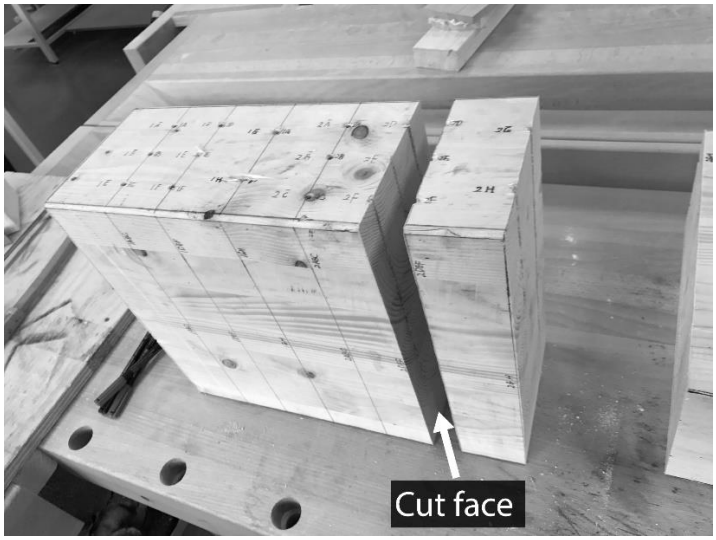

Figure 3-6: A part of the specimen was cut in the transverse direction for inspection.

Table 3-4: Overall inspection result for each group.

	Inspection		Count of cases			
			Group A	Group B	Group C	Group G
With pre-drilled holes	Pre-drilled (<180mm)	Knots in the area*	*3*	*2*	*3*	*2*
		Screw inclination from start	*3*	*1*	*1*	*0*
		Screw bent/inclined due to knots	*0*	*1*	*1*	*0*
		Surge on torque due to knots	*1*	*0*	*2*	*2*
	Below pre-drilled level (>180mm)	Knots in the area*	*0*	*2*	*3*	*3*
		Screw bent due to knots	*0*	*1*	*0*	*0*
		Surge on torque due to knots	*0*	*1*	*0*	*2*
		Screw bent due to annual rings	*3*	*1*	*3*	*1*
	Inspection		Count of cases			
			Group D	Group E	Group F	Group H
Without pre-drilled holes		Knots in the area*	*2*	*4*	*3*	*4*
		Screw inclination from start	*5*	*3*	*5*	*5*
		Screw bent/inclined due to knots	*0*	*2*	*0*	*0*
		Surge on torque due to knots	*1*	*2*	*3*	*2*

** Defined as the number of knots located within the adjacent area (see Figure 3-7).*

As can be seen from Table 3-4, the number of tests that are influenced by knots is evenly distributed in pre-drilled and non pre-drilled groups. For the three groups (A, B and C) using Screw R with pre-drilled holes, 5 out of 15 screws were inclined from the start of installation, among these five screws, four were inclined as the pilot holes were not straight and only one case was influenced by the knots. For the three groups (D, E and F) using Screw R without pre-drilled holes, 13 out of 15 screws were installed inclined from the start. None of the screws in group G (using Screw S with larger diameter) with pre-drilled holes were inclined, in contrast, all five screws in group H without pre-drilled holes were inclined from the start. The above comparison demonstrates one of the main roles of pre-drilled holes is to reduce the chance of inclination of self-tapping screws during installation.

For both pre-drilled and non pre-drilled groups, inspection found that if the screw passes right next to the knot then it is more likely to bend in the direction along the edge of the knot, as shown in Figure 3-7 (a).

For groups (A, B, C and G) with pre-drilled holes, in total 20 screws, none of the screws were bent by the knot above the level of the pre-drilled hole (<180mm). Only one screw, B5, was bent below the level of the pre-drilled hole (>180mm) by the knot, see Figure 3-7 (b). For the groups (D, E, F and H) without pre-drilled holes, two screws were bent by the knot, see Figure 3-8. This might be explained that the high-speed steel (high hardness) drill bits for the pre-drilled hole are less vulnerable to bent when compared to self-tapping screws (made from carbon steel). It demonstrates that pre-drilled holes can help prevent the screws from bending due to the knot.

The growth of European Whitewood is seasonal. At the early stage of the growth period, thin-walled cells (tracheids) appear in the softwood for conduction purposes (the wood is called as earlywood). At the latter stage, thick-walled cells appear in the wood to mainly provide support (the wood is called as latewood). The transformation of the role of the cells leads to a difference in material density whereas early wood is less dense than latewood. As the screw enters to a level below the pre-drilled hole, it tends penetrate the wood where there is less resistance, thus, following the pattern of the annual rings.

For the four groups (A, B, C and G) with pre-drilled holes, some of the screws were found to be bent due to the annual rings, see Figure 3-7 (d). The bending of screws occurs below the level of the pre-drilled holes (180mm deep) indicating the positive effect of pre-drilled holes on screw positioning. As most of the screws were inclined from the beginning in groups without pre-drilled holes, observation of the influence of annual rings on screw positioning is not included in this study.

It was also found that Screw S with larger diameter was less likely to have significant bending due to knots, by comparing groups C & G and groups F & H, respectively. In addition, if the screw passes through the knot, it will not bend significantly. However, the drive-in torque of the screws escalated whenever the screw passed by or through a knot. The count of surge of torque for each group is tabulated in Table 3-4 and the depth of knots that were causing the surge of torque in each specimen is provided in Table 3-5.

The tests that were significantly influenced by knots are discussed first and the torque-depth relationships for these tests are plotted in Figure 3-9.

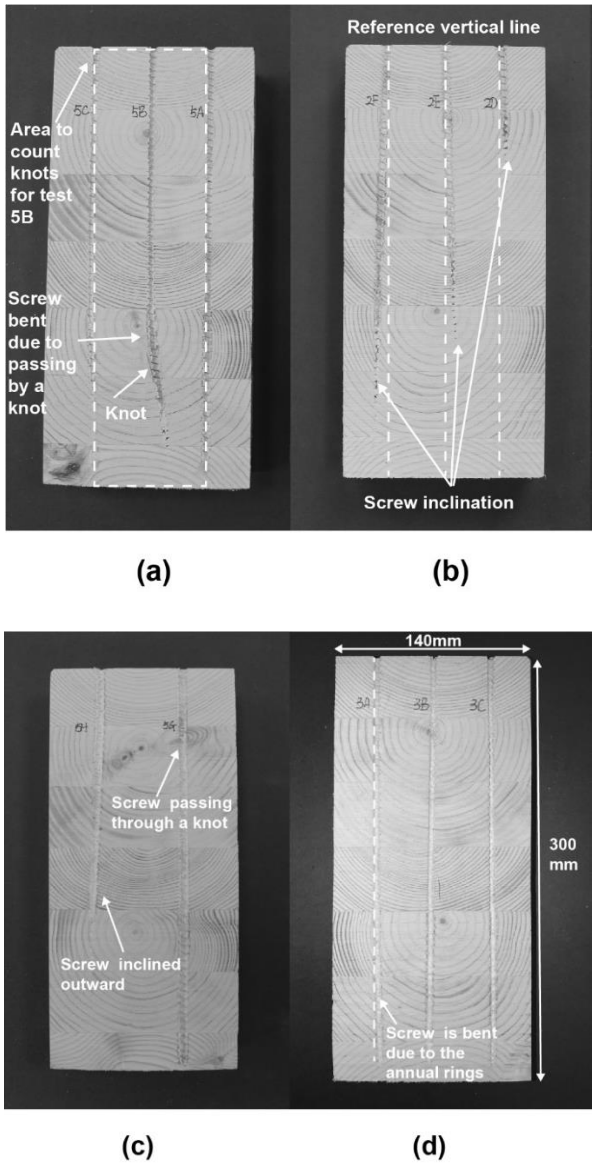

Figure 3-7: Explanation to the terms in Table 3-4. (a): Screw bent due to passing by a knot. (b): Screws inclined inward as the trace of the cut of the screw gradually disappeared inside the specimen. (c): Screw passing through a knot, (d): screw bent due to the annual rings.

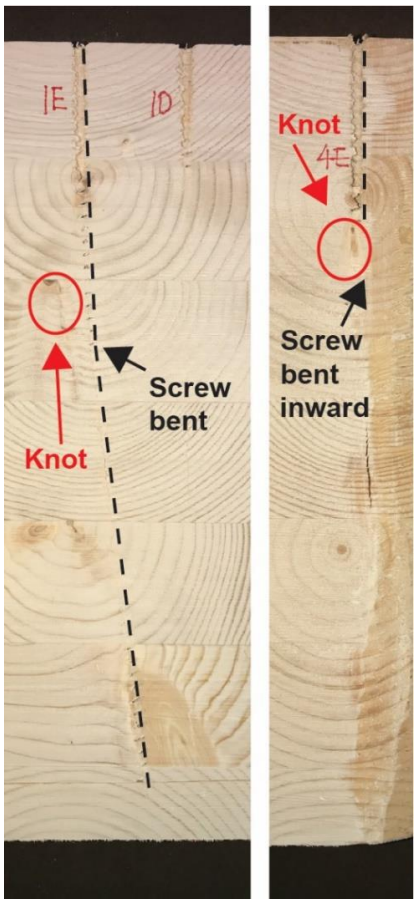

Figure 3-8: Bent of self-tapping screws due to knots.

Table 3-5: Summary of the depths of knots.

Group	A1	B5	C2	C4	G1	G2	G5	
Range of knot depth (mm)	*46-70*	*195-230*	*0-23*	*55-70*	*184-200*	*138-150*	*46-60; 200-210*	
Screw-knot interaction	*Pass through*	*Pass by*	*Pass through*	*Pass through*	*Pass through*	*Pass through*	*Pass through*	
Group	D5	E1	E3	F1	F3	F5	H2	H5
Range of knot depth (mm)	*70-92; 230-270*	*50-60; 230-276*	*276-290*	*180-210*	*23-46*	*0-10; 46-55*	*92-120; 160-184*	*70-92*
Screw-knot interaction	*Pass through*	*Pass through*	*Pass through*	*Pass through*	*Pass through*	*Pass through*	*Pass by*	*Pass through*

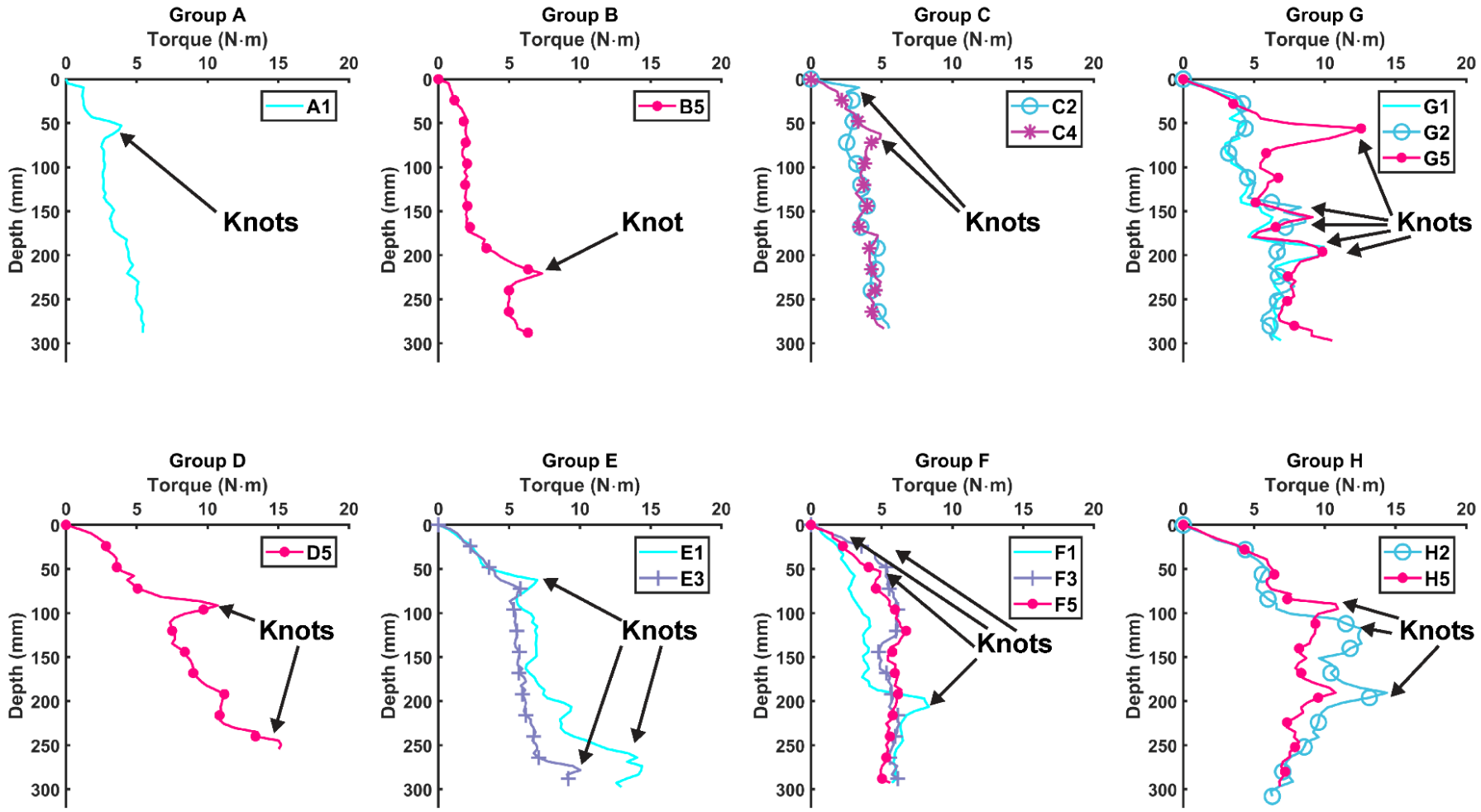

Figure 3-9: Torque-depth relationships for tests that were significantly influenced by knots.

In Table 3-5, if a knot is located near or at the surface of the beam, the corresponding graph will show a rapid increase of the torque with increasing depth; for instance, the curves for tests A1 and C2 in Figure 3-9. Otherwise, the curve will display a surge of torque at the locations of the knot. A good correlation between the knot depth range from Table 3-5 and the change in torque in Figure 3-9 can be found. Furthermore, Table 3-5 also summarises whether the screw passed by or passed through the knot. In Figure 3-9, an increase of torque is shown for both types of interaction. These specimens are therefore excluded from the analysis for better understanding of the influence of screw type, thread configuration and pre-drilled hole.

3.3.2 Results excluding the influence of knots

The depth versus torque results are plotted for the rest of the tests that are not influenced by knots, see Figure 3-10 and Figure 3-11. To fully understand the factors influencing the required torque for installing self-tapping screws, thread configuration, screw point length, reamer and pre-drilled hole depth are presented in the graph by coloured straight lines. The maximum torque for each test is tabulated in Table 3-6.

Table 3-6: Test results after excluding those influenced by knots.

	A	B	C	D	E	F	G	H
1		*5.09*	*5.59*	*10.49*				*9.79*
2	*7.53*	*5.23*		*8.29*	*9.03*	*6.49*		
3	*6.43*	*5.95*	*5.13*	*8.23*			*7.40*	*9.33*
4	*6.59*	*5.73*		*8.39*	*8.55*	*6.07*	*8.19*	*10.05*
5	*8.25*		*5.59*		*8.39*			
Average max torque (N·m)	*7.20*	*5.50*	*5.43*	*8.85*	*8.66*	*6.28*	*7.80*	*9.72*
CoV	*12%*	*7%*	*5%*	*12%*	*4%*	*5%*	*7%*	*4%*

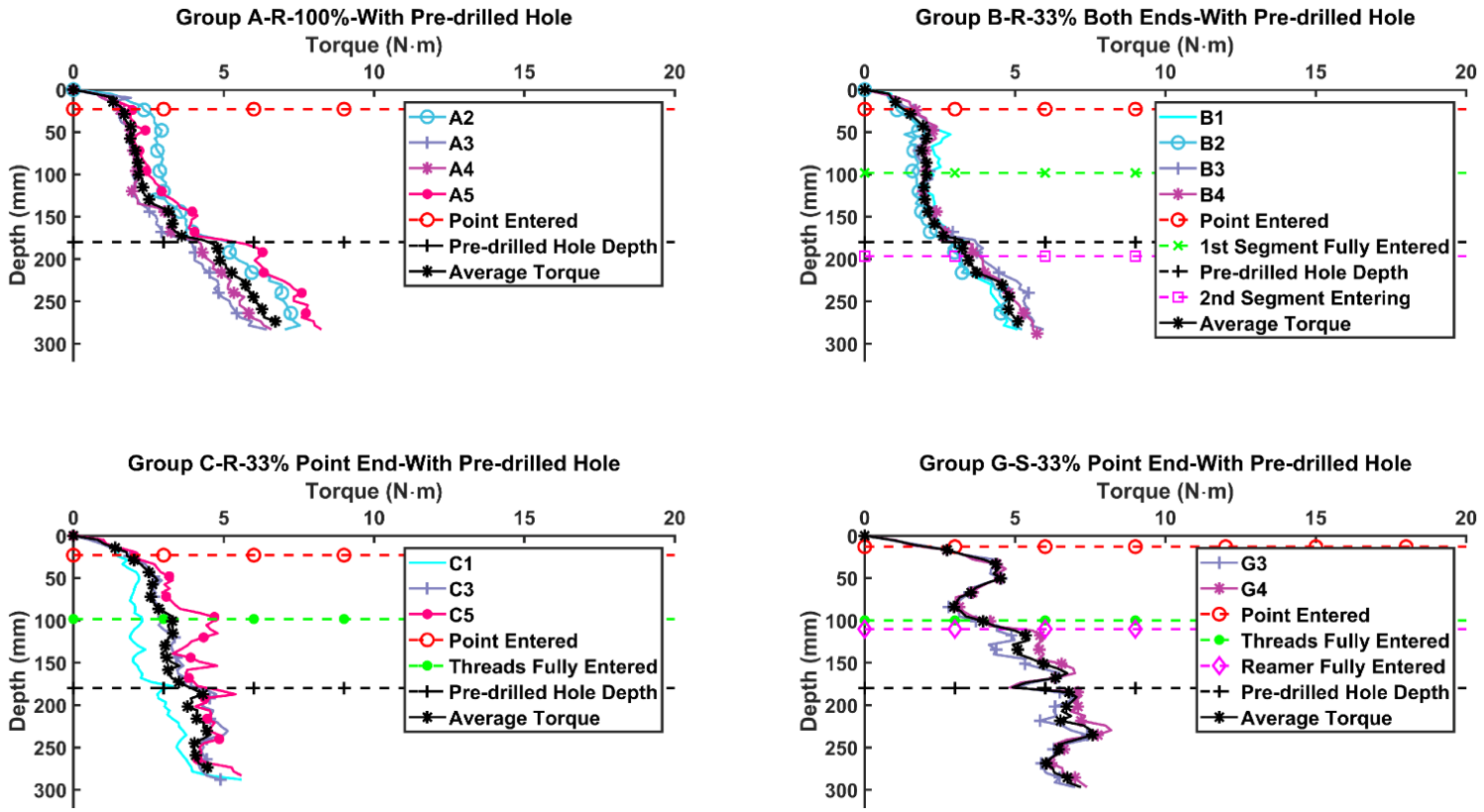

Figure 3-10: Depth versus torque plot for groups with pre-drilled hole (excluding tests significantly influenced by knots).

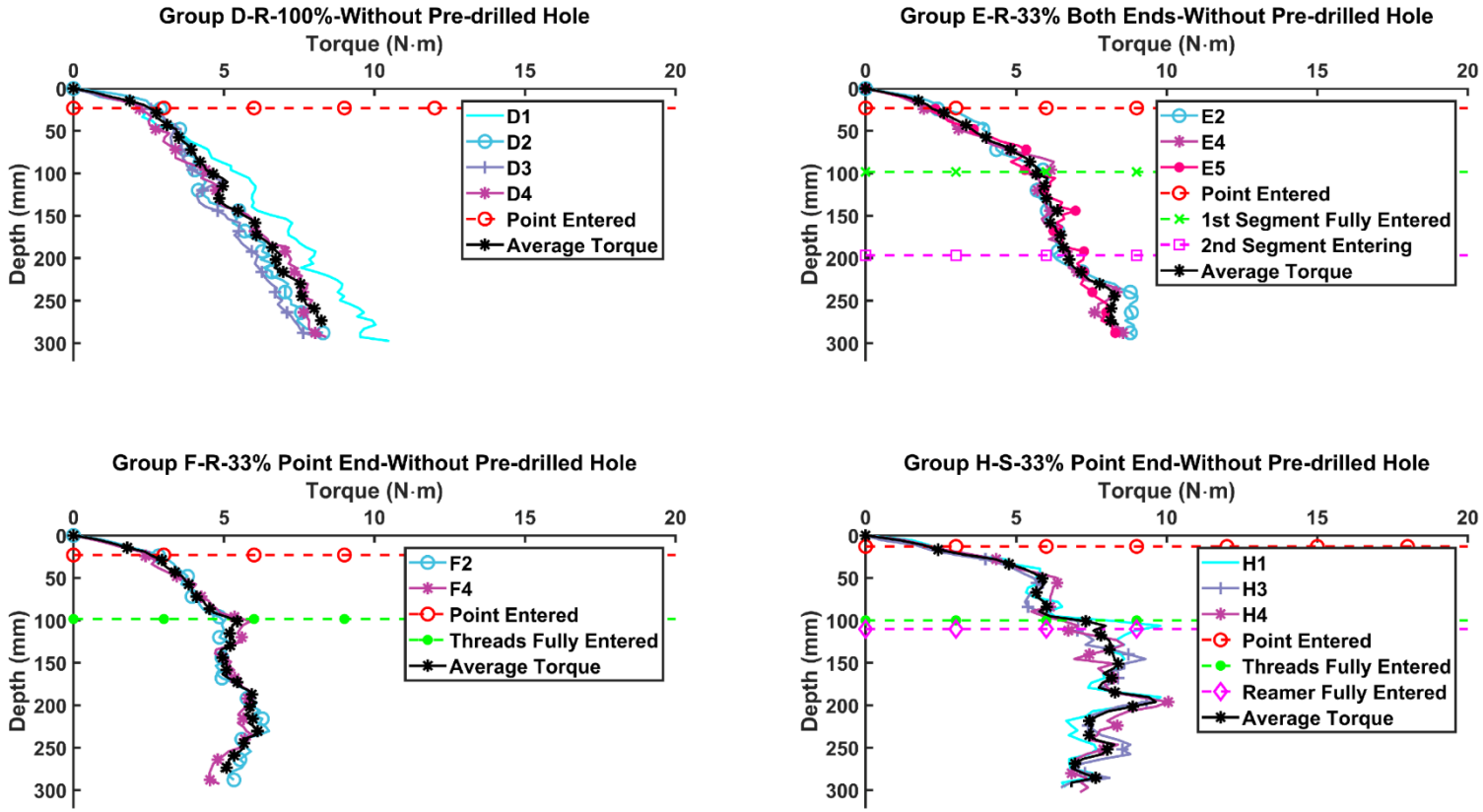

Figure 3-11: Depth versus torque plot for groups without pre-drilled hole (excluding tests significantly influenced by knots).

For the fully threaded Screw R, the torque linearly increased with depth, in both pre-drilled (group A) and without pre-drilled (group D) conditions. The rate of increase was much slower in the 180mm depth pre-drilled hole.

As for Screw R with two thread segments, the increase of torque can also be divided into three parts: entering of the first segment with thread, the middle segment without thread and the second segment with thread. In Figure 3-10 and Figure 3-11, both groups B and E show linear increase of torque for the first 100mm threaded segment, while group B with pre-drilled hole shows a smaller rate of increase. The torque then tends to stabilise with only a small increment as the middle part without thread enters the wood. Finally, the torque rapidly increased as the second segment with thread entered the wood without a pre-drilled hole.

For groups C and F, using Screw R with 33% thread on the point end, the torque linearly increases, with group C showing a smaller rate, as the threaded part first entered the wood. The torque for both groups then tended to stabilise as the polished part started to enter the wood. For group C, the torque slightly increased when the screw reached the end of the pre-drilled hole as more resistance was experienced.

For groups G and H, using Screw S with 33% thread on the point end, the overall trend is identical to that of groups C and F, respectively. However, with a larger size in diameter, the increase of torque is slightly higher as more resistance was experienced when the screw entered the wood. Group G with pre-drilled hole also shows smaller peak torque than that of group H which has no pre-drilled hole.

3.3.3 Comparison between thread configurations

For the groups using Screw R with pre-drilled holes, groups B and C show a stage of stabilisation of torque as the polished shank entered the wood, compared to group A using a fully threaded screw, see Figure 3-10. This difference is also demonstrated on the peak torque. Screw R, with 33% thread on the point end, shows 24.6% reduction in peak torque compared to the fully threaded screw.

In groups without pre-drilled holes, a similar trend is found in the torque-depth curves. The fully threaded screw achieved an average peak torque of 8.85Nm, while the one with two segments achieved 8.66Nm, see Table 3-6. The difference between them is much less in groups with pre-drilled holes. The screw with one segment shows an outstanding result, an average peak torque of only 5.43Nm, 25% of reduction compared to the fully threaded ones.

Results show that the required torque reduces with thread length. In addition, screws with partial thread on the point end achieve the lowest maximum torque, demonstrating its robustness in both with and without pre-drilled hole conditions.

3.3.4 Comparison between conditions with and without pre-drilled holes

In Table 3-6, groups with pre-drilled holes show at least a 13.5% decrease in average maximum torque compared to the corresponding groups without pre-drilled holes (groups C and F). The maximum torque for Screw R with two thread segments is 36.5% lower than those without pre-drilled holes. The results imply that pre-drilled holes are most suitable for screws with 66% thread or more, where at least 18.6% decrease of maximum torque is found.

For Screw S, the difference of maximum torque is similar to that of Screw R; about 20% decrease of peak torque is found in group G with pre-drilled hole.

The impact of pre-drilled holes can also be identified on the torque-depth curves. By comparing the graphs in Figure 3-10 and Figure 3-11, it was found that the influence of a pre-drilled hole is to significantly reduce the increase rate of drive-in torque. The torque is shown to increase drastically when the screw reaches below the depth of the pre-drilled hole.

3.3.5 Comparison between two types of screw

This study used self-tapping screws, R and S, with 33% thread on the point end. As shown in Table 3-1, Screw R is about 14% smaller than Screw S in diameter, while the pitch length for screws R and S are 4.8mm and 5.6mm, respectively. Screw R has a total of 20 complete pitches, 3 more pitches than Screw S with one thread segment. With a finer pitch, the contact area between the wood and screw increases as well as the friction. The penetration depth of Screw R is about 5mm shorter than for Screw S but the difference of depth was not part of the present study.

For both conditions with and without pre-drilled holes, the torque-depth relationships for screws R and S are similar, with Screw S showing higher peak torque than Screw R, 44% and 54%, respectively.

Therefore, even with fewer pitches, Screw S, which is larger in diameter, resulted in a higher maximum torque. This implies that with a smaller difference in pitch counts, the diameter of the screw plays an important role in deciding the drive-in torque.

After the inspection of knots, it was found that Screw R left much deeper and clearer thread cuts on the wood than Screw S, as can be seen in Figure 3-12.

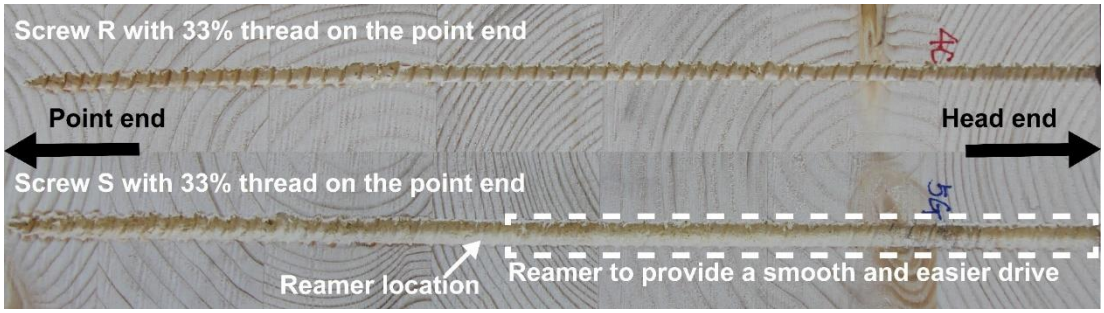

Figure 3-12: Tracks of thread cut of Screws R and S left in the wood.

Screw S shows a shallower cut of the thread on the wood, especially the upper part of the track, than Screw R. One possible explanation is the reamer located 100mm away from the point end of Screw S cleared the passage for the screw shank. According to DeHaitre (1996), the reamer has a larger diameter than the shank and the cutting edges on it will clear the hole for the entrance of the screw shank. Therefore, the track of thread cut in the rectangle area in Figure 3-12 becomes less visible. As for the rest of the part in Screw S, the track of thread cut can be easily identified, but is still less evident than that of Screw R. In Figure 3-13, the double threaded point end on Screw S can cut the wood more than once when the screw spins one turn; thus, leaving a less clear track. The purpose of having the double threaded point is to enable a fast start of installing the screw.

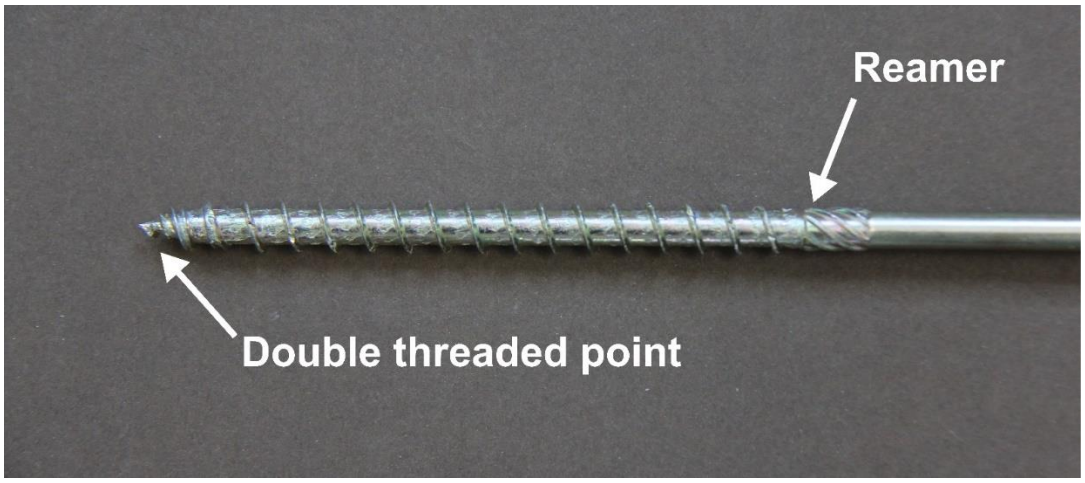

Figure 3-13: Point of Screw S.

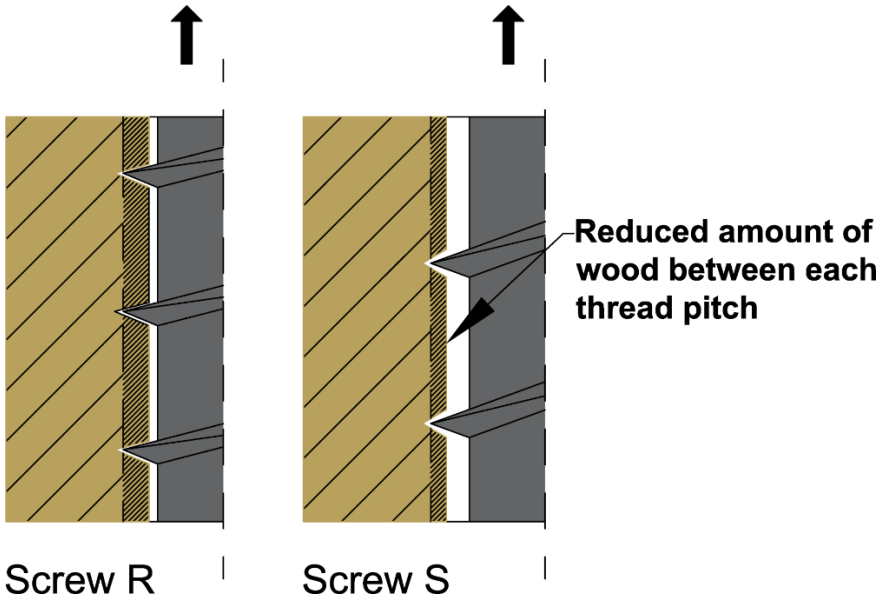

Figure 3-14: Drawing shows the wood-screw interface.

The less obvious track of thread cut for Screw S indicates that the wood in between each thread pitch is reduced, as shown in Figure 3-14. As the withdrawal capacity of the self-tapping screw is determined by shear and the embedment strength of the wood, reducing the shaded part of the wood in and around Screw S can reduce the contact area. This increases the embedding stress and could lead to earlier embedment failure with lower withdrawal capacity of the screw.

3.3.6 Driving self-tapping screws into timber members

The experimental works in Chapter 4 and Chapter 5 demonstrated the use of self-tapping screws as reinforcement on small specimens for embedment and tensile connections tests. With smaller specimens, one may easily identify the knot and avoid installing screws around it. Going by the test results in this chapter, with deeper glulam members, surface inspection cannot ensure the screw completely avoids the area affected by knots; the knots can bend the screw as well as creating a surge of torque, increasing the risks of damaging the screw.

In this study, the use of a pre-drilled hole reduced the maximum driving torque by 13.5%-36.5%. It also prepared an entrance for the self-tapping screw, thus reducing the influence of the knot and reducing the damage to the screw. In addition, the screw can be more accurately driven into position. However, this process is relatively time-consuming in practice. Another method is to use a guide to hold the screw at the exact angle during the driving process. This method can ensure that the screw is initially driven into the correct direction. However, it has no contribution to prevent the increase of drive-in torque when there are knots.

When installing self-tapping screws as reinforcement on connections, preparing pre-drilled holes is a more reliable method than using a guide. An additional benefit of providing pre-drilled holes is to lower the chance of the screw being bent when passing by a knot, see Figure 3-7 (a). When the screws are bent due to the knots, the screws may accidentally pass the prepared hole for the dowels and consequently block the installation of the dowels, especially when the screws are placed at a close distance to the dowels (for instance, at the *1d* distance often used in the tests in later chapters). As discussed in Section 2.2.1, the methods to correctly perform a pre-drilled hole are not specified in EC5. Further investigation on the equipment and methods to ensure a fast and accurate pre-drilling is beneficial to the application of screw reinforcement.

3.4 Summary

This study investigated the relationships between drive-in torque, thread configuration, screw diameter and pre-drilled holes. In total, 40 tests were conducted and the torque to install the screw was measured by a torque analyser. Two types of screws involving three different thread configurations were applied. The required drive-in torque of screws, in conditions with and without pre-drilled holes, was also compared. The torque-depth graphs are plotted and demonstrate how the drive-in torque changes with various parameters, such as pre-drilled hole depth and thread length.

The following points can be concluded:

- A screw passing by or passing through a knot can lead to a surge of torque to drive the screw; inspection of the wood helped to identify which of the tests were affected by knots.
- The required drive-in torque is proportional to the thread length; the screw with 33% thread on the point end achieved the lowest torque which was 75% of the required torque for fully threaded screws in conditions with pre-drilled holes. In groups without pre-drilled holes, the screw with one segment showed an outstanding result, only 71% of the required drive-in torque of fully threaded screws.
- In the pre-drilled hole condition, the screw with two thread segments required slightly higher drive-in torque than the screws with 33% thread on the point end. For the non pre-drilled hole condition, the screw with two thread segments required almost the same amount of drive-in torque of a fully threaded screw.
- From the results, the presence of a pre-drilled hole can significantly reduce the increase of torque. In addition, it is more effective for fully threaded screws and screws with two segments where maximum torque is reduced by at least 18.6%. The

presence of a pre-drilled hole can also ensure that the screw is installed as vertically as possible. About 87% of screws were inclined when installed without pre-drilled holes.

- In pre-drilled and without pre-drilled conditions, Screw S with larger diameter achieved higher maximum torque by 52% and 55% compared to Screw R with the same thread configuration.

In timber construction, adequately reducing the drive-in torque of self-tapping screws not only reduces the risks of damaging the screw but also leads to faster installation. In the future, it will be essential to understand how wood density, screw diameter and pitch length can influence the drive-in torque of self-tapping screws.

Based on the experimental results of this chapter, partially threaded self-tapping screws on the point end ensures easier installation, than fully threaded screws, which is a significant advantage in practice. Therefore, it brings out the research objectives of chapters 4-7, which are to examine the effectiveness of partially threaded self-tapping screws as reinforcement on timber dowel-type connections.

Chapter 4 Single Dowel Embedment Tests with Screw Reinforcement

The majority of the content in Section 4.1 is published in the '*Proceedings of International Network on Timber Engineering Research 2015*'. The content in Section 4.2 has been submitted to the *Journal of Materials in Civil Engineering* and is under review. The content in Section 4.3 has been submitted to the journal of '*Proceedings of the Institution of Civil Engineers – Construction Materials*' and is under review. The content in Section 4.4 has been submitted to the *Proceedings of the Institution of Civil Engineers - Structures and Buildings* and is under review.

This chapter includes a series of experimental studies based on small scale embedment tests. Section 4.1 investigates the relationship between the effectiveness of reinforcement and thread configuration. Section 4.2 focuses on visualising the surface strain distribution of screw-reinforced specimens where various thread configurations and screw to dowel distances are applied. Then, Section 4.3 studies the 'rope effect' in reinforced single dowel specimens and examines its relationship to thread length. The last section (Section 4.4) includes the experimental work on the reinforcement of single dowel specimens with various widths of artificial cracks using self-tapping screws with two different thread lengths.

4.1 Investigation of thread configuration of self-tapping screws as reinforcement for dowel-type connections

4.1.1 Introduction

Dowel-type connections have been widely used in large-scale structures. With the low compressive and tensile strength perpendicular to the grain of the timber member, connections are prone to splitting due to excessive load and moisture induced stresses. Therefore, various methods of reinforcement have been applied to improve the mechanical performance of timber connections.

Studies by Soltis *et al.* (1997) applied GFRP materials onto the timber member of dowel-type connections and significantly improved its load-carrying capacity. Other materials, such

as truss plates, were used to enhance the tensile strength of wood, as demonstrated in Blaß *et al.* (2000).

In recent decades, self-tapping screws have shown the potential to reinforce the timber perpendicular to the grain and prevent splitting of wood around dowels.

Blaß and Schmid (2001) placed screws between fasteners in the connections to enhance the performance and the results have shown significant improvement in ductility. Bejtka and Blaß (2005) and Blaß and Schädle (2011) have further reported that the load-carrying capacity and ductility of the connections were greatly enhanced when the screw was placed in contact with the dowel.

Experimental studies by Lokaj and Klajmonová (2014) on reinforcing round wood connections identified that screw reinforcement has the advantages of simplicity and low cost compared to other forms of metal reinforcement, such as steel plates.

Screw reinforcement can control wood splitting and this ability is governed by the pull-through and withdrawal capacity of the screw. The pull-through capacity is related to the diameter of screw head. The withdrawal capacity is related to the thread length and nominal diameter of the screw. As demonstrated in the previous chapter, fully threaded screws require higher torque during installation. Thus, higher frictional force is produced during the installation process and increases the risk of damaging the screws. Therefore, using self-tapping screws with reduced thread length is more beneficial.

Mastschuch (2000) investigated the influence of screw to dowel distance on the improvement of mechanical performance of connections. The experimental results showed that the screw to dowel distance did not contribute significantly to the enhancement of strength but placing the screw further away from the fastener increased the ductility of the connections.

However, changing thread length and thread location may influence the effectiveness of screw reinforcement, although limited knowledge is available. In addition, there are no design codes which specify the screw to dowel distance when reinforcing timber connections. Therefore, this study aims to understand the influence of thread configuration and screw to dowel distances on the effectiveness of screw reinforcement.

4.1.2 Materials and methods

A series of embedment tests were conducted as embedment strength is an important factor in calculating the load-carrying capacity of connections in Eurocode 5 (EC5 hereafter) (BSI, 2004).

4.1.2.1 Material preparation

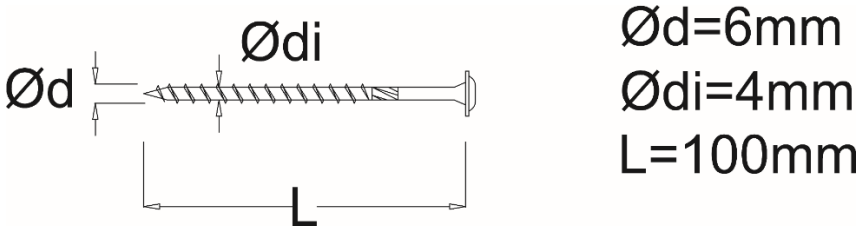

Figure 4-1: Flange head partially threaded self-tapping screw used in this study.

The strength of timber is affected by knots and C24 timber beams have moderate price and less defects than lower grade beams. Therefore, C24 European Whitewood beams were used to prepare the specimens in this study. The beams were stored and prepared at 21.6°C and 59% RH. The specimens have an average density of 456kg/m^3 with an average moisture content of 9.2% (measured by a moisture meter). Details of the self-tapping screws are shown in Figure 4-1. To acquire screws with various thread configurations, part of the thread was removed by a grinder. Figure 4-2 illustrates the original screw and the same type of screw after removing its thread.

Figure 4-2: Original screw (top) and screw without thread (bottom).

4.1.2.2 Embedment test set-up

The test set-up and specimen preparation, as shown in Figure 4-3, followed the European standard, BS EN 383:2007 (BSI, 2007). A 2.5mm diameter pre-drilled hole was drilled at the reinforcement location before the screws were driven in. The embedment tests were performed by DARTEC loading machine with a loading capability of 100kN. The test did not apply two transducers on each side of the specimen to measure the relative displacement of the fastener to the specimen, instead, the displacement of the loading head which was recorded by the data logger, was used. Therefore, the implication of having the steel dowel tilted during the loading stage was not considered in this study.

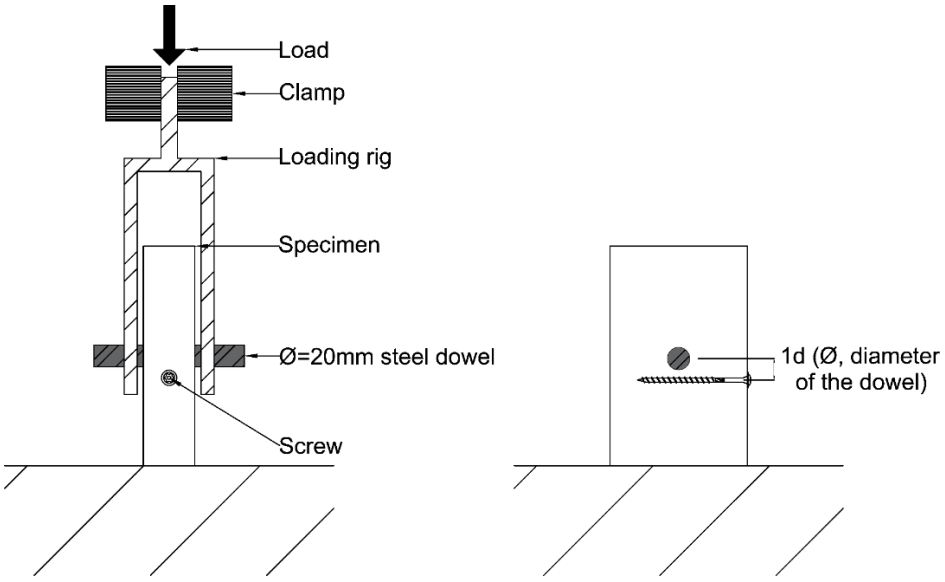

Figure 4-3: Embedment test set-up.

The loading was applied to the specimen parallel to the grain through a 20mm diameter steel dowel and the displacement rate was set to 2mm/min. The loading was stopped after 20% load drop from the peak load had been observed. Table 4-1 summarises the key information for each group in this study and Figure 4-4 demonstrates the thread configurations. This study used 33% and 100% thread on the screws for comparison, a ratio of 1:3 in thread length. The term 100% thread indicate all the thread on the screw was kept but does not indicate the screw is fully threaded. The term 33% thread on point end indicates only 33% of the total length of the threaded part on the screw was kept. The locations of the thread were altered to examine their influence on the performance of screw reinforcement.

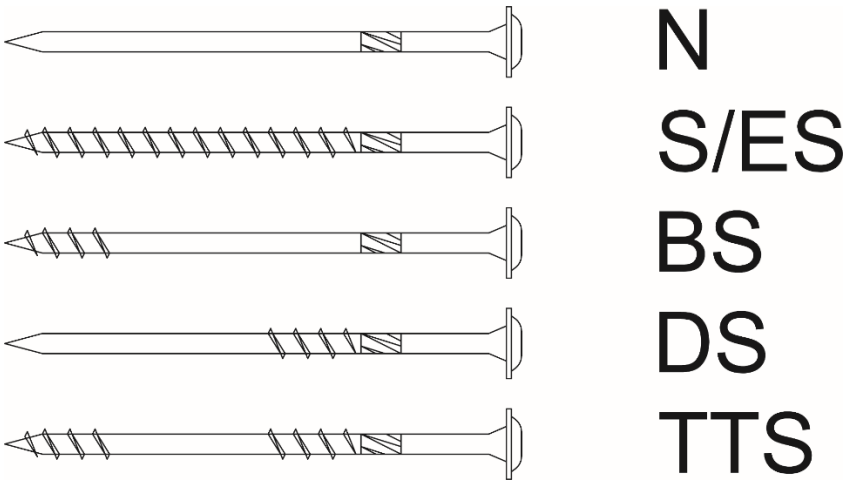

Figure 4-4: Screws with different thread lengths.

Table 4-1: Summary of each group in the embedment test.

Group	Description	Screw to dowel distance	No. of specimens	Mean density (kg/m^3) (CoV)	Mean M.C.% (CoV)
U	*No reinforcement*	*N/A*	*15*	*452 (9%)*	*9.6 (20%)*
N	*0% thread*	*1d*	*15*	*461 (8%)*	*8.6 (21%)*
S	*100% thread*	*1d*	*15*	*453 (6%)*	*8.6 (18%)*
BS	*33% thread on point end*	*1d*	*15*	*459 (5%)*	*9.2 (20%)*
DS	*33% thread on head end*	*1d*	*15*	*456 (9%)*	*9.8 (14%)*
ES	*100% thread*	*0.5d*	*15*	*452 (8%)*	*9.5 (15%)*
TTS	*33% thread on both ends*	*1d*	*15*	*459 (9%)*	*9.3 (18%)*

4.1.3 Results and discussion

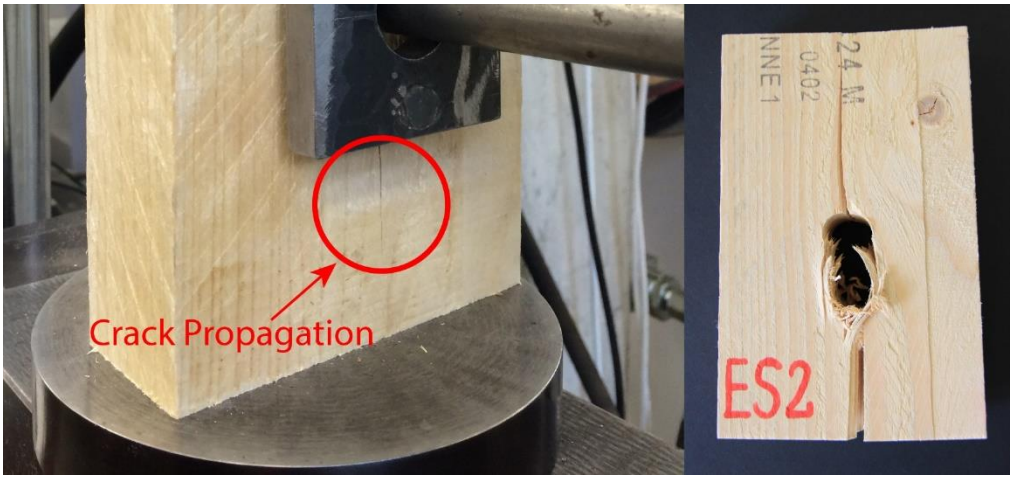

Figure 4-5: Camera captured the crack propagation on the surface of an unreinforced specimen (left) and failed specimen after the embedment test (right).

The splitting failure occurred on all specimens in the embedment tests. In most cases, a crack appearing and propagating below the dowel can be observed, as shown in Figure 4-5 (left). The specimens were cut open to investigate the deformation of the screws. In Figure 4-6 and Figure 4-7, it can be found that screws with partial thread on the point end tend to display a higher deformation together with a noticeable embedment of screw head into the wood.

Figure 4-6: Embedment of screw head: specimens from BS group after test.

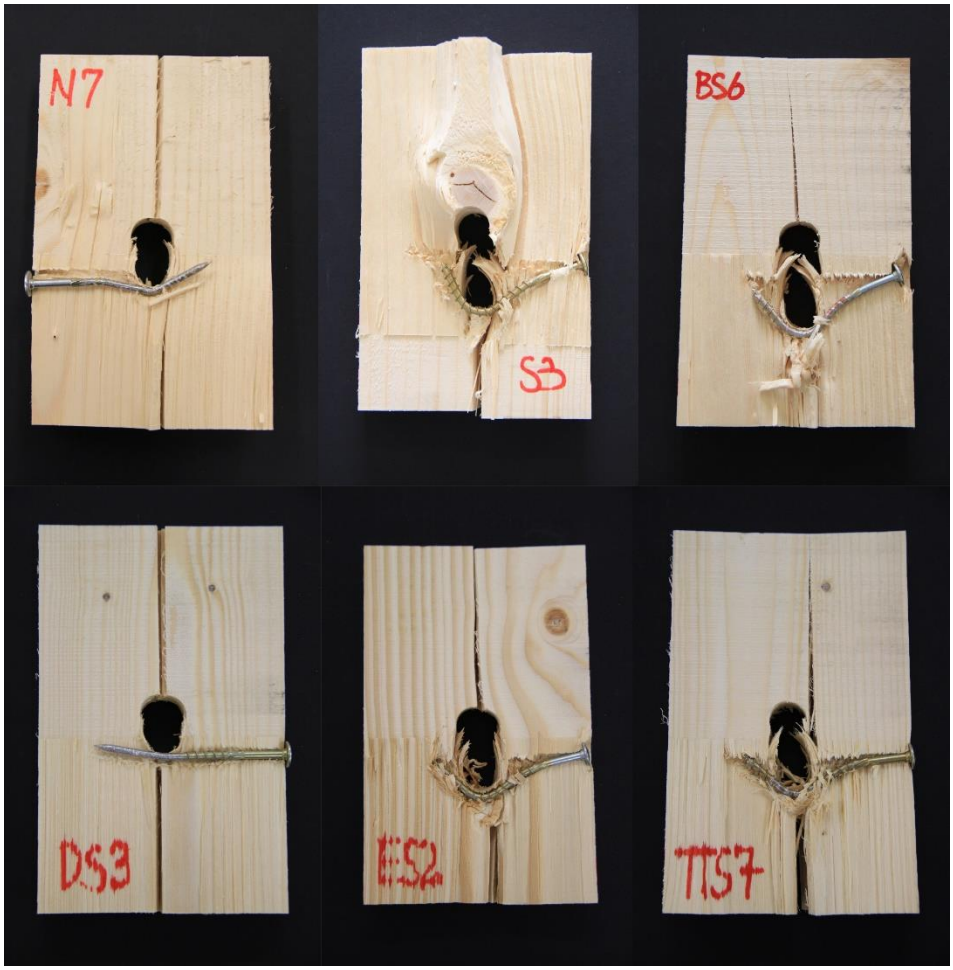

Figure 4-7: Specimens from each reinforced group after embedment test: high level of deformation of screw and embedment of screw head can be seen in groups S, BS, ES and TTS.

Based on test results and observation, reinforcement is effective when restraining forces are present on both ends of the screw. In other words, the thread-wood anchorage at the point end and the pull-through resistance from the screw head can restrain wood splitting. With reduced splitting tendency, the bending strength of the screw can be utilised before the failure of timber, resulting in a higher embedment strength. In contrast, a screw is unable to restrain the propagation of the crack if the thread on the point end is absent and a lower embedment strength can be observed. The mechanism of screw reinforcement is in close relation to the rope effect in dowel-type connections and is discussed in Section 4.3. Figure 4-8 shows the typical load-displacement curves in this study.

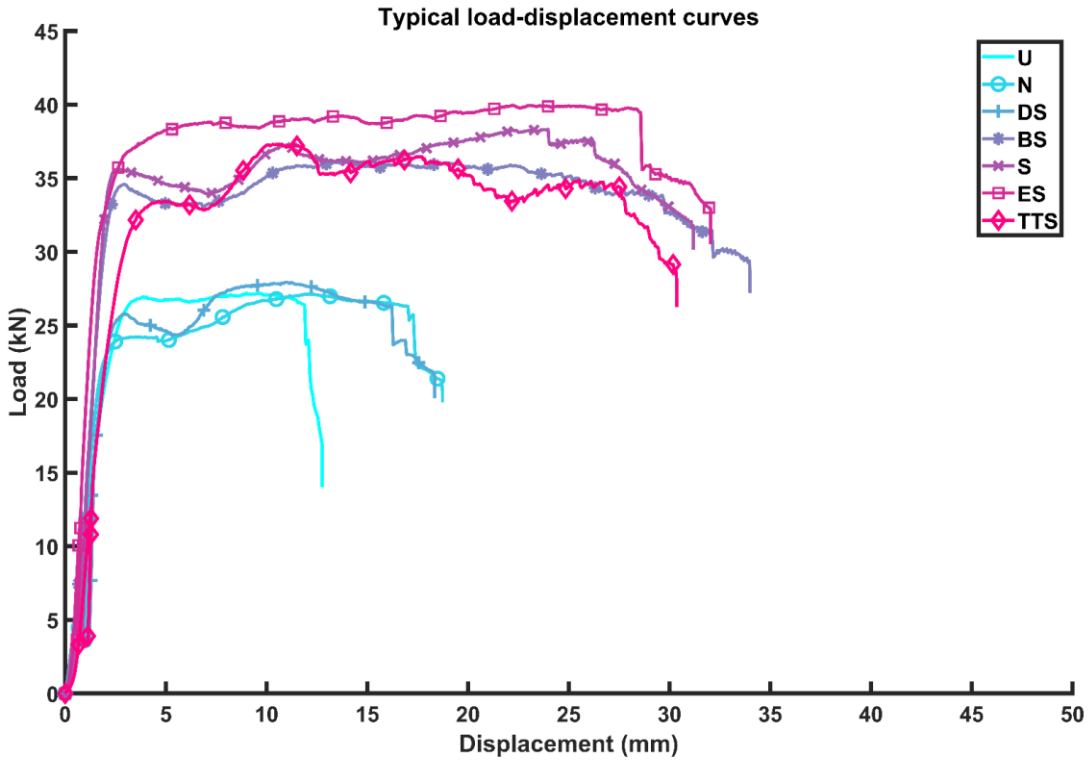

Figure 4-8: Load-displacement curves for embedment test.

This study employs ANCOVA (Analysis of Covariance) to compare the results from different groups. The density of the samples was used as covariance. Table 4-2 presents the adjusted mean value and the enhancement ratio of each reinforced group compared to the unreinforced group.

To identify the difference in effectiveness between each group, ANCOVA pairwise comparison was used to determine whether their difference is significant with the results shown in Table 4-3.

Table 4-2: Results of embedment strength analysed by ANCOVA.

	U	N	S	BS	DS	ES	TTS
Mean embedment strength adjusted by ANCOVA (N/mm^2)	*31.05*	*32.15*	*35.60*	*35.48*	*32.22*	*37.53*	*35.31*
Enhancement ratio	*1.00*	*1.04*	*1.15*	*1.14*	*1.03*	*1.21*	*1.17*

Comparison between groups S and N showed that specimens reinforced by screws with 100% thread achieved significantly higher embedment strength than those reinforced by screws with 0% thread. It shows the effectiveness of a nail as reinforcement is limited and the importance of having thread on the screw.

In groups BS and DS, with the same 33% thread but at different locations (see Figure 4-4), the mean embedment strength of group BS with partial thread on the point end is significantly higher than that of the group DS. The results indicate that the thread on the point end is more effective. This can be explained by having 33% thread and screw head on the both sides of the crack. The screw was able to restrain crack propagation using the withdrawal capacity from the point end and the pull-through resistance from the screw head. Unlike the specimens in group DS, the specimens in group BS had not yet failed when the dowel was bearing on the screw, thus, the bending strength of the screw can be utilised, and a higher embedment strength was achieved.

In addition, the group BS has significantly higher embedment strength than that of the unreinforced group while the group DS shows no significant improvement to the unreinforced group. It again confirms that, to control crack propagation, restraints on both sides of the crack are required. Thus, the group DS cannot utilise the bending strength of the screw to improve the embedment strength, as most of the specimens had failed before the dowels started to bearing on the screw.

As for group TTS using screws with 33% thread on both ends, Table 4-3 shows it has no significant difference to group BS and a significant difference to group DS on embedment strength. It again proves the importance of thread location to the effectiveness of screw reinforcement.

With the screw placed closer to the dowel, group ES showed a higher mean embedment strength than group S, but the difference between them was not significant. With the dowels being placed in contact with the screws, it is presumed that crack initiation was delayed as a restraining force was available as soon as the dowels were loaded.

Table 4-3: Significance of ANCOVA pairwise comparison for embedment test (groups U, N, S, BS, DS, ES and TTS).

	U	N	S	BS	DS	ES	TTS
U							
N	*0.481*						
S	*0.004**	*0.028**					
BS	*0.005**	*0.034**	*0.935*				
DS	*0.452*	*0.963*	*0.031**	*0.038**			
ES	*0.000**	*0.001**	*0.216*	*0.188*	*0.001**		
TTS	*0.001**	*0.009**	*0.652*	*0.594*	*0.010**	*0.431*	

**Sig < 0.05 indicates a significant difference between the two groups.*

Ductility is an important factor in timber connection design. A ductile structure is preferable, as it can provide visual warnings of large deformations before a failure occurs. In seismically active areas, a ductile timber connection can dissipate more energy during the earthquake in order to reduce the damage to the structure.

Ductility from the embedment test is calculated using two methods: the one shown in BS EN12512 (BSI, 2002) and the K&C method proposed by Karacabeyli and Ceccotti (Karacabeyli and Ceccotti, 1996).

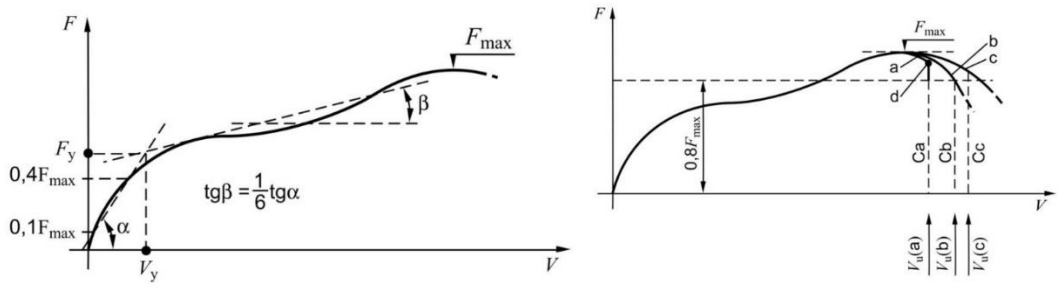

Figure 4-9: Determination of ductility proposed by EN 12512 (BSI, 2002). Determination of the yield point V_y (left) and possible locations of ultimate values V_u (right). V_u(a) is the displacement at failure, V_u(b) is the displacement at 0.8F_{max} and V_u(c) is the displacement equal to 30mm.

Based on EN12512 (BSI, 2002), the ductility of the timber specimens is calculated as follows:

$$D_u = \frac{V_u(b)}{V_y} \qquad (4\text{-}1)$$

where:

D_u is the ductility of the specimen;

$V_u(a)$ is the displacement at failure;

$V_u(b)$ is the displacement at the 80% maximum load as shown in Figure 4-9;

$V_u(c)$ is the displacement equal to 30mm;

V_y is the yield point.

.

Table 4-4: Average ductility of each group calculated by two methods.

Group	U	N	S	BS	DS	ES	TTS
Mean ductility given by EN 12512 method (CoV)	*8.1 (48%)*	*15.4 (52%)*	*21.4 (49%)*	*22.4 (42%)*	*9.4 (45%)*	*19.3 (54%)*	*11.5 (49%)*
Mean ductility given by K&C method (CoV)	*12.2 (47%)*	*24.6 (55%)*	*32.0 (48%)*	*34.8 (42%)*	*14.8 (43%)*	*26.6 (49%)*	*15.6 (37%)*

Table 4-4 summarises the average ductility of each tested group. As can be seen, the unreinforced specimens had the lowest ductility. Groups N and DS had lower average ductility than that of groups S, BS and ES. The screws in groups N and DS lack the ability to restrain crack propagation under loading and hence the single dowel connections demonstrated a less ductile behaviour in test. The method given by the Eurocode shows a more conservative value than the K&C method which uses $0.5F_{max}$ to define the location of the yield point.

4.1.4 Summary

The embedment tests showed that thread configuration can influence the effectiveness of self-tapping screws as reinforcement. Embedment strength and ductility can be significantly improved when the screw is able to provide a restraining force on both sides of the crack by having the screw head on one end and a threaded part on the other end. Statistical methods cannot identify the significant influence of screw to dowel distance, though a higher average embedment strength was achieved by placing the screws in contact with the dowel.

To understand how screw reinforcement can influence the mechanical properties of timber, DIC was used to visualise the strain distribution on the surface of the specimens in the next section.

4.2 Strain distribution of self-tapping screw-reinforced dowel-type connections

4.2.1 Introduction

Earlies studies by Blaß and Schmid (2001), Bejtka and Blaß (2005) and Blaß and Schädle (2011) showed that the mechanical performance of dowel-type connections could be enhanced with fully threaded self-tapping screws that can effectively control the splitting of timber.

As the drive-in torque of screws is related to the thread length, fully threaded screws require higher drive-in toques and the risk of causing damage to the screw increases, especially when they are applied on members with large sizes or high density (e.g. members made of hardwood). The works in Chapter 4 and Chapter 5 have found that partially threaded screws achieved similar reinforcement performance to fully threaded screws. The thread length on partially threaded screws is less than fully threaded screws, ensuring an easy installation.

Due to the geometry of the dowel, the surrounding wood around the dowel is subject to tensile stresses perpendicular to the grain. Since wood has poor tensile strength in this direction, excessive stresses tend to split the timber member from the area that is loaded by the dowel. Surface strain around the crack can escalate as the tensile stress increases. With the application of screw reinforcement, resistance against splitting can be achieved and the propagation of the crack can be controlled. Therefore, it is of interest to visualise the strain distribution on the surface of reinforced specimens. In this study, it is achieved by single dowel embedment tests combined with DIC technique.

The primary research objective of this study is to investigate the influence of thread configuration and screw to dowel distance on the surface strain distribution.

The secondary objective is to understand the influence of design parameters on the accuracy of mapping the strain distribution. As DIC methods can only display the strain distribution on the specimen's surface rather than the cross section where the reinforced screw is placed, the influence of the thickness of specimen should be investigated. In addition, larger diameter of dowels may increase the splitting tendency which is related to the effective number n_{ef} for calculating the load-carrying capacity of timber connections. Therefore, tests for the above two factors were carried out prior to the primary objective in this experiment. Knowledge gained from these tests provided guidance for the primary experiments.

4.2.2 Materials and methods

The timber specimens were prepared from multiple batches of European Whitewood graded to C24. The timber beams were stored and prepared at 21.6°C and 59% RH. They had an average density of 431kg/m^3 (CoV = 10.1%) and an average moisture content (measured by a moisture meter) of 7.8% (CoV=17.4%).

The configuration of the original screw is shown in Figure 4-10. A grinder was used to polish the threaded part of the screw in order to prepare different thread configurations (33% and 100% thread, a ratio of approximately 1:3 as used in Chapter 3 and Section 4.1). This ensured the consistency of material properties of the screws. A 2.5mm diameter pre-drilled hole with 60mm depth was drilled at the location of reinforcement to ensure the accurate positioning of the screw.

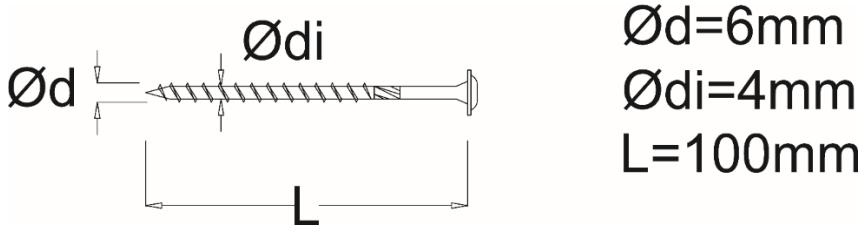

Figure 4-10: Configuration of the self-tapping screws used in this study.

4.2.2.1 DIC principle

DIC is a non-contact optical method to calculate the displacement and strain on a specimen surface through analysing a series of digital images taken during the mechanical test. It requires a picture of the unloaded specimen as reference and pictures during the loading stage as deformed images. A speckle pattern is applied on the specimen surface and is subject to deformation during the loading stage. The deformation of patterns is compared to their initial unloaded image by DIC software which then uses a mathematical correlation to find and generate the strain distribution for each deformed image.

The resolution of a digital image represents the number of pixels it is divided into. Each pixel contains a grey scale value varying from 0 to 255, based on the light intensity reflected by the object on the picture. The DIC method uses this property to locate a pixel on the deformed image by using its grey value from the non-deformed image. However, the grey value of a single pixel is not unique in the entire picture. Thus, a collection of grey values of surrounding pixels is introduced. In DIC, this is called a ‘subset’ or ‘correlation window’. Then, to track a subset in another deformed picture as the tested body moves, the subset is shifted around. The ‘stepsize’ defines the distance (in pixel) a subset is moved when finding

the best match in another picture. The best match is found based on results of a correlation function of total difference in grey values of each pixel within the subset. Finally, the software can determine the displacements and is then able to calculate the strain values for each pixel.

To ensure the matching is accurate, a random, isotropic and high-contrast speckle pattern on the surface is preferred. According to Lionello and Cristofolini (2014), at least three speckle patterns should be included in one subset. Currently, there are a large number of methods to apply the pattern on the specimen, such as paint guns, spray cans and stencils. Salmanpour and Mojsilovic (2013) applied the above methods and recommended using a paint gun to generate a fine, random pattern. Lionello and Cristofolini (2014) investigated the impact of airflow and spraying distance when using an airbrush gun and used it to generate high quality speckle patterns.

4.2.2.2 DIC preparation

In this study, the timber specimens were planed to ensure that curvature on their surface was eliminated. A background using matt white paint and speckle patterns using matt black paint was applied to form a high-contrast speckle pattern so as to avoid false correlation.

The method used to paint the patterns on the surface of the specimen was the same as stencilling. The speckle pattern was designed and applied to the 2mm thick cardboard using a laser cutter, as shown in Figure 4-11. By selecting the appropriate cutting speed and output power, the laser beam leaves openings in the cardboard. It was found that a small and intense pattern makes the cardboard too fragile to use and it broke easily during cutting. Another issue was that small openings made it difficult for the paint to pass through, leaving large blanks on the specimens as a result. Therefore, the size of the pattern and the spacing between each pattern was adjusted to an acceptable range. The adjusted pattern was successfully identified by the DIC software in the trial tests. To ensure the quality of the speckle pattern on the specimen, cardboard stencils were discarded after a few uses, as the black matt paint tended to stick on the surface of the cardboard and blocked the openings, reducing the quality of the pattern. As the area of interest is located on the lower half of the specimen, the speckle pattern did not cover its whole surface, see Figure 4-12.

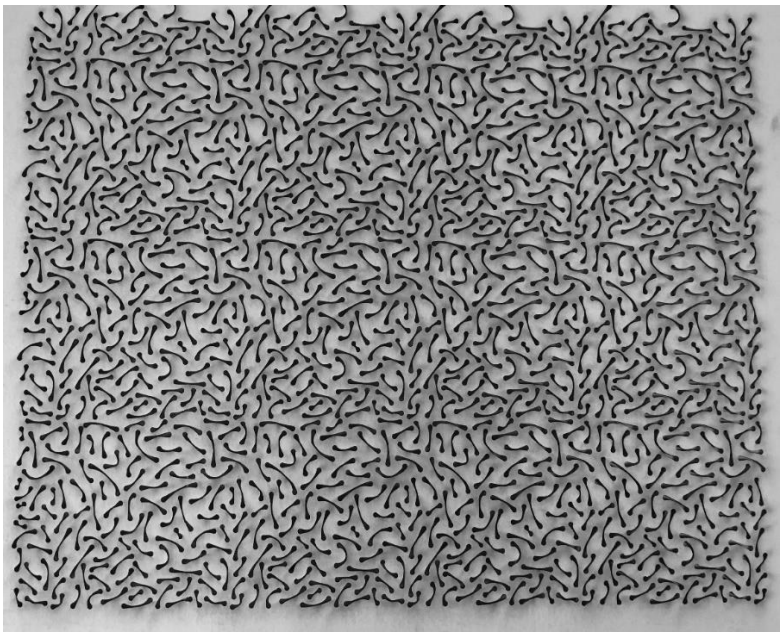

Figure 4-11: Laser cutter prepared patterns on a cardboard.

4.2.2.3 Embedment test set-up

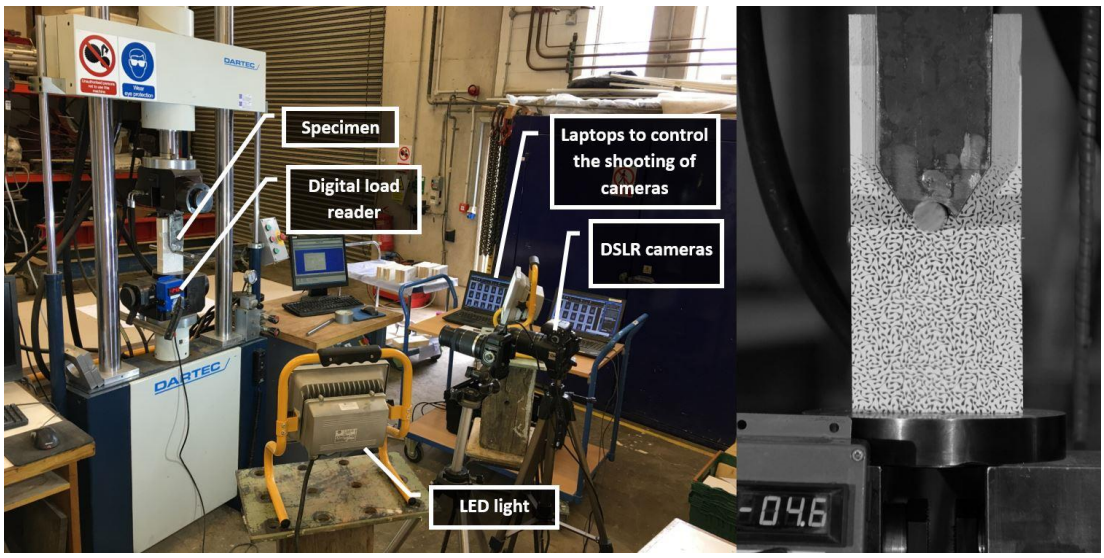

Figure 4-12: Test configurations (left) and a picture of a specimen in black and white for DIC analysis (right).

The embedment test followed the procedure given in BS EN 383:2007 (BSI, 2007) and the test configuration was demonstrated in Figure 4-12 (left). The load was applied to the specimen parallel to the grain through a steel dowel and the displacement rate was set to 2mm/min. The loading was manually stopped when 20% load drop from the peak load was observed. To allow comparison of strain fields among specimens under similar loading, a load display was placed next to the specimen and its readings were captured in the picture, as shown in Figure 4-12 (right). A DARTEC loading machine (100kN capacity) was used to

perform the tests. The displacement of the loading head was used as the relative displacement of the fastener to the specimen assuming no tilting or bending of the steel dowel. The errors due to the fastener tilting or bending were ignored.

Images were taken with an 18MP Canon 60D DSLR camera using 18-200mm lens. The camera was placed towards the patterned face of the specimen. A laptop was connected to the camera to control the shutter so as to capture the images. In addition, a second camera was used to record the test. Two LED working lights were placed at symmetrical positions next to the cameras to provide sufficient light. The images for DIC used the highest resolution settings on the camera (5184 pixels × 3456 pixels). After the test, the original coloured pictures were converted to black and white format and then analysed by DIC software. The details of each group are described in Table 4-5 and the tests are separated into two stages: Stage 1 involves testing different diameters of dowels and thicknesses of specimen, while Stage 2 comprises testing different thread configurations and screw to dowel distances. Figure 4-13 demonstrates the specimen configurations. 16mm and 20mm dowels are commonly used in practice and therefore they were chosen for the test. The screws applied as reinforcement with 33% and 100% thread length in Section 4.1 were used in this study to ensure consistency in material properties.

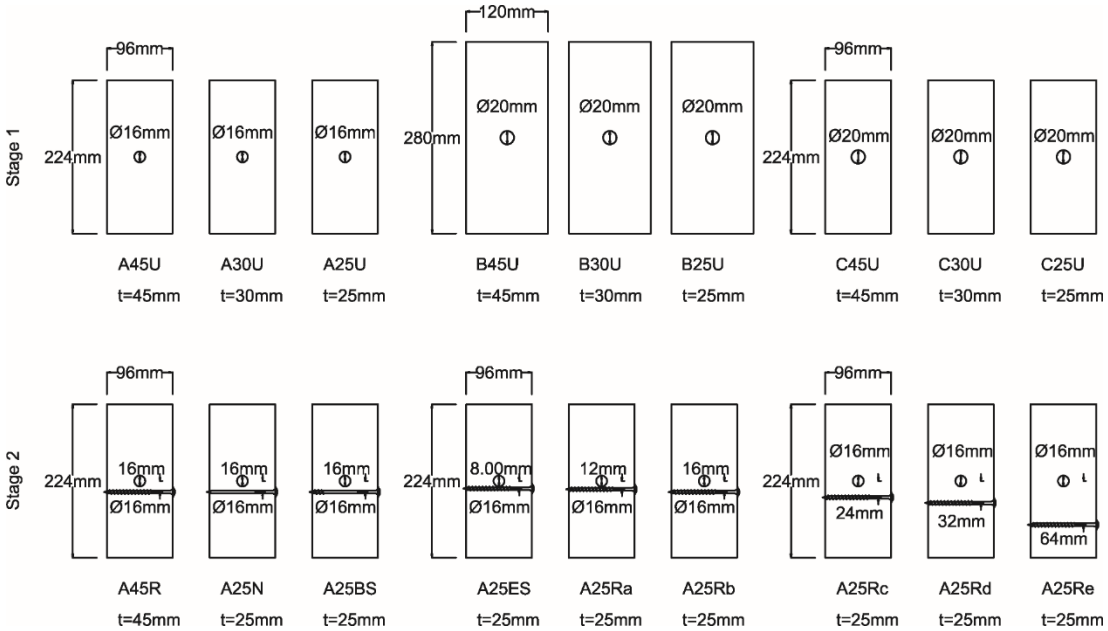

Figure 4-13: Specimen configurations of the two stages.

Table 4-5: Summary of tested group details.

	Group	Dowel diameter (mm)	Specimen size (mm)	Sample size	Description		Mean density (kg/m^3) (CoV)	Mean M.C.% (CoV)
					Reinforcement	Screw to dowel distance *		
Stage 1	A45U	16	224×96×45	3	No reinforcement		434 (10.0%)	7.7 (18.9%)
	A30U		224×96×30	3			422 (15.3%)	8.0 (11.2%)
	A25U		224×96×25	3			405 (13.7%)	9.3 (20.3%)
	B45U	20	280×120×45	3			432 (10.4%)	8.5 (19.1%)
	B30U		280×120×30	3			501 (19.7%)	9.5 (8.1%)
	B25U		280×120×25	3			427 (17.4%)	9.0 (12.6%)
	C45U	20	224×96×45	3			420 (15.5%)	8.4 (12.7%)
	C30U		224×96×30	3			442 (19.0%)	8.1 (4.4%)
	C25U		224×96×25	3			418 (16.4%)	9.8 (19.3%)
Stage 2	A45R	16	224×96×45	3	Complete thread	1d	410 (15.0%)	8.0 (17.7%)
	A25N		224×96×25	6	0% thread	1d	437 (7.4%)	6.3 (2.5%)
	A25BS			3	33% thread on the point end	1d	442 (1.0%)	9.6 (3.3%)
	A25ES			6	Complete thread	0.5d	418 (3.7%)	7.0 (2.6%)
	A25Ra			6		0.75d	438 (7.6%)	6.8 (6.7%)
	A25Rb			7		1d	419 (3.8%)	7.1 (1.8%)
	A25Rc			10		1.5d	430 (5.3%)	7.8 (13.7%)
	A25Rd			3		2d	433 (9.0%)	6.4 (4.0%)
	A25Re			3		4d	435 (9.1%)	6.3 (4.2%)

** d is the diameter of the dowel.*

4.2.3 Results

In the test, all the specimens displayed splitting failure and embedment failure. Screw head embedment was observed in the reinforced groups. Table 4-6 summarises the mechanical properties for each group and the calculation of ductility followed the method described in EN12512 (BSI, 2002). The stiffness of each specimen was found through calculating the gradient between $0.1F_{max}$ and $0.4F_{max}$ on the load-displacement curve.

Table 4-6: Mechanical properties for each tested group.

	Group	Mean strength (N/mm^2)/ (CoV)	Mean ductility / (CoV) EN12512 method	Mean stiffness (kN/mm) / (CoV)
Stage 1	A45U	*22.6/ (19.6%)*	*4.4/ (72.5%)*	*10.0/ (20.0%)*
	A30U	*24.4/ (27.8%)*	*4.7/ (33.9%)*	*9.4/ (28.0%)*
	A25U	*19.4/ (20.9%)*	*6.7/ (69.0%)*	*7.7/ (36.5%)*
	B45U	*23.4/ (12.0%)*	*3.1/ (61.0%)*	*13.6/ (15.5%)*
	B30U	*20.7/ (31.7%)*	*6.5/ (53.9%)*	*11.2/ (55.7%)*
	B25U	*19.8/ (16.1%)*	*4.8/ (60.3%)*	*10.5/ (34.9%)*
	C45U	*22.9/ (4.8%)*	*2.2/ (53.1%)*	*10.7/ (40.1%)*
	C30U	*19.4/ (18.1%)*	*3.6/ (19.5%)*	*11.0/ (36.0%)*
	C25U	*20.1/ (16.6%)*	*6.0/ (47.2%)*	*10.6/ (42.1%)*
Stage 2	A45R	*33.0/ (16.7%)*	*15.6/ (4.4%)*	*8.9/ (18.3%)*
	A25N	*31.3/ (20.2%)*	*7.0/ (61.5%)*	*6.2/ (36.4%)*
	A25BS	*35.2/ (4.6%)*	*21.9/ (12.6%)*	*5.4/ (21.3%)*
	A25ES	*40.3/ (6.3%)*	*23.3/ (21.3%)*	*8.3/ (11.9%)*
	A25Ra	*42.1/ (10.5%)*	*26.0/ (36.8%)*	*9.2/ (14.5%)*
	A25Rb	*39.1/ (8.6%)*	*34.4/ (26.0%)*	*9.8/ (35.6%)*
	A25Rc	*38.5/ (9.7%)*	*30.0/ (21.2%)*	*10.3/ (17.3%)*
	A25Rd	*39.5/ (4.9%)*	*24.1/ (42.4%)*	*9.1/ (46.4%)*
	A25Re	*32.2/ (12.3%)*	*14.7/ (36.1%)*	*7.8/ (17.7%)*

In Stage 1, the unreinforced specimens in configurations *A* and *B* achieved similar mean embedment strength and stiffness even though the thickness of them varies from 25mm to 45mm. The embedment strength of configuration *C* was slightly lower than that of configurations *A* and *B*.

The load-displacement curves in Figure 4-14 shows a less ductile behaviour for the unreinforced specimens in all three configurations. However, the mean ductility of configurations *A* and *B* had similar values and were slightly higher than the value of configuration *C*. This result matched the prediction, as the design of configurations *A* and *B* satisfied the minimum spacing specification given in EC5 (BSI, 2004), while configuration *C* had a larger dowel fitted into the same size of wood as configuration *A*. As a result, using dowels with larger diameter increased the splitting tendency of the wood and led to lower embedment strength. The specimens labelled the third one in each group showed a lower strength but a more ductile failure. One possible explanation is that all of these specimens were prepared from the same timber beam which had lower density but less knots in it than the other timber beams that were used to prepare the first and second specimens.

In Stage 2, with the same thickness, the strength and ductility of reinforced group A45R were significantly higher than the unreinforced group A45U. As for the 25mm thick specimens, the unreinforced group A25U gave the lowest value in strength and ductility. The group A25N, which had a so-called ‘nail’ reinforcement, showed higher strength than A25U but similar low ductility to that of group A25U. The improvement in strength indicated that the dowel had touched the screw, a much stronger material than wood. However, as the screw in group A25N had 0% thread on its shank, very low resistance can be provided to control timber splitting. Therefore, the specimens in group A25N had less ductile failures than those specimens reinforced by screws with thread on point end.

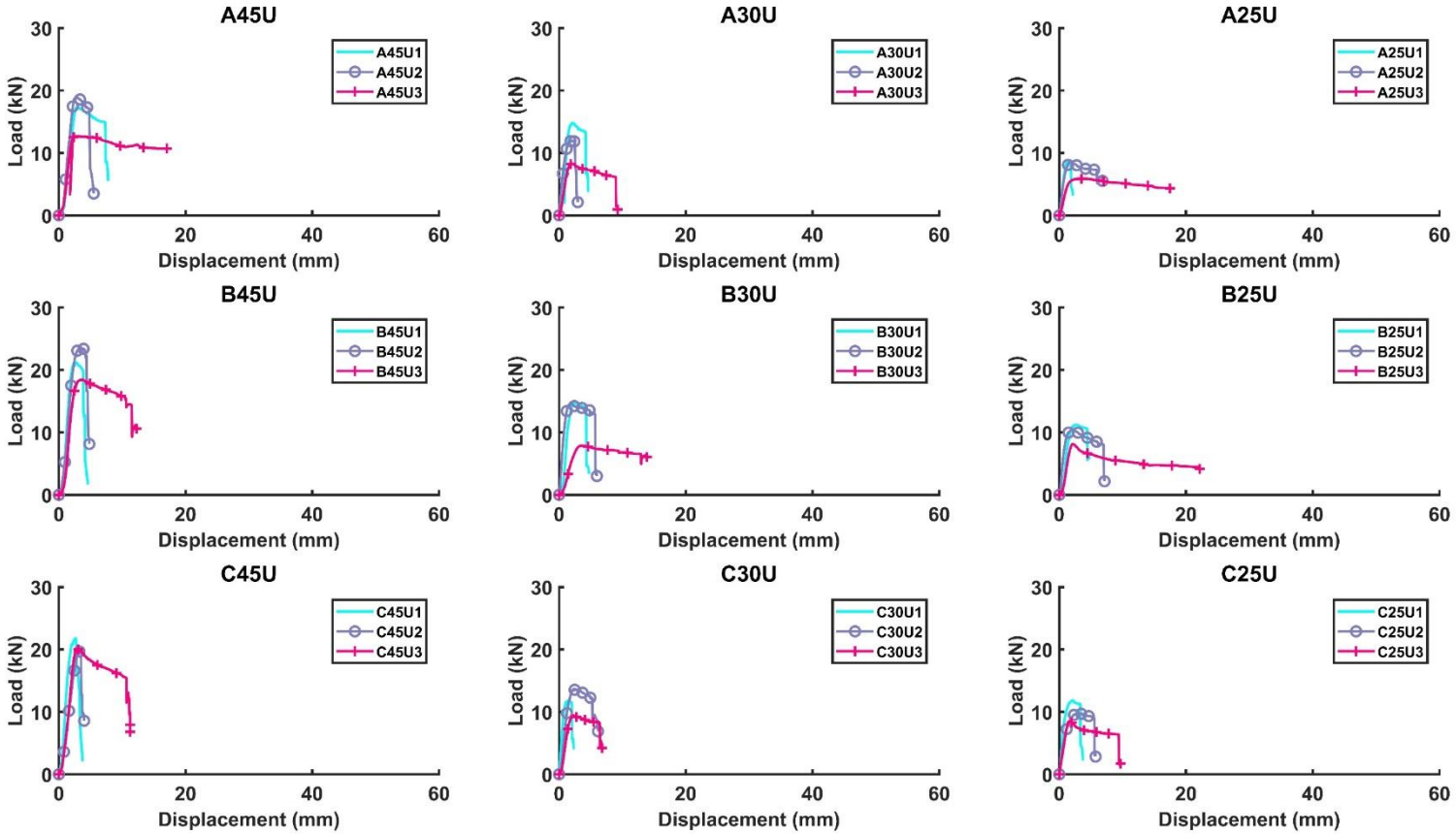

Figure 4-14: Load-displacement curves in Stage 1.

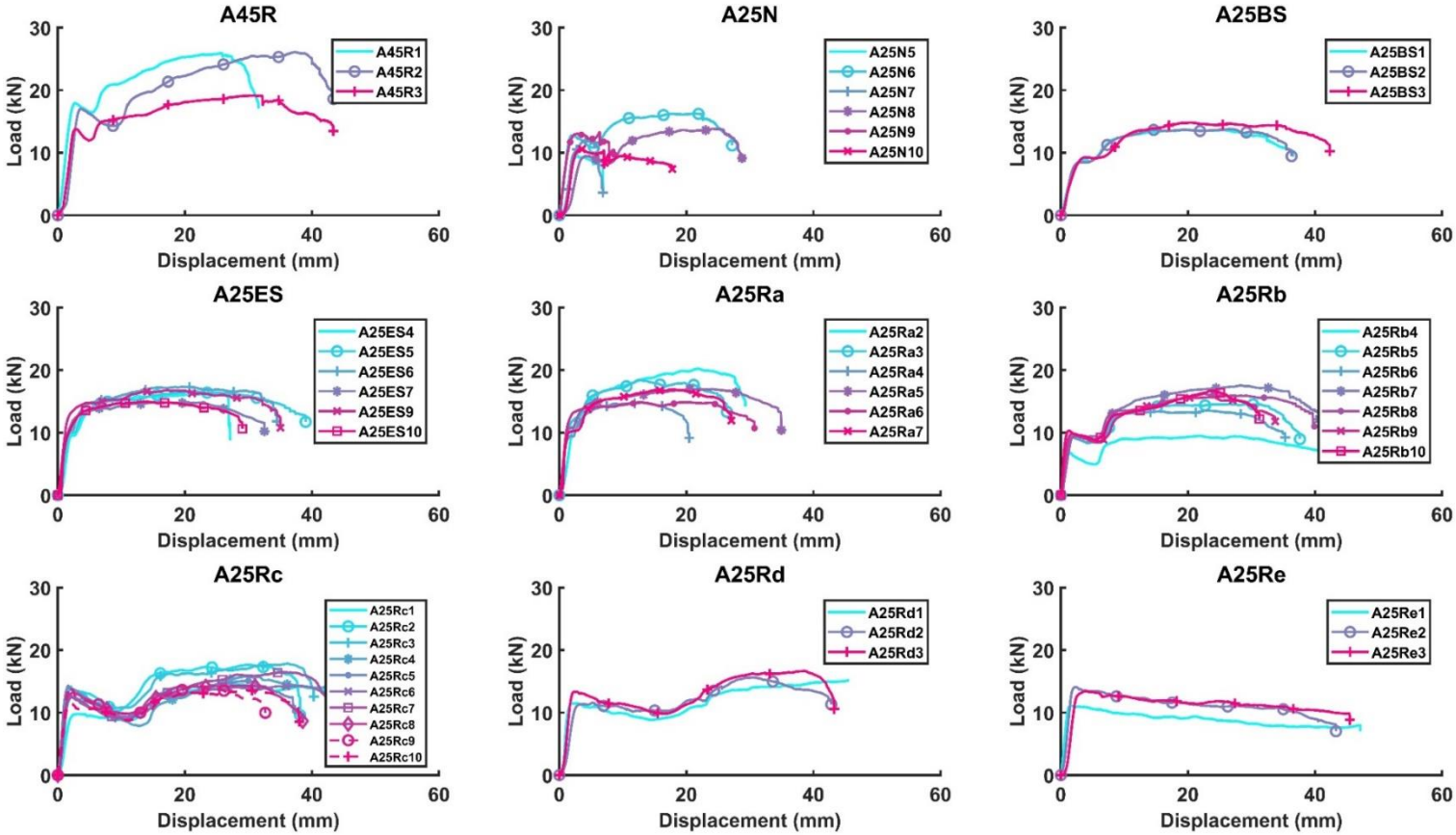

Figure 4-15: Load-displacement curves in Stage 2.

As for group A25BS reinforced by screws with 33% thread on the point end, its mean embedment strength and ductility were approximately 1.8 times and 3 times higher than that of the unreinforced group, respectively. Compared to group A25Rb using screws with complete thread placed at *1d* distance to the dowel, group A25BS showed lower strength and ductility but the difference is not significant.

The last section of Table 4-6 compares the mechanical properties of specimens reinforced by the screw with same thread configuration but placed at different distances to the fastener. All the groups achieved higher mean embedment strength and ductility than the unreinforced group A25U. Embedment strength peaked at 42.1N/mm^2 when the screw was placed at *0.75d*, and ductility peaked at 34.4 when the screw was placed at *1d*. The values gradually reduced as the screws were placed further away from the dowel. From Table 4-6, the reinforcements were highly efficient even if the screws were placed at *2d* distance and, as can be seen in Figure 4-15. The group A25Rd (screws placed at *2d* distance) showed a significant improvement of load-carrying capacity starting from 20mm displacement and achieved considerable ductility. As for group A25Re (screws placed at *4d* distance), it achieved similar improvement as group A25N (screws placed at *1d* distance) but with slightly higher ductility. The enhancement of self-tapping screws was limited as the crack propagated freely before it reached the level where the screw was located. The large screw to dowel distance undermined the capacity of the specimen and a high enhancement of embedment strength was not achieved. However, a strong thread-wood anchorage was provided with 100% thread on the screw. This allowed the screw to hold the specimen in one piece and therefore group A25Re achieved a more ductile behaviour compared to groups A25U and A25N. In terms of stiffness, no significant improvement can be found by using self-tapping screws.

4.2.4 Strain distribution analysis by Digital Image Correlation (DIC)

A series of graphs showing the strain distribution at each loading step for each specimen was produced by DIC software. By observation, crack initiation and propagation mostly occurred beneath the dowel and following the central line of the specimen. The principal strain reached high values near the crack tip, as shown in Figure 4-16. As discussed, the primary objective of this study is to understand how thread configurations and screw to dowel distance can influence the strain distribution at a crack location. But firstly, a parametric study on the influence of the thickness of specimen and diameter of the dowel is discussed.

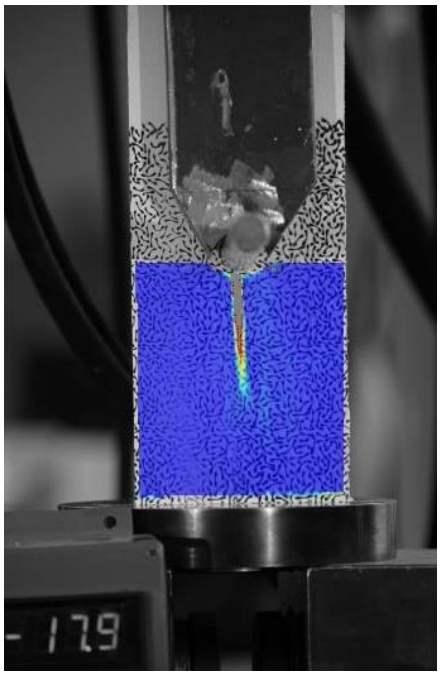

Figure 4-16: Strain concentration at crack location in specimen A45U2.

4.2.4.1 Influence of the thickness of specimen and diameter of the dowel on visualising strain distributions

For reinforced specimens in Stage 2, the DIC analysis can only demonstrate the strain distribution on the surface. However, the screw reinforcement was not located on the surface but at the central plane. Therefore, it is beneficial to establish an understanding of how specimen thickness can influence the surface strain analysis using DIC and to what extent using such technique is reliable.

Results of normalised principal strain vs depth are plotted in Figure 4-17, Figure 4-18 and Figure 4-19 and each figure stands for a configuration type with three different thicknesses. The strain data were extracted from the location of the most significant crack. It should be noted that the starting depth is not the centre of the fastener but the bottom of it. As the crack initiated from the bottom of the dowel and developed downwards, the strain would gradually drop to a value close to zero. To ensure that the results can be compared between different thicknesses, the strain data at similar stress level were selected from a series of DIC outputs. It was difficult to select the exact same stress level for comparison. If a match of similar stress level is impossible, only the ones within an acceptable range are presented, e.g. group A30U in Figure 4-17. The acquired strain data is then normalised from zero to one (all the data points were divided by the maximum value in each test), so that a clearer trend can be demonstrated.

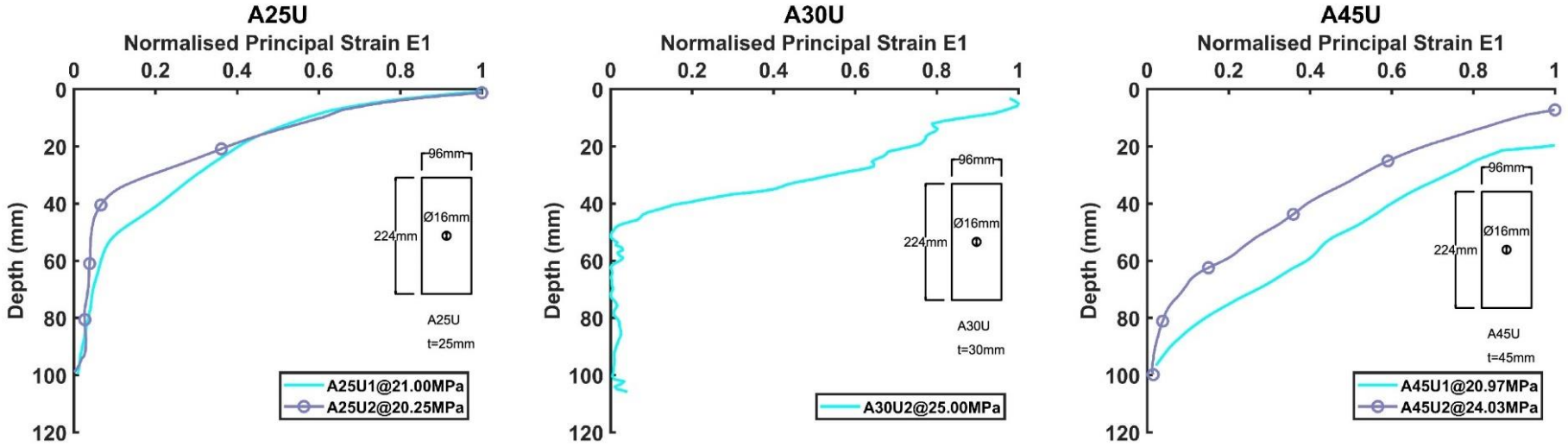

Figure 4-17: Principal strain comparison with changing specimen thickness using configuration A.

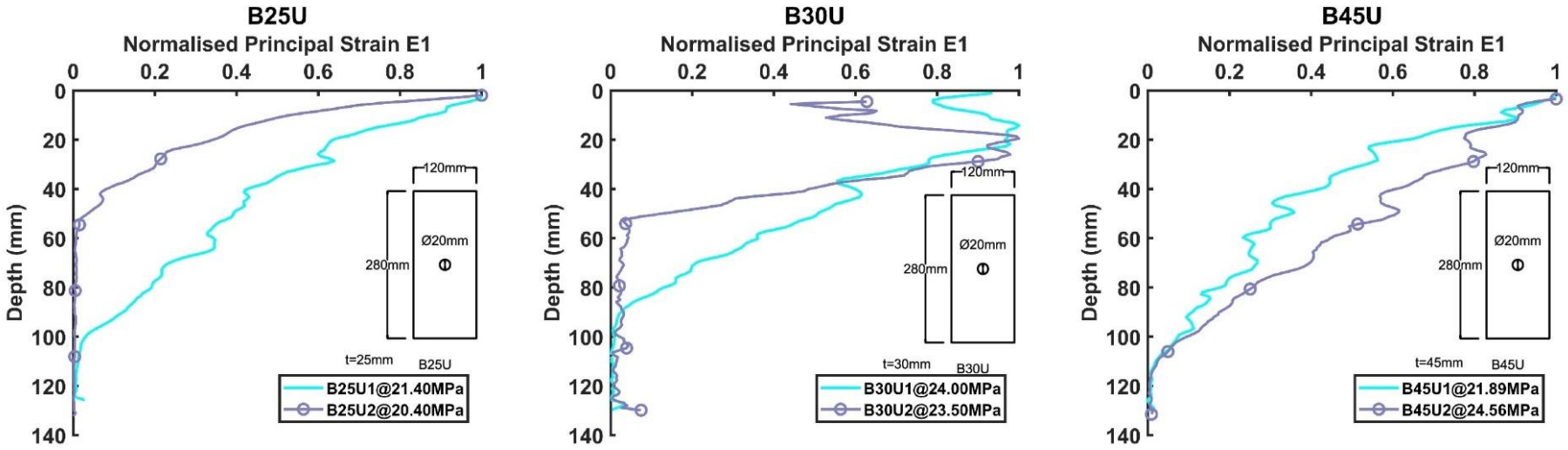

Figure 4-18: Principal strain comparison with changing specimen thickness using configuration B.

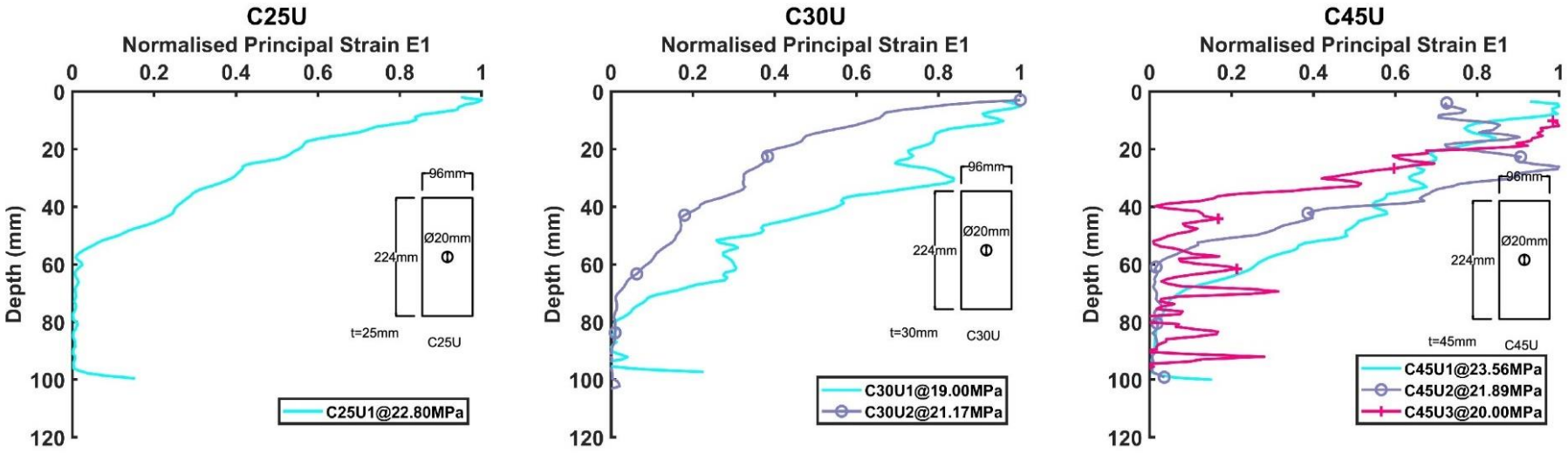

Figure 4-19: Principal strain comparison with changing specimen thickness using configuration C.

For configuration *A*, specimens (A25U) with 25mm thickness showed a higher rate of decrease of principal strain versus depth than that of the 30mm and 45mm thick specimens (A30U and A45U), see Figure 4-17. By comparing the plots at different thicknesses of configuration, *B* and *C*, respectively, it was found that all 25mm thick specimens displayed a higher rate of change in strain than the rest of the thicknesses. In addition, the 30mm thick specimens for all three types of configuration showed slightly higher rates of change than the 45mm thick specimens. With increasing thickness, the accuracy of presenting the strain at the area of interest gradually drops.

It is of importance to acquire the strain distribution as close as possible to the central plane where the screw is located. Thus, this study used the minimum thickness *1.5d* (t=24mm), as suggested by BS EN 383:2007 (BSI, 2007) to obtain the strain distribution at Stage 2. The above results also show that a larger thickness of specimen may not accurately display the strain distribution around the screw. Furthermore, in configuration *C*, the thickness was *1.25d* (25mm thick specimen with 20mm dowel) and the strain distribution can be acquired successfully. Therefore, in future studies, the use of a smaller thickness of specimen may be considered.

Different diameters of steel dowels are expected to vary the strain distribution. According to Thelandersson and Larsen (2003), large and stout dowels act as wedges, increasing tensile stresses perpendicular to the grain. In this study, configuration *C* is expected to have higher splitting tendency and slower strain reduction than other configurations. As can be seen in Figure 4-17 and Figure 4-18, with 25mm thickness configuration, *A* and *B* displayed slightly faster rates of change in strain than configuration *C*. To be more specific, at similar loading stresses at 20mm depth, group A25U had 0.4 normalised strain left, while group C25U had 0.6 normalised strain remaining. This indicated that at similar depth, configuration *C* had developed longer and wider cracks than the rest. By increasing the thickness of the specimen to 30mm and 45mm, see Figure 4-17 to Figure 4-19, all three configurations displayed similar trends for the change of normalised strain versus depth. To summarise, using larger dowels has a tendency to increase the strain distribution and exacerbate crack propagation. In addition, it becomes much easier to observe the influence of the diameter of the dowel on strain distribution at smaller specimen thickness.

4.2.4.2 Strain distributions in unreinforced and reinforced specimens

As screw reinforcement provides effective restraint to crack propagation, it is considered that strain distribution will be influenced. A prediction is that principal strain will decrease at a

faster rate in reinforced specimens than in unreinforced ones. To validate this hypothesis, a measurement was taken by extracting the principal strain values at the crack location of both reinforced and unreinforced specimens at similar loading stresses.

The normalised strain versus depth plot for unreinforced and screw-reinforced specimens at different thicknesses are shown in Figure 4-20. The most important finding is that the reducing rate of normalised strain in reinforced specimens (second row) was much faster than that of the unreinforced ones (first row in Figure 4-20). In the reinforced groups, the normalised strain reduced to 0.1 at approximately 40mm depth while for the unreinforced specimens, the normalised strain remained to around 0.2-0.4. This indicates that the crack propagated faster in unreinforced groups. In other words, the screw reinforcement can effectively control strain distribution and reduce the splitting tendency. For specimens that were reinforced by a screw with 0% thread, in group A25N, it showed similar trends as the unreinforced ones. The normalised strain remains at high values at large depth, indicating severe crack propagation occurred to the specimens. This further confirms that a nail-like reinforcement is inefficient in preventing splitting.

Comparing groups A25BS (reinforced by screws with 33% thread placed at *1d* distance) with A25Rb (reinforced by screws with 100% thread placed at *1d* distance), no significant differences is found between their curves. This comparison indicates that using screws with 33% thread on the point end can effectively prevent splitting. The results also correspond well with the experimental works in Chapter 4 (Section 4.1) and Chapter 5 in embedment strength and load-carrying capacity. The test results match the prediction that screw reinforcement can restrain crack propagation.

The unreinforced groups did not achieve the same high level of stress as the reinforced groups, therefore the strain data at their peak stresses are presented in Figure 4-20 only for reference.

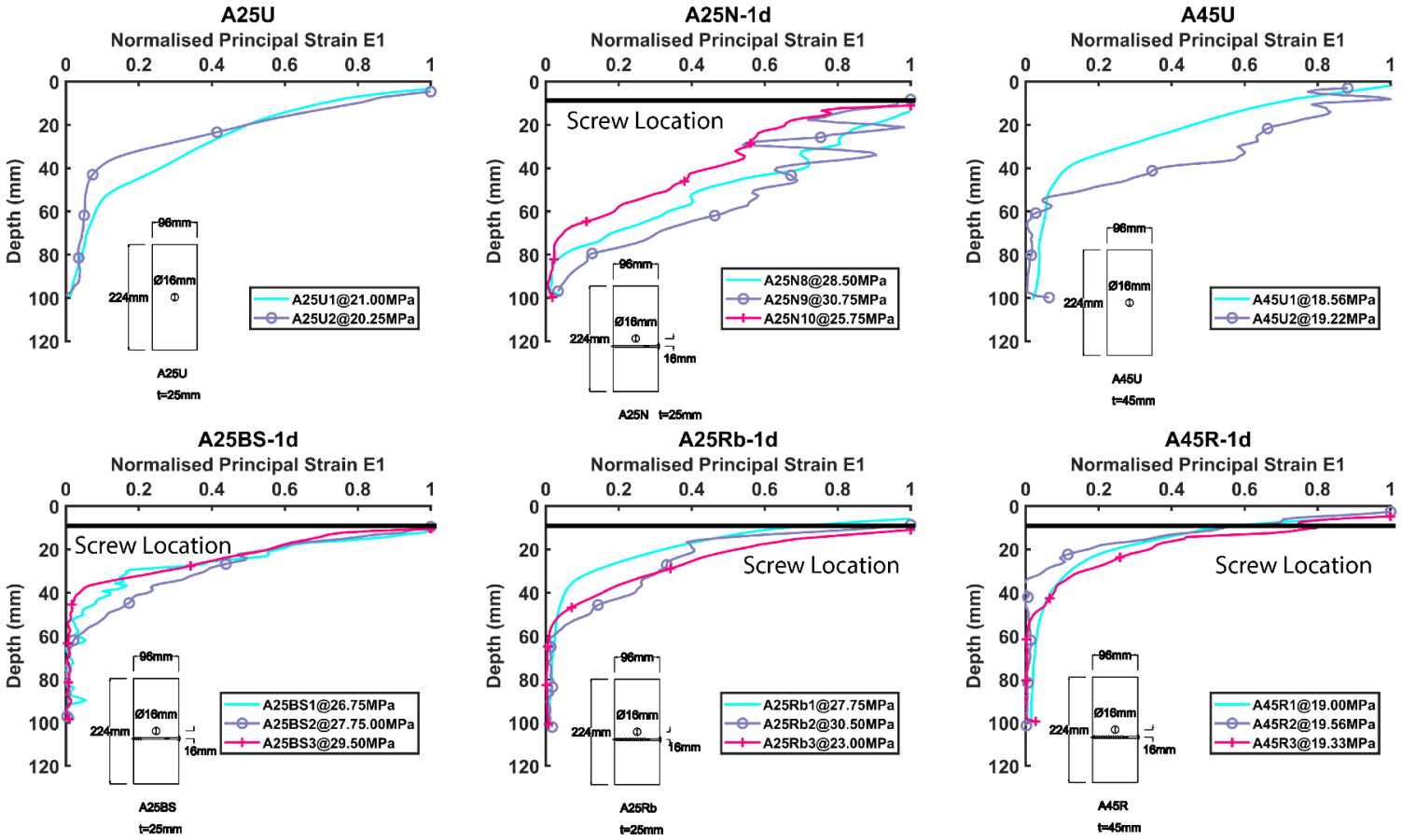

Figure 4-20: Principal strain comparison for reinforced and unreinforced specimens with 25mm and 45mm thickness.

4.2.4.3 Influence of screw to dowel distance on strain distributions

The distance between screw and fastener is an important factor to be considered in the design of screw reinforcement. This study tested six different distances to examine their influence on the strain distribution of reinforced specimens. The strain data were extracted at similar load ranges as shown in Figure 4-21. The screws were placed from *0.5d* (in contact with the dowel) to *4d* distances and the locations of the screw are marked with black straight lines. A clear trend, indicated in Figure 4-21, is that the reducing rate of normalised strain gradually decreases as the screws are placed further away from the dowel. To be more specific, for group A25ES, which had screws in touch with the dowel, the strain reduced to about zero at 30-40mm depth. This depth of zero strain increased to around 45mm for group A25Rb, which had screws placed at *1d* distance to the dowel. Then, in group A25Rd, the strain reduced to zero at 60mm depth, which means the crack had propagated much further than those in group A25ES. For group A25Re, the strain reached to zero at around 80mm, which had screws placed 30mm away from the bottom edge of the specimen. This similar behaviour can also be found in group A25N in Figure 4-20. In other words, placing the screw within *2d* distance of the dowel can effectively slow down the process of wood splitting and this effect increases as the screw is placed closer to the dowel.

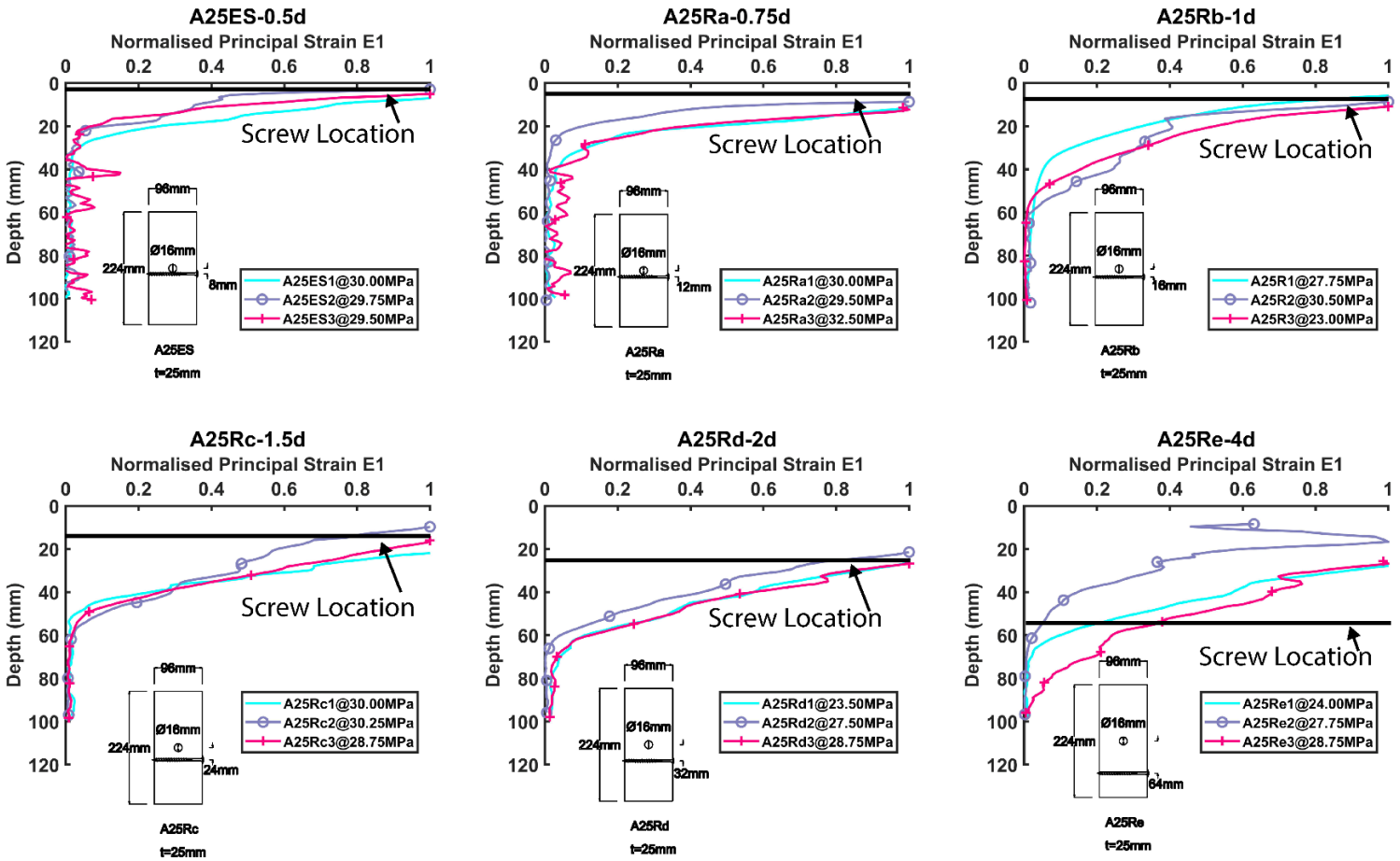

Figure 4-21: Principal strain comparison for different screw to dowel distances using 25mm thick specimens.

4.2.5 Summary

This experimental study investigated the influence of thread configuration and screw to dowel distance on the strain distribution of screw-reinforced dowel-type connections. This study has demonstrated the outstanding capability of DIC technique for strain measurement. The impacts of the diameter of the dowel and thickness of specimen have also been discussed.

The following points can be concluded from this study:

- By plotting the normalised strain vs depth graphs, variation between different specimen thicknesses is found. Specimens with 25mm thickness are recommended because the surface strain is at a closer distance to the plane where the screw is located thus being more accurate. The graphs show that under similar loading stresses, a larger steel dowel displays a lower rate of reduction in strain, which indicates more severe wood splitting and crack propagation has occurred. This trend can only be identified in specimens with 25mm thickness.
  The study also demonstrates the importance of specimen thickness and recommends using the minimum allowed thickness for similar applications, to achieve better accuracy when mapping the strain distribution.
- The normalised strain versus depth graphs reveal that having reinforcement can effectively reduce the strain experienced in unreinforced specimens. Using screws with 33% thread on the point end achieved similar results to those using screws with 100% thread. By having 0% thread on the screw, the specimen showed a less ductile failure, which was similar to the unreinforced groups. The results correspond well with the findings in Chapter 4 (Section 4.1) and Chapter 5.
- The test results confirmed that the screw to dowel distance is essential in preventing splitting failure of wood. The closer the screw is placed to the dowel, the earlier it can control crack propagation. The reinforcement was still efficient in controlling crack propagation when the screw was placed at *2d* distance to the fastener. The mechanical properties and strain distribution obtained from this study provide an insight into where self-tapping screws should be installed in order to achieve better reinforcement efficiency.

4.3 Rope effect of self-tapping screws as reinforcement on dowel-type connections

4.3.1 Introduction

In the experimental work in Chapter 4 (Section 4.1), self-tapping screws were used to enhance the mechanical properties of dowel-type connections. The tests showed that screws with partial thread on the point end achieved similar enhancement in embedment strength and load-carrying capacity as fully threaded screws. Therefore, it is recommended to use partially threaded screws, which reduces the drive-in torque and the risk of damaging the screw. However, the previous work does not explain how a small portion of thread can give the same amount of improvement as a fully threaded screw.

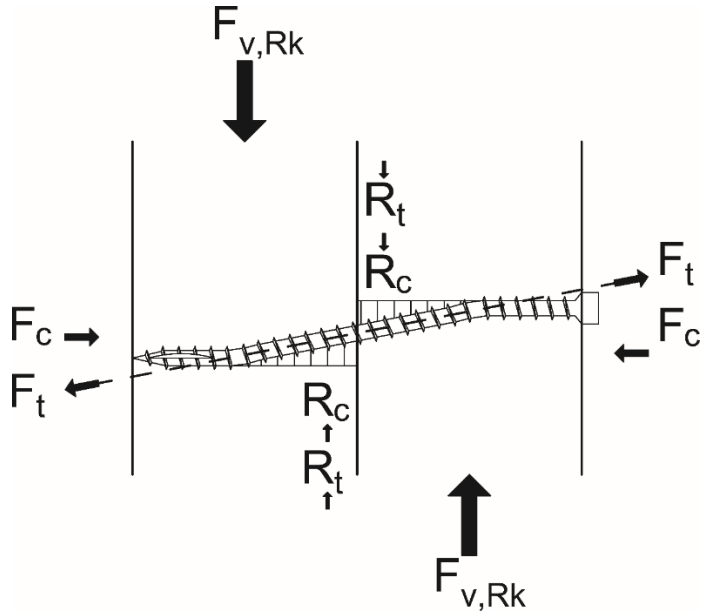

Figure 4-22: The additional capacity R_t and R_c due to the yield of fastener.

In EC5 (BSI, 2004), for fasteners with thread, the calculation of load-carrying capacity is based on a combination of the Johansen yield theory and the rope effect. Rope effect is an increase in load-carrying capacity when the threaded fastener yields. The deformed fastener is subject to a tensile load, F_t, along the fastener. If the tensile load is higher than the withdrawal or pull-through capacity of the fastener, the fastener will be pulled through or withdraw from the connections. Otherwise, a vertical component, R_t, of this load can be added to the load-carrying capacity of the connections, as shown in Figure 4-22. Further additional capacity, R_c, is due to friction from the compressive load F_c on the members as the fastener yields.

An illustration of screw reinforcement in Section 4.1 is shown in Figure 4-23. Due to the geometry of the dowel, the vertical load F, can be resolved into a vertical load, F_v and horizontal components, F_t. The horizontal force will tend to split the specimen and form a crack parallel to the grain. With screw reinforcement, this splitting action is greatly restrained by the thread-wood anchorage and the embedment of screw head, denoted by F_c. As the steel dowel moves downwards and touches the screw, an additional resistance, R_{screw}, can be provided by the screw, which has better mechanical properties than wood. This is a similar action to the rope effect, except that the screw does not penetrate multiple timber members. Moreover, both withdrawal capacity and head pull-through resistance of the screw contribute to the effectiveness of the reinforcement.

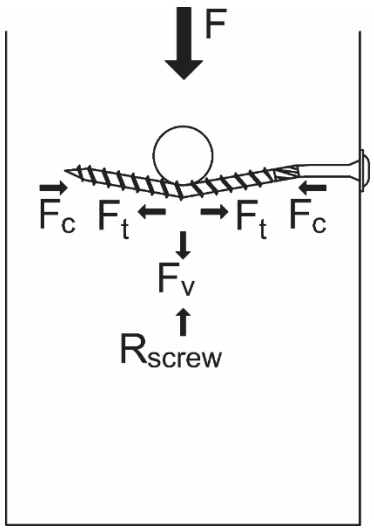

Figure 4-23: Self-tapping screw as reinforcement in the embedment test.

In EC5, the additional load-carrying capacity due to rope effect by friction (R_c) is applied as an additional component of the Johansen yield load part and the additional capacity by the vertical load (R_t) is related to the fastener type and the withdrawal capacity (or pull-through capacity) of the fastener:

$$F_{v,Rk} = frcition\ factor \times Johansen\ yield\ load + min\begin{cases} (F_{ax,Rk}/4) \\ percentage \times frcition\ factor \times Johansen\ yield\ load \end{cases} \quad (4\text{-}2)$$

For steel dowels, the percentage is taken as zero thus dowels do not contribute to the rope effect. For screws, the percentage is taken as 100%, as stated in EC5 clause 8.2.2 (2) (BSI, 2004). EC5 also requires that the penetration length of the threaded part of the screw to be at least six times the outer diameter of the screw.

The term $F_{ax,Rk}$ is the minimum value between the withdrawal capacity and head pull-through capacity of the fastener. Calculation methods can be found in EC5 clause 8.7.2 (5) (BSI, 2004):

$$F_{ax,Rk} = min\begin{cases} \frac{n_{ef} f_{ax,k} d l_{ef} k_d}{1.2cos^2\alpha + sin^2\alpha} & (withdrawal) \\ n_{ef} f_{head,k} d_h^2 \left(\frac{\rho_k}{\rho_a}\right)^{0.8} & (head\ pull\text{-}through) \end{cases} \quad (4\text{-}3)$$

$$f_{\mathrm{ax,k}} = 0.52 d^{-0.5} l_{\mathrm{ef}}^{-0.1} \rho_{\mathrm{k}}$$

$$k_{\mathrm{d}} = min\begin{cases} d/8 \\ 1 \end{cases}$$

where:

n_{ef} is the effective number of fasteners;

$f_{\mathrm{ax,k}}$ is the characteristic withdrawal strength perpendicular to the grain, in N/mm^2;

d is the nominal diameter of the screw, in mm;

l_{ef} is the penetration length of the threaded part, in mm;

α is the angle between the screw axis and the grain direction, with $\alpha \geq 30^{\circ}$;

$f_{\mathrm{head,k}}$ is the is the characteristic pull-through parameter of the screw determined in accordance with BS EN 14592 (BSI, 2009a) for the associated density ρ_{a};

ρ_{a} is the associated density for $f_{\mathrm{ax,k}}$, in kg/m^3;

ρ_{k} is the characteristic density, in kg/m^3;

d_{head} is the diameter of the screw head, in mm.

From the above equations, EC5 has considered the impact of some of the factors of screw specifications on the rope effect. However, the influence of thread configuration, such as thread location, pitch and thread of screws are not included. For rope effect relating to self-tapping screws as reinforcement, consideration of thread configuration should be adapted.

Currently, a large variety of self-tapping screws with different thread configurations are being manufactured. However, neither sufficient understanding of the influence of thread configuration on the rope effect of self-tapping screws as reinforcement, nor guidance to select the suitable forms of screws, is available. Therefore, this study aims to investigate the impact of thread length and location on the rope effect of self-tapping screws as reinforcement, through a series of embedment tests.

4.3.2 Materials and methods

4.3.2.1 Material preparation

The timber specimens were prepared from C24 European Whitewood. The timber beams were prepared at 21.6°C and 59% RH. Their average density and moisture content were 394kg/m^3 (CoV=5.2%) and 7.9% (CoV=2.7%), respectively. The dimension of the specimens was 224×108×45mm, designed according to EC5 (BSI, 2004), and the diameter of the steel dowel was 16mm.

The fully threaded self-tapping screws had a length of 140mm, with a small cylindrical head. They had an inner diameter of 4.6mm and an outer diameter of 7mm. To change the thread configurations of the self-tapping screws, the unwanted threaded part was removed by a grinder and then polished with sandpaper. In total, five different types of thread configurations were prepared and their details are tabulated in Table 4-7.

Table 4-7: Summary of each group in this study.

Group	Thread configuration*	Repetitions	Mean density (kg/m^3) (CoV)	Mean M.C.% (CoV)
RPAS	*1/6 thread on the point end*	*3*	*394 (6.3%)*	*7.8 (2.9%)*
RPBS	*1/3 thread on the point end*	*3*	*393 (6.2%)*	*7.8 (1.5%)*
RPCS	*1/2 thread on the point end*	*3*	*395 (3.6%)*	*7.9 (3.3%)*
RPTTS	*1/3 thread on both ends*	*3*	*396 (6.8%)*	*7.9 (2.6%)*
RPS	*Fully threaded*	*3*	*395 (6.9%)*	*8.0 (3.6%)*

**The length of the threaded part is expressed in a fraction of the total length of the screw.*

The thread configuration for each group is also shown in Figure 4-24. As this study used load cells to measure the axial load from the screw, washers were used to ensure the instrument was working properly and the load from the screw head was uniformly distributed. Therefore, a total of 32mm of the length of the screw were taken by the instrument and the screw's cylindrical head. The threads within this range were also removed, see Figure 4-24, to avoid disturbance to measurement.

For groups RPAS, RPBS and RPCS, the length of their threaded part was no more than 54mm which was exactly half of the width of the specimen. Therefore, there was no thread on the head end meaning that the screw head would fully provide the restraint from one end.

The incremental of thread length between them was 18mm. The readings from the load cell were equal to the resistance provided by the thread on the point end.

For groups RPS and RPTTS, the screw head and thread on the head end both contributed to the resistance. Therefore, it was expected that the force acting on the load cell would be reduced. The screws in Group RPBS have exactly one third of thread of those screws in Group RPS. It ensures a ratio of 1:3 in thread length that is adopted in this research.

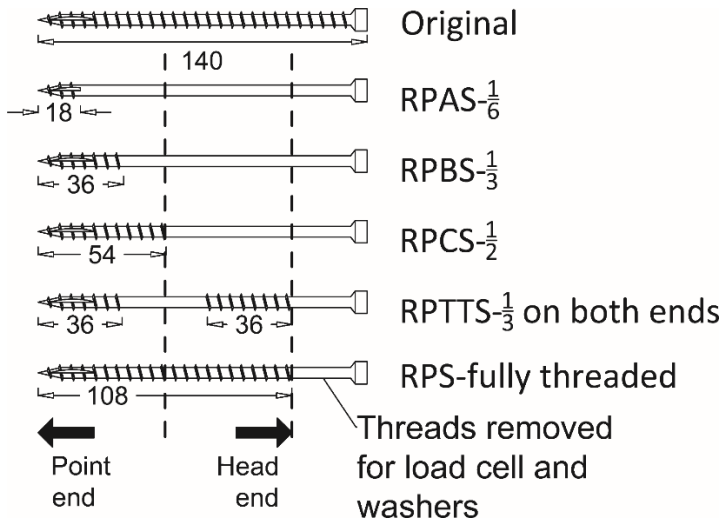

Figure 4-24: Thread configuration for each group compared to the original self-tapping screw.

4.3.2.2 Test set-up

To measure the axial load from the self-tapping screws, an OMEGA LCMWD 10KN load cell was used. As previously explained, to ensure the load cell could work properly, washers were applied and their configurations are shown in Figure 4-25.

The test set-up is shown in Figure 4-26. The washers and load cells were placed in order and aligned to the location of the screw reinforcement. Then, the self-tapping screw was driven into the specimen by a hand drill, and a torque wrench was used for the last few turns of the screw to avoid any excessive pressure on the load cell before the test. The same DARTEC loading machine (100kN capacity) was used to perform the embedment tests as previous sections. The relative displacement of the fastener to the specimen was taken to be the displacement of the loading head assuming no tilting or bending of the steel dowel occurred. The errors due to the fastener tilting or bending were therefore ignored. During the test, the embedment specimens were compressed to failure when 20% of load drop from the peak load was observed.

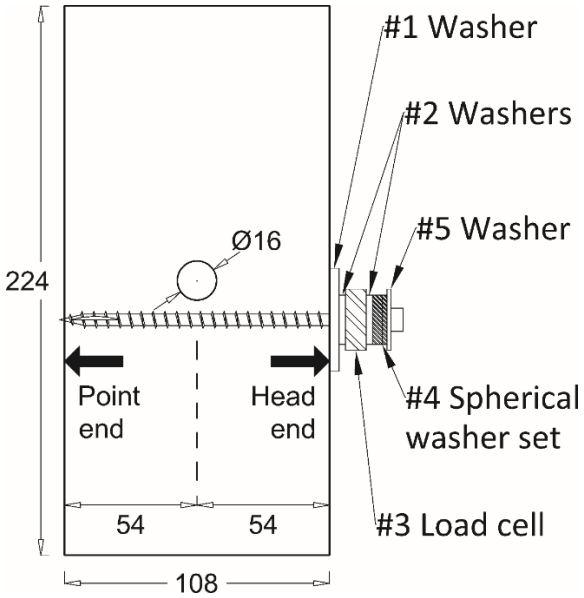

Figure 4-25: Specimen installed with reinforcement and instrument: #1 washer to distribute load on wood; #2 washers to distribute load on both sides of the load cell; #3 load cell connected to data logger; #4 spherical washer set to adjust to any irregular alignment during test and #5 washer to distribute the load from screw head on the spherical washers.

Figure 4-26: Embedment test set-up.

4.3.3 Results

The general trend of load-displacement curves, represented by dotted lines in Figure 4-27 for each group, is similar. They also correspond well with the curves presented in Section 4.1. As the screw was placed at *1d* distance to the dowel, the dowel needed to move downwards for 4mm to be in touch with the screw, considering the outer diameter of the screw. In Figure

4-27, there is an increase of the axial load from the screw head and the load on the specimen at 4-5mm displacement. The axial load from the screw head was much smaller compared to the load from the machine. For groups RPAS, RPBS and RPCS, their measured axial load was higher than groups RPS and RPTTS. The results were as expected, as the thread on the head end, in groups RPS and RPTTS can contribute a part of the resistance, thus reducing the contribution from the screw head. The screw head in groups RPAS, RPBS and RPCS can fully contribute its restraining force, which also increases with the thread length on the point end.

The test results for each group are tabulated in Table 4-8. The stiffness of each specimen was found through calculating the gradient between $0.1F_{max}$ and $0.4F_{max}$ (F_{max} is the peak load) on the load-displacement curve. The sample size in this study is three for each group, therefore, the results can be easily affected by factors, such as density and wood defects, and discussion on the difference between the five groups should be carefully considered. However, an overall trend is that the mechanical properties of the specimen improve with increasing thread length on the point end. To be more specific, groups RPAS and RPBS showed the lowest embedment strength. Group RPCS (specimen reinforced by screw with ½ thread on the point end) achieved the highest strength. Group RPS (with fully threaded screw) achieved the second highest strength, with only 1% lower than group RPCS.

Table 4-8: Summary of test results.

Group	Description	Mean embedment strength (N/mm^2) (CoV)	Mean ductility (CoV) EN12512 method	Mean stiffness (kN/mm) (CoV)	Mean maximum load from screw head (kN) (CoV)
RPAS	*1/6 thread on the point end*	*34.65 (7%)*	*9.21 (7%)*	*6.95 (13%)*	*2.56 (28%)*
RPBS	*1/3 thread on the point end*	*34.59 (5%)*	*10.21 (8%)*	*6.97 (16%)*	*3.47 (26%)*
RPCS	*1/2 thread on the point end*	*39.05 (7%)*	*12.72 (4%)*	*7.19 (14%)*	*4.90 (15%)*
RPTTS	*1/3 thread on both ends*	*36.61 (4%)*	*12.91 (42%)*	*9.67 (61%)*	*1.16 (34%)*
RPS	*Fully threaded*	*38.67 (3%)*	*18.95 (33%)*	*10.42 (33%)*	*1.55 (18%)*

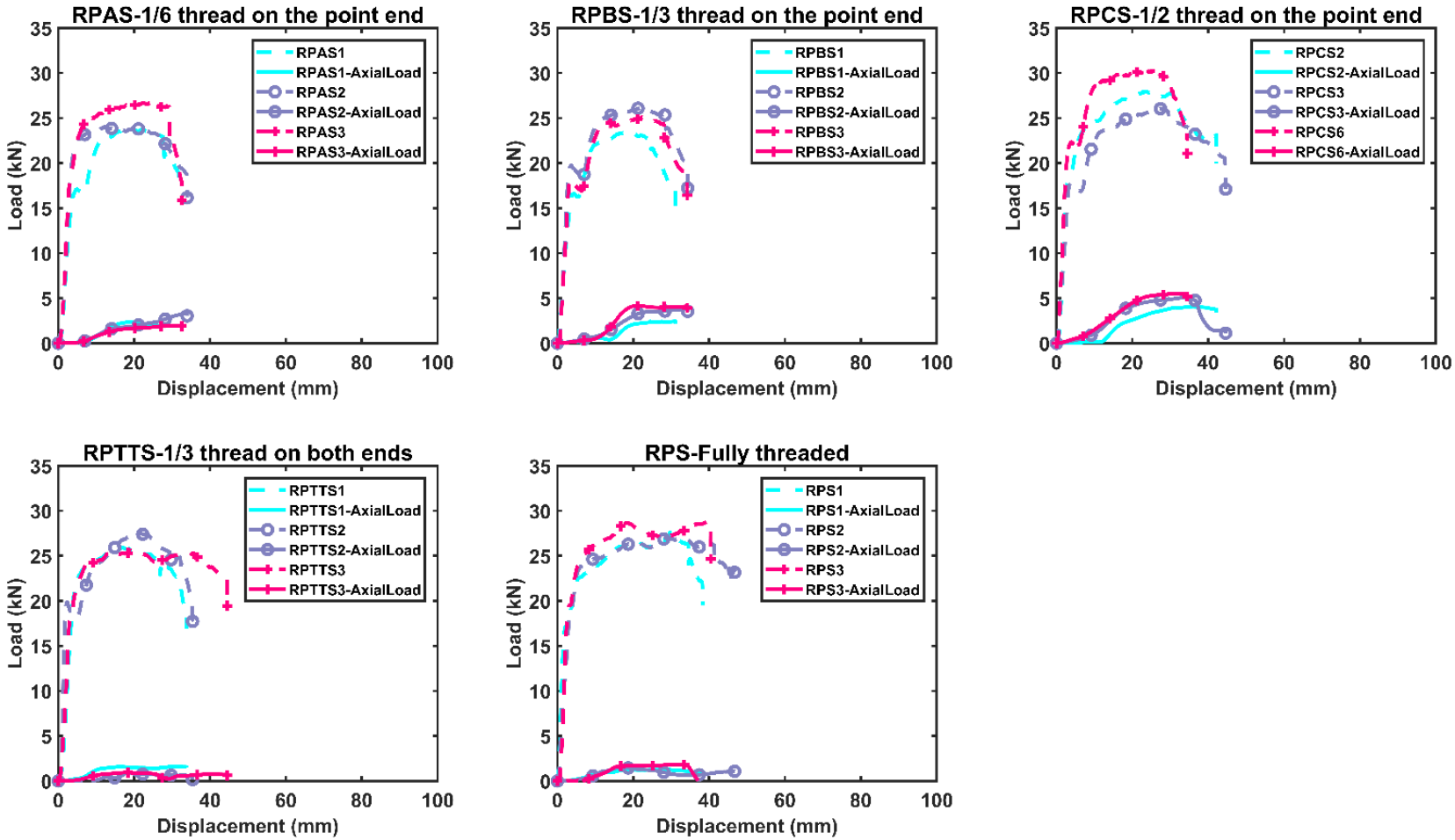

Figure 4-27: Load-displacement curves with axial load from screw head for each group.

As for the maximum load acting on the load cell, the average value increased with increasing thread length on the point end. The value started from 2.56kN for group RPAS (reinforced by a screw with ⅙ thread) and reached to 4.9kN for group RPCS (reinforced by screw with ½ thread on the point end).

For groups using screws with thread on both ends, Table 4-8 shows the maximum load from the screw head was only 65% of the value for group RPAS.

It should be noted that after approximately 8mm of displacement, the steel dowel starts to bear on the screw leading to the deformation of the screw. As the screw is deformed, the axial load on the screw is the combination of the horizontal and vertical forces. The horizontal component is not separated from the vertical component as this study is more interested in the trend between the thread length and the axial load on the screw.

4.3.4 Discussion

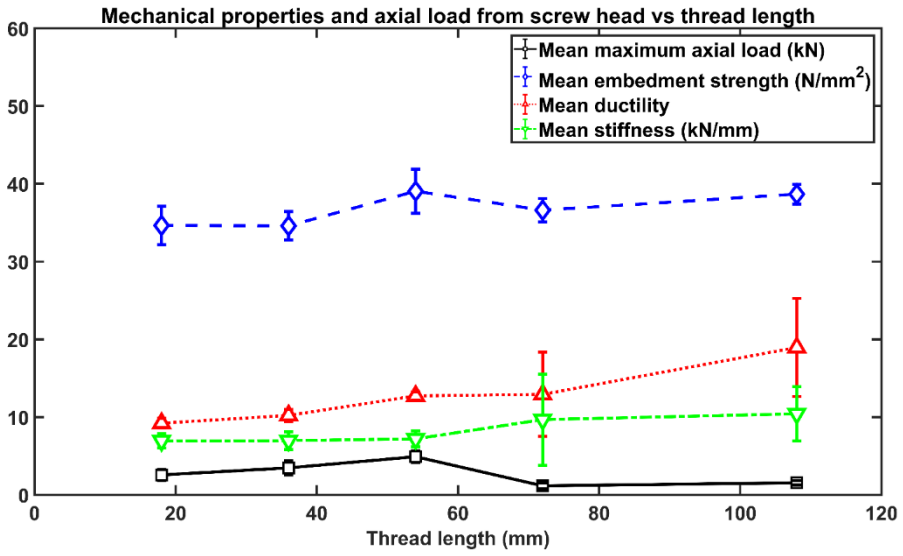

Figure 4-28: Plot of mechanical properties and axial load from screw head versus thread length.

The change of mechanical properties and axial load from screw head versus changing thread length is plotted in Figure 4-28. Combined with the results from Table 4-8, the change of axial load from the screw head is proportional to the thread length when the thread is located on the point end. By adding ⅙ thread (18mm) on the screw, the axial load from screw head (black line) increases by at least 36%.

As for the embedment strength, the specimens reinforced by screws with ½ thread on the point end achieved the highest value. It was about 13% higher than screws with ⅙ thread on the point end. In general, screws with threaded parts on both ends or screws with ½ thread on the point end achieved slightly better enhancement.

The ductility of group RPS, reinforced by fully threaded screws, was influenced by one of its specimens that achieved at least 67% higher ductility than the other two specimens. As for the rest of the groups, the ductility did increase with increasing thread length. Group RPTTS reinforced by screws with ⅓ thread on both ends showed an increase of 40% of ductility when compared with group RPAS that was reinforced by screws with ⅙ thread on the point end.

In this study, increasing thread length on the screw shows slight improvement in embedment strength, a major factor influencing the load-carrying capacity of dowel-type connections. Self-tapping screws with ½ thread on the point end achieved similar reinforcement performance to those using fully threaded screws and have the advantage of reduced drive-in torque discussed in Chapter 3. As the drive-in torque is proportional to the thread length, the less thread length of a screw implies about 50% reduction in required torque, which is beneficial to the installation of self-tapping screws.

As for self-tapping screws with ⅙ thread on the point end, they achieved 89% of the improvement in embedment strength by screws with ½ thread on the point end, but potentially bring the benefits of having a further reduction of required drive-in torque by 66%.

The sample size in this study was limited to three samples and more embedment tests are recommended in the future to have a solid confirmation of the enhancement of mechanical properties.

4.3.5 Summary

In this study, self-tapping screws with five different types of thread lengths were applied as reinforcement on single dowel specimens and the axial load from the screw head was measured by a load cell. When there was no thread on the head end, the axial load from the screw head equalled the resistance provided by the thread on the point end. The mechanical properties of the reinforced specimen were calculated to evaluate the effectiveness of each thread length. The following points can be concluded:

- The resistance from the screw head is proportional to the thread length on the point end. If a screw has thread on both ends, the resistance is from the head end that is contributed by the embedment of screw head and the thread-wood anchorage. Thus, the readings from the load cell cannot represent the actual resistance from the point end for screws with thread on both ends.

- The improvement in embedment strength between the five groups has a difference of 13%. Screws with ½ thread on the point end achieved similar performance to fully threaded screws but reduced the risk of damaging the screw during installation. Using screws with ⅙ thread on the point end further reduced the drive-in torque, as well as the resistance against splitting. They achieved 89% of enhancement in embedment strength of screws with ½ thread on the point end.

4.4 Self-tapping screws as reinforcement on single dowel connections with artificial cracks

4.4.1 Introduction

In a failure analysis by Frese and Blaß (2007), cracking of timber in the grain direction has a higher percentage than shear failure and decay in primary damage distribution. As Franke and Franke (2014) summarised, the causes of crack initiation can be classified into two major aspects: stress induced and moisture induced. The former happens when the strength of bending, shear or tension of the timber is exceeded, e.g. beams with service hole and notches. The latter is caused by the variation of relative humidity in the environment, as the wood changes the moisture contents so as to maintain an equilibrium state. Except for cases where the change of moisture content is above the fibre saturation point (normally 28-30%), any other variations can lead to a moisture exchange in the cell walls and, as a result, a change in timber dimensions (shrinking and swelling) and mechanical properties. This study focused on reinforcing dowel-type timber connections that have moisture induced cracks around the fasteners. Since the wood near the fasteners is restrained from movement, cracking of the timber occurs in many existing timber structures due to moisture fluctuation and may be beneficial.

Previous studies by Blaß and Schmid (2001) and Blaß and Schädle (2011) show the potential of using self-tapping screws to enhance the mechanical properties of undamaged dowel-type connections. However, the only work relating to reinforced cracked dowel-type connections using self-tapping screws has been done by Delahunty *et al.* (2014), where their tests used self-tapping screws to reinforce bolted connections with artificial cracks. Their work showed that screw reinforcement can improve the load-carrying capacity of cracked connections with two or three shear plates. In addition, bolted connections reinforced by two screws, placed at different distances from the bolt, achieved higher capacity than those reinforced by one screw. In existing structures, the width of crack can increase with time. However, in

Delahunty *et al.* (2014), the width of the artificial crack is limited to the width of the saw blade; thus the influence of crack width remained unanswered.

The experimental works in Section 4.1 and Chapter 5 confirmed the effectiveness of using self-tapping screws to reinforce the embedment strength and tensile load-carrying capacity of dowel-type connections. Both works also found that screws with a portion of thread on the point end achieved similar performance to the fully threaded screws in enhancing mechanical properties of connections.

To date, there are limited studies on using self-tapping screws to repair damaged dowel-type connections. Therefore, the aim of this study is to investigate the effectiveness of screw reinforcement on repairing dowel-type connections involving different crack widths. In addition, the effectiveness of using screws with partial thread on the point end in repairing cracked specimens is compared to that of the fully threaded screw.

4.4.2 Materials and methods

In this study, two independent variables were applied: reinforcement type and crack width. The reinforcement type refers to unreinforced specimens, specimens reinforced by a screw with complete thread (a partially threaded screw without changing thread configuration), and a screw with 33% thread on the point end.

The crack widths introduced in this study were 1.5mm, 4.5mm and 6mm, respectively. As the width of the available band saw was 1.5mm, the 1.5mm crack was prepared by having one cut along the central line of the specimen. The 4.5mm and 6mm crack were prepared by having two cuts by the band saw.

As embedment strength is one of the essential parameters to calculate the mechanical properties of dowel-type connections in EC 5 (BSI, 2004), a series of embedment tests were conducted in this section to examine the performance of screws, with various thread configurations, to reinforce cracked timber connections.

4.4.2.1 Material preparation

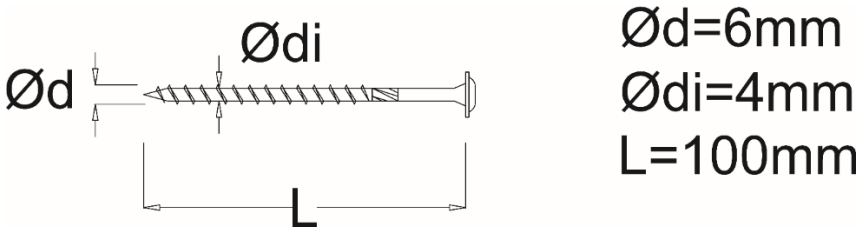

Figure 4-29: Specification of the self-tapping screws applied in this study.

In this study, embedment specimens were prepared from C24 European Whitewood with an average density of 441kg/m^3 (CoV=9.8%). The specimens were conditioned using a climate chamber with 20 °C temperature and 65% RH and achieved an average moisture content of 12% (CoV=13.1%). HECO Topix flange head self-tapping screws which were used in Sections 4.1 and 4.2 were applied as the reinforcement in this study. The details of the screw are shown in Figure 4-29. The original screw is partially threaded (70mm) and has a reamer along its shank.

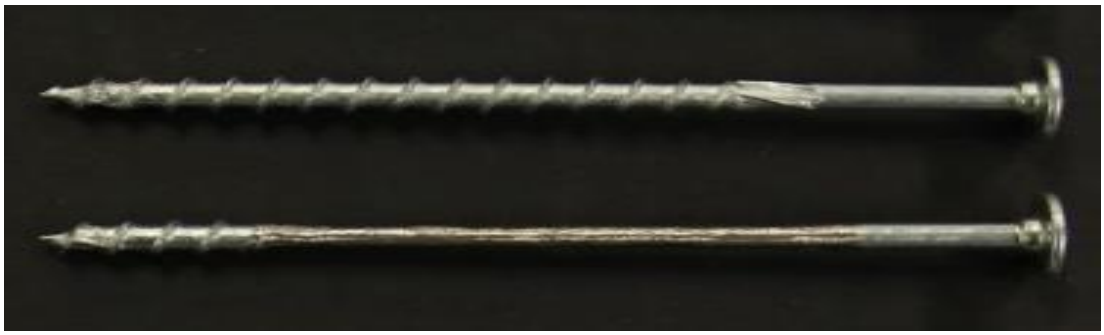

Figure 4-30: Comparison of screw with complete thread (top) and screw with 33% thread on the point end (bottom).

The two thread configurations, 33% and 100% thread, were to ensure the ratio of thread length was kept to 1:3 as that was used in the previous sections of this thesis. To prepare the screw with reduced thread length, the unwanted thread was removed by a grinder. The remaining threaded length was approximately 21mm, about 33% thread of the original one. This procedure ensured consistency of the material properties and the dimensions of the screws. Figure 4-30 illustrates the two types of screws used in this study.

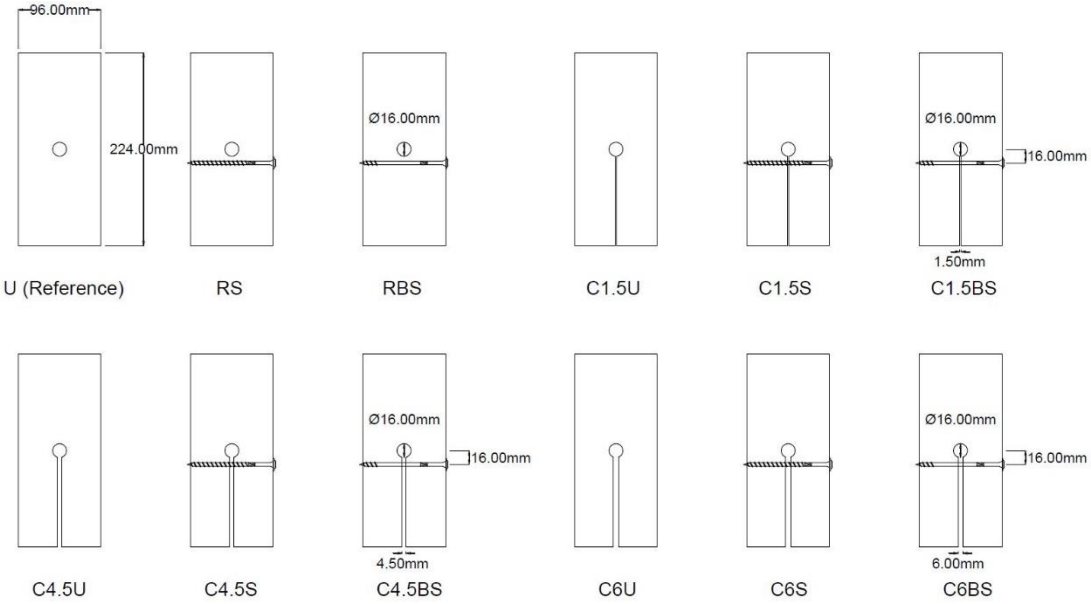

Figure 4-31: Specimen configurations for this study.

The dimensions of the specimen followed the guidance by BS EN 383:2007 (BSI, 2007) and are demonstrated in Figure 4-31; the diameter of the steel dowel was 16mm. After cutting the specimens to the desired size and drilling the holes for the steel dowels, the location of the crack with regard to its width were marked on the surface. The artificial cracks were then prepared by the band saw. To ensure the self-tapping screws could be installed in position as accurately as possible, a 2.5mm diameter (slightly smaller than the inner diameter of the screw) pre-drilled hole was prepared using a pillar drill. After fabrication of the specimens, they were put back in the climate chamber to ensure the moisture content (12%) could be maintained at the preferred level during the test. The details of each group are summarised in Table 4-9.

Table 4-9: Summary of each group.

Group	Description	No of specimens	Mean density (kg/m^3) CoV	Mean M.C.% CoV
U (Reference)	*No crack, unreinforced*	*10*	*450 (11.8%)*	*12.8 (12.8%)*
RS	*No crack, reinforced by screw with complete thread*	*10*	*434 (5.9%)*	*13.1 (12.0%)*
RBS	*No crack, reinforced by screw with 33% thread on the point end*	*10*	*431 (10.2%)*	*12.2 (9.3%)*
C1.5U	*1.5mm crack, unreinforced*	*10*	*442 (9.9%)*	*12.1 (11.2%)*
C1.5S	*1.5mm crack, reinforced by screw with complete thread*	*10*	*448 (8.3%)*	*12.2 (14.4%)*
C1.5BS	*1.5mm crack, reinforced by screw with 33% thread on the point end*	*10*	*439 (9.6%)*	*12.5 (14.2%)*
C4.5U	*4.5mm crack, unreinforced*	*10*	*439 (9.8%)*	*12.7 (11.6%)*
C4.5S	*4.5mm crack, reinforced by screw with complete thread*	*10*	*441 (11.3%)*	*12.9 (7.9%)*
C4.5BS	*4.5mm crack, reinforced by screw with 33% thread on the point end*	*10*	*433 (8.0%)*	*12.6 (11.3%)*
C6U	*6mm crack, unreinforced*	*10*	*435 (10.3%)*	*12.0 (11.8%)*
C6S	*6mm crack, reinforced by screw with complete thread*	*10*	*437 (11.8%)*	*12.5 (12.6%)*
C6BS	*6mm crack, reinforced by screw with 33% thread on the point end*	*10*	*434 (9.4%)*	*12.6 (12.0%)*

4.4.2.2 Embedment test set-up

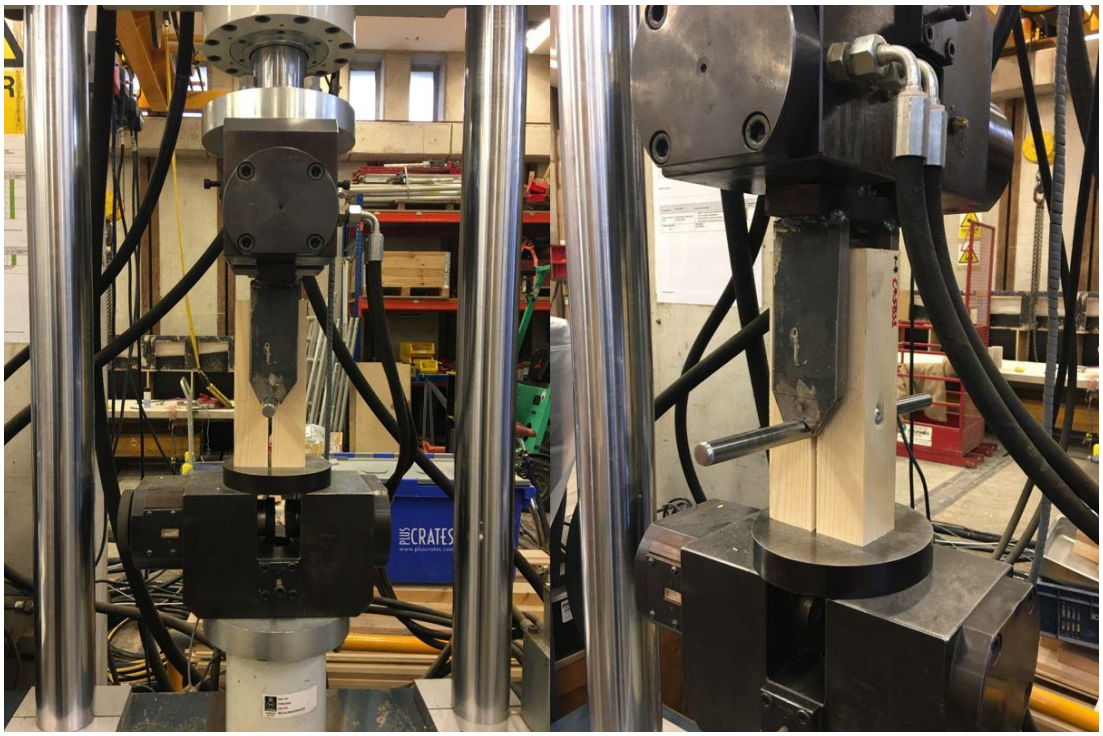

Figure 4-32: Embedment test set-up.

Based on BS EN 383:2007 (BSI, 2007), the embedment test set-up is shown in Figure 4-32. Specimens were loaded parallel to the grain through a 16mm diameter steel dowel. The test was conducted through displacement control with a rate of 4mm/min. The DARTEC loading machine with 100kN capacity was used to conduct the embedment tests. As stated in previous sections, the relative displacement of the fastener to the specimen was taken to be the displacement of the loading head. It should be noted that no significant fastener tilting or bending occurred during the tests, but the results do contain errors from their implications. The tests were either stopped after failure of the specimen with significant load drop or after a 20% load drop from the maximum load had been observed.

4.4.3 Results

Figure 4-33 and Figure 4-34 provide an overview of the load-displacement curves for the groups in this study. Due to the variation of the properties of the timber, even though a similar mean density and corresponding variation was achieved between the groups, a difference within each group still existed. Such differences could be due to a combination of density, wood defects (mainly knots in this case) and moisture content. Thus, the mechanical properties of the specimens may vary. For instance, some of the reinforced specimens in

group C4.5S sustained 20kN of load, while some only achieved 12-15kN. However, this study focuses on identifying a general trend for analysis.

By comparing the unreinforced groups in the first column in Figure 4-33 and Figure 4-34, it can be observed that the maximum load decreased with the introduction of the crack and the increase in crack width. The reference group also had a higher average ductility than the unreinforced cracked ones, which generally failed within 10mm displacement of the dowel.

For the groups with reinforcement, the maximum load also reduced with increasing crack width. However, the reinforced cracked specimens performed with a much more ductile behaviour than the unreinforced cracked specimens. To be more specific, after the elastic stage, the reinforced specimens reached their first peak, which was then followed by a short plastic plateau at around 6-8mm of displacement. Later, the load increased again as the dowel touched the screw. Finally, the specimens fractured after a long stage of plastic deformation.

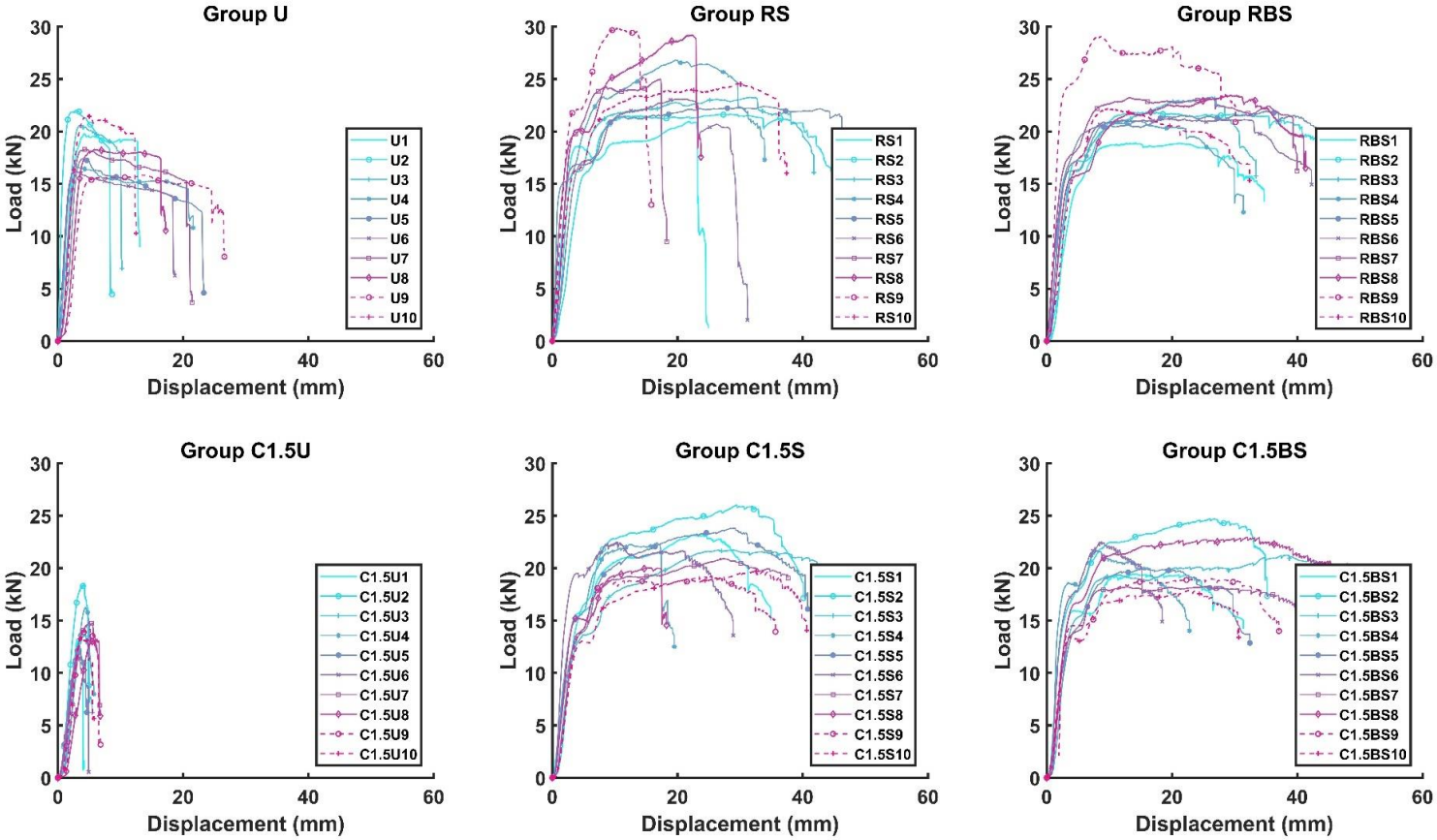

Figure 4-33: Load-displacement curves for the testing groups without cracks and with 1.5mm cracks in this study.

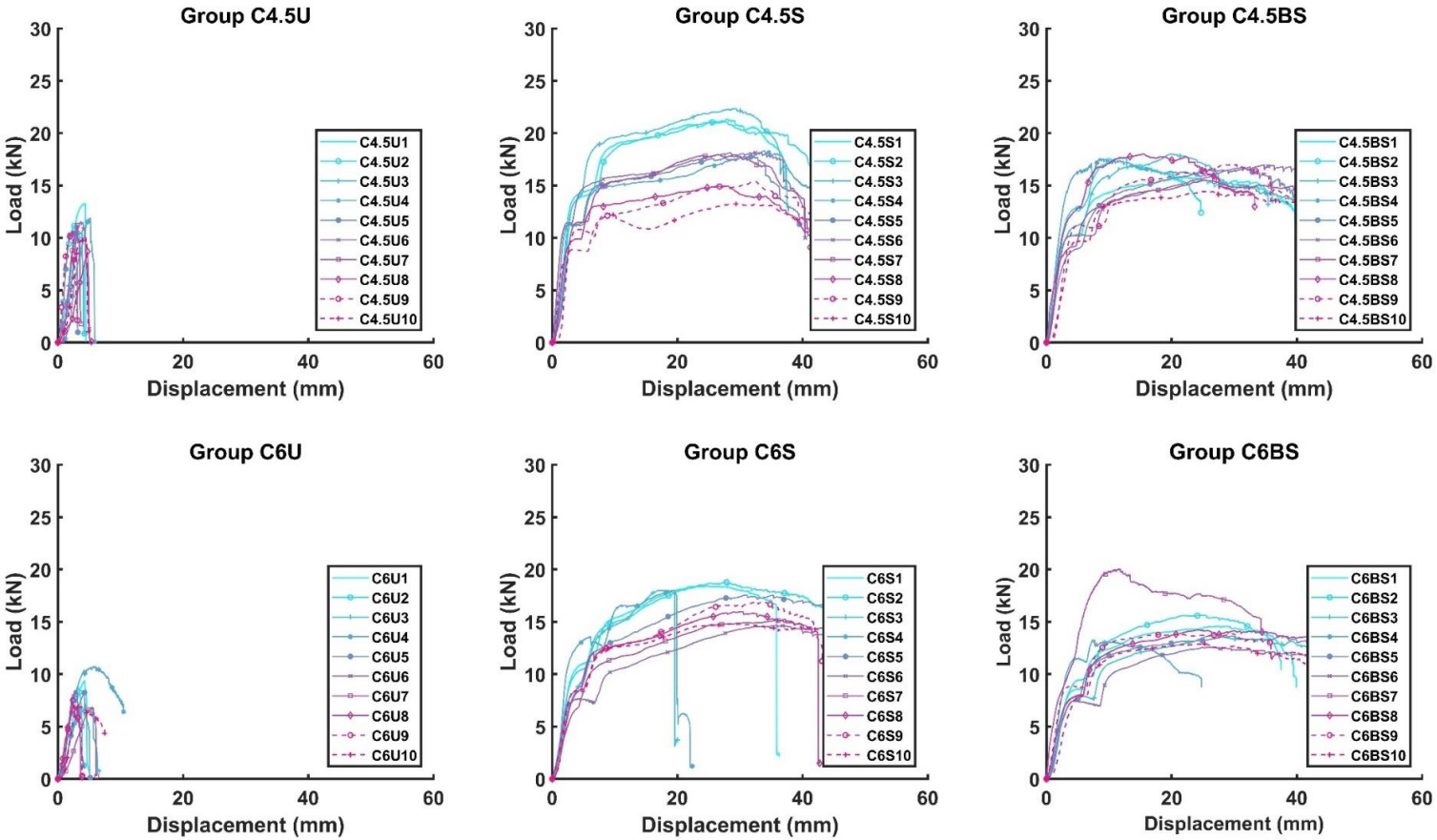

Figure 4-34: Load-displacement curves for the testing groups with 4.5mm cracks and 6mm cracks in this study.

Table 4-10: Summary of mechanical properties of each group.

Group	Mean strength (N/mm^2) (CoV)	ANCOVA adjusted mean strength (N/mm^2)	Mean ductility (CoV) EN12512 method	Mean stiffness (kN/mm) (CoV)
U	*25.9 (12.0%)*	*25.5*	*7.0 (52.0%)*	*10.1 (58.2%)*
RS	*34.3 (12.5%)*	*33.6 **	*15.1 (61.0%) **	*9.3 (51.8%) **
RBS	*31.4 (11.7%)*	*31.7*	*13.7 (28.2%)*	*7.6 (28.3%)*
C1.5U	*19.7 (13.7%)*	*19.6*	*1.9 (19.7%)*	*5.9 (19.6)*
C1.5S	*30.5 (9.5%)*	*30.1*	*10.9 (24.9%)*	*5.9 (37%)*
C1.5BS	*28.8 (10.8%)*	*28.7 **	*13.1 (25.2%) **	*7.0 (24.5%) **
C4.5U	*15.2 (11.0%)*	*15.2*	*1.5 (21.3%)*	*5.7 (28.6%)*
C4.5S	*25.1 (16.3%)*	*25.0*	*19.5 (33.4%)*	*6.9 (16.0%)*
C4.5BS	*23.3 (7.1%)*	*23.5*	*15.1 (28.7%)*	*4.7 (32.0%)*
C6U	*11.2 (16.3%)*	*11.4*	*1.9 (26.6%)*	*3.4 (29%)*
C6S	*23.4 (9.3%)*	*23.5*	*14.8 (29.9%)*	*4.0 (40.1%)*
C6BS	*20.1 (14.9%)*	*20.3*	*14.4 (22.3%)*	*3.4 (20.2%)*

***** *Values excluded the result of specimen RS9 and C1.5BS4 (explanation can be found in the later section).*

Ductility is an essential factor to be considered in timber construction design. A ductile structure can provide visual warnings, such as large deformations. In seismically active areas, a ductile connection can reduce the damage to structures by allowing more energy to be dissipated during an earthquake. Ductility from the tests was calculated using the method provided by BS EN12512 (BSI, 2002) which is described in Section 4.1.

The mechanical properties of each group are tabulated in Table 4-10. For both unreinforced and reinforced groups, the mean embedment strength reduced with increasing crack width. In groups with the same crack width, both reinforced groups showed significantly higher embedment strength than the corresponding unreinforced group. However, specimens reinforced by screws with complete thread showed a higher strength than those reinforced by screws with 33% thread on the point end.

In addition, screw reinforcement significantly enhanced the ductility of cracked specimens. The stiffness of each specimen was calculated using the gradient between $0.1F_{max}$ and $0.4F_{max}$ (F_{max} is the peak load) on the load-displacement curve. The stiffness of the specimen shows a trend to be inversely proportional to the crack width and screw reinforcement

showed no significant improvement in stiffness in comparison to the corresponding unreinforced groups.

4.4.4 Discussion

4.4.4.1 Failure modes

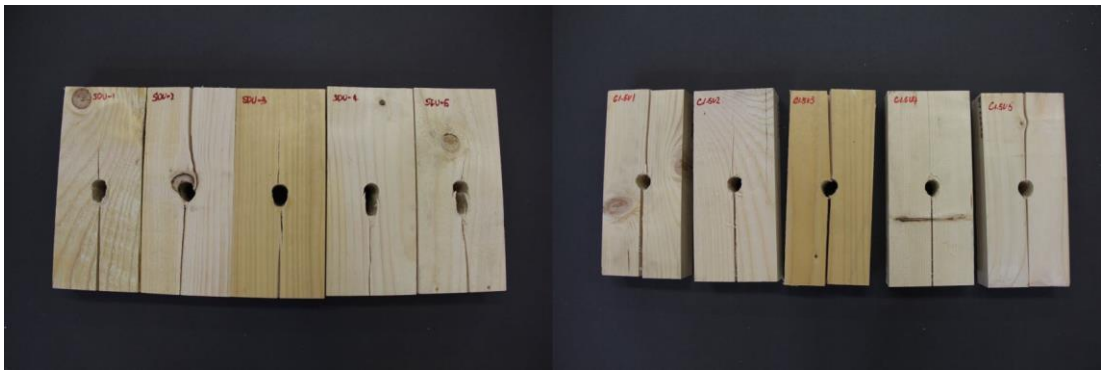

Figure 4-35: Observed failure mode for reference group U (left) and unreinforced cracked group C1.5U.

There were various failure modes observed in this study. For the reference group U, crushing of wood and crack propagation below the dowel was the dominate failure mode. In some cases, the crack was initiated above the dowel and led to a full split of the specimen, as can be seen in some of the specimens in Figure 4-35. For the cracked unreinforced specimens, the crushing of wood was less compared to the uncracked specimens; instead, a rapid fracture of the upper part of the specimen above the dowel can be observed. With the introduction of a crack, less effort was required to cause failure in the timber specimen. Therefore, the unreinforced cracked specimen tended to have less ductile behaviour than the reference group U and this tendency escalated with increasing crack width. The load-displacement in Figure 4-34 further demonstrates such a tendency visually. For unreinforced specimens, both with and without artificial cracks, failure of specimens with sudden load drop was observed.

Figure 4-36: Observed failure of reinforced specimens showing crushed wood and developed cracks (left); embedment of screw head in specimens in group C6S (right).

Splitting failure was also observed in reinforced specimens, with cracks initiated from the top of the dowel and propagated upwards as the dowel kept moving downwards; however, the failure of the specimen was in a much more ductile behaviour. Figure 4-36 (left) demonstrated significant displacement of the dowel with large deformation of wood around the location of the dowel upon failure. In addition, critical embedment of screw head can be observed in Figure 4-36 (right). This was a strong evidence of the thread-wood anchorage in the reinforced specimens. The failure mode for specimens with both types of reinforcement can be summarised as: significant crushing of wood below the dowel, bending of the screw reinforcement with critical screw head embedment and fracture propagating up the specimen. The behaviour of specimens reinforced by screws with two different thread configurations matches the prediction and corresponds well with Section 4.1 in undamaged reinforced specimens.

Figure 4-37: Specimen in C6S showing broken screws with complete thread and fracture of wood.

An interesting finding is that for reinforced specimens with 6mm artificial cracks, some of the fully threaded screws broke into two parts as the specimen failed in tension, see Figure 4-37. This illustrates the significant tensile and bending stresses the screw carried in the specimen.

4.4.4.2 ANCOVA adjusted mean embedment strength

In this study, ANCOVA (Analysis of Covariance) is applied to compare the results between different groups. As the average density of each group varies slightly (from 431-450kg/m^3), it is considered as the covariance in this analysis. ANCOVA first adjusted the mean strength of each group due to the density variation and then used pairwise comparison to determine whether the difference between the two groups was significant. The adjusted value of mean strength is displayed in Table 4-10.

Figure 4-38: Picture showing the surface of C1.5BS4 with a knot above the dowel location.

After the test, it was found that specimen RS9 had a very high density (547 kg/m^3) resulting in a high embedment strength (40.38 N/mm^2) and lower ductility. Its high strength led to a significant difference between groups RS and RBS identified by ANCOVA (sig=0.04).

In addition, a knot appeared right on top of the dowel in specimen C1.5BS4 (with a density of 530 kg/m^3). Figure 4-38 shows that the crack in the failed specimen did not initiate from the top of the prepared hole but rather propagate along the side of the knot. The results of the two specimens are excluded in later analysis.

As can be seen in Table 4-11, a series of comparisons have been made by ANCOVA. For the unreinforced groups U, C1.5U, C4.5U and C6U, their adjusted mean strength (see Table 4-10) decreases with increasing crack width. The difference between each of them is significant.

As for reinforced specimens without cracks or with the same crack width, the adjusted strength is significantly higher than that of the corresponding unreinforced specimens. This implies that screws with two types of thread configuration effectively improved the strength of the cracked specimen.

From Table 4-10, the adjusted mean strength of specimens reinforced by screws with complete thread is higher than that of screws with 33% thread on the point end, with the same crack width. However, as can be seen in Table 4-11, the difference between the two types of thread configuration is only significant (sig = 0.003) when the crack is increased to 6mm. This implies that the effectiveness of using screws with 33% thread on the point end is limited to smaller cracks.

Table 4-11: Pairwise comparison of ANCOVA (excluding the result of specimen RS9 and C1.5BS4).

	U	RS	RBS	C1.5U	C1.5 S	C1.5BS	C4.5U	C4.5S	C4.5BS	C6U	C6S	C6BS
U												
RS	*0.000**											
RBS	*0.000**	*0.075*										
C1.5U	*0.000**	*0.000**	*0.000**									
C1.5S	*0.000**	*0.001**	*0.118*	*0.000**								
C1.5BS	*0.003**	*0.000**	*0.005**	*0.000**	*0.183*							
C4.5U	*0.000**	*0.000**	*0.000**	*0.000**	*0.000**	*0.000**						
C4.5S	*0.643*	*0.000**	*0.000**	*0.000**	*0.000**	*0.001**	*0.000**					
C4.5BS	*0.061*	*0.000**	*0.000**	*0.000**	*0.000**	*0.000**	*0.000**	*0.154*				
C6U	*0.000**	*0.000**	*0.000**	*0.000**	*0.000**	*0.000**	*0.000**	*0.000**	*0.000**			
C6S	*0.056*	*0.000**	*0.000**	*0.000**	*0.000**	*0.000**	*0.000**	*0.144*	*0.972*	*0.000**		
C6BS	*0.000**	*0.000**	*0.000**	*0.498*	*0.000**	*0.000**	*0.000**	*0.000**	*0.002**	*0.000**	*0.003**	

**Sig < 0.05 indicates a significant difference between the two groups.*

4.4.4.3 Relationship between embedment strength and crack width

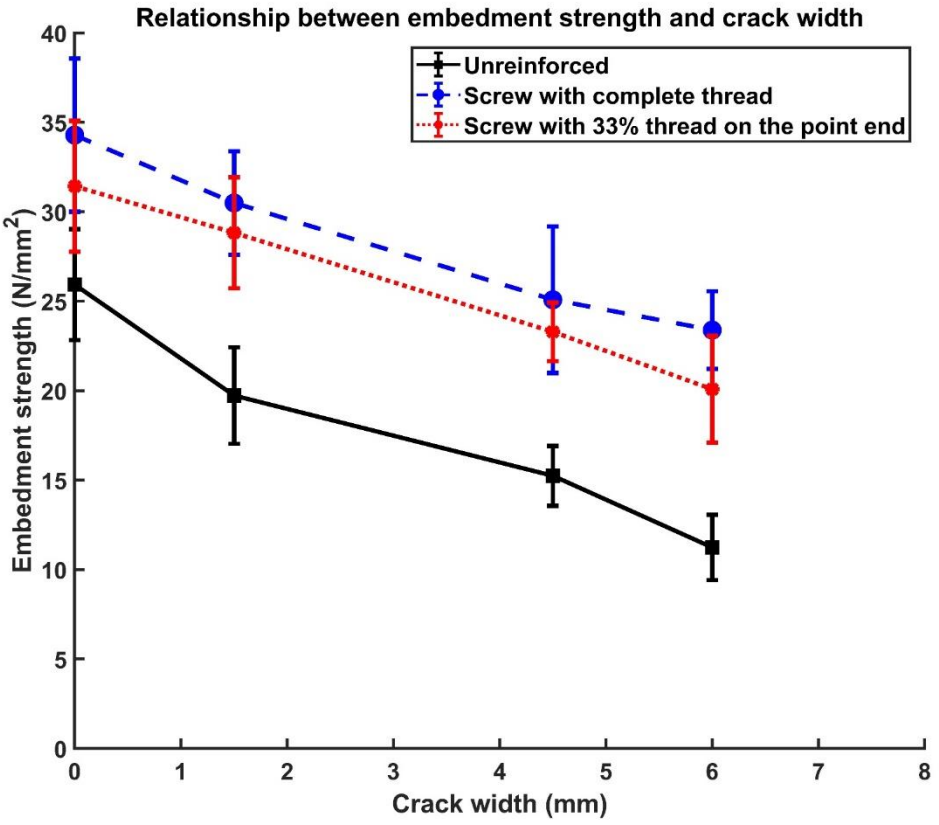

Figure 4-39: Plot of strength versus crack width (excluding the result of specimen RS9 and C1.5BS4).

The relationship between mean embedment strength and crack width is plotted in Figure 4-39. For all unreinforced and reinforced groups, their mean embedment strength decreases linearly with the increase of crack width. Overall, the embedment strength of specimens reinforced by screws with 33% thread on the point end is lower than that of screws with complete thread.

4.4.4.4 Relationship between ductility and crack width

In terms of ductility, the differences between reinforced and unreinforced specimens are significant. The unreinforced cracked groups lost at least 72.9% of original ductility when compared to group U. The difference between the unreinforced cracked groups with regard to the width of crack is not significant, as shown by the black line in Figure 4-40. It shows a trend that when the cracks in timber exceed 1.5mm, the ductility of the connection was reduced. This is because the restraint of movement perpendicular to the grain is heavily reduced by crack.

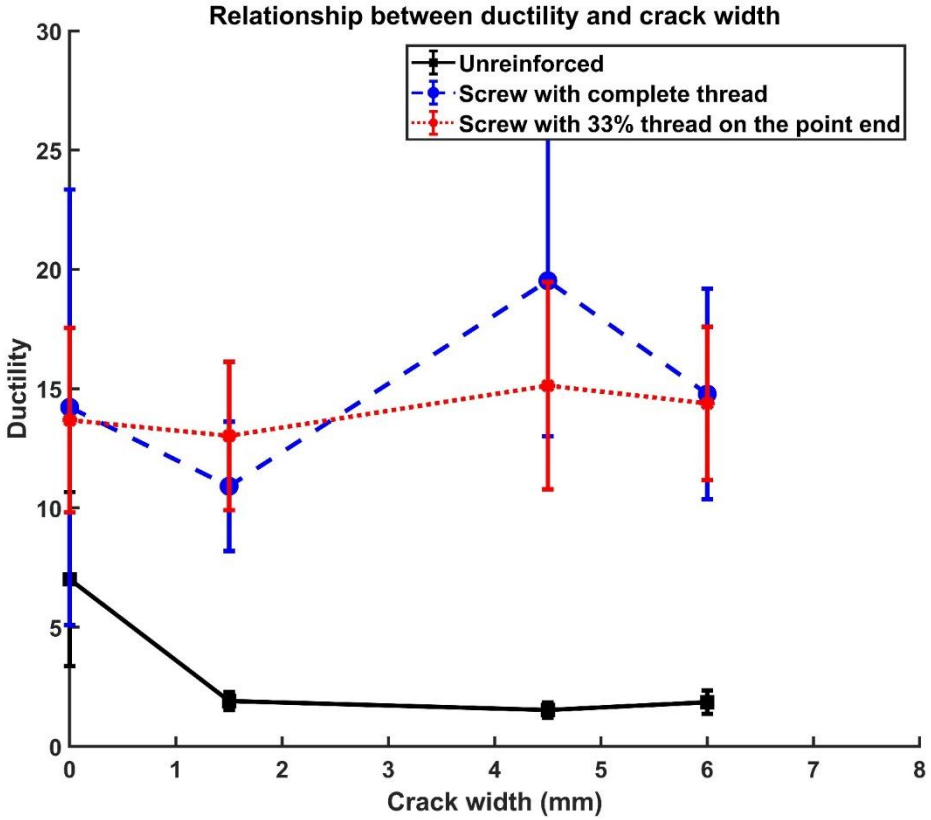

Figure 4-40: Plot of ductility versus crack width (excluding the result of specimen RS9 and C1.5BS4).

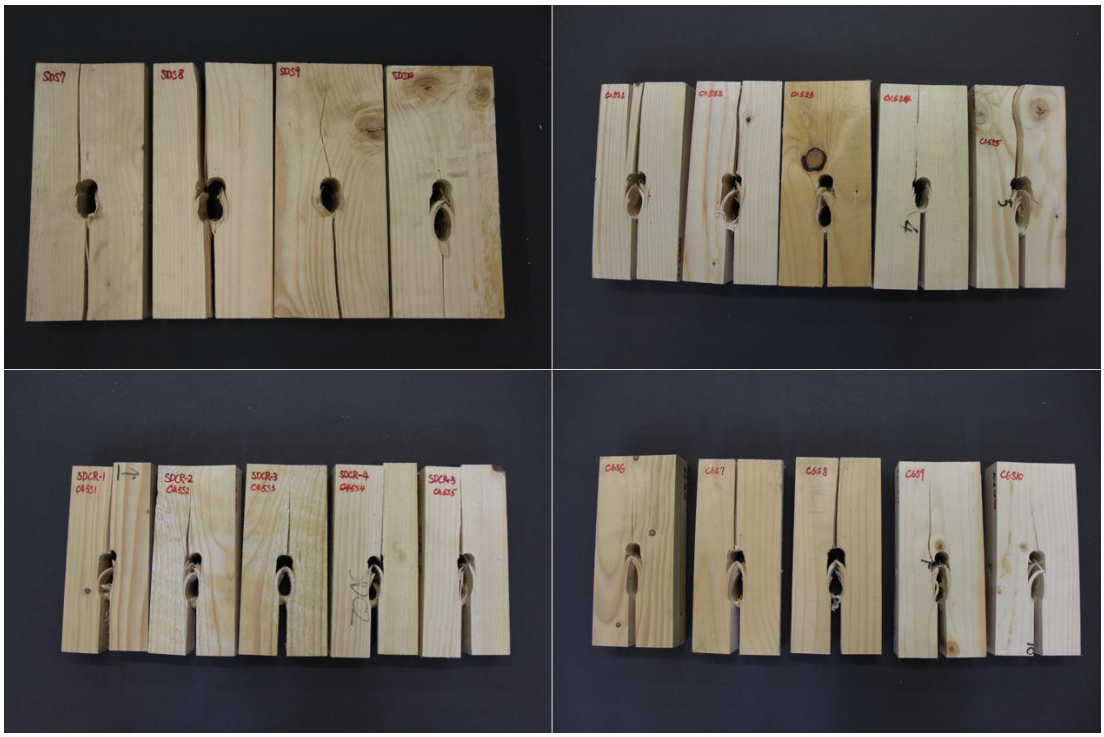

Figure 4-41: Pictures show the surface of specimens in groups: SDS (top left), C1.5S (top right), C4.5S (bottom left) and C6S (bottom right).

As shown in Figure 4-40, there are fluctuations for specimens reinforced by screws with complete thread. Similar fluctuation is also found in stiffness (see Figure 4-42). A possible reason is that the specimens in group C4.5S have fewer knots than those in other groups (see comparison in Figure 4-41). Overall, the two reinforced groups show significant improvement of ductility by at least 5 times when compared to the unreinforced cracked specimens, while the difference between them is not significant.

4.4.4.5 Relationship between stiffness and crack width

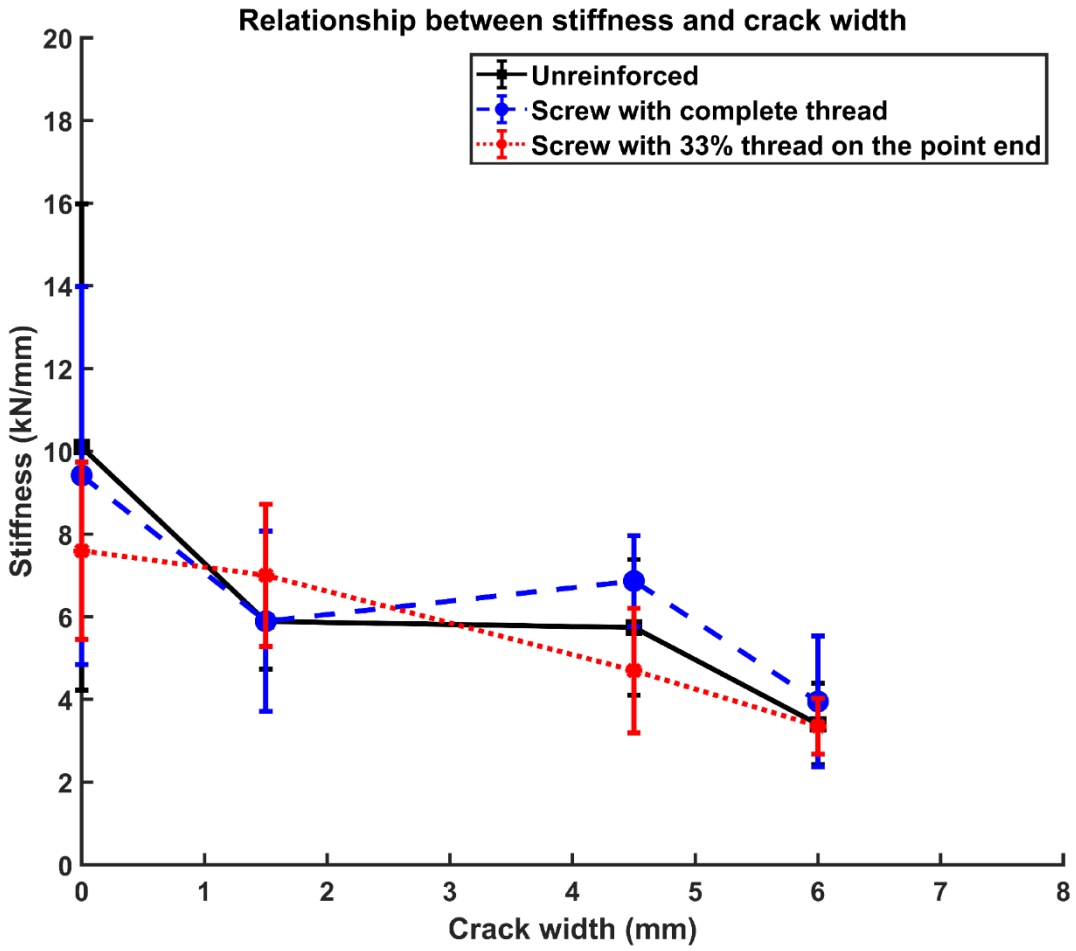

Figure 4-42: Plot of stiffness versus crack width (excluding the result of specimen RS9 and C1.5BS4).

As for the stiffness, a trend of decreasing stiffness with increasing crack width can be observed. The reduction of stiffness does not show significant difference between reinforced and unreinforced specimens with increasing crack widths. Thus, screw reinforcement provides very little improvement to the stiffness of a specimen.

4.4.4.6 Application of self-tapping screws as reinforcement on cracked single dowel connections

In Figure 4-39, with a 4.5mm width of crack, the embedment strength of specimens reinforced by screws with partial thread on the point end is restored to its original state. In addition, the ductility of the specimen with a 4.5mm crack is increased by at least 116% when compared to the undamaged unreinforced group, see Figure 4-40. Therefore, it implies the possibility that self-tapping screws with either of the thread configurations applied in this study can restore the strength and further enhance the ductility of a single dowel connection with a crack width up to 4.5mm.

4.4.5 Summary

This study investigated the performance of self-tapping screws in enhancing the mechanical properties of damaged single dowel connections. In total, 12 groups of tests, involving two types of thread configurations and three different sizes of crack width, were conducted through embedment tests. The following points can be concluded from the results in this study:

- Self-tapping screws showed effective performance in reinforcing cracked single dowel connections. The reinforced groups showed at least 53% improvement in embedment strength and over four times improvement in ductility when compared with unreinforced specimens with the same width of the artificial crack.
- The mean embedment strength of specimens reinforced by screws with 33% thread on the point end was generally lower than that of specimens reinforced by screws with 100% thread. However, the difference was only significant when the crack width was increased to 6mm. This implies that screws with 33% thread on the point end might only be applicable to uncracked dowel-type connections or those which only develop small cracks.
- A linear relationship between embedment strength and the width of crack is found in unreinforced and reinforced groups.
- The ductility was significantly improved by screws regardless of the type of thread configuration. The results also imply that with an artificial crack, the ductility of unreinforced specimens does not change significantly with increasing crack width. Similarly, in screw-reinforced specimens, ductility is not greatly influenced by the introduction of a crack and increasing crack width.

In the next chapter, the experimental study on reinforcing multiple-dowel timber connections using self-tapping screws is presented. The mechanical performance of the connections reinforced by screws with different thread configuration is compared and discussed. This study aims to confirm the results from the first section of this chapter that screws with reduced thread are as effective as fully threaded screws when they are applied on multiple-dowel connections.

Chapter 5 Multiple-Dowel Tensile Connections with Screw Reinforcement

The content of this chapter is published in the '*Proceedings of World Conference on Timber Engineering 2016*'.

5.1 Introduction

In timber dowel-type connections, the geometry of the fastener determines whether there are tensile stresses perpendicular to the grain and a tendency to form a crack in the wood adjacent to the fastener. Reinforcement using self-tapping screws can control the splitting of wood by providing restraints on both sides of the crack. At one side, the screw head provides pull-through resistance. At the other side, it is the anchoring of the thread in the wood.

Chapter 3 identified the risks of damaging the self-tapping screw due to the high drive-in torque required for fully threaded screws and suggests using partially threaded screws. In Chapter 4 (Section 4.1), it is identified that thread configuration can influence the enhancement of embedment strength and ductility of single dowel connections. In addition, using self-tapping screws with partial thread on the point end achieved similar enhancement to the fully threaded screws. However, the findings cannot reflect the impact of thread configuration on more practical cases, such as a connection with multiple dowels.

Therefore, Chapter 5 aims to investigate the influence of thread configuration and screw to dowel distances on multiple-dowel connections, through experimental tests.

5.2 Materials and methods

5.2.1 Material preparation

The connections were prepared from several batches of C24 European Whitewood beams with an average density of 467kg/m^3 (CoV=11.6%) and an average moisture content of 11% (CoV=10.91%). The timber beams were prepared indoor at 21.6°C and 59% RH. The self-tapping screws were the same as used in Chapter 4 to ensure consistency in material properties. The thread configurations (0%, 33% and 100% thread) were also kept the same as used in Chapter 4. A grinder was used to remove the thread on the screws to achieve various thread configurations.

5.2.2 Tensile connections test set-up

The design of the timber-steel-timber connections followed the guidance given by EC5 (BSI, 2004). Details of the test set-up of the tensile connections are shown in Figure 5-1. The upper part of the connection was clamped to the loading head and was pulled upwards during the test. The lower part had the same geometry as the upper part and the middle steel plate was clamped to the base of the loading machine. For the convenience of observation, this study intended to control the failure of connections to the upper part by reinforcing the lower part. For all connections tested in this study, both unreinforced and reinforced, additional steel reinforcement was screwed to the sides of the timber members on the lower part. Linear Variable Displacement Transducer (LVDT) was attached to the connections to measure their displacements.

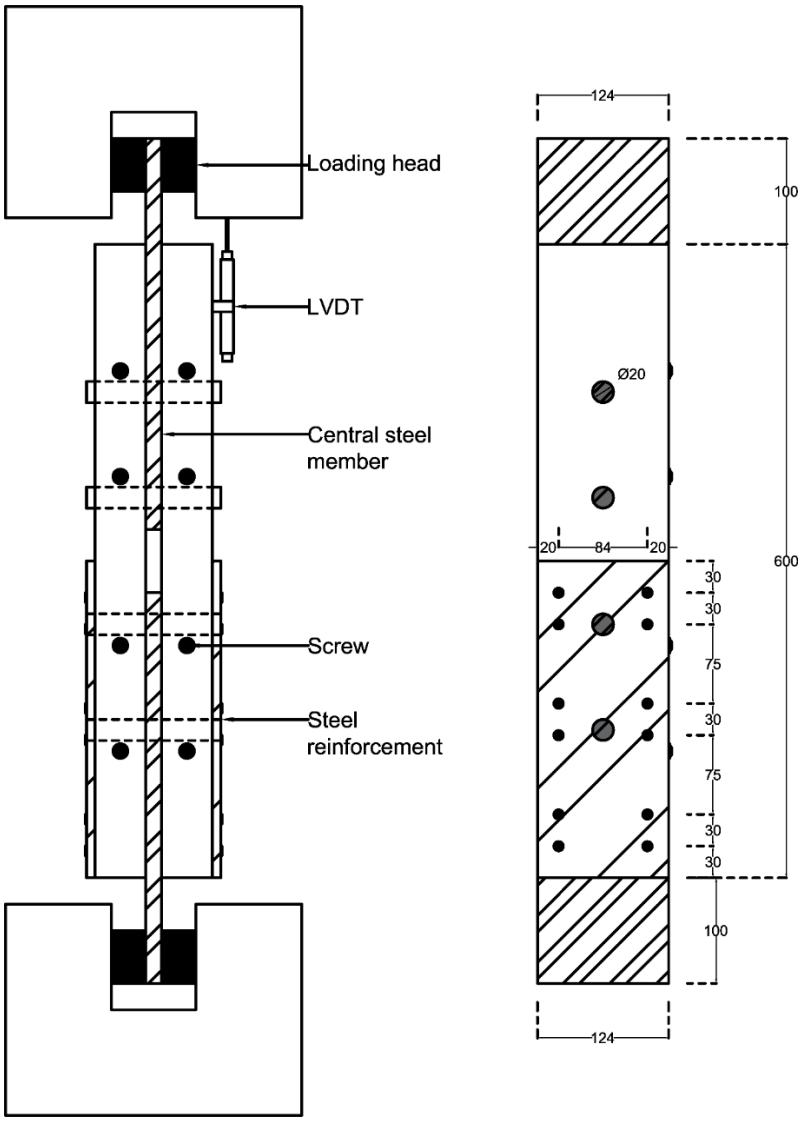

Figure 5-1: Specimen set-up (left) and dimensions for the specimen (right).

Table 5-1: Summary of groups in the connection tensile test.

Group	Description	Screw to dowel distance	No. of specimens	Mean density (kg/m^3) CoV	Mean M.C.% CoV
UC	*Unreinforced*	*N/A*	*10*	*459 (13%)*	*10.7 (10%)*
SNC	*Reinforced by screw with 0% thread (N)*	*1d*	*10*	*459 (10%)*	*11.0 (10%)*
SFC	*Reinforced by screw with 100% thread (S)*	*1d*	*10*	*475 (13%)*	*11.2 (12%)*
SPC	*Reinforced by screw with 33% thread on the point end (BS)*	*1d*	*10*	*476 (12%)*	*11.0 (12%)*

A total of four groups, each with 10 repetitions, were conducted and their details are tabulated in Table 5-1. Figure 5-2 shows the screws used in this study.

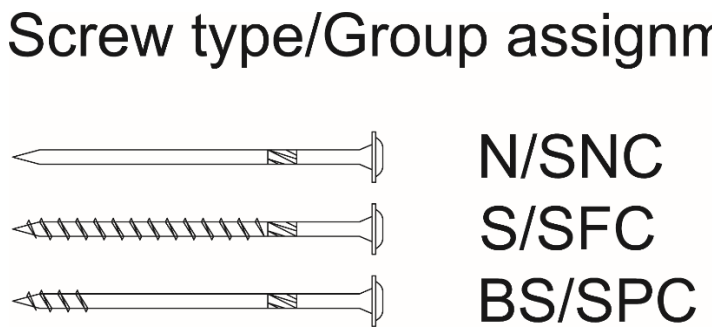

Figure 5-2: Screw types and corresponding group assignment.

The tensile tests were performed by the DARTEC loading machine with a capacity of 2000kN. The connection specimens were loaded in tension with a constant displacement rate of 2mm/min. The tests were stopped after a 20% load drop from the peak load had been observed.

5.3 Results and discussion

The load-displacement curves for each group are shown in Figure 5-3. Groups SFC and SPC show a higher load-carrying capacity and ductility than groups UC and SNC.

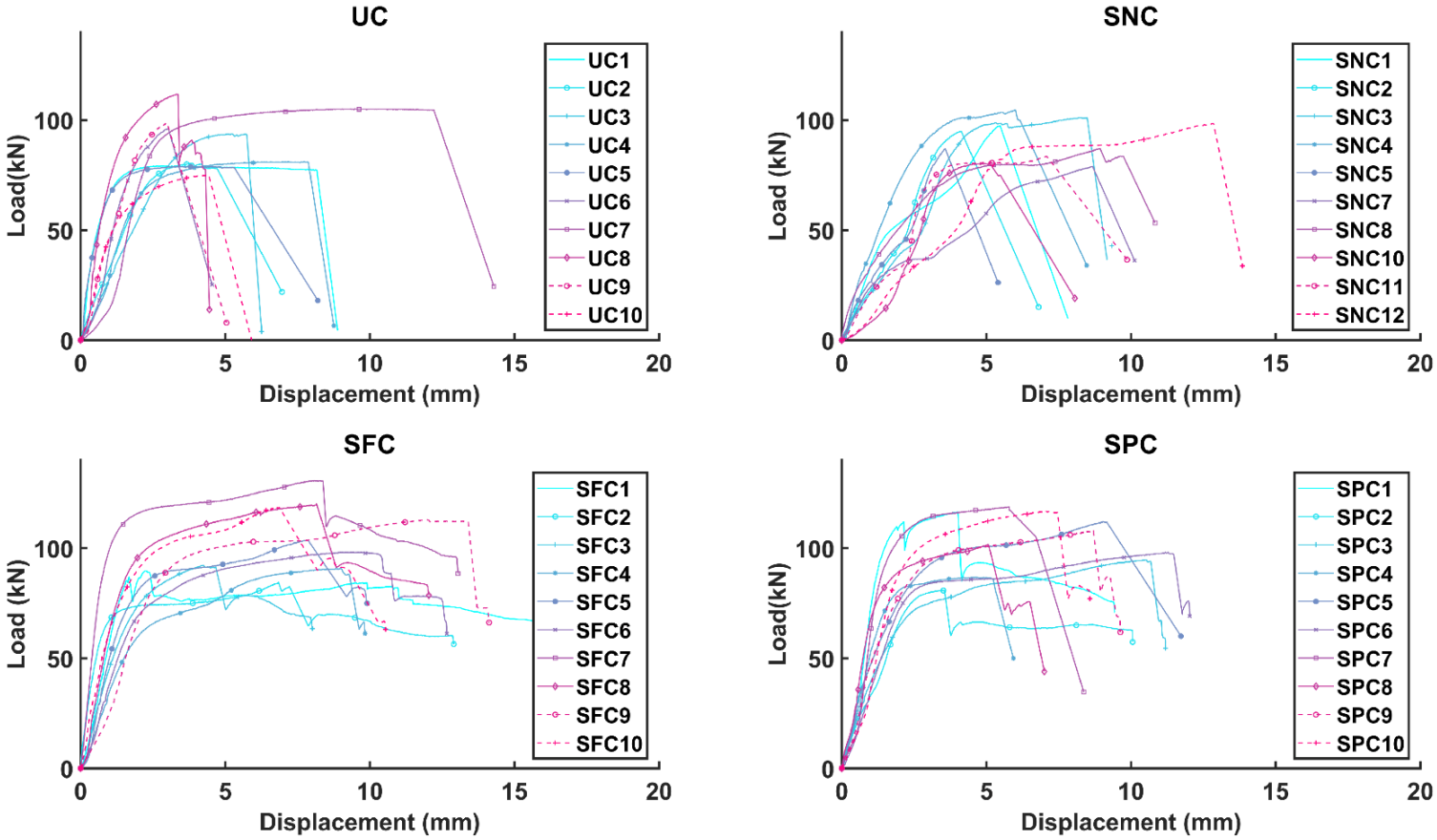

Figure 5-3: Load-displacement curves for each group in this study.

In the connection tests, splitting failure was observed to occur in the upper part of all specimens. After splitting of the wood, the load acting on the connections dropped dramatically for the group UC and SPC, while specimens in the reinforced groups SFC and SPC failed in a more ductile way with a gradual reduction of load. For most of the specimens in groups SFC and SPC, slight screw head embedment was observed. The screws in these groups were bent by the dowels as shown in Figure 5-4.

As the timber connections for each group were prepared from different batches of timber beams, the variation in density (see Table 5-1) may have resulted in different embedment strength and load-carrying capacities. To reduce this effect, the load-carrying capacity of the connections were adjusted by ANCOVA, based on their corresponding timber densities. The mean capacity for each group, after adjustment of ANCOVA, is presented in Table 5-2.

Figure 5-4: Timber members of connection specimens after failure showing deformation of screws. Top: connections reinforced by screws with complete thread (SFC). Bottom: connections reinforced by screws with 33% thread on the point end (SPC).

The load-carrying capacity of groups SFC and SPC showed at least 11% increase compared to the unreinforced group UC. The connections reinforced by screws without thread in group SNC only shows a slight increase of 0.3% when compared to the unreinforced connections.

Table 5-2: Results of load-carrying capacity adjusted by ANCOVA.

	UC	SNC	SFC	SPC
Mean load-carrying capacity adjusted by ANCOVA (kN)	*92.2*	*92.5*	*103.6*	*102.2*
Mean stiffness adjusted by ANCOVA (kN/mm)	*68.11*	*24.09*	*63.94*	*61.00*

Table 5-3: Results of pairwise comparison using ANCOVA.

	UC	SNC	SFC	SPC
UC				
SNC	*0.963*			
SFC	*0.018**	*0.020**		
SPC	*0.037**	*0.041**	*0.756*	

**Sig < 0.05 indicates a significant difference between the two groups.*

Table 5-3 shows that the load-carrying capacity was significantly improved in the two reinforced groups (SFC and SPC) when compared to the unreinforced group (UC). The load-carrying capacity between groups SFC and SPC does not differ significantly. For group SNC, the difference to group UC is not significant and its mean capacity is significantly lower than that of groups SFC and SPC. Overall, there is good agreement with previous results from the embedment tests in Section 4.1. The connection tests also confirmed that the thread on the point end is key to maintaining the effectiveness of reinforcement.

The stiffness of each connection was calculated using the gradient between $0.1F_{max}$ and $0.4F_{max}$ (F_{max} is the peak load) on the load-displacement curve. ANCOVA does not detect significant difference between group UC, SFC and SPC, indicating that screw reinforcement has less effect in strengthening the stiffness of connections. The stiffness of group SNC was found significantly lower than the other three groups. The members for Group SNC was prepared from a different batch of timber beams which may explain the variation in stiffness.

5.4 Implementing the embedment strength of reinforced specimen in connection design

Currently, there are no available methods to predict the load-carrying capacity of screw-reinforced dowel-type connections. Embedment strength, f_h, can provide a path to predicting the theoretical capacity of reinforced connections. Based on BS EN 14358:2016 (BSI, 2016), the corresponding characteristic values of the embedment strength (from Section 4.1) and the load-carrying capacity of connections (in this study) were calculated and shown in Table 5-4.

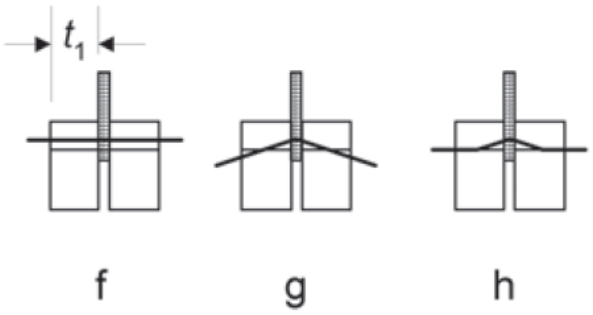

Figure 5-5: Failure modes for steel-to-timber connections that has a steel plate of any thickness as the central member of a double shear connection (EC5) (BSI, 2004).

According to EC5 (BSI, 2004), the load-carrying capacity for steel-to-timber connections are calculated using Equation (5-1) and Figure 5-5 shows the corresponding failure modes.

$$F_{v,Rk} = min \begin{cases} f_{h,1,k} t_1 d & (f) \\ f_{h,1,k} t_1 d \left[\sqrt{2 + \frac{4 M_{y,Rk}}{f_{h,1,k} d t_1^2}} - 1 \right] + \frac{F_{ax,Rk}}{4} & (g) \\ 2.3 \sqrt{M_{y,Rk} f_{h,1,k} d} + \frac{F_{ax,Rk}}{4} & (h) \end{cases} \quad (5\text{-}1)$$

where:

$F_{v,Rk}$ is the characteristic load-carrying capacity per shear plane per fastener;

$f_{h,1,k}$ is the characteristic embedment strength in the timber member;

t_1 is the smaller of the thickness of the timber side member or the penetration depth;

d is the fastener diameter;

$M_{y,Rk}$ is the characteristic fastener yield moment;

$F_{ax,Rk}$ is the characteristic withdrawal capacity of the fastener.

The calculated characteristic embedment strength of the reinforced specimen has been substituted into Equation (5-1) to replace the $f_{h,1,k}$ in the equation. The values from theoretical prediction are lower than the characteristic value from the connection test results, see Table 5-4. This implies that the prediction is conservative and offers the possibility of developing a method to predict the load-carrying capacity of screw-reinforced connections.

Table 5-4: Characteristic embedment strength, characteristic load-carrying capacity and theoretical prediction.

	U	N	S	BS
Characteristic embedment strength from Section 4.1 (N/mm^2)	*24.35*	*26.44*	*27.40*	*27.54*
	UC	SNC	SFC	SPC
Characteristic load-carrying capacity calculated based on 10 repetitions (kN)	*69.46*	*73.68*	*77.87*	*77.49*
Theoretical prediction using the characteristic value of embedment test (kN)	*65.49*	*68.93*	*70.52*	*70.75*

Previous studies, such as Bejtka and Blaß (2005), did not apply ANCOVA to include the influence of density, and consequently their results were scattered due to the variation in density. In this study, the influence of density was taken into consideration by ANCOVA, thus giving a more reliable comparison between group means.

The ductility of the connections has also been calculated using the method proposed by BS EN12512 (BSI, 2002) and the results are shown in Table 5-5.

Table 5-5: Average ductility of each group in connection test.

Group	UC	SNC	SFC	SPC
Mean ductility given by BS EN 12512 method (CoV)	*3.7 (54%)*	*2.9 (49%)*	*9.0 (52%)*	*4.9 (29%)*
Mean ductility given by K&C method (CoV)	*5.4 (52%)*	*2.9 (30%)*	*11.6 (44%)*	*7.1 (21%)*

By comparing the results from BS EN 12512 (BSI, 2002) and the Karacabeyli and Ceccotti method (K&C method) (Karacabeyli and Ceccotti, 1996), it shows that the European standard is more conservative in showing a lower ductility.

5.5 Summary

The connection tests showed good agreement with the embedment tests. This confirms that self-tapping screws can enhance load-carrying capacity and ductility. In addition, the results demonstrated that screws with partial thread on the point end achieved similar reinforcement performance to screws with complete thread.

The experimental work in this chapter established a foundation for Chapter 6 to further investigate the use of self-tapping screw with partial thread on the point end to reinforce multiple dowel-type connections when subject to a moment. The design of a connection to have adequate moment-resisting capacity is crucial in seismically active areas.

Chapter 6 Moment-Resisting Dowel-Type Connections with Screw Reinforcement

The majority of the content in Section 6.1 has been submitted to the journal of '*Construction and Building Materials*' and is under revision. The content in Section 6.2 is published in the '*Proceedings of World Conference on Timber Engineering 2018*'.

6.1 Screw reinforcement of cracked timber dowel-type moment-resisting connections

6.1.1 Introduction

Dowel-type connections are widely used in timber construction. As timber is weak in transferring load perpendicular to the grain, international standards have set ground rules to prevent splitting by limiting the minimum fastener spacing, end and edge distance in design. However, cracks can occur to existing timber connections due to moisture fluctuations. As the relative humidity varies in the environment, the wood tends to change its moisture content to achieve a balance. The material will change in size as it swells (increase in moisture content) or shrinks (decrease in moisture content). As the dimension of the wood changes, the fasteners in the connections tend to restrain this movement and stress will be concentrated in the wood around the fasteners. Excessive stresses can lead to cracking of the timber member and reduce the moment-resisting capacity and ductility of the connections. The moment-resisting capacity and ductility of a connection is usually critical, especially for high-rise timber buildings and structures in seismically active areas.

Pizzo *et al.* (2013), D'Ambrisi *et al.* (2014) and Metelli *et al.* (2016) have used steel plates and FRPs as reinforcement to repair damaged timber members. However, both reinforcement methods require a large amount of work and involve complex installation procedures. In addition, when such reinforcement is to be placed on the timber member, accessibility to a large surface area of the structural components is usually required and this can limit their application when repairing certain historical buildings.

Recent studies by Blaß and Schmid (2001), Bejtka and Blaß (2005) and Blaß and Schädle (2011) have indicated the potential use of self-tapping screws as reinforcement to dowel-type connections. Their work shows that self-tapping screws can effectively reduce the splitting tendency of the connections. Lam *et al.* (2008), Lam *et al.* (2010), Gehloff *et al.* (2010) and Closen and Lam (2012) investigated the effectiveness of using self-tapping screws as reinforcement in bolted timber connections under dynamic load. Lam *et al.* (2010) reported that screw reinforcement increased the moment-resisting capacity by 170% under reverse cyclic loading. In addition, self-tapping screws are easy to install and are less intrusive. A practical use of self-tapping screws to repair cracked dowel-type connections is shown in Figure 6-1.

The experiments in Chapter 4 (Section 4.1) and Chapter 5 have investigated the influence of thread configuration of self-tapping screws as reinforcement to dowel-type connections. The results indicated that screws with 33% thread on the point end achieved similar performance as reinforcement to that of screws with complete thread. The works in previous chapters suggested using partially threaded screws, as fully threaded screws are prone to damage due to the high frictional force induced during installation.

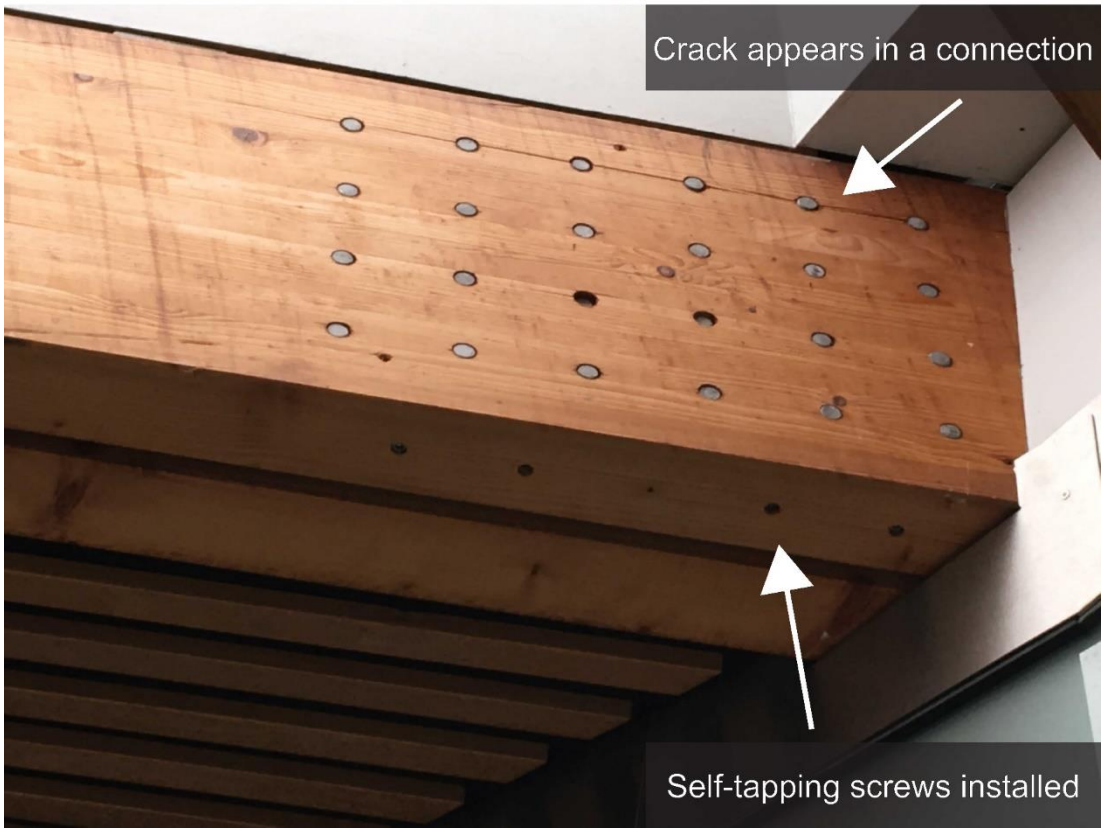

Figure 6-1: Self-tapping screws are installed from the bottom to repair the connection at the Forum, Exeter.

Delahunty *et al.* (2014) applied self-tapping screws to reinforce connections with artificial cracks and confirmed that the reinforcement can improve the load-carrying capacity of cracked connections. However, their work is limited to bolted connections loaded parallel to the grain.

Currently, there is limited knowledge on using self-tapping screws to reinforce or repair dowel-type moment-resisting connections. Therefore, the purpose of this study is to examine the effectiveness of self-tapping screws with various thread configurations in enhancing the moment resistance of timber connections with and without artificial cracks.

6.1.2 Materials and methods

The experimental tests in this study are sub-divided into two sections. First, the performance of the proposed screws with partial thread on the point end (herein referred to as Screw X) as reinforcement on moment-resisting connections. In the second section, the performance of screws with different thread configurations (herein referred to as Screw Y) as reinforcement on moment-resisting connections. Simpson Strong Tie ESCR 8.0×300 screws and Rothoblaas VGZ 7.0×300 screws, available on the commercial market, are used for Screws X and Y, respectively.

6.1.2.1 Repairing cracked connections with partially thread self-tapping screws

In this section, two independent variables are introduced: unreinforced and reinforced beams; undamaged beams and beams artificially damaged by cutting a crack at the location of fasteners.

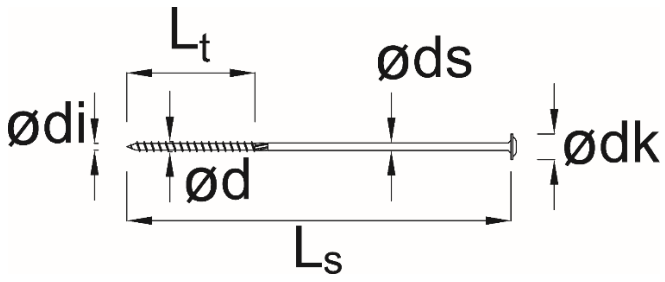

Figure 6-2: Self-tapping Screw X (8.0mm×300mm) used in this study.

In Chapter 3, Screw Y with 33% thread demonstrated a lower drive-in torque than the fully threaded screws. Therefore, this study tends to use self-tapping screws with reduced thread length along their shank. This is practically necessary when long screws are used to reinforce members in large-scale timber structures. The fully threaded screws are vulnerable to

damage during installation as large friction forces are generated. Thus, 300mm long self-tapping screws (Screw X), with 100mm threaded part on the point end, were used to examine the performance of reinforcement.

The commercial glulam beams in this test were prepared from European Whitewood (*Picea abies*) classified to GL24c. They were conditioned to equilibrium moisture content before and after fabrication (at 21.6°C temperature and 59% RH). The measured average density is 419kg/m^3 (CoV=3.5%) and average moisture content is 8.4% (CoV=10.0%). A drawing of the screw with flange head is shown in Figure 6-2 and its detailed specifications and material properties from the technical approval (OIB, 2017) are listed in Table 6-1.

Table 6-1: Specifications of the self-tapping screw.

L_s (mm)	L_t (mm)	ød$_s$ (mm)	ød$_i$ (mm)	ød$_s$ (mm)	ød$_k$ (mm)
Screw length	Thread length	Shank diameter	Inner diameter	Outer diameter	Head diameter
300.00	100.00	8.00	5.30	5.90	20.00
Characteristic yield moment (Nm)			Characteristic tension resistance (kN)		
22.6			8.56		

In this study, the specimen was simplified to one timber member to simulate a timber-steel-timber connection. The span of the glulam beam was 1500mm and was taken to be sufficient to keep the effect of shear deflection in the beam to a negligible value.

Table 6-2: Summary of each groups.

Group	Description	No of tests	Mean density (kg/m^3) (CoV)	Mean M.C.% (CoV)
MCU	*Moment Connection Unreinforced*	*6*	*419 (6.0%)*	*7.8 (11.7%)*
CMCU	*Cracked Moment Connection Unreinforced, 1.5mm crack width*	*6*	*419 (2.2%)*	*8.8 (5.0%)*
MCBS	*Moment Connection Reinforced by Screw X*	*6*	*419 (2.5%)*	*8.8(5.5%)*
CMCBS	*Cracked Moment Connection Reinforced by Screw X, 1.5mm crack width*	*6*	*421(5.4%)*	*7.8 (15.9%)*

In total, 24 tests using 9 glulam beams were conducted and Table 6-2 lists the details of each group. The specimens for group CMCU were prepared from the tested groups MCU and MCBS using 6 beams (three from each group). One end of the tested beams was cut off and new fastener holes were prepared on the remaining part.

The timber-steel-timber connections consisted of 5mm steel plates slotted into the glulam beam with 67mm thickness on each timber side member. The configuration of the connections was designed according to EC5 (BSI, 2004) and the details are shown in Figure 6-3. The diameter of the dowel was 12mm and a 3×3 fastener group was used for the connections. The steel dowels and steel plates were made from bright mild steel 080A15T and S275, respectively.

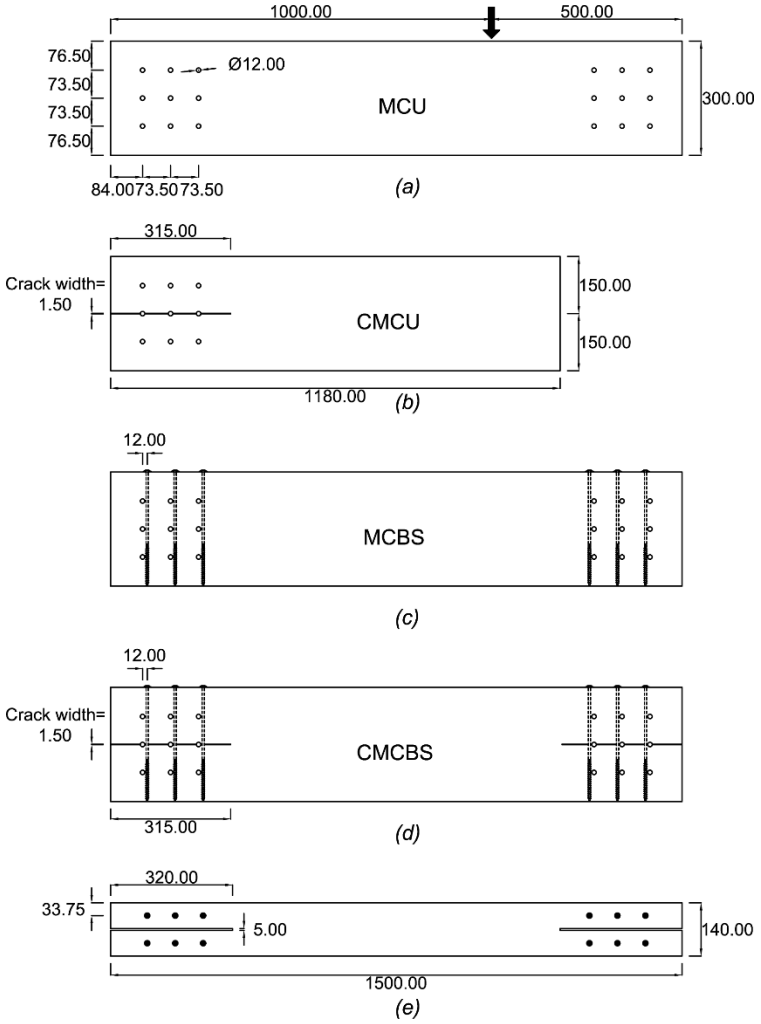

Figure 6-3: Specimen configurations: (a) Moment Connection Unreinforced (MCU), (b) Cracked Moment Connection Unreinforced (CMCU), (c) Moment Connection Reinforced with Screw (MCBS), (d) Cracked Moment Connection Reinforced with Screw (CMCBS) and (e) top view of the glulam beam indicating the positions of the screw reinforcement.

The artificial crack was prepared using a bandsaw which had a width of the saw of 1.5mm. The crack was located at the middle row of the dowels and the length was 315mm. A 6mm wide slot was then cut using the bandsaw on both ends of the beam for mounting the 5mm steel plate as the central member. A pre-drilled hole with 5.5mm diameter and 80mm depth was prepared using a pillar drill to ensure the 300mm self-tapping screw could be placed perpendicular to the grain.

After fabrication of the specimens, one side of the glulam beam on both ends was painted with black speckle patterns in a matt white background for DIC. The painted side covered an area of 300mm×315mm where the fastener group was located. DIC was used to track crack propagation and observe surface strain distribution. The painted surface had no difference from the non-DIC side; therefore, cracks could not be controlled to appear on the painted side for analysis.

Test set-up

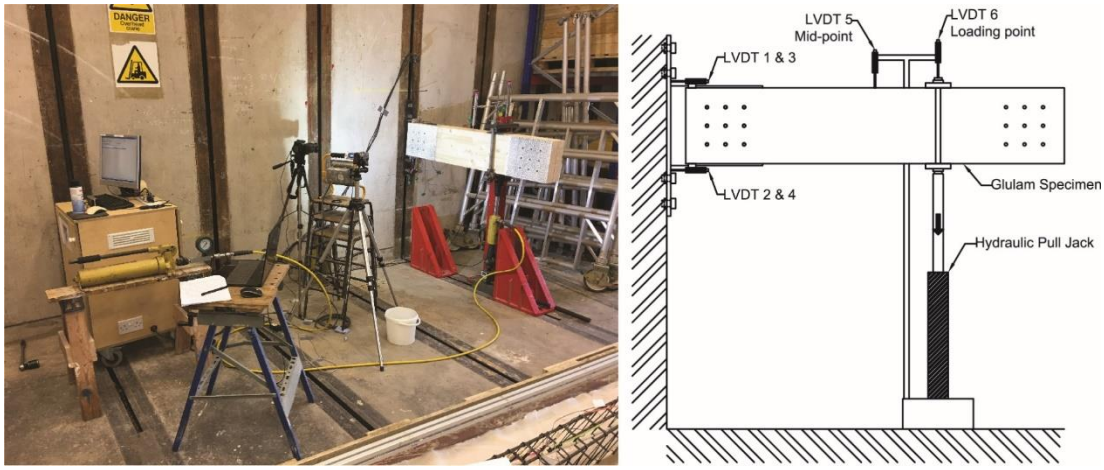

Figure 6-4: Moment-resisting connection test set-up (left) and locations of the LVDTs (right).

A general view of the test set-up is shown in Figure 6-4. The glulam beam and the steel plate were placed at 1200mm above the ground and a hydraulic pull jack (with 100kN capacity and 150mm stroke) was bolted to the strong floor in the laboratory. The hydraulic jack pulled the beam downwards 1 metre away from the fixed end and the load was distributed through a steel plate. In this static test, the connection specimens were loaded to failure with around 15-20% load drop from where the peak load was observed. The test was conducted in load-control and at each 0.5kN increment a picture was taken for DIC analysis.

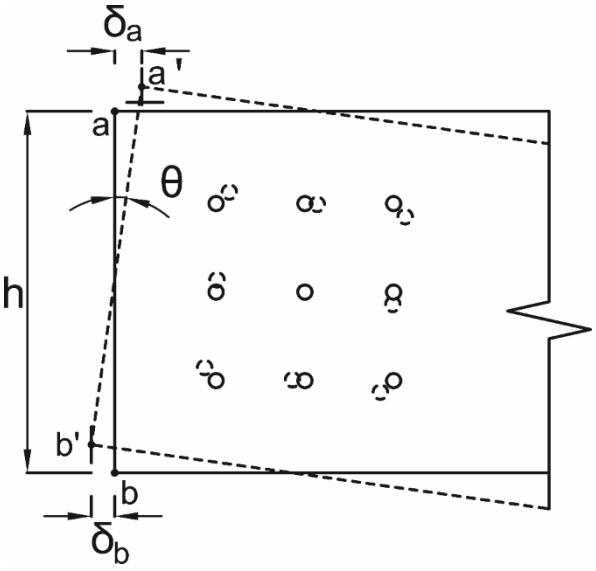

Figure 6-5: Schematic to measure the rotation of the connections.

A total of 6 LVDTs (100mm stroke, ±0.01mm accuracy) were deployed in each test and Figure 6-4 (right) shows their locations. LVDT 5 and 6 measured the vertical displacement at the mid-point (750mm away from both ends) and loading point (1000mm away from the left end of the beam), respectively. The rotation of the connections is calculated by considering the relative displacement between the LVDT on top and bottom of the beam. As shown in Figure 6-5, LVDT 1 measured the horizontal displacement from *a* to *a'* and LVDT 2 gave the measurement from *b* to *b'*. The angle of rotation of the connections can be calculated as:

$$\theta = arctan\left\{\frac{(a'-a)+(b'-b)}{h}\right\} = arctan\left\{\frac{\delta_a+\delta_b}{h}\right\} \qquad (6\text{-}1)$$

where:

h	is the vertical distance between the top and bottom LVDTs and was measured as 335mm in this study;
δ_a *and* δ_b	are the relative horizontal displacements of the two LVDTs.

6.1.2.2 Influence of thread configurations on enhancing moment-resisting capacity

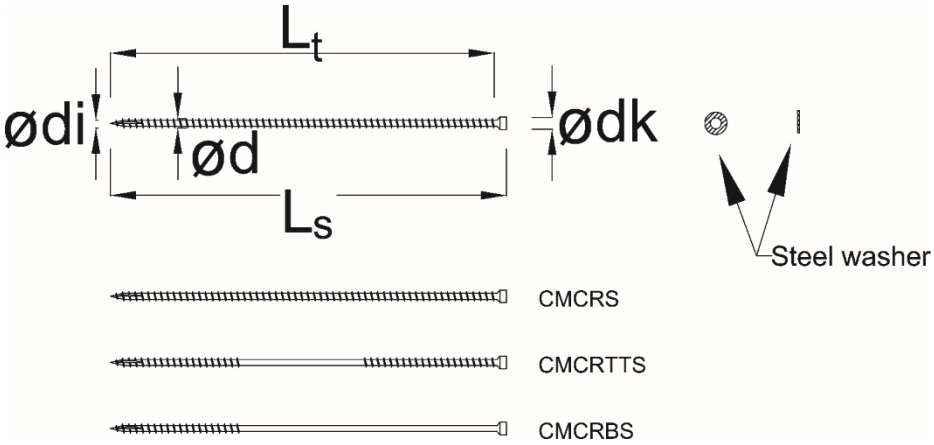

Figure 6-6: Drawings of screws with different thread configurations and washer used in this study.

The works in Chapter 4 (Section 4.1) and Chapter 5 only demonstrated the influence of thread configuration on embedment strength and tensile connection load-carrying capacity. This study intended to establish an understanding of how various thread configurations can influence the moment-resisting capacity of damaged connections. The beams were prepared from GL24c glulam timber. The timber beams were prepared at 21.6°C temperature and 59% RH. A different type of Screw *Y* (fully threaded) was used and its details are listed in Table 6-3. The self-tapping screw had a small cylindrical head thus a high strength steel washer was used. The washer had an inner diameter of 8.35mm and an outer diameter of 16.90mm with a thickness of 1.4mm. Details for the self-tapping screw and washer are shown in Figure 6-6.

Table 6-3: Specifications of the self-tapping screw Y.

L_s (mm)	L_t (mm)	ød (mm)	ødi (mm)	ødk (mm)
Screw length	Thread length	Outer diameter	Inner diameter	Head diameter
300.00	*290.00*	*7.00*	*4.60*	*9.50*

In total, three different thread configurations were used for comparison and each had three test repetitions. Their details and material properties are given in Table 6-4. The thread length ratio of screws in Groups CMCRBS and CMCRS was set to 1:3 as it was used in previous chapters. An artificial crack with 1.5mm width was applied to the middle row of the fastener group in the connections.

Table 6-4: Summary of each group.

Group	Description	No of tests	Mean density (kg/m^3) (CoV)	Mean M.C.% (CoV)
CMCRS	*1.5mm crack, reinforced by Screw Y with complete thread*	*3*	*422 (0.8%)*	*7.7 (3.7%)*
CMCRTTS	*1.5mm crack, reinforced by Screw Y with 33% thread on both ends*	*3*	*422 (3.0%)*	*7.9 (5.3%)*
CMCRBS	*1.5mm crack, reinforced by Screw Y with 33% thread on the point end*	*3*	*422 (1.4%)*	*7.7 (6.0%)*

The specimens used the same configuration as in the previous section. A total of nine tests were conducted over five glulam beams by using both ends of the beams. Figure 6-7 shows the specimen configuration and different thread configurations used on the screws.

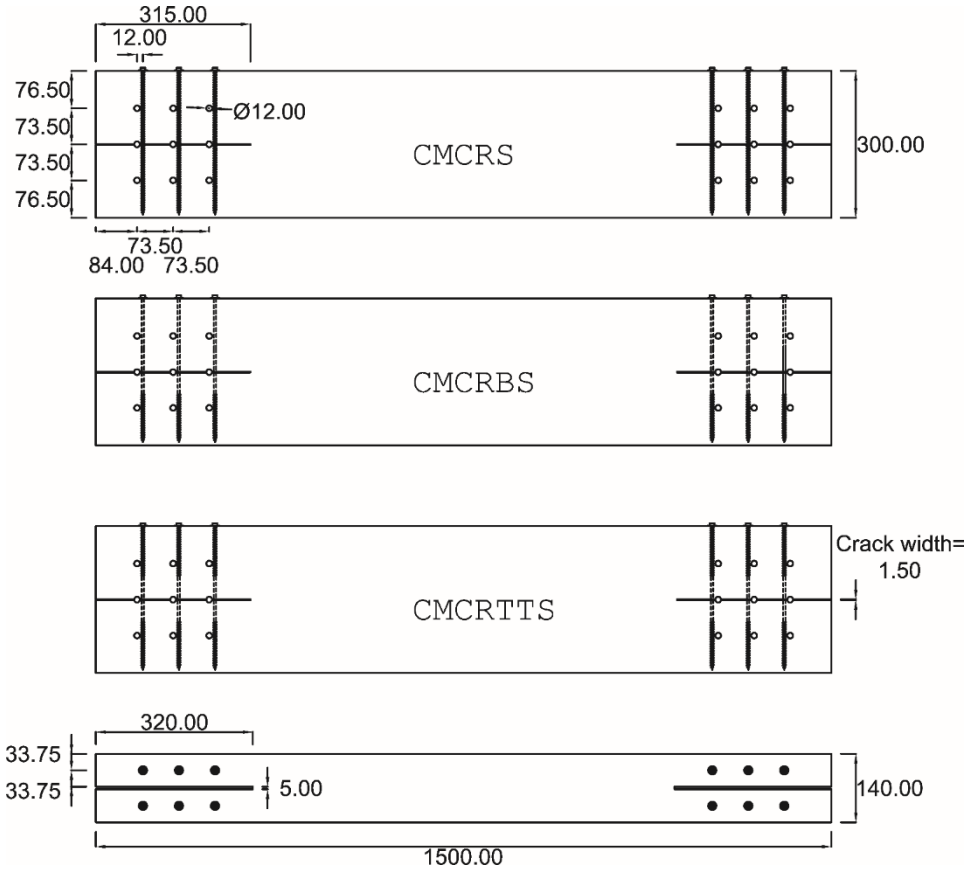

Figure 6-7: Specimen configurations: reinforced by fully threaded screws (CMCRS), reinforced by screws with 33% thread on the point end (CMCRBS) and reinforced by screws with 33% thread on both ends (CMCRTTS).

Test set-up

The test configuration was identical to the previous section except DIC was not applied in this test. The LVDTs were placed as shown in Figure 6-4. The specimens were either loaded to failure when 20% of load drop from maximum load was observed or when the 150mm stroke on the hydraulic jack was reached.

6.1.3 Results and discussion

6.1.3.1 Repairing cracked connections with partially thread self-tapping screws

Moment-rotation curves

Figure 6-8 demonstrates the moment-rotation curves for the four groups. During the test, the readings of some LVDTs stopped as the stroke on the LVDT was reached or the LVDT stuck due to the movement of the beam. Therefore, to reflect the actual rotational capacity of the connections, the rotation of the connections in the last image from DIC was calculated. A final point can be plotted with the rotation and the corresponding moment. A straight line is drawn between the last available data from the LVDT measurement and the calculated final point. Another method is to use the displacement of LVDT 5 which was placed at the mid-point of the beam. It was used to check the results of the former method. The average percentage difference is found to be 8.9% between the two methods.

As can be seen in Figure 6-8, even though a similar mean density and variation has been achieved (see Table 6-2), the connections within a group still display variation in moment-rotation curves. This could result from factors relating to local material defects, such as knots.

Table 6-5 summarises the results of the moment-resisting connection test. The rotational stiffness of each connection was calculated using the gradient between $0.1M_{max}$ and $0.4M_{max}$ (M_{max} is the peak moment resistance) on the moment-rotation curve. The density of connections varies in a range of 398-447kg/m^3 and is considered to have an impact on the test results. A higher density of wood can lead to higher embedment strength and thus a higher moment-resisting capacity. ANCOVA (Analysis of Covariance) is applied to examine the difference between the three groups after effectively removing the influence of density variation.

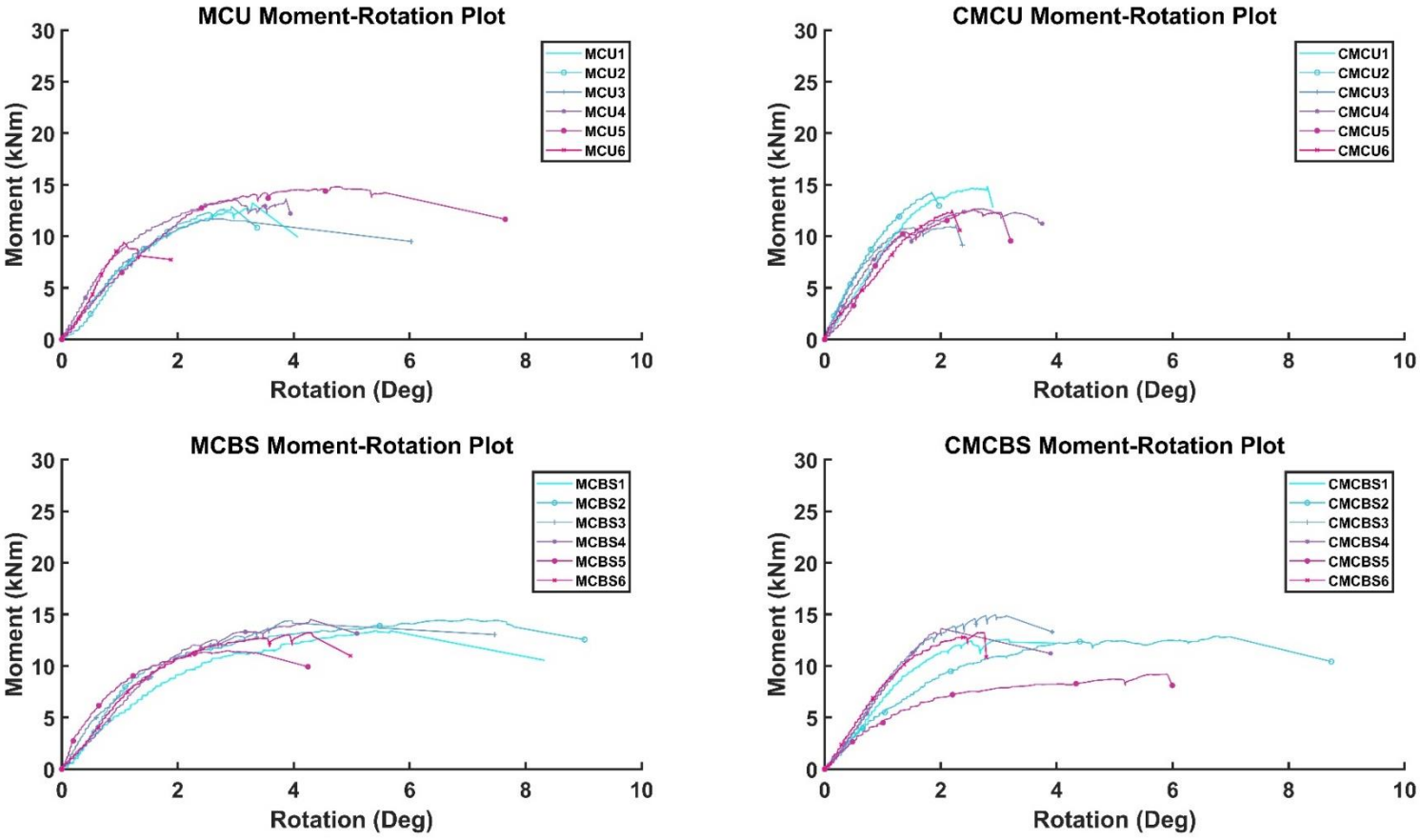

Figure 6-8: Moment-rotation curves for each group.

Table 6-5: Summary of results for each group.

Group	Mean moment-resisting capacity (kNm) (CoV)*	Mean maximum rotation (degree) (CoV) *	Mean rotational stiffness (kNm per degree) (CoV) *	Mean rotational stiffness (kNm per radian) (CoV) *
MCU	*13.07 (13%)*	*4.47 (49%)*	*9.26 (20%)*	*530.49 (20%)*
CMCU	*13.35 (10%)*	*2.74 (23%)*	*11.30 (22%)*	*647.24 (22%)*
MCBS	*13.92 (8%)*	*6.51 (31%)*	*9.18 (26%)*	*526.03 (26%)*
CMCBS	*13.35 (15%)*	*4.95 (44%)*	*8.28 (25%)*	*474.71 (25%)*

** The values are adjusted by ANCOVA, except the CoV remains for the value before the adjustment.*

In terms of moment-resisting capacity, no significant difference was found between the four groups in Table 6-5. The average capacity of the reinforced group MCBS is about 6.5% higher than the unreinforced group MCU. This implies that partially threaded self-tapping screws can slightly improve the moment-resisting capacity when placed at *1d* distance to the dowel. Comparing with group CMCU, it shows that screw reinforcement in group CMCBS did not effectively improve the moment-resisting capacity when the connection was damaged by an artificial crack.

For the connections designed in this study, a crack due to moisture variation may appear on the top, middle and bottom rows of the fastener group. This study focuses exclusively on connections that have a crack developed at the middle row. Group MCU shows a slightly lower capacity than group CMCU, which has a crack located at the middle row. The result may indicate that a crack located at the middle row may not significantly influence the moment-resisting capacity of a connection. The moment-resisting calculations later in this section also indicate that the middle dowels have the lowest capacity as the force acts perpendicular to the grain (wood with the lowest embedment strength), and they also have the shortest distance to the rotation centre.

For a connection, both the moment-resisting capacity and ductility are important. In this study, the rotational capacity of the connections is considered as an indicator of the ductility of the connections. A crack located at the middle row did not significantly reduce the moment-resisting capacity but it significantly reduced the rotational capacity of the connections which is a crucial factor for designing structures in seismic areas.

In terms of average rotation, the unreinforced group CMCU, with artificial cracks showed the lowest value; it had only 61% capacity of the original unreinforced group MCU. This

indicates that timber cracking can greatly reduce the rotational capacity of a connection. The reinforced group CMCBS that contained artificial cracks achieved the second-best maximum rotation; it had a capacity even higher than the unreinforced, undamaged ones, by 10.7%. This implies that screw reinforcement can restore the rotational capacity of damaged connections. Finally, the reinforced group MCBS showed the highest rotation, which met expectations, it improved the rotational capacity by 45.6%, when comparing with group MCU. The variation of rotation angle was higher for group MCU and CMCBS which could be a result of the inherent variability of wood materials.

As mentioned in the previous section, the specimens in group CMCU were prepared from the tested beams in groups MCU and MCBS. Specimens CMCU1-3 were prepared from MCU1, 3 and 6, respectively. Using the same beam reduces the variation of material properties due to defects, and a comparison of the moment-resisting capacity before and after the application of an artificial crack was made. Overall, it showed an increase of moment-resisting capacity of 13%, 19% and 11% for CMCU1-3 with an artificial crack. Such increase may explain why the group CMCU achieved higher moment-resisting capacity than group MCU. A possible explanation could be due to the local defects, as knots were identified in the glulam beams. After the beams were reused, the fastener groups were located on different locations. Thus, different locations of the fastener group along the beam may have different numbers of defects and the implication is difficult to measure. Therefore, more tests are recommended to minimise the influence of local defects.

For CMCU4-6, the specimens were prepared from group MCBS. However, a similar comparison is not possible with two variables because group CMCU contains artificial cracks without reinforcement while group MCBS contains reinforcement without artificial cracks.

A similar calculation of rotation angle is performed for the connections in groups MCU and CMCU using the same timber beams. An average of 73% of reduction of rotation angle was found when a crack was applied to the middle row. The results provide good correlation to the comparison of the rotation angle between groups MCU and CMCU.

To summarise, self-tapping screws with thread on the point end can slightly improve the moment-resisting capacity and rotational capacity of dowel-type connections when placed at *1d* distance from the dowel. It can also restore the rotational capacity of damaged connections to their original status.

Failure modes

Table 6-6: Summary on specimens after failure.

Specimen	Crack location and longest length on the DIC side	Crack location and longest length on the non-DIC side
MCU1	*Top row, 311mm*	*No crack*
MCU2	*Top row, 228mm*	*No crack*
MCU3	*No crack*	*No crack*
MCU4	*Top row, 559mm*	*No crack*
MCU5	*Bottom row, 459mm*	*No crack*
MCU6	*No crack*	*Top row, 402mm*
CMCU1	*No crack*	*Top row, 227mm*
CMCU2	*Top row, 353mm*	*No crack*
CMCU3	*Top row, 446mm*	*Top row, 312mm*
CMCU4	*Top and bottom row, 677mm*	*Top and bottom row, 617mm*
CMCU5	*Top and middle row, 273mm*	*Top and middle row, 246mm*
CMCU6	*No crack*	*Top row, 273mm*
MCBS1	*No crack*	*No crack*
MCBS2	*Top row, 159mm*	*No crack*
MCBS3	*Top row, 151mm*	*No crack*
MCBS4	*No crack*	*No crack*
MCBS5	*No crack*	*No crack*
MCBS6	*No crack*	*No crack*
CMCBS1	*Top row, 229mm; stress concentration on artificial crack*	*No crack*
CMCBS2	*Top row, 214mm; stress concentration on artificial crack*	*Top and bottom row, 221mm*
CMCBS3	*No crack; stress concentration on artificial crack*	*No crack*
CMCBS4	*No crack; stress concentration on artificial crack*	*No crack*
CMCBS5	*No crack; stress concentration on artificial crack*	*No crack*
CMCBS6	*No crack; stress concentration on artificial crack*	*No crack*

The major failure mode during this test was splitting failure of the beam parallel to the grain and the cracks were mostly located at the top rows of the fasteners group. All of the observed splitting of timber was sudden and accompanied by significant load drop. Table 6-6 provides a summary of the inspection of each specimen after failure. As the test configuration cannot control the initiation of crack to happen on a specific side, it is difficult to give a detailed observation of the cracks that appeared on the non-DIC side, which had no recording from the DSLR camera or digital video camera. The crack length on the DIC side was measured by the DIC software and for cracks on the non-DIC side, a tape measure was used.

As can be seen in Table 6-6, the majority of the unreinforced undamaged specimens had splitting on either side of the beam and all the unreinforced specimens with artificial cracks had significant wood splitting. The crack initiated around the end of the beam and most of the crack propagated either to or beyond the third dowel on the top row. An example of crack propagation in the unreinforced group is shown in Figure 6-9 (a). The average crack lengths for groups MCU and CMCU were 392mm and 356mm, respectively.

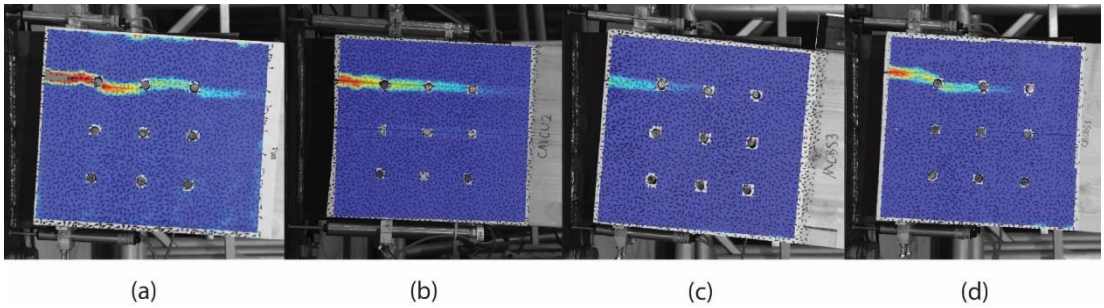

Figure 6-9: Observation from DIC on crack propagation at failure point (from left to right): (a) MCU1, (b) CMCU2, (c) MCBS3 and (d) CMCBS1.

In the reinforced group without artificial cracks, only two specimens, MCBS3 and MCBS4, developed a crack on the top row and their cracks reached the second dowel, at the point of failure. An example of crack on specimen MCBS3 is shown in Figure 6-9 (c). The average crack length for group MCBS was 155mm, approximately 60% reduction in length when compared with the unreinforced group MCU.

As for the reinforced specimens with artificial cracks, two of the connections developed new cracks apart from the existing pre-made crack. Their developed cracks reached the third dowel but did not propagate any further at the point of failure, as illustrated in Figure 6-9 (d). The rest of the group developed no additional cracks and DIC showed stress concentration along the artificial crack, as shown in Figure 6-10. The stress concentration along the crack was insignificant compared to the crack developed on the top row in Figure 6-9 (d) and thus

was not shown in the image. The average crack length for group CMCBS was 223mm which is 37% shorter than that of the cracked unreinforced group CMCU.

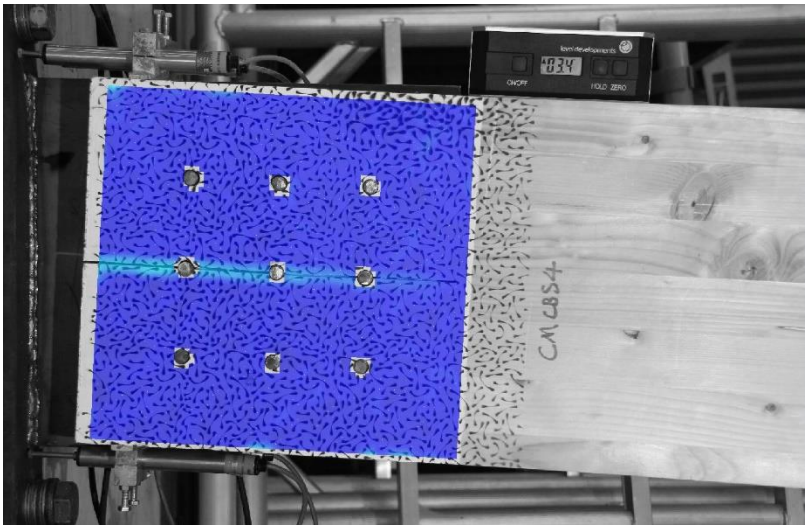

Figure 6-10: DIC analysis showing stress concentration around the artificial crack at the failure point of specimen CMCBS4.

By comparing the occurrence of splitting failure in the four groups, a preliminary conclusion is that self-tapping screws with partial thread on the point end can reduce the chance of crack initiation and effectively prevent crack propagation in moment-resisting dowel-type connections. The cracks in both reinforced groups show significant reduction in length compared to the unreinforced groups.

Figure 6-11: Bending of 5mm steel plates (left) and 15mm steel base plate (middle) and yielding of steel dowels (right).

In the test, bending of the steel dowels and steel plates was also observed, as shown in Figure 6-11. All the dowels except the central one in the moment-resisting connections displayed a level of yielding with a hinge formed at the midpoint of the axial length of the dowels. The yielding of the screw explains the reason for some connections showing load drop without the formation of a crack in Table 6-6. According to EC5, the failure mode of the connections

is mode type 2 which is a combination of embedment failure and single yield failure of the fastener.

However, none of the self-tapping screws used in this study displayed significant screw head embedment into the wood as shown in Figure 6-12. In the experiments in Chapter 4 (Section 4.1) and Chapter 5, screw head embedment is a result of a combination of bending of the screw and the action to split the wood by tensile load perpendicular to the grain. The self-tapping screws were retrieved after the test while visual observation does not identify significant damage to the screws.

Figure 6-12: The specimen from MCBS5 shows no sign of screw head embedment after the test.

One possible explanation is that some dowels were not in contact with the screw at the point of failure, because the self-tapping screws were placed at *1d* (≈ 12mm) distance from the dowel. The purpose of a *1d* spacing was to avoid the risk of the screw passing through the holes for the fasteners due to the existence of knots that may have caused the screw to deviate from its original vertical course during installation. The action of bending of the screw was not possible, thus, the embedment of the screw head was insignificant. The connection part of MCBS2 was cut off from the beam and a band saw was used to separate the part into two for inspection. In Figure 6-13, it is observed that, as suggested above, the dowels were not in contact with the screws by the point of failure of the connection.

Therefore, the tendency for screw head embedment mainly depends on the splitting action of wood. However, as recorded in Table 6-6, the reinforced connections showed no significant cracking, indicating that the splitting action is also reduced. This implies that self-tapping screws as reinforcement can effectively control crack propagation as a higher rotational capacity is found in the reinforced groups in Table 6-5.

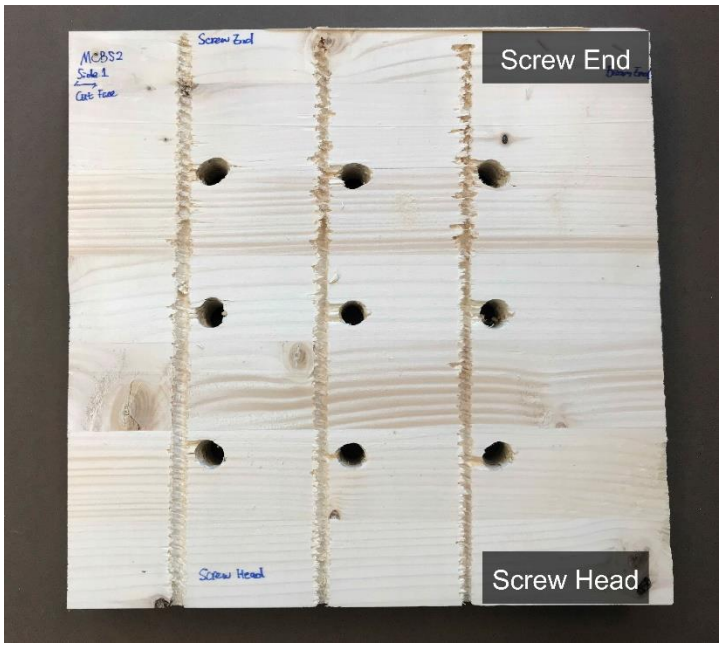

Figure 6-13: Inspection of screw and dowel interaction in the connection area in group MCBS2.

6.1.3.2 Theoretical prediction of moment-resisting capacity of dowel-type connections

Currently, the industry is promoting the use of glulam products and proposing large-scale, high-rise timber buildings. Studies have indicated that self-tapping screws are effective as reinforcement and also possess the advantage of simplicity, as they are easy to install and require less space than steel or FRP reinforcement. On the other hand, there is no guidance given in standards to calculate the moment-resisting capacity of dowel-type connections reinforced by self-tapping screws. Therefore, this study proposes a method to calculate the moment-resisting capacity of screw-reinforced dowel-type connections.

Assumption and procedures

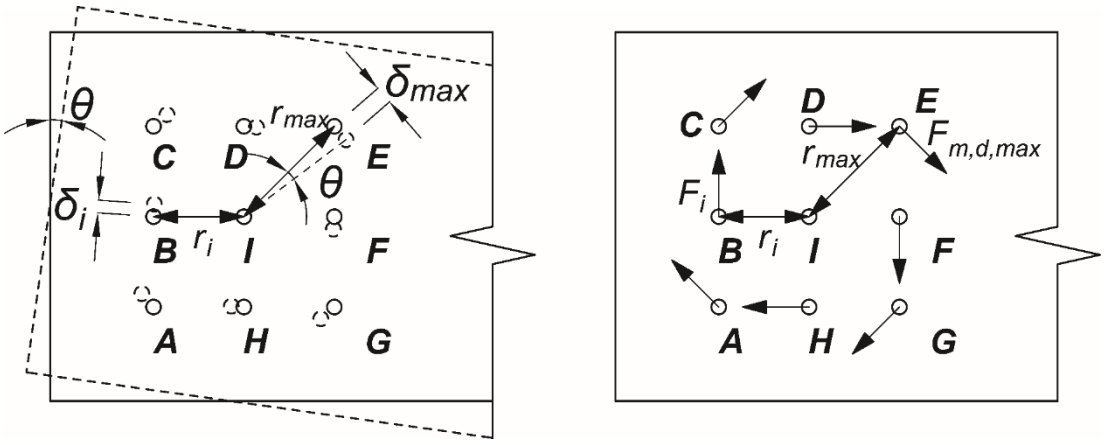

Figure 6-14: The rotational behaviour of the fasteners in the tested specimen.

Key points of the proposed prediction method are summarised in the following paragraphs.

The connection is regarded as rotationally rigid. For a rigid model, one important assumption is that the centre of rotation remains fixed under loading. In addition, the centre of rotation is taken as the centre of the fastener group and all the fasteners are applied with the same linear-stiffness behaviour in the analysis. Figure 6-14 shows the rotation of fasteners around the centre at angle, θ, and transfer loads normal to the direct distance from the centre.

The method is based on the calculation model that was demonstrated in Blaß (1995) and Porteous and Kermani (2013) for a rotationally rigid connection:

$$M_d = \left(\frac{F_{m,d,max}}{r_{max}} \sum_{i=1}^{n} r_i^2\right) \cdot n_{sp} \qquad (6\text{-}2)$$

where:

M_d	is the design moment-resisting capacity of the connections;
$F_{m,d,max}$	is the maximum load normal to its distance to the centre of rotation due to the moment imposed on the connections;
r_{max}	is the maximum distance between the dowel and the centre of rotation;
n	is the number of dowels;
i	represents the dowel in the connections;
r_i	is the distance between the dowel and the centre of rotation;
n_{sp}	is the number of shear planes.

In the experimental tests of this entire chapter, mode type 2 failure (including the embedment failure of wood and single yield failure of the dowel) was observed. For convenience, the labels for the dowels are used to represent the area where mode type 2 failure has occurred. For instance, '*failure of Area A'* indicates that dowel *A* and the wood around it has failed.

In the proposed method, the vertical load, *F*, acting on the beam is considered into calculation. With the additional vertical load, the angle of the total load on the dowel to the grain direction is changed and the corresponding embedment strength can be different, leading to various $F_{m,d,max}$ and M_d, for the dowels furthest from the centre of rotation (e.g. dowels *A* and *C* comparing to dowels *E* and *G* in Figure 6-15 (b) in the next section). Therefore, the fastener areas may not fail simultaneously even though they have same direct distance to the centre of rotation, as the local mechanical properties are influenced by the loading direction, reinforcement and artificial damage.

Thus, the fundamental idea of the proposed method is to input the characteristic embedment strength from Chapter 4 (listed in Table 6-7) to predict the $F_{m,k,max}$ and M_k based on the loading condition of each dowel. Then, finding the sequence of failure of the areas by sorting the acquired M_k values from the smallest to the largest. Finally, calculating the characteristic moment-resisting capacity of the connections by considering the early failure of certain areas.

The proposed method estimates the moment-resisting capacity at ultimate load. Due to the nature of the reinforcement method, not all the fasteners are bearing on the reinforced wood. Some of the fasteners are bearing on unreinforced wood leading to a lower load-carrying capacity and that area around it would tend to fail earlier than those having fasteners bearing on reinforced wood. It is less accurate to use the load-carrying capacity, which is calculated based on the condition that the fastener is bearing on unreinforced wood, to predict the moment-resisting capacity of the reinforced connections. Therefore, an assumption is made that the connection is effective until failure has occurred to three or four fastener areas, and the failed areas continue to provide their full load-carrying capacity and support to vertical load until the total number of failed areas reaches to 3 or 4. This is done in order to include the reinforcement effect when calculating the capacity of reinforced connections. To ensure consistency, this assumption is applied to all types of connections tested in this study.

Furthermore, this study assumes the vertical load on the dowels is evenly distributed. In a real connection, there is a lack of fit of the dowels (gaps around the dowels) at the beginning and the gaps close as the dowels take up load progressively. Therefore, the prediction in this study is based on the situation after initial rotation has closed the gaps around the dowels.

The characteristic moment-resisting capacity of the four types of connections are given in Table 6-8 and a demonstration of calculation is shown for the reinforced connections without crack.

Reinforced connections MCBS

The perpendicular distance L of the vertical load, F, to the centre of rotation of the connections is 842.5mm and the load is equally divided into nine components acting on the fasteners by two shear planes with each denoted as, F_v, as shown in Figure 6-15. The forces on the dowels due to the moment, M, are denoted as, F_X. The total forces acting on the dowels are represented by F_{TX} and their angles to the grain direction are represented by α_{TX} as demonstrated in Figure 6-15 (b) where X is the letter representing the dowel as shown in Figure 6-15. The direction of the total force on each dowel is different depending on the combination of the imposed loads. The maximum and minimum perpendicular distances from a fastener to the centre of rotation are 103.94mm (r_{max}) and 73.50mm (r_i), respectively.

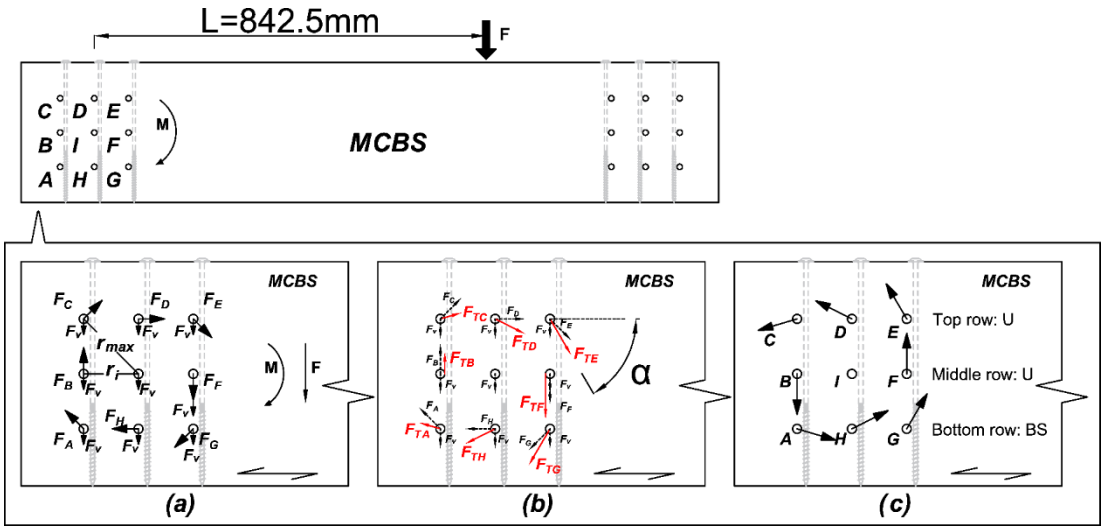

Figure 6-15: Forces and their directions on each dowel in group MCBS: (a) vertical load F_V and load due to rotation F_X imposed on each dowel; (b) total load F_{TX} and its direction α_{TX}; (c) the relative direction of movement of the dowels due to rotation.

Based on the demonstration in Figure 6-15, it can be found that dowels E and G are the critical points as they sustain the highest total load, which is a combination of the load due to moment and the vertical load. However, as indicated in Figure 6-15 (c), the relative movement of the dowels is anti-clockwise. Thus, only dowels A, H and G are bearing on screw-reinforced wood with a higher embedment strength and a higher load-carrying capacity. Therefore, it is assumed that failure occurs to Area E first.

The moment-resisting capacity of the connections, M_k can be expressed as:

$$M_k = FL = [(F_A + F_C + F_E + F_G) \cdot r_{max} + (F_B + F_D + F_F + F_H) \cdot r_i] \cdot n_{sp} \qquad (6\text{-}3)$$

where:

F is the vertical load acting on the beam in Figure 6-15;

L is the perpendicular distance of the vertical load, F, to the centre of rotation of the connections and is measured to be 842.5mm in this study;

r_{max} is the distance from the centre of the fastener group to the furthest fastener;

r_i is the distance from the centre of the fastener group to the furthest fastener;

n_{sp} is the number of shear planes.

In this study, a moment acting on the connection causes a rotation of θ and a displacement of δ_{max} in dowel E as shown in Figure 6-14. The load on the dowel due to the rotation is the product of the slip modulus and the displacement. For a rigid model, the dowels with equal perpendicular distance, either r_{max} or r_i, to the centre of rotation are subject to the same amount of load assuming they have same slip modulus, K, and rotation angle, θ. Thus:

$$F_A = F_C = F_E = F_G = K \cdot \delta_{max} = K \cdot r_{max} \cdot \theta \quad (6\text{-}4)$$

$$F_B = F_D = F_F = F_H = K \cdot \delta_i = K \cdot r_i \cdot \theta \quad (6\text{-}5)$$

where:

K is the slip modulus for each fastener and assumed to be a constant in here;

δ is the displacement of the fastener;

θ is the rotation of the connection.

The force F_E, acting on dowel E is under consideration in this step. The forces on dowels B, D, F and H are the same and their magnitude can be found by knowing the proportion between r_{max} and r_i based on Equations (6-4) and (6-5), therefore:

$$F_B = F_D = F_F = F_H = \frac{F_E}{r_{max}} \cdot r_i \quad (6\text{-}6)$$

The loads on dowels A, C, E and G are the same and substituting the load on each fastener in relation to the load on dowel E into Equation (6-3), the equation to calculate the characteristic moment-resisting capacity of the connections can be simplified and expressed as:

$$M_k = FL = (4F_E \cdot r_{max} + 4\frac{F_E}{r_{max}} \cdot r_i^2) \cdot n_{sp} \quad (6\text{-}7)$$

Rearranging the equation:

$$F_E = \frac{FL}{4n_{sp}} \cdot \frac{1}{(r_{max} + \frac{r_i^2}{r_{max}})} \tag{6-8}$$

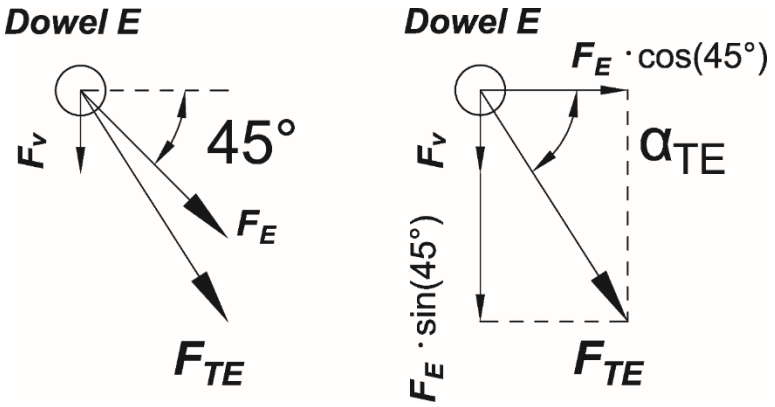

Figure 6-16: (a) The loads acting on dowel E; (b) Resolving the loads into vertical and horizontal components.

As shown in Figure 6-16 (b), the magnitude and angle of the total load on dowel *E*, F_{TE}, can be found by resolving F_v and F_E into horizontal and vertical components. The load due to moment, F_E, is at 45° to the horizontal direction. The load in the vertical direction is the sum of the F_v and the components of F_E:

$$F_{vertical} = F_v + F_E \cdot sin(45°) = \frac{F}{n_{sp}n} + F_E \cdot sin(45°) = \frac{F}{2\times9} + \frac{\sqrt{2}}{2}F_E = \frac{F}{18} + \frac{\sqrt{2}}{2}F_E \tag{6-9}$$

where:

F_v is the vertical load on the fastener;

F_E is the load on the fastener due to moment;

F is the vertical load on the connection;

n_{sp} is the number of shear planes;

n is the number of fasteners.

The horizontal component is contributed from the load F_E only. Therefore, the following equation can be established:

$$tan(\alpha_{TE}) = \frac{(\frac{F}{18} + \frac{\sqrt{2}}{2}F_E)}{\frac{\sqrt{2}}{2}F_E} \tag{6-10}$$

By substituting Equation (6-8) and the values for L, n_{sp}, r_{max} and r_i into Equation (6-10), the angle of F_{TE} to the grain direction, α_{TE} is:

$$\alpha_{TE} = tan^{-1}\left[1 + \frac{8\sqrt{2}}{18L} \cdot (r_{max} + \frac{r_i^2}{r_{max}})\right] = 48.15° \quad (6\text{-}11)$$

Thus, the total load on the dowel F_{TE} should not exceed the load-carrying capacity in this direction. The load-carrying capacity can be calculated using the following equations from EC5 (BSI, 2004):

$$F_{v,Rk} = min\begin{cases} f_{h,1,k} t_1 d & (f) \\ f_{h,1,k} t_1 d \left[\sqrt{2 + \frac{4M_{y,Rk}}{f_{h,1,k} d t_1^2}} - 1\right] + \frac{F_{ax,Rk}}{4} & (g) \\ 2.3\sqrt{M_{y,Rk} f_{h,1,k} d} + \frac{F_{ax,Rk}}{4} & (h) \end{cases} \quad (6\text{-}12)$$

where:

$f_{h,1,k}$ is the characteristic embedment strength in the timber member;

t_1 is the smaller of the thicknesses of the timber side member or the penetration

d is the fastener diameter;

$M_{y,Rk}$ is the characteristic fastener yield moment;

$F_{ax,Rk}$ is the characteristic withdrawal capacity of the fastener and is equal to zero for steel dowels.

$F_{v,Rk}$ depends on the characteristic embedment strength of the wood, $f_{h,1,k}$, in the loaded angle, α_{TE}, to the grain direction and in here is 0°, 45° and 90° as shown in Figure 6-14. Based on the characteristic embedment strength parallel to the grain, $f_{h,0,k}$, acquired from Chapter 4 Section 4.1, as shown in Table 6-7, and, $f_{h,1,k}$, can be calculated through the Hankinson formula given in clause 8.5.1.1 (2) in EC5:

$$f_{h,\alpha,k} = \frac{f_{h,0,k}}{k_{90} sin^2\alpha + cos^2\alpha} \quad (6\text{-}13)$$

where:

k_{90} is equal to 1.53 for a member made of softwood and connected by 12mm diameter dowels.

The embedment tests from Table 6-7 were acquired from previous tests of European Whitewood using 16mm dowels, with same material properties for the 12mm dowels used in this study. The loading direction of the embedment test was parallel to the grain.

There is other available literature that presents values of embedment strength of screw-reinforced wood such as Lederer *et al.* (2016). However, for several reasons, the results of their work are considered to be less reliable for the use of the prediction method in this study. Firstly, the screw to dowel distance is *1d* in this study whereas screw to dowel distance in Lederer *et al.* (2016) is '*in contact*' or '*at 2d distance*'. Secondly, this study uses the characteristic embedment strength to predict the characteristic moment-resisting capacity while the only available data from Lederer *et al.* (2016) is the mean value of embedment strength.

As mentioned previously, the wood that dowel *E* is bearing on is unreinforced due to the relative movement of the dowel during rotation; and, for a connection with dowel *E*, the load-carrying capacity can be found by using the unreinforced embedment strength (*U*) at 48.15˚ to the grain direction. For unreinforced wood, if no reference values are available from tests, the use of the formulas in EC5 Equation 8.31 is recommended to calculate the characteristic embedment strength. Another approach is to acquire the embedment strength experimentally following BS EN 383:2007 (BSI, 2007) and using BS EN 14358:2016 (BSI, 2016) to calculate the characteristic value.

Table 6-7: Summary of characteristic values calculated based on previous tests from Chapter 4.

Group	Description	Characteristic embedment strength from previous test, $f_{h,0,k}$ (N/mm^2)
U	*No crack, unreinforced*	*20.07*
BS	*No crack, reinforced by screw with 33% thread on the point end*	*24.80*
C1.5U	*1.5mm crack, unreinforced*	*14.91*

Thus, from Equation (6-12), $F_{v,Rk}$ is calculated to be 6.74kN (mode type 2 failure) and F_{TE} is not greater than this value. As the horizontal component of F_{TE} is contributed by F_E (see Figure 6-16), a relationship between F_{TE} and F_E is demonstrated below:

$$F_{TE} \cdot cos(48.15^{\circ}) = \frac{\sqrt{2}}{2} F_E \qquad (6\text{-}14)$$

Therefore, F_E equals to 6.36kN when the maximum value of 6.74kN is assigned to F_{TE}. Substituting the value of F_E into Equation (6-7), the characteristic moment-resisting capacity of the reinforced connections based on the load-carrying capacity of a connection contains dowel *E* is found to be 7.93kNm.

By this point, only one area has failed and the prediction does not consider the enhancement of embedment strength due to the screw reinforcement. Therefore, the predicted value is not

accurate enough for a reinforced connection. As previously mentioned, the failed area will still provide the load-carrying capacity and vertical support until two or three more areas fail. The ultimate state of the connections has not yet been reached.

To have a more accurate prediction, the capacity of the reinforced connections is checked regarding to Areas *C*, *F* and *G*, respectively, based on the failure of Area *E* (a combination of embedment failure and fastener failure). The connections are likely to fail at these locations with a higher total load (see Figure 6-15 (b)). A new equation is established based on the load on dowel *C* (F_C is equal to F_A) for demonstration:

$$M_k = FL = (3F_C \cdot r_{max} + 4\frac{F_C}{r_{max}} \cdot r_i^2 + F_E \cdot r_{max}) \cdot n_{sp} \qquad (6\text{-}15)$$

Rearranging the equation:

$$F_C = \frac{FL - F_E \cdot r_{max} \cdot n_{sp}}{(3 \cdot r_{max} + 4 \cdot \frac{r_i^2}{r_{max}}) \cdot n_{sp}} \qquad (6\text{-}16)$$

The above equation can be represented by:

$$F_C = xF - y \qquad (6\text{-}17)$$

Substituting the constants and the values for F_E from the previous calculation into the expressions:

$$x = \frac{L}{(3 \cdot r_{max} + 4 \cdot \frac{r_i^2}{r_{max}}) \cdot n_{sp}} = 0.81 \qquad y = \frac{F_E \cdot r_{max} \cdot n_{sp}}{(3 \cdot r_{max} + 4 \cdot \frac{r_i^2}{r_{max}}) \cdot n_{sp}} = 1.27 \qquad (6\text{-}18)$$

$$\therefore F_C = 0.81F - 1.27 \qquad (6\text{-}19)$$

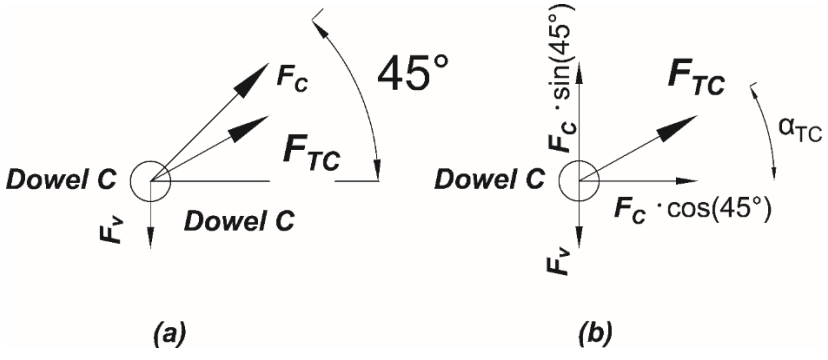

Figure 6-17: (a) The loads acting on dowel C; (b) Resolving the loads into vertical and horizontal components.

The angle between the total load on dowel *C* and the grain direction, α_{TC}, is assumed to be the angle when failure occurs to Area *E*. Unlike the expression in Equation (6-10), the load F_C, due to moment acting on dowel *C*, is in the opposite direction to the vertical load F_v, see

Figure 6-15 (b) and Figure 6-17 (a). Therefore, the relationship between α_{TC} and the horizontal and vertical components of F_{TC} is now:

$$tan(\alpha_{TC}) = \frac{\left(\frac{\sqrt{2}}{2}F_C - \frac{F}{18}\right)}{\frac{\sqrt{2}}{2}F_C} = 1 - \frac{F}{18} \cdot \frac{\sqrt{2}}{F_C} \qquad (6\text{-}20)$$

The corresponding load F_C on dowel *C* at that moment can be found using the relationship identified in Equation (6-4). Dowels *C* and *E* have the same distance to the centre of rotation r_{max}, slip modulus *K* and rotation angle θ:

$$F_C = \frac{K \cdot r_{max} \cdot \theta}{K \cdot r_{max} \cdot \theta} F_E \qquad (6\text{-}21)$$

The vertical load F_v on dowel *C* at that moment is the vertical load *F* on the beam divided by 18 (with nine dowels and two shear planes) (when dowel *E* has failed) and is calculated to be 0.52kN (from previous calculation on dowel *E*). Thus, the angle of the total load on dowel *C* can be found by substituting Equation (6-21) into Equation (6-20) and knowing the value of load F_E also from previous calculation on dowel *E*:

$$\alpha_{TC} = tan^{-1}\left[\frac{\left(\frac{\sqrt{2}K \cdot r_{max} \cdot \theta}{2\ K \cdot r_{max} \cdot \theta} F_E - \frac{F}{18}\right)}{\frac{\sqrt{2}K \cdot r_{max} \cdot \theta}{2\ K \cdot r_{max} \cdot \theta} F_E}\right] = tan^{-1}(1 - \frac{F}{18} \cdot \frac{\sqrt{2}}{F_E}) = 41.47° \qquad (6\text{-}22)$$

Dowel *C* will move away from the self-tapping screw (see Figure 6-15 (c)), meaning that the wood it bears on is not reinforced. Thus, the embedment strength is taken for the unreinforced value (*U*) in Table 6-7 at 41.47˚ to the grain direction, using the Hankinson formula (Equation (6-13)). The embedment strength is then substituting into the load-carrying capacity equations for a connection (Equation (6-12)). Therefore, the load-carrying capacity of a connection contains dowel *C* can be found as 7.01kN and the total load F_{TC} cannot be greater than this value.

For dowel *C*, a relationship between the total load F_{TC}, the load F_C due to the moment and the vertical load F_v can be established (see Figure 6-17 (b)):

$$F_{TC}^2 = (\frac{\sqrt{2}}{2}F_C)^2 + (\frac{\sqrt{2}}{2}F_C - \frac{F}{18})^2 \qquad (6\text{-}23)$$

Substituting Equation (6-19) into Equation (6-23), a quadratic equation with unknown *F* can be written as following:

$$0 = (x^2 - \frac{x\sqrt{2}}{18} + \frac{1}{324})F^2 + (-2xy + \frac{y\sqrt{2}}{18})F + (y^2 - F_{TC}^2) \qquad (6\text{-}24)$$

Where F_{TC} can be found using Equations (6-12) and (6-13) and the above equation can be solved which gives the values of *F* to be 10.72 or -7.43. The value of the load *F* is taken to be the positive solution of the quadratic equation. The characteristic moment-resisting capacity of the reinforced connections at the ultimate state is the product of the load on the beam (*F*) and the perpendicular distance of load to the centre of rotation (*L*) and is calculated to be 9.03kNm.

Using the same method for Area *C*, the characteristic moment-resisting capacity of the connections can be found when Areas *F* (at 9.15kNm) and *G* (at 9.17kNm) fail respectively, with prior failure to Area *E*. With a higher moment-resisting capacity than 9.03kNm, it implies that areas fail in a sequence of *E*, *C*, *F* and *G*. The next step is to find the moment-resisting capacity of the connections when Area *F* fails with Areas *E* and *C* having already failed. Similarly, an equation can be established as follows:

$$M_k = FL = (2F_F \cdot r_{max} + 4\frac{F_F}{r_{max}} \cdot r_i^2 + F_E \cdot r_{max} + F_C \cdot r_{max}) \cdot n_{sp} \qquad (6\text{-}25)$$

Repeating the above steps and using the unreinforced embedment strength (*U*) for the wood around dowel *F*, the characteristic moment-resisting capacity of the connections when Areas *E*, *C* and *F* have failed is 9.13kNm. As can be seen, the moment-resisting capacity has increased 16% from the first failure of Area *E*. However, the additional capacity due to the enhanced embedment strength from reinforcement is not considered as the wood around dowels *E*, *C* and *F* is unreinforced due to the movement of the dowels.

Thus, the final step is to calculate the moment-resisting capacity of the connections based on Area *G* with Areas *E*, *C* and *F* having failed already. Another equation is established:

$$M_k = FL = (2F_G \cdot r_{max} + 3\frac{F_G}{r_{max}} \cdot r_i^2 + F_E \cdot r_{max} + F_C \cdot r_{max} + F_F \cdot r_i) \cdot n_{sp} \qquad (6\text{-}26)$$

The wood around dowel *G* is assumed to be reinforced with an enhanced embedment strength calculated from (*BS*) in Table 6-7 and the final characteristic moment-resisting capacity of the reinforced connections MCBS is found to be 9.14kNm.

6.1.3.3 Predicted values for characteristic moment-resisting capacity

Table 6-8 lists the calculation steps for each group tested in this study. In groups CMCU and CMCBS, the dowels *B* and *F* will tend to move parallel to the grain direction and a crack passes through the dowels. Therefore, cracked unreinforced embedment strength of wood (*C1.5U*) from Table 6-7 is used.

Table 6-8: Summary of predicted values for the connections in this study and details for each calculation steps.

	Step	Calculation based on dowel	Early failure of area	Embedment strength based on previous study	Total load to grain angle α	Load on the early failed dowel (kN)	Moment-resisting capacity (kNm)
MCU				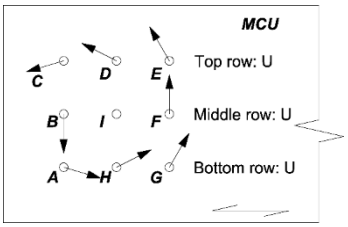			
	1	*E (G) **	*N/A*	*U*	*48.15˚*	*N/A*	*7.93*
	2	*C (A) **	*N/A*	*U*	*41.47˚*	*N/A*	*9.27*
	3	*C (A) **	*E & G*	*U*	*41.47˚*	*F_E=6.36*	*8.80*

$$M_k = FL = (2F_C \cdot r_{max} + 4\frac{F_C}{r_{max}} \cdot r_i^2 + F_E \cdot r_{max} + F_G \cdot r_{max}) \cdot n_{sp}$$

CMCU				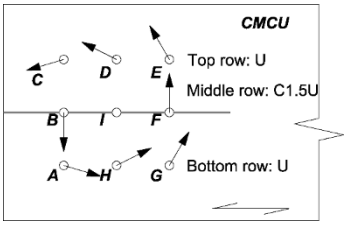			
	1	*F*	*N/A*	*C1.5U*	*90.00˚*	*N/A*	*7.55*
	2	*E (G) **	*F*	*U*	*48.15˚*	*F_F=4.28*	*7.90*

$$M_k = FL = (4F_E \cdot r_{max} + 3\frac{F_E}{r_{max}} \cdot r_i^2 + F_F \cdot r_i) \cdot n_{sp}$$

	Step	Calculation based on dowel	Early failure of area	Embedment strength based on previous study	Total load to grain angle α	Load on the early failed dowel (kN)	Moment-resisting capacity (kNm)
				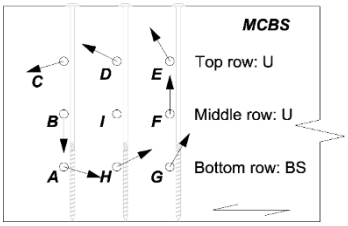			
MCBS	*1*	*E*	*N/A*	*U*	*48.15˚*	*N/A*	*7.93*
	2	*G*	*E*	*BS*	*48.15˚*	*F_E=6.36*	*9.17*
	3	*F*	*E*	*U*	*90.00˚*	*F_E=6.36*	*9.15*
	4	*C*	*E*	*U*	*41.47˚*	*F_E=6.36*	*9.03*
	5	*F*	*E & C*	*U*	*90.00˚*	*F_E=6.36, F_C=7.42*	*9.13*
	6	*G*	*E, C & F*	*BS*	*48.15˚*	*F_E=6.36, F_C=7.42, F_F=5.33*	*<u>9.14</u>*

$$M_{\mathrm{k}} = FL = (2F_{\mathrm{G}} \cdot r_{\max} + 3\frac{F_{\mathrm{G}}}{r_{\max}} \cdot r_{\mathrm{i}}^2 + F_{\mathrm{E}} \cdot r_{\max} + F_{\mathrm{C}} \cdot r_{\max} + F_{\mathrm{F}} \cdot r_{\mathrm{i}}) \cdot n_{\mathrm{sp}}$$

				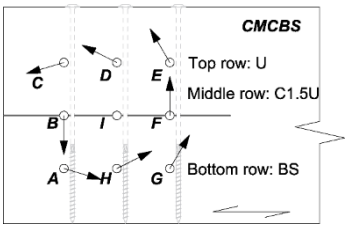			
CMCBS	*1*	*F*	*N/A*	*C1.5U*	*90.00˚*	*N/A*	*7.55*
	2	*E*	*F*	*U*	*48.15˚*	*F_F=4.28*	*7.90*
	3	*C*	*F & E*	*U*	*41.47˚*	*F_F=4.28, F_E=6.36*	*8.88*
	4	*G*	*F & E*	*BS*	*48.15˚*	*F_F=4.28, F_E=6.36*	*9.02*
	5	*G*	*F, E & C*	*BS*	*48.15˚*	*F_F=4.28, F_E=6.36, F_C=7.40*	*<u>8.99</u>*

$$M_{\mathrm{k}} = FL = (2F_{\mathrm{G}} \cdot r_{\max} + 3\frac{F_{\mathrm{G}}}{r_{\max}} \cdot r_{\mathrm{i}}^2 + F_{\mathrm{E}} \cdot r_{\max} + F_{\mathrm{C}} \cdot r_{\max} + F_{\mathrm{F}} \cdot r_{\mathrm{i}}) \cdot n_{\mathrm{sp}}$$

**Dowel in the brackets fail simultaneously.*

Table 6-9 summarises the predicted capacity compared with the characteristic moment-resisting capacity from the connection tests. The characteristic moment-resisting capacity from the connection tests is calculated according to the 5-percentile method in BS EN 14358:2016 (BSI, 2016).

As can be seen from Table 6-9, the calculation method gives underestimated values when compared to the characteristic values calculated from the test, which is in line with expectation that prediction should provide a conservative value. Comparing the calculated characteristic values with the predicted values, the unreinforced group MCU shows a 5% difference. This implies that the method is conservative but is still an accurate estimation of the moment-resisting capacity of the connections. As for the other three groups, the prediction method is also conservative but with a higher percentage error. The proposed method is based on the existing method which does not consider the influence of crack and reinforcement. Applying the embedment strength for each different situation in the proposed method would gain a more accurate estimation but the reduction of the percentage error requires further investigation and modification of the method. The proposed method provides an insight into predicting the moment-resisting capacity of screw-reinforced dowel-type connections.

Table 6-9: Calculated characteristic moment-resisting capacity from tests and estimated characteristic moment-resisting capacity based on proposed calculation method.

	MCU	CMCU	MCBS	CMCBS
Characteristic moment-resisting capacity calculated based on six repetitions (kNm)	*9.26*	*10.41*	*12.94*	*12.06*
Characteristic moment-resisting capacity of connections estimated by using the characteristic value of embedment tests (kNm)	*8.80*	*7.90*	*9.14*	*8.99*
Percentage error between the characteristic test and predicted values	*5.0%*	*24.1%*	*29.4%*	*25.5%*

As screw reinforcement involves strengthening the wood material, it has been assumed that such reinforcement could change the basic assumption that all the steel dowels rotate around the centre of the fastener group. To further validate the credibility of the proposed modes, DIC analysis was used to identify the movement of fasteners under certain rotations of the connections. Specimen rotation at 2.5˚ was chosen and the corresponding images were selected. DIC analysis can show the horizontal and vertical displacement of points around

the dowels on the images, and the movement of the dowels (displacement and direction) can be calculated. This method helps to demonstrate whether the fasteners in the reinforced specimens rotate around the centre of rotation, as illustrated in Figure 6-14.

The result is shown in Figure 6-18, with the theoretical rotation direction of the dowels represented by a solid line with an arrow. The actual rotation direction of the dowel is represented by a dashed line. The theoretical displacement can be found by calculating the distances between the dowels and the centre of rotation but is not displayed in Figure 6-18. Overall, the realistic movement of the fastener in all specimens showed good correlation to theoretical movement in both displacement and rotation. Therefore, it confirms that specimens reinforced by self-tapping screws placed at *1d* fastener spacing follows the assumption that all fasteners rotate around the centre of the fastener group and validates the proposed method for calculating the moment-resisting capacity of reinforced dowel-type connections.

Furthermore, DIC analysis calculated the displacement of the centre dowel as shown in Figure 6-18. The values of displacement for all four groups are small and negligible. This confirms the previous assumption that the centre of the fastener group remains fixed. The displacements of the centre dowels at smaller theoretical and measured rotation (e.g. 1° and 2°) are not shown in this study, while their values are also found to be small.

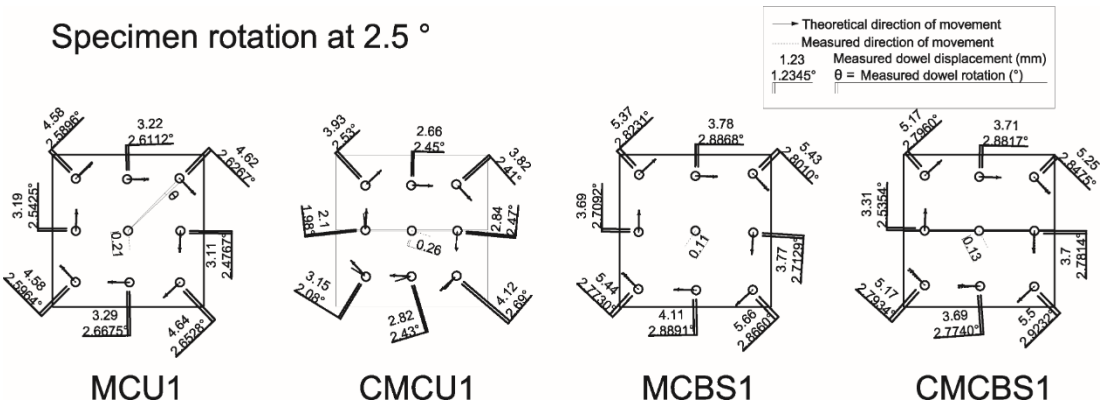

Figure 6-18: Measured dowel displacement at 2.5° rotation angle. Most of the dashed lines representing the actual direction are hardly visible due to the high correlation with the theoretical direction.

6.1.3.4 Influence of thread configurations on enhancing moment-resisting capacity

Failure modes

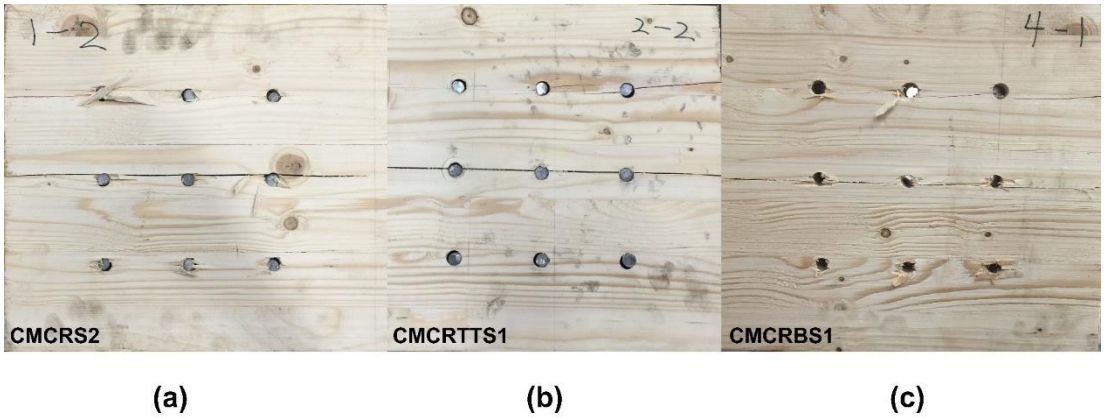

Figure 6-19: Splitting of timber occurred in each group: (a) CMCRS2, (b) CMCRTTS1 and (c) CMCRBS1.

During the test, timber cracking could be heard and splitting of the beam parallel to the grain was observed. In addition, sudden splitting was always accompanied with significant load drop. The splitting of timber around the fasteners is shown in Figure 6-19. Table 6-10 summarises the inspection of specimens after testing.

Table 6-10: Summary of the inspection of specimens after test.

Specimen	Observation	Description
CMCRS1	*No crack*	*N/A*
CMCRS2	*Top row on both sides*	*Crack initiated from end and around dowels, propagated to the second dowel*
CMCRS3	*No crack*	*N/A*
CMCRTTS1	*Top row on both sides*	*Crack initiated from end and around dowels, propagated to the second dowel*
CMCRTTS2	*No crack*	*N/A*
CMCRTTS3	*No crack*	*N/A*
CMCRBS1	*Top row on one side*	*Crack initiated from end and around dowels, propagated to the third dowel*
CMCRBS2	*No crack*	*N/A*
CMCRBS3	*Top row on both sides*	*Crack initiated from end and around dowels, propagated to the second dowel on one side and third dowel on another side.*

Compared to group CMCU in Table 6-6 (unreinforced connections with artificial crack), all the reinforced groups show better performance in controlling crack propagation. Only CMCRBS3 developed a crack to the third dowel while the rest have either not developed a crack at all or a crack has only reached to the second dowel from the edge. Group CMCRBS using screws with 33% thread on the point end, has higher occurrence of crack development but this should be further confirmed with more tests. The observed embedment failure of wood and the single yield failure of the dowels indicate a mode type 2 failure of the connections.

Embedment of screw head and washer into the wood was not observed in this test (see example in Figure 6-20 (left)). After the test, screws were retrieved, and no significant bending or physical damage were identified (as shown in Figure 6-20 (right)). A possible explanation has already been given in previous Section 6.1.3.1.

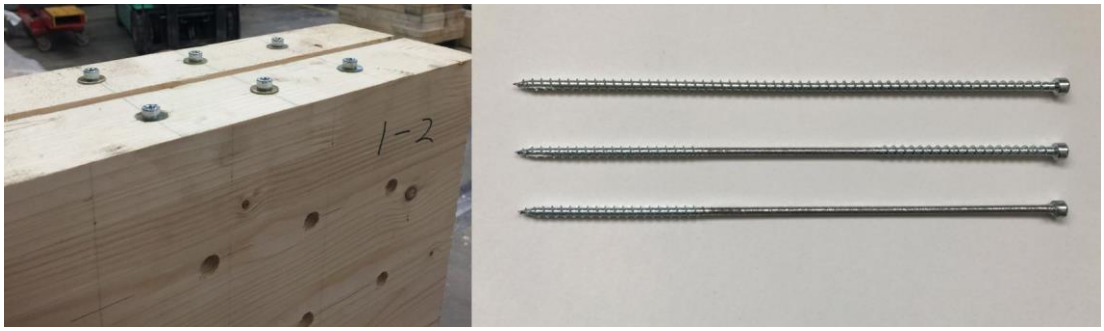

Figure 6-20: No significant screw head embedment observed in CMCRS2 (left) and self-tapping screws retrieved after test (right).

Moment-rotation curves

In Figure 6-21, the reinforced groups showed higher ductility and slightly improved moment resistance compared with the unreinforced cracked group CMCU from the previous section. Most of the tests in the reinforced groups were stopped due to the hydraulic jack running out of stroke, therefore, specimen failure could not be achieved. Within the three reinforced groups, the moment resistance and ductility were similar except that CMCRS1 failed in a less ductile way. The results imply that the applied thread configuration has limited influence on the effectiveness of screw reinforcement.

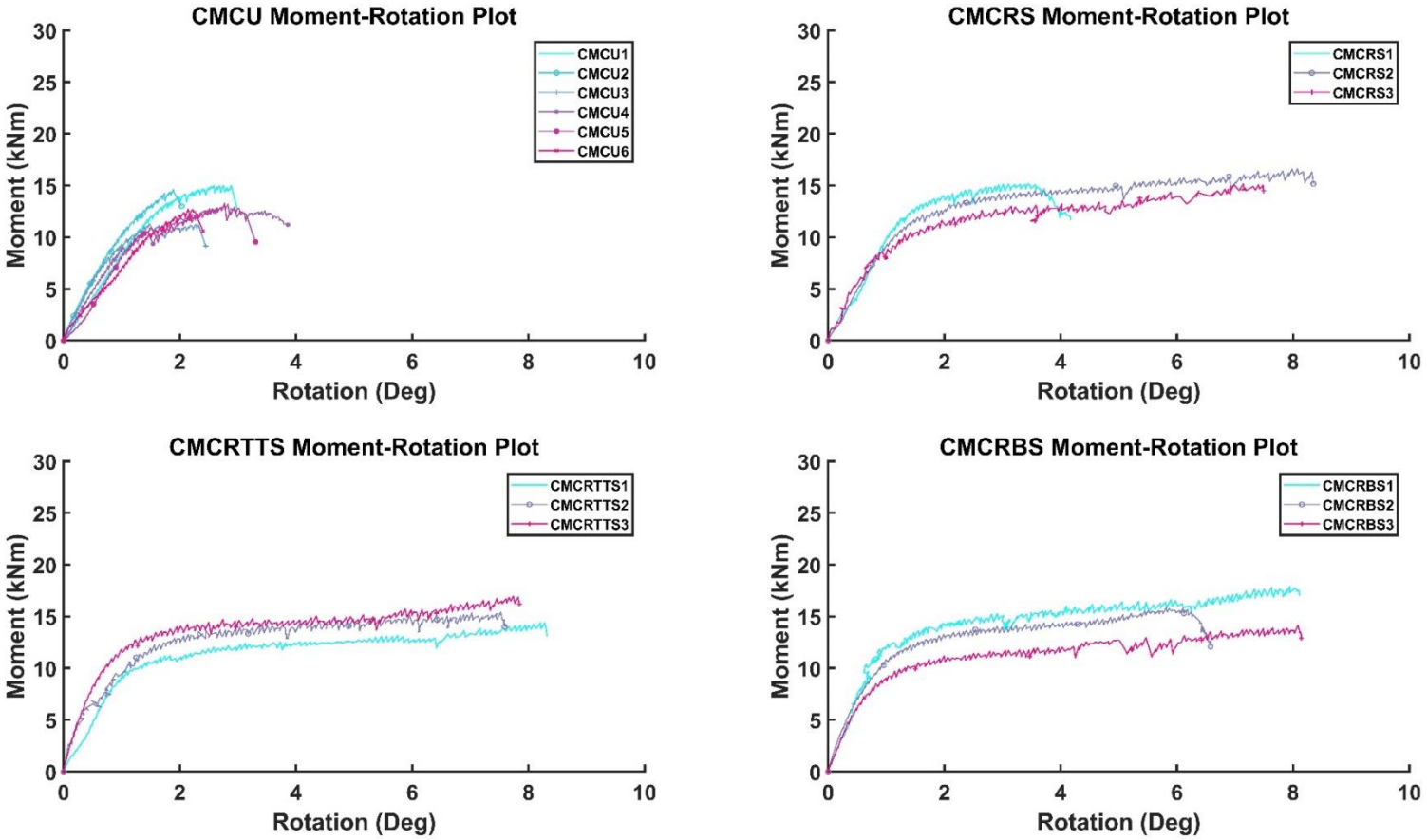

Figure 6-21: Plot of moment-rotation curves for group CMCU (top left), CMCRS (top right), CMCRTTS (bottom left) and CMCRBS (bottom right).

The mechanical properties of each group have been adjusted by ANCOVA, using density as covariance (shown in Table 6-11). The rotational stiffness was calculated using the gradient between $0.1M_{max}$ and $0.4M_{max}$ (M_{max} is the peak moment resistance) on the moment-rotation curve. The reinforced groups show similar values in moment-resisting capacity, rotational capacity and stiffness. A comparison with the unreinforced cracked group shows a significant improvement in moment-resisting capacity and rotational capacity. This has demonstrated the positive effects of screw reinforcement.

To summarise, the applied thread configurations have limited influence on the performance of reinforcement. Therefore, a recommendation is to use screws with thread on the point end rather than fully threaded screws as they are less vulnerable to damage from the friction generated during the installation process. However, the sample size in this study was limited, more repetitions are required for confirmation.

Table 6-11: Summary of the mechanical properties of each group.

Group	Mean moment-resisting capacity (kNm) (CoV)*	Mean maximum rotation (degree) (CoV)*	Mean rotational stiffness (kNm per degree) (CoV)*	Mean rotational stiffness (kNm per radian) (CoV)*
CMCU	*15.70 (10%)*	*2.73 (23%)*	*11.28 (22%)*	*633.26 (22%)*
CMCRS	*18.71 (5%)*	*6.72 (32%)*	*12.19 (17%)*	*710.66 (17%)*
CMCRTTS	*18.56 (8%)*	*7.94 (4%)*	*14.83 (33%)*	*855.51 (33%)*
CMCRBS	*19.03 (12%)*	*7.61 (11%)*	*15.77 (9%)*	*911.50 (9%)*

** The values are adjusted by ANCOVA except the CoV remains for the value before the adjustment.*

Theoretical prediction of moment-resisting capacity of dowel-type connections

Section 6.1.3.2 proposed a method to calculate the moment-resisting capacity of screw-reinforced dowel-type connections. The method is applied in this section to predict the capacity of a reinforced cracked connection.

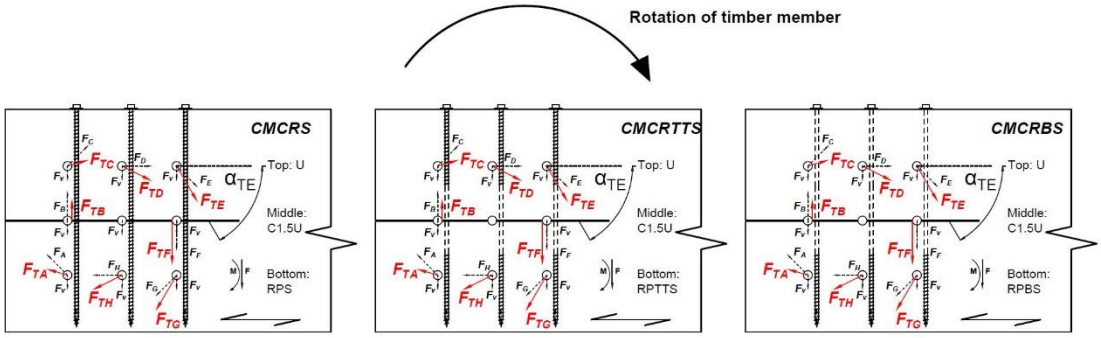

Figure 6-22: Demonstration of the loads acting on each dowel in groups CMCRS (left), CMCRTTS (middle) and CMCRBS (right). Arrows indicate the actual load acting on the fasteners as the connections rotate clockwise but they will bear on the wood opposite to this direction.

Table 6-12: Summary of characteristic embedment strength.

Group	Description	Characteristic embedment strength from previous test, $f_{h,0,k}$ (N/mm^2)
RPS	*No crack, reinforced by fully threaded screw Y*	*34.87*
RPTTS	*No crack, reinforced by screw Y with 33% thread on both ends*	*32.23*
RPBS	*No crack, reinforced by screw Y with 33% thread on the point end*	*29.18*

The loads imposed on the dowels in each group are shown in Figure 6-22. The available embedment strength for each case is listed in Table 6-12. The characteristic moment-resisting capacities are also calculated using the five-percentile method in BS EN 14358:2016 (BSI, 2016). It should be noted that the sample size for the embedment strength is three, which is small. A comparison of predicted and test-based characteristic values of each group is shown in Table 6-13.

Table 6-13: Comparison of test based and predicated characteristic moment-resisting capacity.

	CMCRS	CMCRTTS	CMCRBS
Characteristic moment-resisting capacity calculated based on three repetitions (kNm) (measured)	*13.20*	*11.98*	*10.92*
Characteristic moment-resisting capacity of connections estimated by using the characteristic value of embedment test (kNm) (predicted)	*10.86*	*10.36*	*9.80*

The characteristic values calculated from test results show a difference between the three reinforced groups. However, it is recommended that more repetitions should be carried out for confirmation. Comparing the two types of characteristic values, it can be easily identified that the predicted values are more conservative, which gains confidence in the proposed calculation method.

6.1.4 Summary

This study investigates the performance of dowel-type moment-resisting connections reinforced by self-tapping screws compared with unreinforced connections. Enhancement of screw reinforcement on artificially damaged connections is also investigated. The following points can be concluded from the results in this study:

- Partially threaded self-tapping screws placed at one fastener spacing to the dowel can enhance rotational capacity while the improvement in moment-resisting capacity is slight.
- When a connection was damaged by making a 1.5mm artificial crack at the middle row of its fastener group, self-tapping screws as reinforcement restored the rotational capacity to its original undamaged state.
- Based on experimental observation, the tendency of splitting failure was greatly controlled by the application of self-tapping screws. In addition, according to images from DIC, crack propagation was also controlled by having self-tapping screws. The average crack lengths in the unreinforced groups MCU and CMCU were 392mm and 356mm, respectively. The average crack lengths in the reinforced groups MCBS and CMCBS were 155mm and 223mm, respectively. The average crack length in reinforced specimens was at least 37% shorter than in the unreinforced ones.
- A calculation method for predicting the moment-resisting capacity of connections reinforced by screws is proposed and shows conservative values when compared with experimental results (percentage error ranging from 5-29.4%). The displacement results from DIC also validated that the steel dowels in the reinforced specimen followed the assumption that they rotate around the centre of the fastener group. Therefore, the proposed method can be used to predict the moment-resisting capacity of screw-reinforced dowel-type connections with similar configuration of connections and screw reinforcement.
- Fully threaded screws, screws with 33% thread on both ends and screws with 33% thread on the point end were applied to examine the influence of thread configurations. Results confirmed the enhancement of mechanical properties using

these screws but revealed no significant difference between different thread configurations. The results correspond well with previous findings in Chapter 4 and Chapter 5. As long fully threaded screws are prone to damage during installation, screws with a small portion of threaded part that can achieve equal reinforcement performance could be a good option. More tests are recommended to make a solid confirmation.

An important conclusion in this study is that screw reinforcement leads to a more ductile, safer failure. It may not be worth using the screws with partial thread for increased strength, but it is certainly worth using them to restore the ductility after the development of cracks and ensure a less brittle failure.

In addition, the proposed calculation method establishes a path to find the moment-resisting capacity of dowel-type connections reinforced by self-tapping screws. The experiment is based on a small sample size and more repetitions should be performed to reduce the variability in the results that is induced by the inherent material characteristic of wood. Furthermore, the applicability of the proposed method to other configurations of reinforced connections can be achieved with available embedment strength of timber that is reinforced by screw with similar thread configuration and screw to dowel distance.

6.2 Reinforcement of beam-to-column dowel-type connections using self-tapping screws

6.2.1 Introduction

In recent years, self-tapping screws have been widely used in timber construction, not only as connecters but also as reinforcement for various situations. Experimental works in Chapter 4 and Chapter 5 confirmed the effectiveness of self-tapping screws on improving embedment strength and tensile load-carrying capacity of dowel-type connections. The results of the studies also showed that specimens reinforced by screws with thread on the point end achieved similar performance to connections reinforced by fully threaded screws. As the drive-in torque of a screw is related to its thread length, a fully threaded screw has higher risk of being damaged during the installation process.

In timber structures, a dowel-type moment-resisting connection is a critical part for load transfer. With weak strength perpendicular to the grain, the mechanical properties of the connections could be limited due to timber splitting parallel to the grain. Lam *et al.* (2010), Gehloff *et al.* (2010) and Closen and Lam (2012) used self-tapping screws to reinforce

bolted connections and found significant improvement in moment-resisting capacity. Currently, there is limited research on the reinforcement of moment-resisting connections, made using steel dowels, by self-tapping screws.

The aim of this study is to examine the mechanical performance of beam-to-column dowel-type connections reinforced by partially threaded self-tapping screws. A comparison with two unreinforced connections is made.

6.2.2 Materials and methods

The timber-steel-timber connections in this study were retrieved from two portal frames which had been previously tested for frequency measurement without any damage. The design of the portal frame followed the guidance by EC5 (BSI, 2004).

The connections were made of commercial GL24c glulam beams using European whitewood timber which had an average density of 394 kg/m^3 (CoV= 3.7%) and moisture content of 7% (CoV=9.7%). The timber beams were stored and prepared at 21.6°C temperature and 59% RH. In total, four beam-to-column connections were prepared and two of them were reinforced by Screw X as used in Section 6.1 in order to reduce the drive-in torque. The diameter of the steel dowel was 16mm and the screws were placed at *1d* distance from the centre of the dowel to the centre of the screw. Figure 6-23 shows details of the screw and its specifications.

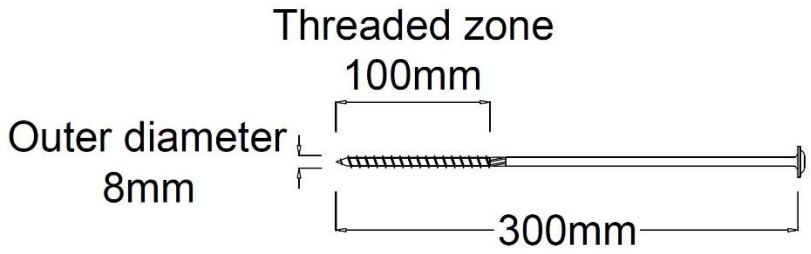

Figure 6-23: The partially threaded self-tapping screw used in this study.

Pre-drilled holes, with 180mm depth, were prepared to ensure the screws could be placed as accurately as possible. Figure 6-24 shows the original locations of the connections on the portal frames and the geometry of the connections with screw reinforcement. The original design of the portal frame left a 10mm gap between the timber members. The details of the two groups are summarised in Table 6-14.

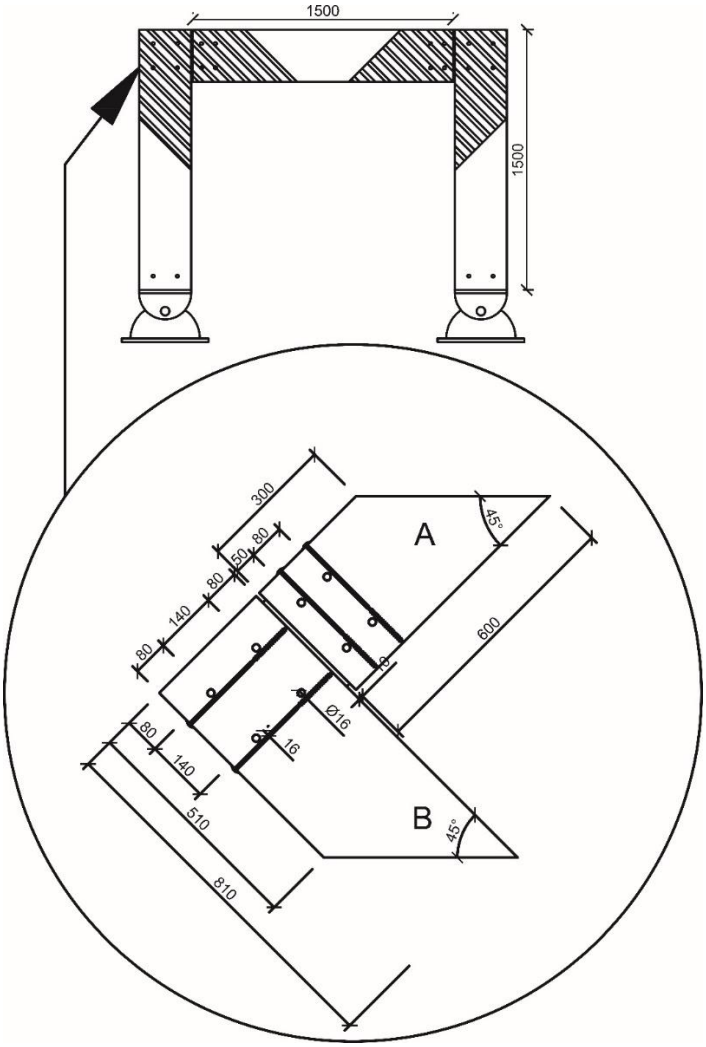

Figure 6-24: Drawings of the portal frame and the shaded parts are the beam-to-column connections tested in this study.

Table 6-14: Details of each group.

Group	Description	Tests	Mean density (kg/m^3) (CoV)	Mean M.C. (%) (CoV)
ULC	*Unreinforced*	*2*	*393 (3.1%)*	*6.3 (8.5%)*
RLC	*Reinforced by screws with 100mm thread (33% thread on the point end)*	*2*	*396 (4.7%)*	*6.9 (9.7%)*

6.2.2.1 Test set-up

The beam-to-column connections were placed on a flat platform so that the loading head above them would compress the levelled surface of part A. Two LVDTs (100mm stroke with

±0.01mm accuracy) on each side of the specimen were installed to measure the rotation of the connections, see Figure 6-25. The connections were loaded to failure (when 20% of load drop from the peak load was observed).

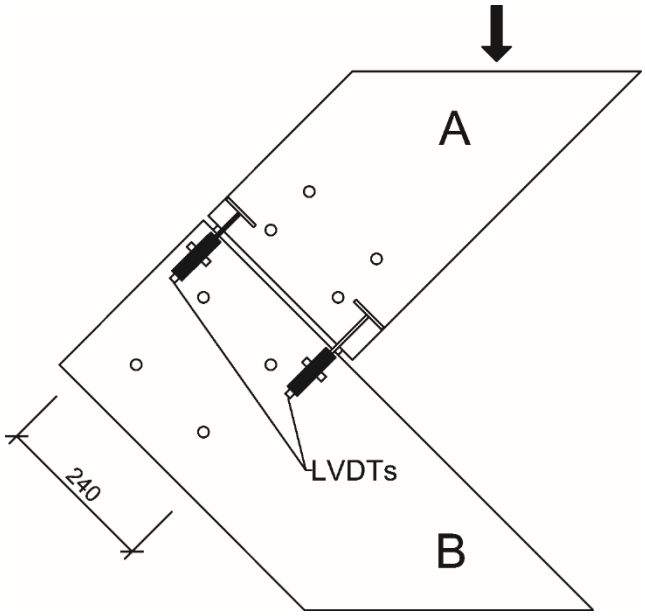

Figure 6-25: Locations of LVDTs for rotation measurement.

6.2.3 Results and discussion

6.2.3.1 Failure of specimens

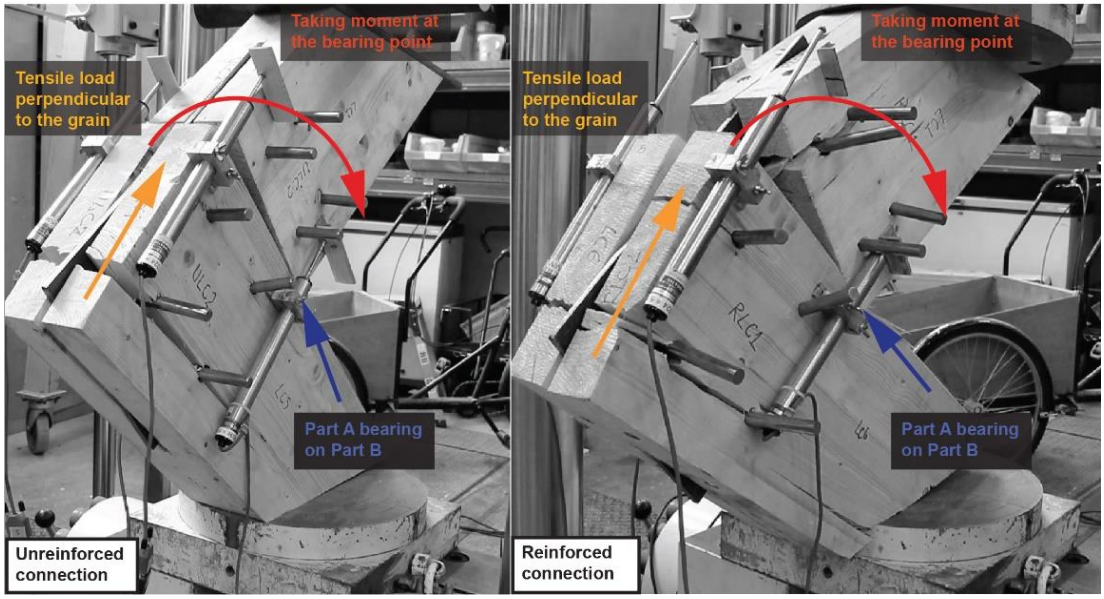

Figure 6-26: Pictures of unreinforced (left) and reinforced specimens (right).

Due to the nature of the test configuration, the connections were also in compression during loading. As the top part A was compressed, the 10mm gap between the two pieces gradually

closed and finally the corner of part A rested onto part B as shown in Figure 6-26. In both tests of unreinforced and reinforced specimens, interaction between the two members was observed. This interaction shifted the centres of rotation from the centroid to the bearing point for the rest of the loading stage. The location of the bearing point for each specimen was measured to be approximately 300mm from the end of part B, as indicated in Figure 6-29. The observed bearing also resulted in a tensile load perpendicular to the grain of part B, which then led to the splitting of the wood.

For the unreinforced specimens, cracks developed parallel to the grain in both parts and failed in a less ductile manner. For the reinforced specimens, as the crack developed in the member, the self-tapping screws restrained the movement of wood perpendicular to the grain, thus, rotational capacity of the connections was enhanced. The screw head embedded into the wood as it held the timber member against splitting, see Figure 6-27. Mode type 2 failure (EC5 defines it to be embedment failure and single yield failure of the fastener) for both groups of connections was observed.

Figure 6-27: Embedment of screw head in reinforced connection.

6.2.3.2 Load-displacement curves

The moment on the connections is the product of the load on piece A and the perpendicular distance to the bearing point (approximately 219mm). The moment-rotation curves in Figure 6-28 shows that reinforced specimens displayed a higher rotation and moment-resisting

capacity. The mechanical properties of the connections are tabulated in Table 6-15. The rotational stiffness of the beam-to-column connection was calculated using the gradient between $0.1M_{max}$ and $0.4M_{max}$ (M_{max} is the peak moment resistance) on the moment-rotation curve.

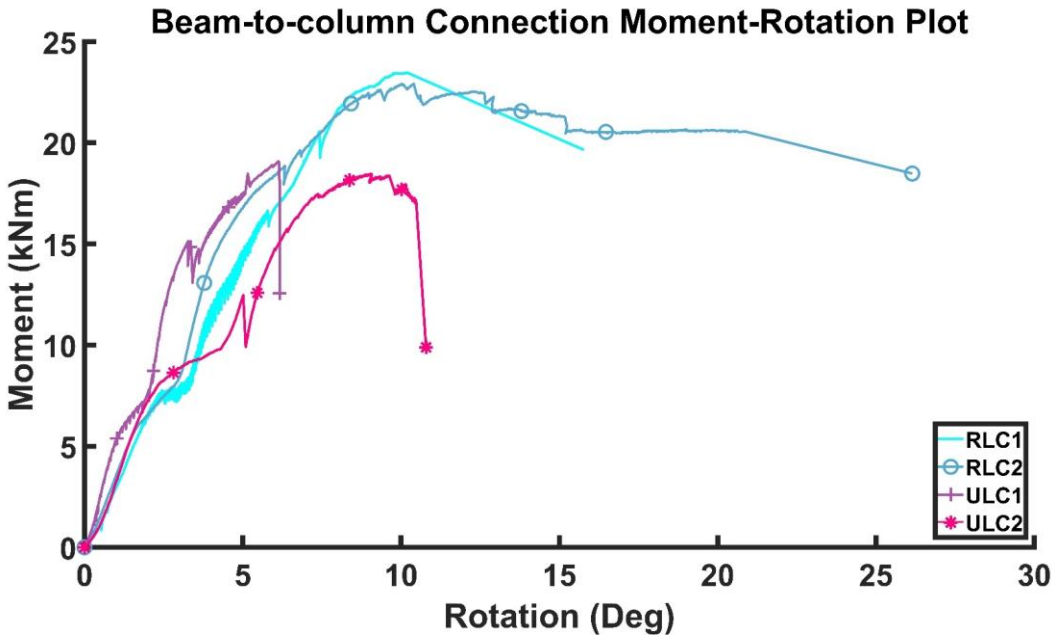

Figure 6-28: Experimental moment-rotation curves for unreinforced and reinforced connections.

Table 6-15: Mechanical properties of each group.

Group	Mean maximum moment-resisting capacity (kNm) (CoV)	Mean maximum rotation (degree) (CoV)	Mean rotational stiffness (kNm per degree) (CoV)	Mean rotational stiffness (kNm per radian) (CoV)
ULC	*18.78 (2.4%)*	*8.50 (38.3%)*	*17.6 (7.4%)*	*1007.51 (4.1%)*
RLC	*23.20 (1.7%)*	*20.95 (34.8%)*	*12.4 (4.1%)*	*711.16 (7.4%)*

In this research, rotation angle is considered as an indicator of the ductility of the connections. The rotation of reinforced connections was approximately 2.5 times better than unreinforced groups. Their maximum moment resistance was also 24% higher than the unreinforced ones. The results demonstrate that partially threaded self-tapping screws can greatly enhance the mechanical properties of beam-to-column connections. The unreinforced specimens had slightly higher stiffness than the reinforced ones. In a study by Leijten and Brandon (2013), the analytical calculation shows that the smaller initial gap between the two timber members in a reinforced column-beam connection can lead to higher rotational

stiffness. This is caused by the contact of the two timber members. Therefore, it is possible that the higher mean stiffness value of the unreinforced connections in this study is due to the size of the initial gap being smaller than that of the reinforced connections (the sizes of gaps in unreinforced and reinforced connections were 5.7mm and 8.9mm, respectively). The difference in initial gap could be due to errors when manufacturing the members or during assembly of the connections.

6.2.4 Theoretical prediction of moment-resisting capacity

Current design codes have no relevant methods for prediction of the moment-resisting capacity of screw-reinforced dowel-type connections. In this study, a calculation method is proposed based on the following Equations (6-27) and (6-28) presented in Porteous and Kermani (2013) for a semi-rigid connection:

$$M_{sp} = \left(\frac{K_{ser}}{1+\psi_2 k_{def}}\right) \sum_{i=1}^{n} r_i^2 \, \theta_u \qquad (6\text{-}27)$$

$$k_u = \left(\frac{K_{ser}}{1+\psi_2 k_{def}}\right) \sum_{i=1}^{n} r_i^2 \qquad (6\text{-}28)$$

where:

M_{sp} is the moment-resisting capacity of the connections per shear plane;

k_u is the rotational stiffness of the connections per shear plane;

K_{ser} is the slip modulus of the dowel at serviceability limit states;

ψ_2 is factor for the quasi-permanent value of the action causing the largest stress in relation to the strength;

k_{def} is the factor for the evaluation of creep deformation taking into account the relevant service class;

n is the number of fasteners;

n_{sp} is the number of shear planes;

i indicates a specific fastener;

r_i is the distance of the specific fastener to the centre of rotation;

θ_u is the assumed rotation in the connections.

For ultimate limit states (ULS), the slip modulus of fasteners should use K_u and for serviceability limit states (SLS), the slip modulus is K_{ser}. However, according to Porteous and Kermani (2013), even at ultimate limit states, many fasteners are only stressed to

serviceability limit states. Thus, for this calculation at ultimate state, the serviceability slip modulus of fasteners, K_{ser}, is used rather than K_u.

The proposed method splits the loading stage of the connections into two stages: before (Stage 1) and after gap closed (Stage 2).

The rotation of the entire connection when the gap is fully closed can be calculated using the trigonometric functions by knowing the width of the gap and the depth of the beam. This study assumes each fastener group in Part A and B rotates around its centre of rotation. The rotation of each part, θ_A and θ_B, is inversely proportional to the rotational stiffness of each part, which can be calculated using Equations (6-27) and (6-28) and the values are shown in Table 6-16. The sum of θ_A and θ_B is equal to the angle between the two parts when the gap is fully closed. Figure 6-29 shows the geometry of the specimen and the theoretical rotation of each fastener at Stage 1.

Table 6-16: Values of factors and prediction results for unreinforced connections at Stage 1.

	Part A	Part B
ρ_m for GL24c (kg/m^3)	*400*	*400*
d (mm)	*16*	*16*
r_i (mm)	*81*	*99*
K_{ser} (N/mm)	*5565*	*5565*
Ψ_2	*0.3*	*0.3*
k_{def}	*0.8*	*0.8*
k_u (kNm)	*223*	*352*
θ_{peak} (rad)	*0.020*	*0.013*
Angle to grain, α (˚)	*29.75*	*45*
n_{sp}	*2*	*2*
$M_{Stage\ 1}=n_{sp}*k_u*\theta$ (kNm)	*4.68*	*4.68*

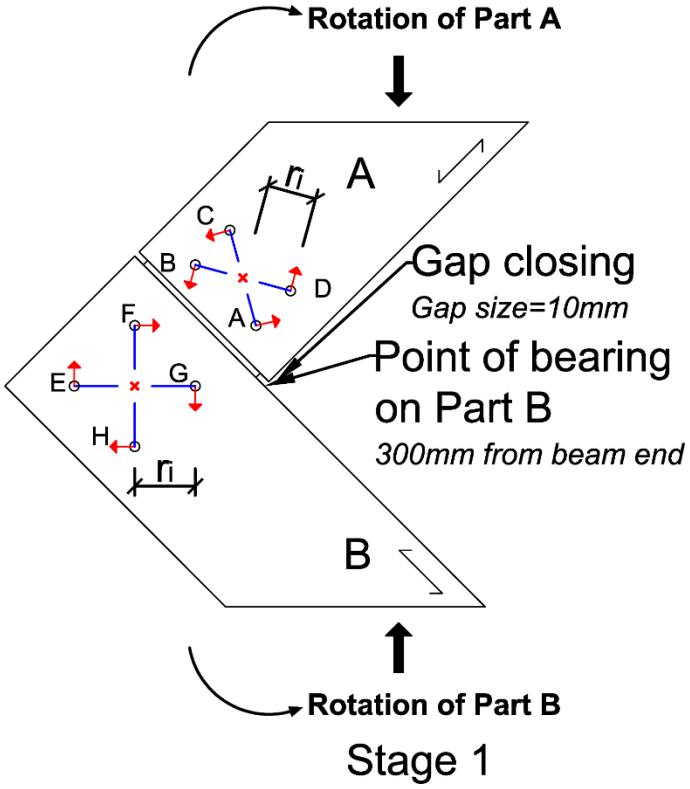

Figure 6-29: Assumptions made for the unreinforced connections before gap is closed. Red arrow indicates the direction the wood is loaded.

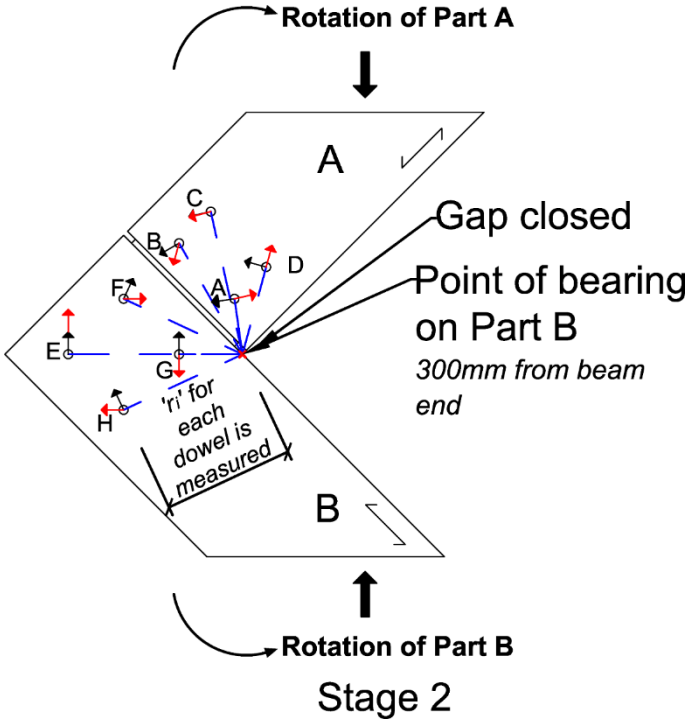

Figure 6-30: Assumptions made for the unreinforced connections after gap is closed, drawing not showing the rotation of each part. Red arrow indicates the direction the wood is loaded.

After the gap is closed, Part 1 continues to bear on Part 2 and rotate around the bearing point which has become the centre of rotation of the fastener in both parts as shown in Figure 6-30. During the tests, a crack first appeared around dowel *E* in all specimens. This is due to excessive tensile stresses perpendicular to the grain causing splitting failure of the connections. Therefore, using the splitting capacity of the connections provides a path to calculate the moment-resisting capacity of the unreinforced connections.

The characteristic splitting capacity of each dowel is calculated using the Equation provided in EC5 (BSI, 2004):

$$F_{90,Rk} = 14bw\sqrt{\frac{h_e}{(1-\frac{h_e}{h})}} \qquad (6\text{-}29)$$

where:

$F_{90,\,Rk}$ is the characteristic splitting capacity;

b is the member thickness (64mm for all members in this study);

w is a modification factor and is equal to '*1'* for dowel-type fastener;

h_e is the loaded edge distance to the centre of the most distant fastener;

h is the timber member height (300mm for all members).

In this study, h_e is measured for each fastener to the corresponding loaded edge (as demonstrated in Figure 6-31) in each part. To determine the rotation of the connections when splitting occurs, it is essential to understand the load on the wood from each fastener. This study assumes, at Stage 2, the wood around a fastener is subject to the vertical load (from the loading machine), the load from the fastener (due to the moment at Stage 1) and the load from the fastener (due to the moment at Stage 2), see Figure 6-31 for a demonstration of the loads on dowel *H*. The characteristic splitting capacity of the wood should not be smaller than the load perpendicular to the grain as Equation (6-30) demonstrated:

$$F_{90,Rk} \geq F_{v,i,90} + F_{m,i,stage\,,90} + F_{m,i,stage\,2,90} \qquad (6\text{-}30)$$

The aim of the calculation method is to assume a range of rotations of the connections at Stage 2 and calculate the total load acting on the wood from each fastener. The component of the total load perpendicular to the grain is the force trying to split the timber. The direction of this force is essential to decide the loaded edge for each fastener and the distance to the loaded edge, which is an important factor to find the splitting capacity in Equation (6-29).

When the load exceeds the splitting capacity of the wood, a crack will form and the corresponding rotation of the connections can be found.

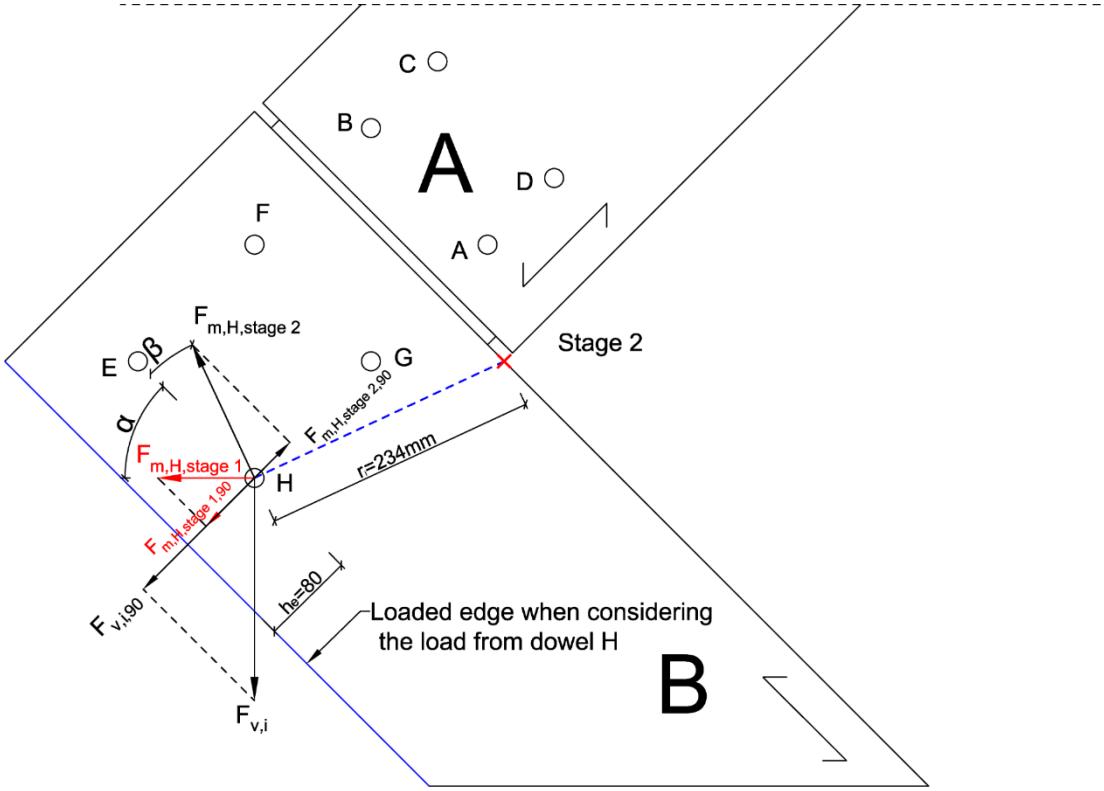

Figure 6-31: Demonstration of the loads acting on dowel H at stage 2.

Calculation of the vertical load

The vertical load from each fastener acting on the wood is comprised of two parts, the vertical load from Stage 1 and another from Stage 2, in this study, the load is calculated per shear plane:

$$F_{v,sp} = F_{v,sp,\,stage\,1} + F_{v,sp,stage\,2} \tag{6-31}$$

The vertical load is in relation to the moment on the connections and the perpendicular distance of the vertical load to the bearing point (L=219mm as mentioned in the previous section):

$$F_{v,sp} = \frac{M_{sp,stage\,1} + M_{sp,stage\,2}}{L} \tag{6-32}$$

And the moment per shear plane can be found using the following equation:

$$M_{sp} = k_{u,sp} \cdot \theta = \left(\frac{K_{ser}}{1+\varphi_2 k_{def}}\right) \cdot \sum r_i^2 \cdot \theta \tag{6-33}$$

Therefore, the vertical load on the four fasteners per shear plane can be expressed as:

$$F_{v,sp} = \frac{k_{u,sp,stage\,1} \cdot \theta_{peak} + k_{u,sp,\,stage\,2} \cdot \theta}{L} \quad (6\text{-}34)$$

where:

θ_{peak} is the maximum rotation of the specific part at Stage 1 and can be found in Table 6-16 for each part of the connections;

θ is an assumed rotation of the specific part at Stage 2;

$k_{u,sp,stage\,1}$ is the rotational stiffness per shear plane at Stage 1. Its value can be found in Table 6-16;

$k_{u,sp,stage\,2}$ is the rotational stiffness per shear plane at Stage 2. Its value can be found in Table 6-17.

For each fastener per shear plane, the vertical load is (divided by four dowels):

$$F_{v,i} = \frac{k_{u,sp,stage\,1} \cdot \theta_{peak} + k_{u,sp,\,stage\,2} \cdot \theta}{4L} \quad (6\text{-}35)$$

Thus, the component force of the vertical load acting perpendicular to the grain direction of the member is (when the vertical load is acting 45° to the grain direction on part 2):

$$F_{v,i,90} = \frac{(k_{u,sp,stage\,1} \cdot \theta_{peak} + k_{u,sp,\,stage\,2} \cdot \theta) \cdot sin(45°)}{4L} \quad (6\text{-}36)$$

Calculation of the load due to moment

The fasteners are subject to two stages of loads due to moment acting on the connections, the magnitude and direction of the loads vary dependently. The load on each dowel per shear plane at Stage 1 is denoted as $F_{m,i,s1}$ (where *i* represents the symbol of the dowel, marked with red arrows) and is shown in Figure 6-30. Depending on its direction, the load on each dowel at Stage 1 will either accumulate with the load at Stage 2 (increasing the occurrence of splitting as total load is relatively higher) or have a counter effect to reduce the total load perpendicular to the grain at Stage 2 (delaying the splitting of wood).

The loads on fastener *i* in the two stages are:

$$F_{m,i,stage\,1} = \frac{M_{m,i,\,stage\,1}}{r_{i,stage\,1}} \quad (6\text{-}37)$$

$$F_{m,i,stage\,2} = \frac{M_{m,i,stage\,2}}{r_{i.stage\,2}} \quad (6\text{-}38)$$

The moment is the product of the rotational stiffness and the rotation angle:

$$F_{m,i,stage\,1} = \frac{k_{i,\,sp,stage\,1} \cdot \theta_{peak}}{r_{i,stage\,1}} \quad (6\text{-}39)$$

$$F_{m,i,\,stage\,2} = \frac{k_{i,sp,stage\,2} \cdot \theta}{r_{i.stage\,2}} \quad (6\text{-}40)$$

The rotational stiffness can be expressed as in Equation (6-28), thus, Equations (6-37) and (6-38) are transformed into:

$$F_{m,i,stage\,1} = \left(\frac{K_{ser}}{1+\varphi_2 k_{def}}\right) \cdot r_{i,stage\,1} \cdot \theta_{peak} \quad (6\text{-}41)$$

$$F_{m,i,stage\,2} = \left(\frac{K_{ser}}{1+\varphi_2 k_{def}}\right) \cdot r_{i,stage\,2} \cdot \theta \quad (6\text{-}42)$$

The combined load on a fastener *i*, due to moment at Stage 1 and 2, per shear plane is:

$$F_{m,i,90} = \left(\frac{K_{ser}}{1+\varphi_2 k_{def}}\right) \cdot r_{i,stage\,1} \cdot \theta_{peak} \cdot sin\alpha + \left(\frac{K_{ser}}{1+\varphi_2 k_{def}}\right) \cdot r_{i,stage\,2} \cdot \theta \cdot sin\beta \quad (6\text{-}43)$$

where:

α is the angle of the load to the grain direction at Stage 1. Its value can be found in Table 6-16;

β is the angle of the load to the grain direction at Stage 2. Its value is calculated using manufacturing drawings and shown in Table 6-17.

Table 6-17: Parameters for calculating the characteristic splitting capacity based on each dowel.

Part A		r_i (mm)	Angle to grain, β (˚)	k_u (kNm)	h_e (mm)
Dowel	A	*100*	*37*	*1400*	*220*
	B	*228*	*15*		*80*
	C	*261*	*32*		*80*
	D	*161*	*60*		*220*
Part B		r_i (mm)	Angle to grain, β (˚)	k_u (kNm)	h_e (mm)
Dowel	E	*311*	*45*	*1967*	*80*
	F	*234*	*70*		*220*
	G	*113*	*45*		*220*
	H	*234*	*20*		*80*

The total load acting on the wood from each fastener can be calculated and the loaded edge is then determined for each fastener, as shown in Table 6-18. This study assigned values for θ to substitute into Equation (6-30), when the sum of the acquired load and the tensile load

perpendicular to the grain exceeds the splitting capacity, cracking occurs and the corresponding rotation of the connections can be found. It should be noted that θ does not include the angle from the previous stage and starts from zero. In addition, the two parts rotate at different angles as they have different rotational stiffness.

$$F_{90,Rk} \geq \frac{\left(k_{u,sp,stage\ 1} \cdot \theta_{peak} + k_{u,sp,\ stage\ 2} \cdot \theta\right) \cdot \sin(45°)}{4L} +$$

$$\left(\frac{K_{ser}}{1+\varphi_2 k_{def}}\right) \cdot r_{i,stage\ 1} \cdot \theta_{peak} \cdot sin\alpha + \left(\frac{K_{ser}}{1+\varphi_2 k_{def}}\right) \cdot r_{i,stage\ 2} \cdot \theta \cdot sin\beta \qquad (6\text{-}44)$$

Table 6-18: Comparing the tensile load perpendicular to the grain with the characteristic splitting capacity using assumed rotation of the connections.

θ_{total} (rad) *			*0.0050*	*0.0150*	*0.0183*
θ_{total} (°) *			*0.2865*	*0.8594*	*1.0456*
$\theta_{Part\ A}$ (rad) *			*0.0029*	*0.0088*	*0.0107*
$\theta_{Part\ B}$ (rad) *			*0.0021*	*0.0062*	*0.0076*
Part A			$F_{90,Rk}$-($F_{v,i,90}$+$F_{m,i,stage\ 1,90}$+$F_{m,i,stage\ 2,90}$) (kN)		
	Dowel	A	*3.01*	*1.29*	*0.73*
		B	*19.38*	*17.62*	*17.05*
		C	*7.49*	*7.17*	*7.06*
		D	*23.85*	*23.49*	*23.37*
Part B			$F_{90,Rk}$-($F_{v,i,90}$+$F_{m,i,stage\ 1,90}$+$F_{m,i,stage\ 2,90}$) (kN)		
	Dowel	E	*23.05*	*22.24*	*21.98*
		F	*6.67*	*5.87*	*5.61*
		G	*18.77*	*16.96*	*16.37*
		H	*2.39*	*0.59*	*0.00***

**Does not include the rotation at Stage 1.*
***Marks the point the splitting capacity is exceeded.*

The results of the calculation are tabulated in Table 6-18. It shows that the wood around dowel *H* fails first as the tensile load perpendicular to the grain on the fastener exceeds the splitting capacity of wood. The rotation of the entire connection when splitting occurs is at 2.95˚ (including the rotation at Stage 1). The ultimate moment-resisting capacity of the connections before splitting failure is:

$$M_k = n_{sp} k_u \theta + M_{Stage\ 1} = 19.61 kNm \qquad (6\text{-}45)$$

To reflect the splitting failure, this study assumes dowel *H* with surrounding cracks does not contribute to the rotational stiffness of the connections; thus, after splitting occurs, the rotational stiffness of Part B per shear plane is recalculated as:

$$k_u = \left(\frac{K_{ser}}{1+\psi_2 k_{def}}\right)(r_E^2 + r_F^2 + r_G^2) n_{sp} = 738 kNm \qquad (6\text{-}46)$$

And the prediction of moment-resisting capacity of the connections is based on Equation (6-45). Calculations shows that, after splitting occurs around dowel *H*, the characteristic

moment-resisting capacity of the connections drops to 15.87kNm, approximately 20% drop, meaning the connections fail.

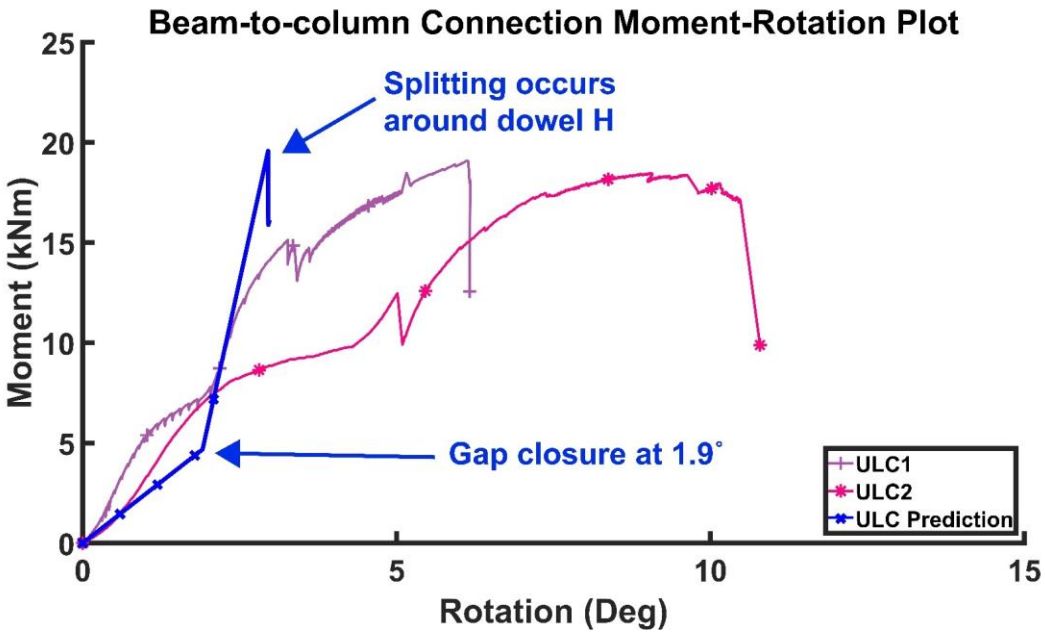

Figure 6-32: Experimental and theoretical moment-rotation curves for unreinforced connections.

A predicted moment-rotation curve for the unreinforced connections is shown in Figure 6-32. The prediction shows slightly higher values than the actual test results. In addition, as observed in the test, splitting failure first occurred around dowel *E* rather than dowel *H*. The results indicate there are other factors that might influence the failure mode of the connections. In this study, the prediction assumes the timber around the fasteners has the same capacity, nevertheless, timber is non-homogenous, and the material properties vary. Material defects, such as knots, can also undermine the splitting capacity of wood. Therefore, future investigation is required and more experimental tests are necessary.

As the bearing behaviour of the connections shifted the rotation centre to the bearing point, the dowels tend to move away from the self-tapping screws rather than moving towards them. Thus, the load-carrying capacity cannot be predicted by using the embedment strength of reinforced embedment samples. The proposed prediction method derived in this study therefore cannot predict the moment-resisting capacity of the reinforced connections.

However, self-tapping screws can provide restraint to splitting and the tested reinforced connections showed higher rotation angle and moment-resisting capacity than unreinforced ones. The splitting resistance provided by the screws effectively controlled crack

propagation and allowed the yielding of fasteners, thus higher mechanical performance of the connections can be achieved.

6.2.5 Screw reinforcement design

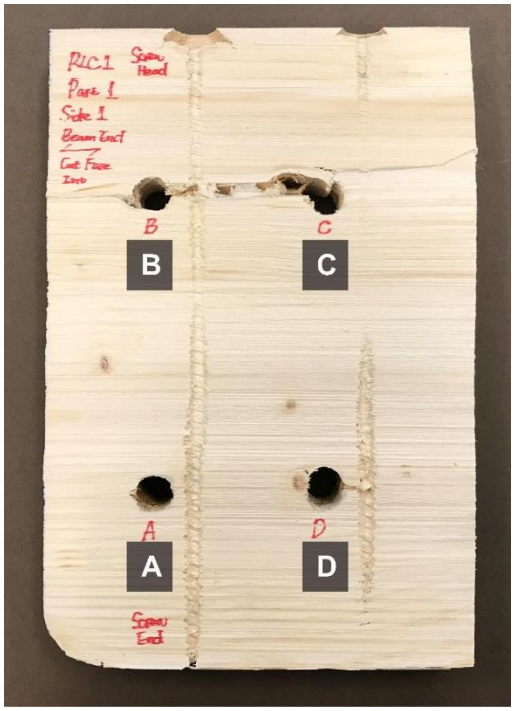

Figure 6-33: Picture of Part 1 of reinforced connection (RLC1) cut open after test.

The purpose of screw reinforcement in this study is to provide splitting resistance and enhance the capacity of the connections when the steel dowels bear on the screws. However, as stated in the previous section, the centre of rotation is shifted to the bearing point making it impossible for the dowels to bear on the self-tapping screws. After the test, the reinforced connections were dismantled and cut open for inspection. In Figure 6-33, none of the dowels in Part A showed the movement to bear on the self-tapping screws. As for the dowels *F* and *G* in Part 2 in Figure 6-34, they showed a tendency to move towards the self-tapping screws but, overall, the deformation of the screws was insignificant in both parts, see Figure 6-35 and Figure 6-36. The self-tapping screws in this study did not provide the extra improvement in the embedment strength using their bending capacity. However, the deformation of a few screws due to the splitting failure and the embedment of screw head indicated restraining resistance was provided by the screws.

The results of this study provide insights into the effective positioning of the self-tapping screws regarding the design of the connections. Installing the screws at the locations where the dowels can rest on the screws may result in a higher capacity and rotation of the connections. In addition, the self-tapping screws were placed at *1d* distance to the dowels

and decreasing this spacing may utilise the bending capacity of the screw and further enhance the moment-resisting capacity of the connections.

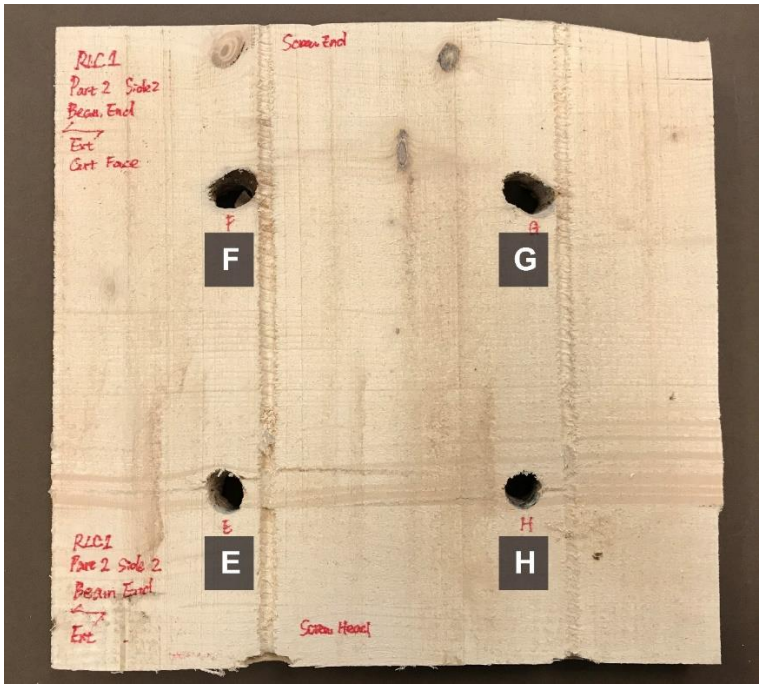

Figure 6-34: Picture of Part 2 of reinforced connection (RLC1) cut open after test.

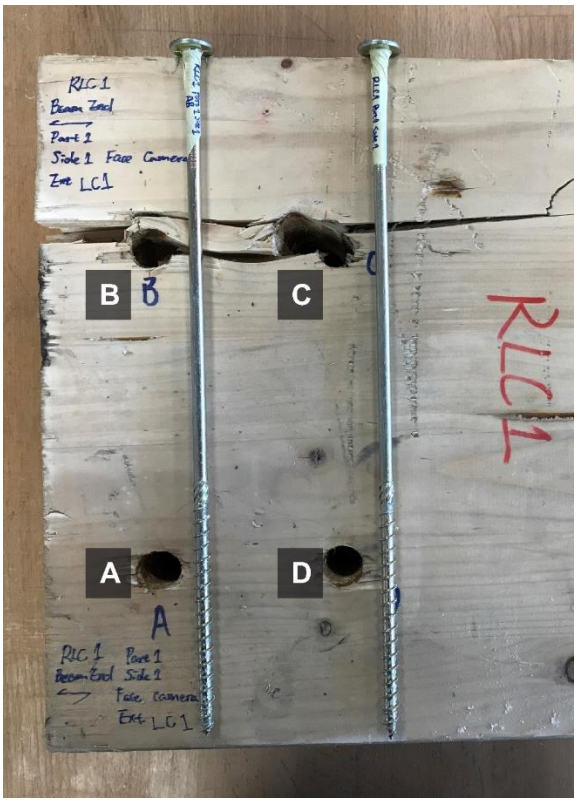

Figure 6-35: Picture of the screws retrieved from Part 1 of the reinforced connection (RLC1).

Figure 6-36: Picture of the screws retrieved from Part 2 of the reinforced connection (RLC1).

6.2.6 Summary

In this study, a total of four beam-to-column dowel-type connections were tested. The mechanical properties between unreinforced and reinforced connections are compared and the following points can be concluded:

- Self-tapping screws show a tendency to improve the moment-resisting capacity and rotational capacity of beam-to-column connections. The variation in stiffness could be a result of the difference of the initial gap between the two timber members during manufacture. A larger gap can reduce the rotational stiffness.
- The screws transformed the failure mode. Reinforced connections exhibited a more ductile failure.
- A theoretical calculation of moment-resisting capacity of unreinforced connections is presented. The moment-rotation curve produced by this method reflects the behaviour of the connections when the gap gradually closes and the two timber members start bearing on each other. This leads to excessive tensile stresses perpendicular to the grain and finally splitting failure.
- A larger sample size of the experimental test is required to examine the accuracy and robustness of the presented method. The bearing behaviour shifted the centre of rotation in each fastener group to the bearing point causing the dowels to move away

from the self-tapping screws. Consequently, the dowels did not bear on the self-tapping screws that were observed in embedment tests in previous work. Thus, the moment-resisting capacity of the reinforced connection is not predicted in this study.

This study considers that the location of self-tapping screws is essential to utilise the mechanical properties of the screw as reinforcement. Furthermore, the design of the connections, such as the size of the gap between the two parts in this study, can have a critical impact on determining the location of the screw.

The next chapter extends the experimental work on full-scale structures, aiming to investigate the effectiveness of partially threaded self-tapping screws to improve the moment-resisting capacity and rotational capacity of dowel-type connections as reinforcement.

Chapter 7 Dowel-Type Connected Portal Frame with Screw Reinforcement

The content of this chapter has been published in the journal of '*Engineering Structures*'.

7.1 Introduction

Timber as construction material has the advantage over concrete and steel of having a low self-weight. However, due to its low capacity of strength perpendicular to the grain, the application of tall timber structures has been limited (Jorissen and Leijten, 2008). For instance, timber dowel-type connections are commonly used in design, but their moment-resisting capacity is much lower than that of a timber member, making it the most vulnerable link in a timber structure (Leijten and Brandon, 2013).

A moment connection with sufficient capacity is vital in a portal frame structure. Therefore, in past decades, efforts have been made to strengthen the capacity of dowel-type timber connections with various types of reinforcement.

With the development of FRP, considerable research has been conducted into using FRP as reinforcement for timber connections. Studies by Soltis *et al.* (1997) and Chen (1999) reported that FRPs improved the load-carrying capacity and prevented splitting failure of the connections. Haller and Wehsener (1999) used FRP reinforcement combined with densified timber to improve the load-carrying capacity of dowel-type connections to two times that of the unreinforced connections. In the tests of Kasal *et al.* (2004), timber frames reinforced by FRP and densified wood showed less reduction in structural stiffness than unreinforced timber frames. Recent works by D'Ambrisi *et al.* (2014) used FRP to repair damaged timber beams and successfully restored their mechanical properties. Other reinforcing techniques, as summarised by Blaß and Schädle (2011), used glued-on wood-based panels and truss plates. However, the above methods using different materials often require complex preparation and sufficient accessible space to conduct the work. In addition, some of them may not be feasible for repairing historic buildings as they are limited by accessibility and aesthetic requirements.

Under the construction stage of timber structures, it is always more convenient to assemble a dowel-type connection with slightly oversized holes. However, due to the gap between the drilled hole and the dowel, unexpected deformation of the structure is likely to occur; thus, Leijten (1998), Rodd and Leijten (2003), Leijten *et al.* (2006) proposed the use of expanded tube fasteners combined with densified veneer wood (DVW) reinforcement in moment-resisting connections. The expanded steel tube helped to make a tight fit for the fastener so as to avoid slack load take-up, as well as enhancing stiffness (Leijten and Brandon, 2013). The DVW reinforcement controls splitting parallel to the grain but also enhances the embedment strength of the connections. Test results from Rodd and Leijten (2003) showed that such reinforcement significantly improved the moment-resisting capacity and stiffness of connections compared to unreinforced ones. Bakel *et al.* (2017) examined the seismic performance of this type of connection and results showed it had very high capacity to dissipate energy. However, this reinforcement design can significantly increase the total thickness of the connections to over 500mm if glued laminated timber is used. Therefore, Leijten and Brandon (2013) and Brandon and Leijten (2014) proposed the use of a thin steel plate as the middle member in order to reduce the total thickness. The loss of rotational stiffness, by replacing the middle timber member with a steel flitch plate, can be compensated by decreasing the gap between the two timber side members so as to create a rotational suppressing effect. However, the procedure to fabricate such connections involves using a hydraulic jack to compress the tube to fit and attaching the DVW reinforcement is time-consuming and complex.

In the last two decades, studies by Blaß and Schmid (2001), and Blaß and Schädle (2011) demonstrated that self-tapping screws can effectively reduce the splitting tendency of the connections. Lam *et al.* (2008), Lam *et al.* (2010) and Gehloff *et al.* (2010) investigated the effectiveness of using self-tapping screws as reinforcement on bolted timber connections under dynamic load. Lam *et al.* (2010) found that self-tapping screws as reinforcement could increase the moment-resisting capacity by 170% under reverse cyclic loading. He and Liu (2015) compared the reinforcement effectiveness of plain round rods and self-tapping screws on post-to-beam connections. Their work found that screw reinforcement outperformed the plain round rods in maximum moment enhancement, ductility and energy dissipation. In Chapter 4 and Chapter 5, the experimental works also showed the effectiveness of screw reinforcement and suggested the use of self-tapping screws with partial thread on the point end to reduce the drive-in torque so as to reduce the damage to the screws during the installation process.

Currently, there is no experimental testing on timber portal frames using dowel-type connections reinforced by self-tapping screws. Therefore, the aim of this paper is to compare

the mechanical performance of unreinforced and screw-reinforced portal frames. As in large timber structures, long screws are required and higher friction forces are inevitable when the screw is fully threaded. Therefore, the portal frames in this study used screws with partial thread on the point end in order to reduce the drive-in torque.

7.2 Materials and methods

7.2.1 Material preparation

Two timber portal frames were fabricated for the test, each frame consisting of three glulam beams made from European Whitewood, classified to GL24c. The timber beams were prepared at 21.6°C temperature and 59% RH. The measured average volume density was 456 kg/m^3 (CoV=1.5%) and the average moisture content was 10.2% (CoV= 17.9%) measured by a moisture meter. The screw used in this study is the Screw X that was used in Chapter 6. It had a flange head and its details and specifications, according to OIB (2017), are shown in Figure 7-1.

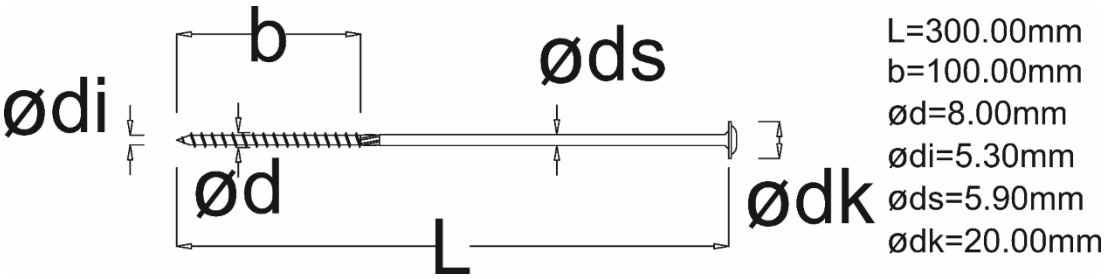

Figure 7-1: The partially threaded self-tapping screw used in this study.

The configuration of timber-steel-timber connections in the portal frame was designed according to EC5 (BSI, 2004) and the details are shown in Figure 7-2. A 3×3 fastener group consisting of 12mm dowels was adopted for the connections, the geometry of the fastener groups in the columns and beams being identical. An 8.5mm wide slot was used to accommodate the 8mm steel plate as the central member. The steel dowels and steel plates were made from bright mild steel classified to 080A15T and S275, respectively. To ensure the 300mm self-tapping screws could be accurately installed, a pre-drilled hole with 5mm diameter and 300mm depth was prepared using a pillar drill. The self-tapping screw was placed at *1d* distance (12mm) to the dowel, so that the screw was not in contact with the dowel.

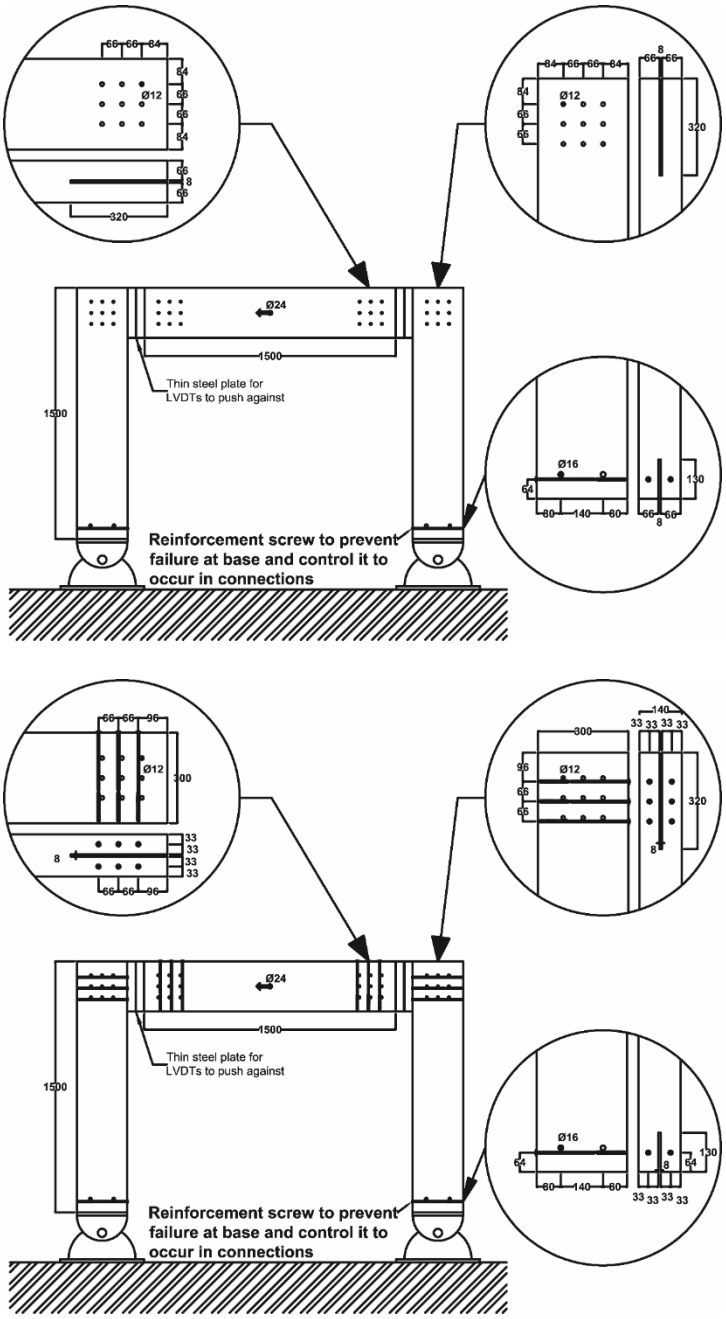

Figure 7-2: Configuration of unreinforced portal frame (top); Configuration of reinforced portal frame (bottom).

As the portal frame was to be subjected to a horizontal force, the base of each of the two columns was designed to sustain an opposing force to reach equilibrium. Therefore, a shear force acting parallel to the cross section of the beam could lead to shear splitting failure of the column. To avoid failure at the base of the frame, both the unreinforced and reinforced frames were reinforced by self-tapping screws at the base, as shown in Figure 7-2, while calculation had shown sufficient shear resistance at base. Table 7-1 summarises the properties of the two tested portal frames.

Table 7-1: Summary of the two groups.

Group	Description	Mean density (kg/m^3) (CoV)	Mean M.C.% (CoV)
UPF	*Unreinforced*	*458 (0.5%)*	*10.5 (23.5%)*
RPF	*Reinforced*	*458 (0.5%)*	*9.6 (18.2%)*

7.2.2 Portal frame test set-up

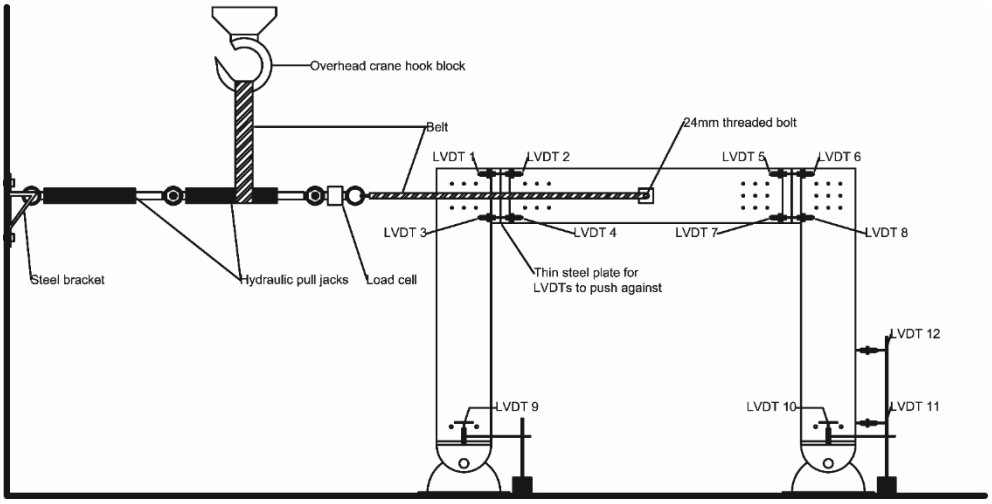

Figure 7-3: Layout of the portal frame test.

A general overview of the test layout is shown in Figure 7-3. The portal frames had pinned supports bolted to the strong floor and the frame was loaded horizontally by two hydraulic pull jacks (100kN capacity). The hydraulic jacks were placed in series with one end connected to a steel triangle bracket fixed to the wall and the other end connected to a load cell. One of the jacks was linked to the hook block of an overhead crane by a belt to ensure the hydraulic jacks were held in position vertically. Another belt was used to transfer the load from the hydraulic jack to the 24mm bolt installed in the frame, as demonstrated in Figure 7-3. In this static loading test, the portal frame was pulled to failure or the load was stopped when the stroke of the jack reached the 300mm limit (with 150mm strokes for each jack). The loading of the test followed BS EN 26891:1991 (BSI, 1991) which describes that a pre-load should be performed from 10% to 40% of the estimated load-carrying capacity before the frame is ramp loaded to failure. 12 LVDTs (100mm stroke with ±0.01mm accuracy) were installed to measure the rotation in each member of the frame.

7.3 Results and discussion

7.3.1 Unreinforced portal frame

In this study, the unreinforced portal frame was unloaded when the capacity of the frame was 20% lower than the peak load. During the loading stage, splitting of the timber in the two columns occurred with a large wood cracking noise. A total of 8 major cracks were found in the two columns. After failure, it was observed that cracks were located at the top and bottom rows parallel to the grain of the columns, as shown in Figure 7-4. Some of the wide and deep cracks propagated to the mid-span of the timber member. The columns rotated around the pinned supports to allow deformation of the frame, and the fasteners in the columns rotated around the centre dowel to take the moment generated during the movement of the frame. For the dowels at the corner of the square-shape fastener group in the column, the four dowels sustained the highest moment as they were located furthest from the centre of the rotation. The load on them was at 45° to the grain direction and the force component perpendicular to the grain was the cause of the splitting in the wood parallel to the grain. Cracks appeared on both sides of the columns in the unreinforced portal frame. The initiation of the crack on the right-hand side of the column appeared along the bottom row of dowels with an initial length of 202mm at 26kNm. At the point of failure, this crack propagated to about 551mm. A second crack appeared on the top row of dowels, before the failure point, and propagated to 407mm at the end of the loading stage. The beam member of the frame, however, did not rotate substantially relative to the steel plate as the two columns did (see Figure 7-9) and no cracks could be observed at the point of failure of the unreinforced frame.

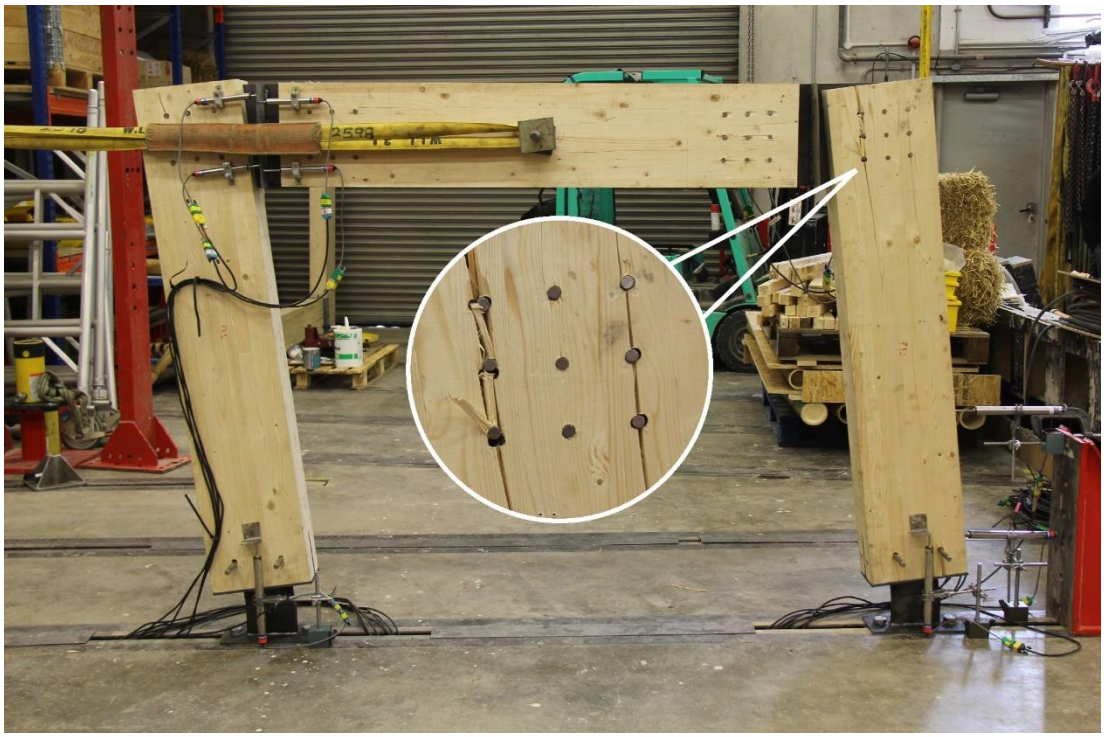

Figure 7-4: Unreinforced portal frame during testing, significant cracks can be observed on the column on the right-hand side (one along the top row and another along the bottom row parallel to the grain direction).

7.3.2 Reinforced portal frame

For the reinforced portal frame, loading was stopped when the full stroke of the jack had been reached. The reinforced frame did show a small load reduction when the timber split, but the load did not drop below 80% of the peak load as observed in the unreinforced frame. There were two cracks at the lower row of fasteners parallel to the grain of the column on the right-hand side. The cracks were much shorter than those in the unreinforced frame and did not pass through all three dowels in a row, as shown in Figure 7-5 below. The two side columns rotated at the pinned supports and at a higher angle of rotation than the unreinforced. The central beam again had much smaller rotation relative to the steel plates and no cracks were found on the beam. In the last few minutes of the test, the 100mm LVDT (No.12) exceeded the stroke capacity and the final width of the gap between the tip of the LVDT and the surface of the column was measured to be 30mm. For the reinforced portal frame, the significant load perpendicular to the grain of the column was intended to split the wood, but the crack propagation was restricted by the screw reinforcement, as expected. The first crack initiated at 33kNm with a length of 129mm. At the end of the loading stage, its length remained to be the same. A second crack developed after 35kNm with an initial length of 108mm and propagated to 126mm at the end of the loading stage. The screw reinforcement effectively used the restrains provided by the embedment of the screw head

and the thread-wood anchorage. Figure 7-6 shows the embedment of the screw head in the reinforced portal frame.

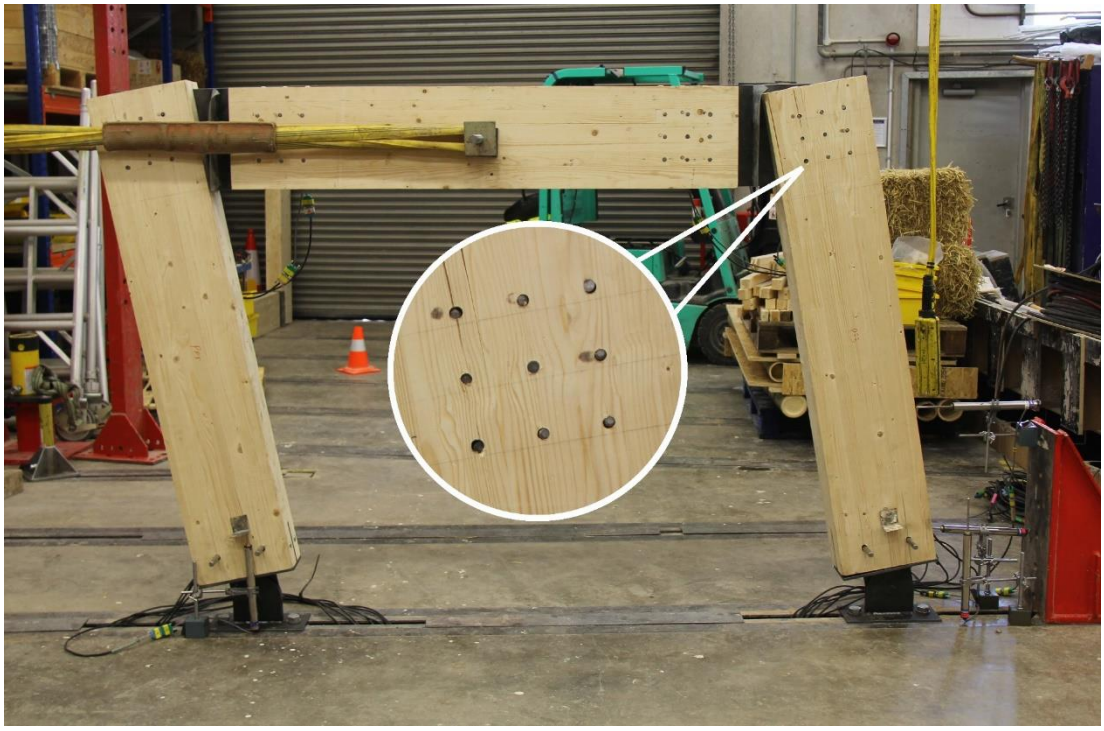

Figure 7-5: Reinforced portal frame during testing, two short cracks located on the right-hand side column is zoomed.

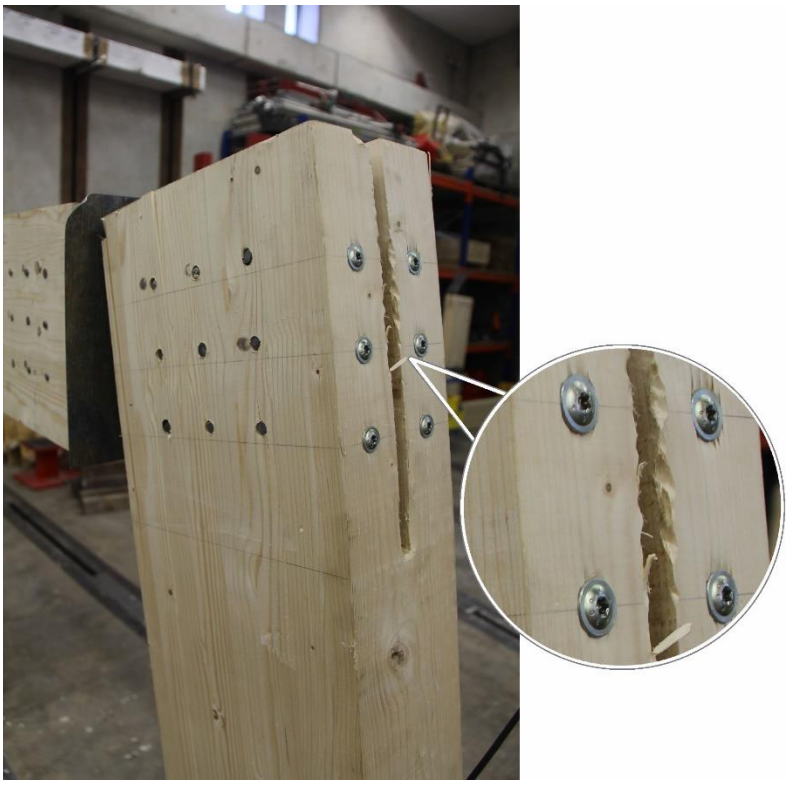

Figure 7-6: Embedment of screw head in the reinforced portal frame.

7.3.3 Comparison between unreinforced and reinforced portal frames

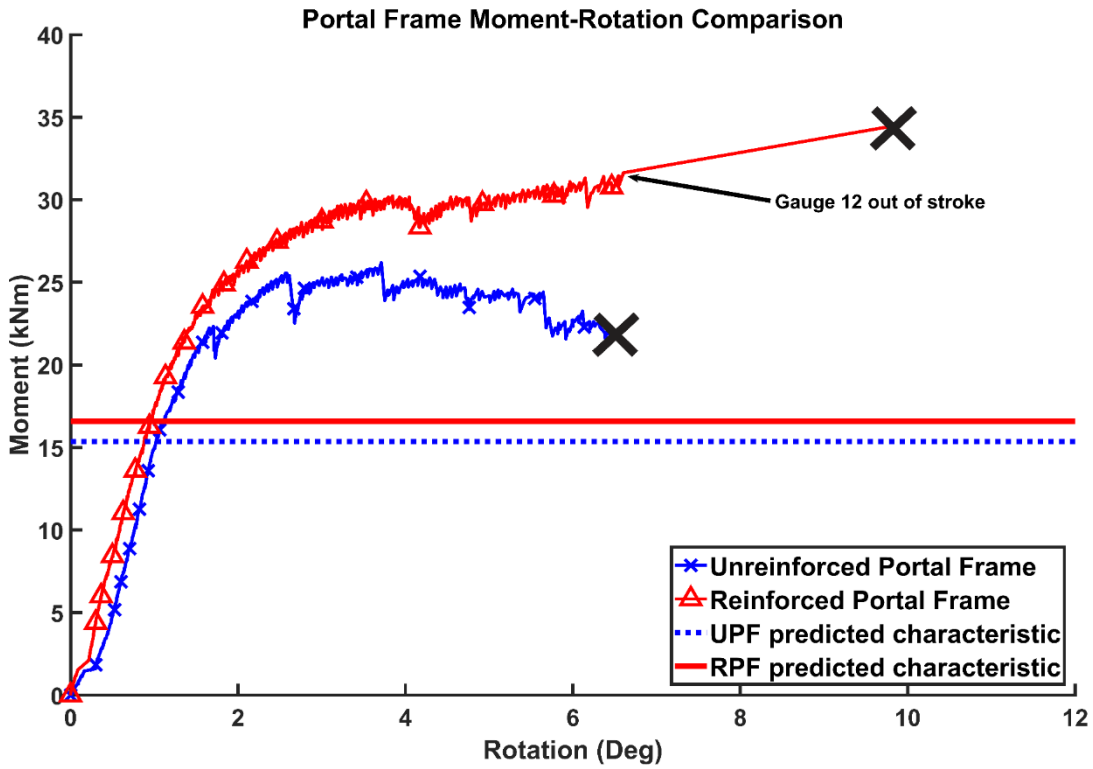

Figure 7-7: Moment-rotation curves for the two tested frames. For the UPF, the black X-mark indicates the 20% load drop from the peak load. For the RPF, the marker indicates the end of stroke of the hydraulic jack. The pre-loading stage is excluded in the graph.

The moment-rotation curves for both frames are plotted in Figure 7-7. For the unreinforced frame, the moment-resisting capacity dropped as the crack developed in the connections. The unreinforced frame reached its peak moment at 26.19kNm and splitting failure of the timber columns led to 20% load drop. The ultimate rotation for the unreinforced frame was 6°.

As for the reinforced frame, the moment first peaked at 30kNm with a rotation of 4°. The capacity then slightly dropped with crack propagation; however, as the steel dowels were bent and started to bear on the screw reinforcement, the connections regained their moment-resisting capacity. At approximately 6° of rotation, the capacity increased to about 32kNm when the full stroke of LVDT 12 (100mm) was reached and the reading of LVDT 12 remained to be a constant. Then, the capacity kept increasing to 34.47kNm until the full stroke of the jack was reached, at which point the load was removed. However, as the full stroke of LVDT 12 had already been reached, the rotation of frame during this stage is not available. Therefore, a tape was used to measure the additional stroke from the tip of LVDT 12 to the surface of the column and the distance was 30mm (see Figure 7-8). The measured

30mm was added to the last reading of LVDT 12. Together with the reading of LVDT 11 at the point the full stroke of the jack was reached, the rotation of the frame at the final point was calculated to be 9.8°. The corresponding moment-resisting capacity of the reinforced frame was 34.47kNm and is marked with ***X*** in the graph. The interval points, between the point when the full stroke of LVDT 12 was reached and the point when the full stroke of the hydraulic jack was reached, were not available and a straight line was drawn in Figure 7-7.

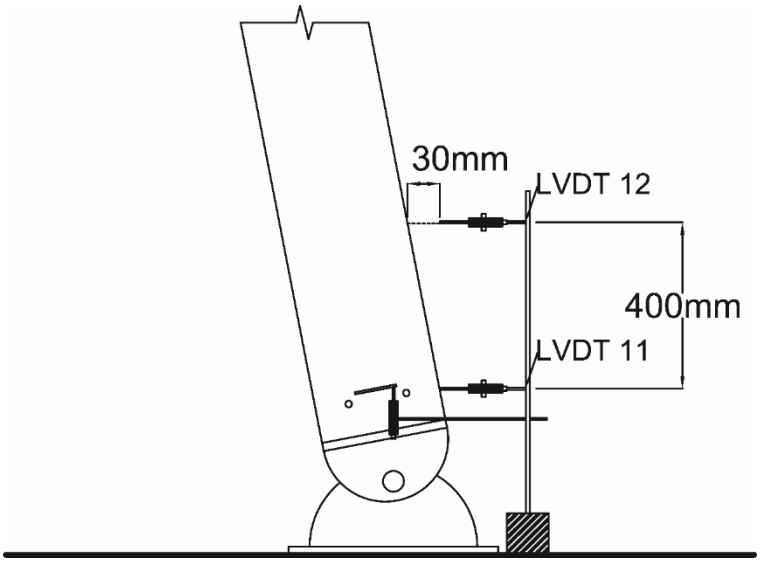

Figure 7-8: At the point the full stroke of the hydraulic jack was reached, the distance between the tip of LVDT 12 and the column was 30mm.

The reinforced portal frame demonstrated high moment-resisting capacity and ultimate rotation compared to the unreinforced one. A higher ultimate rotation in a dowel-type connection is an indicator for a higher ductility.

Table 7-2: Summary of calculated mechanical properties for the two frames.

Group	Mean maximum moment-resisting capacity (kNm)	Mean ultimate rotation (degree)	Mean rotational stiffness (kNm per degree)	Mean rotational stiffness (kNm per radian)
UPF	*26.19*	*6.50*	*9.03*	*1035.73*
RPF	*34.47 **	*9.80 **	*10.00*	*1146.90*

** This is not the maximum value of the reinforced portal frame, but the final reading when the stroke on the hydraulic jack was reached.*

The calculated mechanical properties of the two frames are listed in Table 7-2. As can be seen, the screw reinforcement effectively improved the moment-resisting capacity and

ultimate rotation of the frame with dowel-type timber connections. The rotational stiffness of the frame was calculated using the gradient between $0.1M_{max}$ and $0.4M_{max}$ (M_{max} is the peak moment resistance). However, the stiffness did not show significant enhancement and correlated well with previous results on screw-reinforced moment-resisting connections.

Figure 7-9 displays the beam to steel plate rotation and column to steel plate rotation for both frames. It shows that the beam did not rotate significantly around the plate, while the column in the reinforced frame showed a larger angle of rotation around the plate than that of the unreinforced frame.

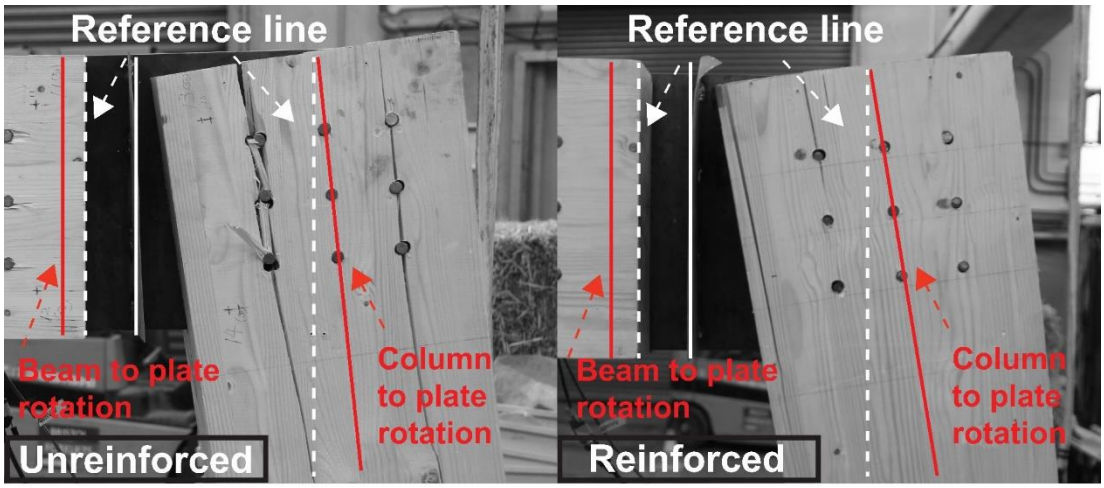

Figure 7-9: Pictures showing the beams and columns to plates rotation for unreinforced portal frame (left) and reinforced portal frame (right).

7.3.4 Theoretical prediction of moment-resisting capacity of portal frames

Current EC5 does not provide any methods of calculations for screw-reinforced timber structures. In this study, the connections in the portal frame are assumed to be rotationally rigid, where the centre of rotation is the centroid of the fastener group and remains fixed.

The calculation method is based on the model presented in Blaß (1995) and Porteous and Kermani (2013) and, for the three by three moment connection in this study, is expressed as:

$$M_k = FL = [(F_A + F_C + F_E + F_G) \cdot r_{max} + (F_B + F_D + F_F + F_H) \cdot r_i] \cdot n_{sp} \qquad (7\text{-}1)$$

where:

M_k is the characteristic moment-resisting capacity of the connection;

F is the load acting perpendicular to the grain;

F_x represents the load acting on the dowel due to the moment (see Figure 7-10);

r_{max} is the maximum distance between the dowel and the centre of rotation;

r_i is the distance between the dowel and the centre of rotation;

n_{sp} is the number of shear planes.

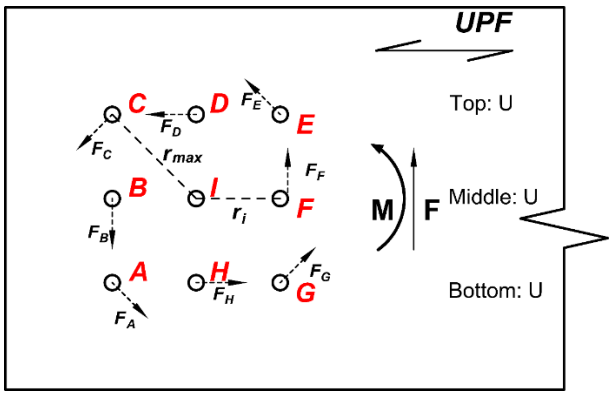

Figure 7-10: The drawing indicates the unreinforced column connections on the right-hand side only and for convenience, they have been rotated 90˚ in the anti-clockwise direction. The black arrows represent the load on the dowel due to the moment.

As the connections in the beam member did not have significant rotation, the theoretical prediction only considers the fastener groups at the columns which are subject to a horizontal load and moment. The calculation method assumes the connection is rigid and the dowels have same slip modulus and rotation angle. Therefore, for a three by three connection, the dowels having same perpendicular distance to the centre of rotation are subject to the same amount of load due to pure moment:

$$F_A = F_C = F_E = F_G = K \cdot \delta_{max} = K \cdot r_{max} \cdot \theta \qquad (7\text{-}2)$$

$$F_B = F_D = F_F = F_H = K \cdot \delta_i = K \cdot r_i \cdot \theta \qquad (7\text{-}3)$$

Thus, the equation for the characteristic moment-resisting capacity of the connections can be re-written based on the load on one dowel; taking dowel *E* for example:

$$M_k = FL = (4F_E \cdot r_{max} + 4\frac{F_E}{r_{max}} \cdot r_i^2) \cdot n_{sp} \qquad (7\text{-}4)$$

The method considers the influence of a load on the connections, when also subject to a moment at the centre of rotation. The load, either in the vertical or the horizontal direction, can change the angle of the total load on the dowel, see Figure 7-11. F_{TX} represents the total load on dowel *X* due to the moment and the horizontal load F_h. The angle of the total load can be found by using the resolution of F_{TX}, F_h and F_x into horizontal and vertical

components. The magnitude of the total load should not be greater than the load-carrying capacity derived using the equations in EC5.

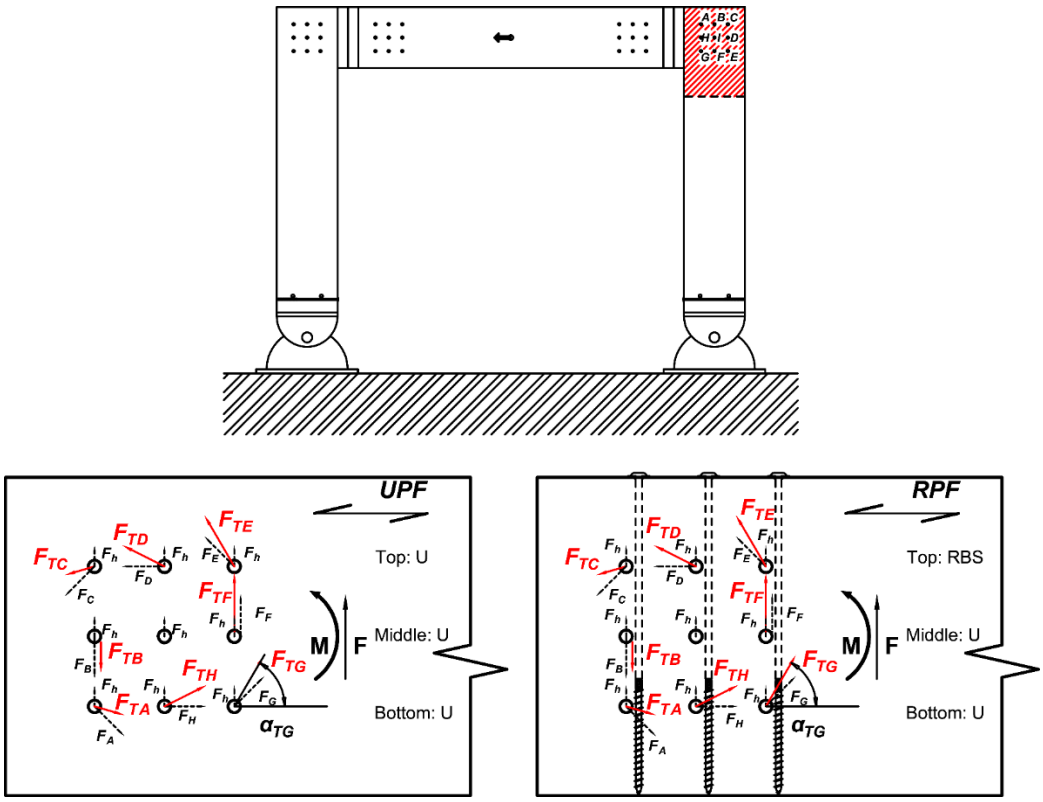

Figure 7-11: The drawings indicate the column connections on the right-hand side (refer to Figure 7-4 and Figure 7-5) only. Reinforcement scenario assigned for the two frames: unreinforced portal frame (left) and screw-reinforced portal frame (right). Red arrows indicate the total loads on the dowels from the timber members due to the rotation and horizontal loading.

The load-carrying capacity can be found by knowing the embedment strength and the angle of the load to the grain direction. As the embedment strength varies with the angle of load to the grain direction, the load-carrying capacity will be different. For the unreinforced connections, the characteristic embedment strength for each dowel is calculated based on the unreinforced embedment test (group *U*) as shown in Figure 7-11.

To find the magnitude of F_{TX}, characteristic embedment strength from single dowel embedment tests are applied. The characteristic embedment values are acquired from the original data using the five-percentile method described in BS EN 14358:2016 (BSI, 2016). As the characteristic values are only available for loading parallel to the grain, $f_{h,0,k}$, the characteristic embedment strength, $f_{h,1,k}$, in various loading directions (denoted as α_{TX} in Figure 7-11 where *X* represents the fastener), can be calculated using the Hankinson formula illustrated in EC5 Clause 8.5.1.1 (BSI, 2004). Table 7-3 lists the characteristic values obtained from the embedment test.

Table 7-3: Characteristic values calculated from embedment test.

Group	Description	Repetition	Characteristic embedment strength (N/mm^2)
U	*Unreinforced*	*10*	*20.07*
RBS	*Reinforced by screw with 33% thread on the point end*	*10*	*24.80*

After the magnitude of the total load acting on a certain dowel is found, the value of F_x, can be worked out by resolving F_{TX} into horizontal and vertical components.

Since the characteristic moment-resisting capacity of the connections can be represented by the load F_x on a certain dowel, such as Equation (7-4), the moment-resisting capacity of a connection can be calculated. With different magnitude and angle of the total loads on the dowels, the value of F_x and the moment-resisting capacity of the connection shall vary with the dowel that is under consideration.

Consequently, the dowels and the surrounding wood shall fail in a sequence because their load-carrying capacities are different. In this study, mode type 2 failure (a combination of embedment failure of wood and single yield failure of the fastener) was observed in the experiment. For simplification purposes, this study uses the label of the dowels to indicate the area of the occurrence of mode type 2 failure. For example, '*failure of Area E*' indicates that both embedment failure of the wood and single yield failure of the dowel have occurred to dowel *E*.

The calculation method first involves finding the sequence of failure, then, calculating the moment-resisting capacity of the connections by considering the loads on the failed areas. It requires considering three areas to fail in a connection for an accurate prediction. The purpose for such requirement is because the area that has dowels bearing on unreinforced wood tend to fail first and considering the failure of three areas would involve at least one case of the failure with a dowel bearing on reinforced wood to occur. The moment-resisting capacity of the reinforced connections would be underestimated if they are calculated using only the load-carrying capacity from an unreinforced area of the connection. Furthermore, the calculation methods assume the failed areas would maintain their peak load-carrying capacity until three areas have failed.

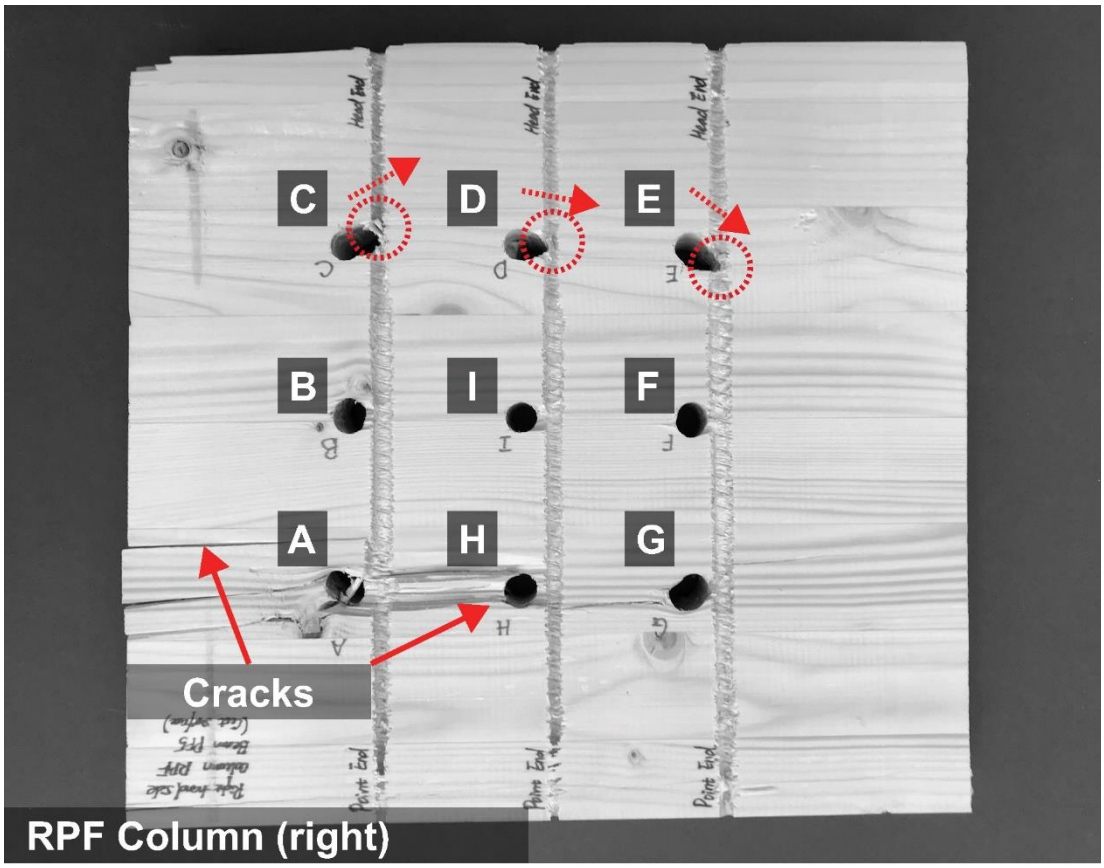

Figure 7-12: The column from reinforced portal frame was cut open for inspection of the interaction between dowels and screws.

For the reinforced connections, the sequence of failure (defined as the load-carrying capacity being exceeded) includes two unreinforced area and one reinforced area.

In the reinforced connections, only the top row of the fasteners *C*, *D* and *E*, have the movement of bearing on the screw reinforcement. This is also confirmed by the inspection of the reinforced portal frame specimen which was cut open, see Figure 7-12. It should be noted the movement of the dowel is opposite to the direction of the total load acting on the dowel, as shown in Figure 7-11. In other words, the embedment strength for these locations is enhanced. Therefore, the embedment strength of group *RBS*, in Table 7-3, is applied. As for the middle and bottom dowels, their rotation directions determine that they will not bear on the screws. Therefore, the wood at these locations are defined as 'unreinforced' and applied with unreinforced values (*U*). The load-carrying capacity of each dowel is acquired by using the Equations *(f)*, *(g)* and *(h)* from clause 8.2.3 in EC5 (BSI, 2004).

The characteristic moment-resisting capacity of the portal frame is the sum of the capacity of the two column connections. The predicted maximum values for the unreinforced and reinforced portal frames were 15.38 and 16.60kNm, respectively; they are shown by the horizontal lines in Figure 7-7.

In addition, the maximum moment-resisting capacity of the reinforced portal frame is approximately 8% higher than the unreinforced frame for the theoretically predicted values.

The 8% increase of theoretical moment-resisting capacity of the frame is a result of the higher embedment strength of the wood around the dowels *C*, *D* and *E*. As shown in Figure 7-11, only these areas are considered to be effectively reinforced by the self-tapping screws. To further enhance the capacity of the frame, one possible method is to enhance the remaining part of the connection, which is shown in Figure 7-13.

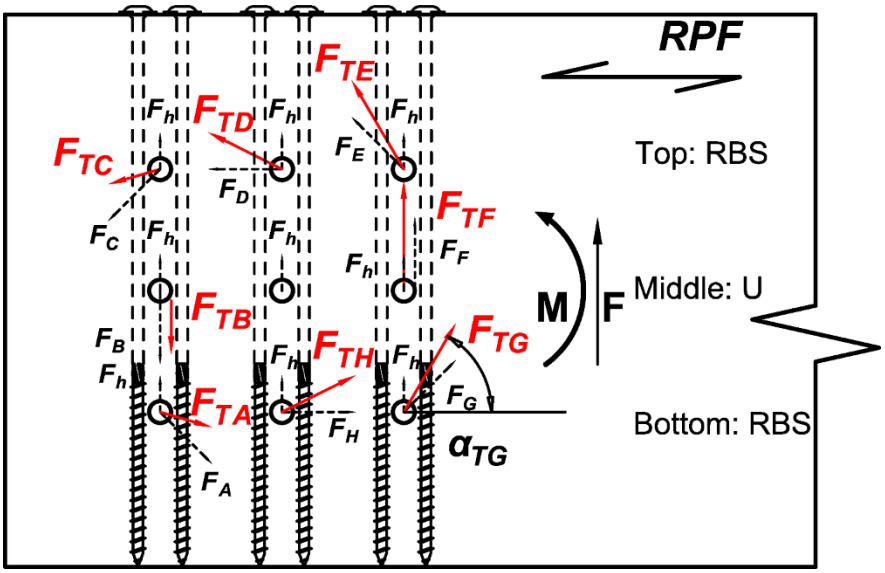

Figure 7-13: Proposed reinforcement approach to further enhance the moment-resisting capacity of portal frames. Red arrows indicate the total loads on the dowels from the timber members due to the rotation and horizontal loading.

In Figure 7-13, these 3 additional screws are placed at *1d* distance to the dowels, opposite to the existing screws. These screws are applied to enhance the embedment strength of Areas *A*, *G* and *H*. For steel dowels *B* and *F*, their movements are perpendicular to the grain. As the embedment strength of the wood is lowest in the perpendicular to the grain direction, using self-tapping screws to enhance their strength is less effective than enhancing those with higher strength, in 45° or parallel to the grain direction. The theoretical moment-resisting capacity of this type of reinforced frame is 17.47kNm, 14% higher than the unreinforced frame.

The results of this study are limited by the number of tests. It will be necessary in the future, to increase the sample size and use the 5-percentile method in BS EN 14358:2016 (BSI, 2016) to calculate the characteristic moment-resisting capacity of the test results. The characteristic values can then be used to demonstrate whether the characteristic values, obtained by the proposed calculation method in this study, are appropriate and conservative.

7.4 Summary

This study compares the mechanical performance of dowel-type moment-resisting timber frames that are unreinforced and reinforced by self-tapping screws. The sample size of the experiment in this study is small and a large number of tests are required in the future for confirmation. The following points were concluded based on the results of this study:

- Self-tapping screws with 33% thread on the point end placed at one fastener spacing to the dowel showed a tendency to effectively enhance the moment-resisting capacity and ultimate rotation of timber portal frames. The experiment demonstrates the potential of using self-tapping screws with partial thread as reinforcement on dowel-type connections. The screws with partial thread offer better installation compared with fully threaded screws.
- Screw reinforcement has demonstrated an effective behaviour in controlling crack initiation and propagation. The restraining force is provided through screw head embedment and thread-wood anchorage.
- The study does not find a tendency for screw reinforcement to improve structural stiffness. This result corresponds well with previous findings on moment-resisting connection tests.
- A simple calculation method for predicting the moment-resisting capacity of screw-reinforced portal frames is proposed. The method uses results from embedment tests to predict the load-carrying capacity of each area that is assigned different reinforcement scenarios. The summation of the moment resistance of the fastener group represents a structure's characteristic moment-resisting capacity.
- The predicted values are smaller than those of the experimental results, but more repetitions of test are required to validate whether the method is conservative. With further confirmation, the proposed method may be used to predict the safe moment-resisting capacity of certain types of screw-reinforced dowel-type timber structures, if the corresponding embedment data is available.

The next chapter concludes the experimental results of the research works in this thesis and identifies the gaps of research on reinforcing dowel-type connections with self-tapping screws for future study.

Chapter 8 Conclusion

8.1 Summary

Self-tapping screws are often used as connectors and this research has demonstrated their strong potential as reinforcement for dowel-type timber connections. However, the standardisation of screw reinforcement is still at an early stage of adoption. With the current lack of knowledge, no confidence can be assured in choosing the most suitable form of self-tapping screws out of the huge number available on the market. With insufficient guidance, no confidence can be established in using screws as effective reinforcement.

Screws with full thread require higher drive-in torque to be installed. Therefore, this study investigated reduced thread lengths on the screw and aims to prove that partially threaded screws can effectively improve the mechanically properties of timber dowel-type connections.

In addition, two factors are chosen in this study, thread configuration and screw to dowel distance, in order to understand their influence on the effectiveness of screw reinforcement for dowel-type timber connections. The experimental work of this study aims to provide insight for the future use of self-tapping screws as reinforcement.

8.1.1 Relationship between drive-in torque and thread configuration

Validating the influence of thread configuration on the drive-in torque has been a core task in this study. A torque analyser was used to measure drive-in torque of the screw. Tests revealed that the screws with 33% thread on the point end only required 75% and 71% of the torque to install a fully threaded screw, in conditions with and without pre-drilled holes, respectively. It demonstrated that the risks due to torsional damage are reduced with partially threaded screws. In addition, the tests also identified the negative impact of knots on drive-in torque and positioning of screws. This study has also confirmed the benefits of having pre-drilled holes; these include the reduction in drive-in torque by at least 18.6% and increased accuracy of positioning of screws. Since it is difficult to locate knots inside the timber member, having pre-drilled holes can neutralising the influence of knots.

8.1.2 Embedment strength of reinforced single dowel connections

Embedment tests on timber specimens demonstrated that thread location and length impact the enhancement of embedment strength. Self-tapping screws with thread on the point end achieved similar improvement in strength when compared to screws with complete thread. The use of DIC also identified that screws with thread on the point end can effectively reduce the principal strain at the location of cracks. With the restraining force provided by the screw head and the thread-wood anchorage at the point end, the splitting of the wood is controlled, and the embedment strength of the wood is improved, as higher loads are required to bend the screws. With less thread, the drive-in torque is reduced and the screw can be less vulnerable to torsional damage during the installation process.

The study did not indicate a significant difference in embedment strength and ductility between specimens reinforced by screws placed at *0.5d* (technically, in touch with the dowel) and *1d* distance to the dowel. However, visualisation of the strain distributions on the surface of the specimen indicated a faster rate of strain reduction in the specimen reinforced by screw placed at *0.5d*. The results from DIC also indicated that, under similar magnitude of loading, the rate of stress reduction decreases with increasing screw to dowel distance (*0.5d* to *4d*). In addition, placing the screws at *4d* distance did not enhance the embedment strength of the wood, as it was too far for the dowel to bear on the screw before the failure of the wood occurred. However, as the screw still provided restraint to wood splitting, the ductility of the specimens was enhanced.

To provide evidence that the restraining force from the screw is connected to the thread length, the axial load on the screw was measured by a load cell. Results indicated that resistance is proportional to the thread length on the point end. The resistance from the head end is contributed by the screw head and the threads on the head end. Reducing the thread length on the point end to ⅛ of the total length of the screw reduces the improvement in embedment strength by 10% when compared to a fully threaded screw.

The above experimental tests indicated that screws with partial thread on the point end can achieve similar performance to fully threaded screws but have better workability, as its thread profile reduces the drive-in torque.

8.1.3 Mechanical performance of reinforced multiple-dowel tensile connections

Multiple-dowel connections subject to tensile loading parallel to the grain were conducted to examine the performance of screws with 33% thread on the point end. The connections reinforced by screws with 33% thread on the point end achieved significantly higher performance than unreinforced connections and connections reinforced by screws with 0% thread. The tensile connection tests also confirmed that screws with thread on the point end can compete with screws with complete thread in terms of reinforcement performance, as the difference in the load-carrying capacities of connections reinforced by them is insignificant.

8.1.4 Moment-resisting capacity of reinforced dowel-type connections

To further investigate the performance of screws with 33% thread on the point end, static loading on reinforced moment-resisting connections are conducted. Compared with unreinforced connections, the moment resisting capacity and rotational capacity showed slight improvement in the reinforced connections. The artificial crack located at the middle row of a three by three dowel-type fastener group reduced the rotational capacity. However, as the three dowels at the middle row did not provide a significant portion of the moment resistance of the connections, the reduction of moment-resisting capacity due to the crack was not significant. Reinforcing the damaged connections with screws can restore the rotational capacity by controlling crack propagation. Furthermore, self-tapping screws can effectively control crack propagation in both damaged and undamaged specimens. The average crack length in reinforced connections is approximately 37% shorter than the cracks in unreinforced connections. Screws with partial thread on the point end, which have the benefit of easier installation than fully threaded screws, have demonstrated their ability to ensure a more ductile failure in timber connections.

A series of moment-resisting connection tests were carried out to compare the effectiveness of screws with different thread configurations: screws with full thread, screws with 33% thread on both ends and screws with 33% thread on the point end. Screws with all three types of thread configuration improved the mechanical properties of damaged moment-resisting connections. This research provides positive evidence that screws with the proposed partial thread on the point end can work as effectively as fully threaded screws. To confirm the effectiveness of reinforcement, in the future, the sample size should be increased.

Based on the assumption that the reinforced connections rotate around the centroid of the fastener group, the theoretical moment-resisting capacity of reinforced connections can be predicted using results of embedment test in this study. The predicted values from the analytical model is shown to be conservative when compared to the characteristic values of the test results.

Tests on beam-to-column connections also provide positive results, showing that screws with the proposed partial thread on the point end can enhance the moment-resisting capacity (by 24%) and rotational capacity (by approximately 2.5 times) compared with unreinforced connections.

8.1.5 Mechanical performance of dowel-type connected portal frames

To examine the effectiveness of self-tapping screws with 33% thread on the point end on a complete structure, static test on reinforced portal frame was conducted. The screw reinforcement showed a tendency to improve the moment-resisting capacity and rotational capacity of the frame by approximately 32% and 51%, respectively, when compared to the unreinforced frame. Observation of the reinforced frame found that the propagation of crack was effectively controlled. The prediction of the characteristic moment-resisting capacity of the reinforced frame, using the analytical model, shows conservative values.

By a series of experimental tests, positive evidence was found that self-tapping screws with 33% thread on the point end can work as effectively as fully threaded screws to reinforce timber structures with dowel-type connections. Enlarging the sample size of testing screw-reinforced portal frames is required for confirmation.

Overall, the experiments in this study demonstrated the effectiveness of screws with partial thread on improving the mechanical performance of dowel-type timber connections. More importantly, partially threaded self-tapping screws are easier to install than fully threaded screws.

8.2 Potential future work

This thesis has identified some areas for future investigation. As stated by Bejtka and Blaß (2005), placing the self-tapping screws beyond the hinge location can make the reinforcement inefficient, as the dowel is unable to bear on the screw. However, placing screws closer to the edge of the member could cause splitting of the wood. The current design edge distance for screw connections is specified in EC5 (BSI, 2004). Therefore, it is

possible for the hinge distance to fall within the required edge distance (see Figure 2-40). In this case, it is essential to review whether the design requirement is conservative, and new design standards should be developed for screw reinforcement.

The investigation of thread configuration in this study is only limited to the thread location and length. Other design parameters, such as thread depth, thread angle and pitch length should be investigated in aiming to reduce the drive-in torque, while maintaining the thread-wood anchorage.

Similar to other reinforcement materials, the long-term durability of screw reinforcement should be investigated. In some conditions, such as coastal areas, the corrosion of the screw reinforcement can be critical. To protect the thread-wood anchorage and the screw itself, the performance of protective coating on the screw against extreme conditions should be evaluated. Accelerated artificial ageing processes of screw-reinforced members may be a possible method. Durability is an important factor in the service life of screw reinforcement, especially when applied to the repair of historic buildings, which require a minimum amount of intervention to the original structure.

The entire experimental work carried out in this study was under static loading. However, in practice, buildings are subject to dynamic loading from human activities, wind loading, and possibly seismic loads. These dynamic loadings can cause discomfort to the users, deformation of the structure or even failure. Using materials with superior mechanical performance and increasing member sizes can mitigate the problem but increases the cost. Therefore, the behaviour of connections reinforced by self-tapping screw under dynamic loading should be understood, particularly in ductility and energy dissipation. A structure with better ductility can sustain larger deformation before failure and good energy dissipation can damp the vibration.

This study has demonstrated that screw reinforcement can restore the mechanical properties of connections damaged by cracks. However, two problems arise with screw reinforcement. First, the influence of screw reinforcement on the dimensional change of the connection area during moisture variation. The screw itself may restrain the free movement of wood during swelling or shrinking, which has the possibility of causing new cracks. Secondly, during the shrinking phase of the wood, a gap may appear between the screw head and the wood. In this study, the performance of the screw head is essential, as it provides the only restraining force to wood splitting (no thread is available on the head end in the proposed thread configuration). As the screw head is no longer in contact with the surface of the wood, the pull through strength of the screw is no longer available thus splitting of the wood can occur. This led to the idea of keeping a portion of threaded part on the head end of the screw in

order to maintain the gripping force on the wood. The drive-in torque and reinforcement effectiveness (the improvement in embedment strength and moment-resisting capacity) of using this type of thread configuration has been demonstrated in Chapters 3-6. Experimental exploration of the influence of moisture variation on screw-reinforced timber dowel-type connections is an essential part of future work.

In Chapter 3, it is recommended to use pre-drilled holes for self-tapping screws as reinforcement. The advantage is in ensuring the positioning of screws, reducing the drive-in torque and neutralising the negative impact from knots. However, it can be a costly and time-consuming process, particularly for reinforcements in a large timber structure. Current EC5 does not give specifications on the method and tools to prepare pre-drilled holes. The development of methods to quickly and accurately prepare pre-drilled holes are essential for their use in screw reinforcement and should be investigated in the future. In Chapter 7, it is proposed to place two screws on each side of the dowels to enhance the moment-resisting capacity by allowing more dowels to bear on the self-tapping screws. This doubles the amount of reinforcement, work time and cost. Therefore, it is recommended that a feasibility study be conducted on the use of screw reinforcement regarding the total time and cost involved. The relationships between the effectiveness, time and cost of screw reinforcement should be addressed.

Bibliography

Aicher, S. and Höfflin, L., 2009. Glulam beams with holes reinforced by steel bars. *International Council for Research and Innovation in Building and Construction-Working Commission W18-Timber Structure (CIB-W18)*.

Aicher, S., 2011. Glulam beams with internally and externally reinforced holes-tests, detailing and design. *International Council for Research and Innovation in Building and Construction, Working Commission W18-Timber Structures*. Alghero, Italy.

Akbiyik, A., Lamanna, A.J. and Hale, W.M., 2007. Feasibility investigation of the shear repair of timber stringers with horizontal splits. *Construction and Building Materials,* 21(5), pp. 991-1000.

Alam, P., Ansell, M.P. and Smedley, D., 2009. Mechanical repair of timber beams fractured in flexure using bonded-in reinforcements. *Composites Part B: Engineering,* 40(2), pp. 95-106.

Alhayek, H. and Svecova, D., 2012. Flexural stiffness and strength of GFRP-reinforced timber beams. *Journal of Composites for Construction,* 16(3), pp. 245-252.

André, A., 2006. *Fibres for strengthening of timber structures.* Luleå tekniska universitet.

André, A., Johnsson, H. and Carolin, A., 2006. Natural fibre composites for strengthening of glued-laminated timber in tension perpendicular to the grain. *3rd International Conference on FRP Composites in Civil Engineering*.

Angst, V. and Malo, K.A., 2012. Effect of self-tapping screws on moisture induced stresses in glulam. *Engineering Structures,* 45, pp. 299-306.

Ardalany, M., Fragiacomo, M., Deam, B. and Buchanan, A., 2012. Design of reinforcement around holes in laminated veneer lumber (LVL) beams. *World Conference on Timber Engineering 2012*. Auckland, New Zealand. pp. 539-547.

Ardalany, M., Fragiacomo, M., Carradine, D. and Moss, P., 2013a. Experimental behavior of Laminated Veneer Lumber (LVL) joists with holes and different methods of reinforcement. *Engineering Structures,* 56, pp. 2154-2164.

Ardalany, M., Fragiacomo, M., Moss, P. and Deam, B., 2013b. An analytical model for design of reinforcement around holes in Laminated Veneer Lumber (LVL) beams. *Materials and Structures,* 46(11), pp. 1811-1831.

Bakel, R., Rinaldin, G., Leijten, A. and Fragiacomo, M., 2017. Experimental‐numerical investigation on the seismic behaviour of moment‐resisting timber frames with densified veneer wood‐reinforced timber joints and expanded tube fasteners. *Earthquake Engineering & Structural Dynamics,* 46(8), pp. 1307-1324.

Bejtka, I. and Blaß, H., 2005. Self-tapping screws as reinforcements in connections with dowel-type fasteners. *International Council for Research and Innovation in Building and Construction-Working Commission W18-Timber Structure (CIB-W18)*. Karlsruhe, Germany. Karlsruhe, Germany: Universität Karlsruhe.

Bejtka, I. and Blaß, H., 2006. Self-tapping screws as reinforcements in beam supports. *International Council for Research and Innovation in Building and Construction-Working Commission W18-Timber Structure (CIB-W18)*. Florence, Italy.

Blaß, H.J., 1995. *Timber engineering. Step 1: basis of design, material properties, structural components and joints.*

Blaß, H.J., Schmid, M., Litze, H. and Wagner, B., 2000. Nail plate reinforced joints with dowel-type fasteners. *6th World Conference on Timber Engineering*.

Blaß, H.J. and Schmid, M., 2001. Self-tapping screws as reinforcement perpendicular to the grain in timber connections. In: S. Aicher and H.W. Reinhardt, eds. *RILEM Symposium: Joints in Timber Structures*. Stuttgart, Germany. Paris, France: RILEM, pp. 163-172.

Blaß, H.J. and Schädle, P., 2011. Ductility aspects of reinforced and non-reinforced timber joints. *Engineering Structures*, 33(11), pp. 3018-3026.

Borri, A., Corradi, M. and Grazini, A., 2005. A method for flexural reinforcement of old wood beams with CFRP materials. *Composites Part B: Engineering*, 36(2), pp. 143-153.

Borri, A. and Corradi, M., 2011. Strengthening of timber beams with high strength steel cords. *Composites Part B: Engineering*, 42(6), pp. 1480-1491.

Borri, A., Corradi, M. and Speranzini, E., 2013. Reinforcement of wood with natural fibers. *Composites Part B: Engineering*, 53, pp. 1-8.

Brandon, D. and Leijten, A., 2014. Structural performance and advantages of DVW reinforced moment transmitting timber joints with steel plate connectors and tube fasteners. *Materials and Joints in Timber Structures.* Springer, pp. 255-263.

Brunner, M. and Schnüriger, M., 2005. Timber beams strengthened by attaching prestressed carbon FRP laminates with a gradiented anchoring device. *International symposium on bond behaviour of FRP in structures (BBFS 2005)*. Citeseer, pp. 465-471.

BS 4174:1972: 1972. *Specification for self-tapping screws and metallic drive screws*. BSI.

BS EN 26891:1991: 1991. *Timber structures. Joints made with mechanical fasteners. General principles for the determination of strength and deformation characteristics*. BSI.

BS EN 12512:2001: 2002. *Timber structures. Test methods. Cyclic testing of joints made with mechanical fasteners*. BSI.

BS EN 1995-1-1:2004+A2:2014: 2004. *Eurocode 5: Design of timber structures. General. Common rules and rules for buildings*. BSI.

BS EN 383:2007: 2007. *Timber structures. Test methods. Determination of embedment strength and foundation values for dowel type fasteners*. BSI.

BS EN 14592:2008+A1:2012: 2009a. *Timber structures. Dowel type fasteners. Requirements*. BSI.

BS EN 15737:2009: 2009b. *Timber structures. Test methods. Torsional resistance of driving in screws*. BSI.

BS EN 14358:2016: 2016. *Timber structures. Calculation and verification of characteristic values*. BSI.

Bulleit, W.M., Sandberg, L.B. and Woods, G.J., 1989. Steel-reinforced glued laminated timber. *Journal of Structural Engineering*, 115(2), pp. 433-444.

Chen, C.-J., 1999. Mechanical behavior of fiberglass reinforced timber joints. *World Conference on Timber Engineering*

Closen, M. and Lam, F., 2012. Performance of moment resisting self-tapping screw assembly under reverse cyclic load. *World Conference on Timber Engineering*. Auckland, New Zealand. pp. 433-440.

Corradi, M. and Borri, A., 2007. Fir and chestnut timber beams reinforced with GFRP pultruded elements. *Composites Part B: Engineering,* 38(2), pp. 172-181.

Crocetti, R., Gustafsson, P., J, Ed, D. and Hasselqvist, F., 2012. Compression Strength Perpendicular To Grain – Full-Scale Testing Of Glulam Beams With And Without Reinforcement. *COST Action FP1004, Early stage researchers conference*. April 19-20, 2012 Zagreb, Croatia.

D'Ambrisi, A., Focacci, F. and Luciano, R., 2014. Experimental investigation on flexural behavior of timber beams repaired with CFRP plates. *Composite Structures,* 108, pp. 720-728.

Davis, G. and Mettem, C., 1997. The use of resin adhesives in the repair of structural timber members. *WIT Transactions on the Built Environment,* 26.

De Luca, V. and Marano, C., 2012. Prestressed glulam timbers reinforced with steel bars. *Construction and Building Materials,* 30, pp. 206-217.

DeHaitre, L., 1996. *Low torque wood screw*.

Delahunty, S., Chui, Y.H. and McCormick, M., 2014. Use of double-threaded self-tapping screws for in-situ repair of cracked timber connecitons. *World Conference on Timber Engineering*. Quebec City, Canada.

Dietsch, P., Kreuzinger, H. and Winter, S., 2013. Design of shear reinforcement for timber beams. *International Council for Research and Innovation in Building and Construction-Working Commission W18-Timber Structure (CIB-W18).*

Dietsch, P. and Brandner, R., 2015. Self-tapping screws and threaded rods as reinforcement for structural timber elements–A state-of-the-art report. *Construction and Building Materials,* 97, pp. 78-89.

DIN EN 1995-1-1/NA:2013-08: 2013. *National Annex - Nationally determined parameters - Eurocode 5: Design of timber structures - Part 1-1: General - Common rules and rules for buildings*. DIN.

Echavarría, C., 2007. Bolted timber joints with self-tapping screws. *Revista EIA,* (8), pp. 37-47.

Ed, D. and Hasselqvist, F., 2011. *Timber compression strength perpendicular to the grain.* Lund Institute of Technology, Lund.

ETA-Danmark, 2016. *European Technical Assessment ETA-11/0030 of 2016-04-07.* Danmark.

Fawwaz, M. and Hanna, A., 2012. *Structural behavior of notched glulam beams reinforced by means of plywood and FRP.*

Flores, E.S., Saavedra, K., Hinojosa, J., Chandra, Y. and Das, R., 2016. Multi-scale modelling of rolling shear failure in cross-laminated timber structures by homogenisation and cohesive zone models. *International Journal of Solids and Structures,* 81, pp. 219-232.

Fossetti, M., Minafò, G. and Papia, M., 2015. Flexural behaviour of glulam timber beams reinforced with FRP cords. *Construction and Building Materials,* 95, pp. 54-64.

Franke, S. and Franke, B., 2014. Causes, assessment and impact of cracks in timber elements. *COST Workshop–Highly Performing Timber Structures: Reliability, Assessment, Monitoring and Strengthening*. pp. 15-21.

Franke, S., Franke, B. and Harte, A.M., 2015. Failure modes and reinforcement techniques for timber beams–state of the art. *Construction and Building Materials*, 97, pp. 2-13.

Frese, M. and Blaß, H., 2007. Failure analysis on timber structures in Germany. *COST Action E55, First Workshop*. Graz University of Technology, Austria. Graz: Graz University of Technology.

Gehloff, M., Closen, M. and Lam, F., 2010. Reduced edge distances in bolted timber moment connections with perpendicular to grain reinforcements. *World Conference on Timber Engineering*.

Gentile, C., Svecova, D., Saltzberg, W. and Rizkalla, S., 2000. Flexural strengthening of timber beams using GFRP. *3rd International Conference in Advanced Composites Materials in Bridge and Structures*. Ottawa, Canada. pp. 637-644.

Gentile, C., Svecova, D. and Rizkalla, S.H., 2002. Timber beams strengthened with GFRP bars: development and applications. *Journal of Composites for Construction,* 6(1), pp. 11-20.

Glišović, I., Stevanović, B. and Todorović, M., 2016. Flexural reinforcement of glulam beams with CFRP plates. *Materials and Structures,* 49(7), pp. 2841-2855.

González-Bravo, C., Arriaga, F. and Díez, R., 2008. Bending reinforcement of wooden beams with steel cross sections. *10th World Conference on Timber Engineering*. Miyazaki, Japan.

González-Bravo, C., Arriaga-Martitegui, F., Maldonado-Ramos, L. and Díez-Barra, R., 2010. Bending reinforcement of timber beams with steel cross sections on the upper face. *Materiales de Construcción,* 60(298), pp. 123-135.

Gustafsson, P., 1995. Notched beams and holes in glulam beams B5. *Timber Engineering STEP*, 1, p. B5.

Haller, P. and Wehsener, J., 1999. Use of technical textiles and densified wood for timber joints. *1st International RILEM Symposium on Timber Engineering*. Stockholm, Sweden. pp. 717-726.

He, M.-j. and Liu, H.-f., 2015. Comparison of glulam post-to-beam connections reinforced by two different dowel-type fasteners. *Construction and Building Materials*, 99, pp. 99-108.

Heiduschke, A. and Haller, P., 2008. Performance of composite-reinforced timber joints using single dowel-type fasteners. *10th World Conference on Timber Engineering.*

Hockey, B., Lam, F. and Prion, H.G., 2000. Truss plate reinforced bolted connections in parallel strand lumber. *Canadian Journal of Civil Engineering*, 27(6), pp. 1150-1161.

IStructE, 2007. *Manual for the design of timber building structures to Eurocode 5*. The Institution of Structural Engineers.

Jasieńko, J. and Nowak, T.P., 2014. Solid timber beams strengthened with steel plates–Experimental studies. *Construction and Building Materials,* 63, pp. 81-88.

Jockwer, R., Frangi, A., Serrano, E. and Steiger, R., 2013. Enhanced design approach for reinforced notched beams. *International Council for Research and Innovation in Building and Construction-Working Commission W18-Timber Structure (CIB-W18) 46*. Timber Scientific Publishing, pp. 69-84.

Jockwer, R., 2014. *Structural behaviour of glued laminated timber beams with unreinforced and reinforced notches.* ETH Zurich.

Jönsson, J., 2005. Load carrying capacity of curved glulam beams reinforced with self-tapping screws. *Holz als Roh-und Werkstoff,* 63(5), pp. 342-346.

Jorissen, A. and Leijten, A., 2008. Tall Timber Buildings in The Netherlands. *Structural Engineering International,* 18(2), pp. 133-136.

Karacabeyli, E. and Ceccotti, A., 1996. Quasi-static reversed-cyclic testing of nailed joints. *International Council for Research and Innovation in Building and Construction-Working Commission W18-Timber Structure (CIB-W18).*

Kasal, B. and Heiduschke, A., 2004. Radial reinforcement of curved glue laminated wood beams with composite materials. *Forest Products Journal,* 54(1), p. 74.

Kasal, B., Pospisil, S., Jirovsky, I., Heiduschke, A., Drdacky, M. and Haller, P., 2004. Seismic performance of laminated timber frames with fiber‐reinforced joints. *Earthquake Engineering & Structural Dynamics,* 33(5), pp. 633-646.

Kliger, R., Al-Emrani, M., Johansson, M. and Crocetti, R., 2007. Strengthening glulam beams with steel or CFRP plates. *Asia-Pacific Conf. on FRP in Structures (APFIS2007), International Institute for FRP in Construction*. ON, Canada. pp. 291-296.

Kliger, R., Johansson, M. and Crocetti, R., 2008. Strengthening timber with CFRP or steel plates–short and long-term performance. *World Conference on Timber Engineering*. Miyazaki, Japan.

Kliger, R., Haghani, R., Brunner, M., Harte, A.M. and Schober, K.-U., 2016. Wood-based beams strengthened with FRP laminates: improved performance with pre-stressed systems. *European Journal of Wood and Wood Products,* 74(3), pp. 319-330.

Lam, F., Schulte-Wrede, M., Yao, C. and Gu, J., 2008. Moment resistance of bolted timber connections with perpendicular to grain reinforcements. *10th World Conference on Timber Engineering* Miyazaki, Japan.

Lam, F., Gehloff, M. and Closen, M., 2010. Moment-resisting bolted timber connections. *Proceedings of the Institution of Civil Engineers-Structures and Buildings,* 163(4), pp. 267-274.

Lederer, W., Bader, T.K., Unger, G. and Eberhardsteiner, J., 2016. Influence of different types of reinforcements on the embedment behavior of steel dowels in wood. *European Journal of Wood and Wood Products,* 74(6), pp. 793-807.

Leijten, A., 1998. *Densified veneer wood reinforced timber joints with expanded tube fasteners.* TU Delft, Delft University of Technology.

Leijten, A., Ruxton, S., Prion, H. and Lam, F., 2006. Reversed-cyclic behavior of a novel heavy timber tube connection. *Journal of Structural Engineering,* 132(8), pp. 1314-1319.

Leijten, A. and Brandon, D., 2013. Advances in moment transfering dvw reinforced timber connections–Analysis and experimental verification, Part 1. *Construction and Building Materials,* 43, pp. 614-622.

Li, Y.-F., Xie, Y.-M. and Tsai, M.-J., 2009. Enhancement of the flexural performance of retrofitted wood beams using CFRP composite sheets. *Construction and Building Materials,* 23(1), pp. 411-422.

Lionello, G. and Cristofolini, L., 2014. A practical approach to optimizing the preparation of speckle patterns for digital-image correlation. *Measurement Science and Technology*, 25(10), p. 107001.

Lokaj, A. and Klajmonová, K., 2014. Round timber bolted joints exposed to static and dynamic loading. *Wood Research*, 59(3), pp. 439-448.

Lu, W., Ling, Z., Geng, Q., Liu, W., Yang, H. and Yue, K., 2015. Study on flexural behaviour of glulam beams reinforced by Near Surface Mounted (NSM) CFRP laminates. *Construction and Building Materials*, 91, pp. 23-31.

Mastschuch, R., 2000. *Reinforced multiple bolt timber connections.* University of British Columbia.

McConnell, E., McPolin, D. and Taylor, S., 2014. Post-tensioning of glulam timber with steel tendons. *Construction and Building Materials*, 73, pp. 426-433.

Mestek, P., Kreuzinger, H. and Winter, S., 2011. Design concept for CLT-reinforced with self-tapping screws. *International Council for Research and Innovation in Building and Construction-Working Commission W18-Timber Structure (CIB-W18)*. Alghero, Italy.

Metelli, G., Preti, M. and Giuriani, E., 2016. On the delamination phenomenon in the repair of timber beams with steel plates. *Construction and Building Materials*, 102, pp. 1018-1028.

Mohammad, M., Salenikovich, A. and Quenneville, P., 2006. Investigations on the Effectiveness of Self-tapping Screws in Reinforcing Bolted Timber Connections.

Nardin, A., Boström, L. and Zaupa, F., 2000. The effect of knots on the fracture of wood. *World Conference on Timber Engineering*, British Columbia, Canada.

Nielsen, J. and Ellegaard, P., 1999. Moment capacity of timber reinforced with punched metal plate fasteners. *1st RILEM Symposium on Timber Engineering*. RILEM Publications SARL, pp. 129-137.

Nowak, T.P., Jasieńko, J. and Czepiżak, D., 2013. Experimental tests and numerical analysis of historic bent timber elements reinforced with CFRP strips. *Construction and Building Materials*, 40, pp. 197-206.

Oberg, E., Jones, F.D., Horton, H.L., Ryffel, H.H. and Geronimo, J.H., 2016. *Machinery's handbook.* Industrial Press, Incorporated.

OIB, 2017. *European Technical Approval ETA-13/0796 of 15.12.2017.*

Osmannezhad, S., Faezipour, M. and Ebrahimi, G., 2014. Effects of GFRP on bending strength of glulam made of poplar (Populus deltoids) and beech (Fagus orientalis). *Construction and Building Materials*, 51, pp. 34-39.

Palma, P., Frangi, A., Hugi, E., Cachim, P. and Cruz, H., 2013. Fire resistance tests on steel-to-timber dowelled connections reinforced with self drilling screws. *2nd CILASCI–Ibero-Latin-American Congresso n Fire Safety Engineering*. Eidgenösische Technische Hochschule Zürich.

Pizzo, B. and Schober, K., 2008. On site interventions on decayed beam ends. *Core document of COST action E*, 34.

Pizzo, B., Gavioli, M. and Lauriola, M.P., 2013. Evaluation of a design approach to the on-site structural repair of decayed old timber end beams. *Engineering Structures*, 48, pp. 611-622.

Plevris, N. and Triantafillou, T.C., 1992. FRP-reinforced wood as structural material. *Journal of Materials in Civil Engineering*, 4(3), pp. 300-317.

Porteous, J. and Kermani, A., 2013. *Structural timber design to Eurocode 5*. John Wiley & Sons.

Quenneville, J. and Mohammad, M., 2000. Anti-check bolts as means of repair for damaged split ring connections. *6th World Conference on Timber Engineering*.

Radford, D., Van Goethem, D., Gutkowski, R. and Peterson, M., 2002. Composite repair of timber structures. *Construction and Building Materials,* 16(7), pp. 417-425.

Raftery, G., Whelan, C. and Harte, A., 2012. Bonded-in GFRP rods for the repair of glued laminated timber. *World Conference on Timber Engineering* Auckland, New Zealand.

Raftery, G.M. and Harte, A.M., 2011. Low-grade glued laminated timber reinforced with FRP plate. *Composites Part B: Engineering,* 42(4), pp. 724-735.

Raftery, G.M. and Whelan, C., 2014. Low-grade glued laminated timber beams reinforced using improved arrangements of bonded-in GFRP rods. *Construction and Building Materials,* 52, pp. 209-220.

Raftery, G.M. and Kelly, F., 2015. Basalt FRP rods for reinforcement and repair of timber. *Composites Part B: Engineering,* 70, pp. 9-19.

Raftery, G.M. and Rodd, P.D., 2015. FRP reinforcement of low-grade glulam timber bonded with wood adhesive. *Construction and Building Materials,* 91, pp. 116-125.

Rodd, P. and Leijten, A., 2003. High‐performance dowel‐type joints for timber structures. *Progress in Structural Engineering and Materials,* 5(2), pp. 77-89.

Rotafix, 2014. *Timber Resin Splice Brochure.* Swansea: Rotafix. Available from: *http://rotafix.co.uk/*.

Salmanpour, A. and Mojsilovic, N., 2013. Application of digital image correlation for strain measurements of large masonry walls. *5th Asia Pacific Congress on Computational Mechanics*. Queens Town, Singapore. Singapore: Association for Computational Mechanics (Singapore), SACM, pp. 11-14.

Schober, K.-U., Harte, A.M., Kliger, R., Jockwer, R., Xu, Q. and Chen, J.-F., 2015. FRP reinforcement of timber structures. *Construction and Building Materials,* 97, pp. 106-118.

Schober, K. and Rautenstrauch, K., 2007. Post-strengthening of timber structures with CFRP's. *Materials and Structures,* 40(1), pp. 27-35.

Soltis, L.A., Ross, R.J. and Windorski, D.E., 1997. Effect of fiberglass reinforcement on the behavior of bolted wood connections. *A Journal of Contemporary Wood Engineering,* 8(3), p. 6.

Tascioglu, C., Goodell, B. and Lopez-Anido, R., 2003a. Bond durability characterization of preservative treated wood and E-glass/phenolic composite interfaces. *Composites Science and Technology,* 63(7), pp. 979-991.

Tascioglu, C., Goodell, B., Lopez-Anido, R., Peterson, M., Halteman, W. and Jellison, J., 2003b. Monitoring fungal degradation of E-glass/phenolic fiber reinforced polymer (FRP) composites used in wood reinforcement. *International Biodeterioration & Biodegradation,* 51(3), pp. 157-165.

Thelandersson, S. and Larsen, H.J., 2003. *Timber engineering.* John Wiley & Sons.

Trautz, M. and Koj, C., 2009. Self-tapping screws as reinforcement for timber structures. *Symposium of the International Association for Shell and Spatial Structures (50th. 2009. Valencia). Evolution and Trends in Design, Analysis and Construction of Shell and Spatial Structures: Proceedings*. Editorial Universitat Politècnica de València.

Triantafillou, T.C. and Deskovic, N., 1992. Prestressed FRP sheets as external reinforcement of wood members. *Journal of Structural Engineering,* 118(5), pp. 1270-1284.

Triantafillou, T.C., 1997. Shear reinforcement of wood using FRP materials. *Journal of Materials in Civil Engineering,* 9(2), pp. 65-69.

UBC, 2017. *Brock Commons – Tallwood House* [Online]. The University of British Columbia. Available from: *http://vancouver.housing.ubc.ca/residences/brock-commons/* [Accessed 10th January].

Wheeler, A. and Hutchinson, A., 1998. Resin repairs to timber structures. *International Journal of Adhesion and Adhesives,* 18(1), pp. 1-13.

Widmann, R., Jockwer, R., Frei, R. and Häni, R., 2012. Comparison of different techniques for the strengthening of glulam members. *Enhance mechanical properties of timber, engineered wood products and timber structures: COST Action FP1004 Early Stage Researchers Conference*. pp. 57-62.

Yang, Y.-l., Liu, J.-w. and Xiong, G.-j., 2013. Flexural behavior of wood beams strengthened with HFRP. *Construction and Building Materials,* 43, pp. 118-124.

List of Publications

Published:

Zhang, C., Chang, W. and Harris, R., 2018. Screw reinforcement on beam-to-column dowel-type connection. *World Conference on Timber Engineering*, August 20-23, 2018 Seoul, Republic of Korea.

Zhang, C., Chang, W. and Harris, R., 2016. Investigation of thread configuration of self-tapping screws as reinforcement for dowel-type connection. *World Conference on Timber Engineering*, August 22-25, 2016 Vienna, Austria. pp. 1440-1448.

Zhang, C., Chang, W. and Harris, R., 2015. Investigation of thread configuration for self-tapping screws as reinforcement for embedment strength. *International Network on Timber Engineering Research*. 2015 Šibenik. Croatia. pp. 449-451.

Zhang, C., Guo, H., Jung, K., Harris, R. and Chang, W., 2018. Using self-tapping screw to reinforce dowel-type connection in a timber portal frame. *Engineering Structures*, Volume 178, Pages 656-664.

Under review:

Zhang, C., Guo, H., Jung, K., Harris, R. and Chang, W. Screw reinforcement on dowel-type moment-resisting connection with cracks. *Construction and Building Materials*. Under revision.

Zhang, C., Harris, R. and Chang, W. Rope effect of self-tapping screw as reinforcement on dowel-type connections. *Proceedings of the Institution of Civil Engineers – Construction Materials*. Under review.

Zhang, C., Harris, R. and Chang, W. Strain distribution of self-tapping screw-reinforced dowel-type connections. *Journal of Materials in Civil Engineering*. Under review.

Zhang, C., Jung, K., Harris, R. and Chang, W. Drive-in torque for self-tapping screws into timber. *Proceedings of the Institution of Civil Engineers - Construction Materials*. Under review.

Zhang, C., Harris, R. and Chang, W. Self-tapping screws as reinforcement on single dowel connections with artificial cracks. *Proceedings of the Institution of Civil Engineers - Structures and Buildings*. Under review.

Statement of Authorship

<table>
<tr><td colspan="10">This declaration concerns the article entitled:</td></tr>
<tr><td colspan="10">Using self-tapping screw to reinforce dowel-type connection in a timber portal frame.</td></tr>
<tr><td colspan="10">Publication status (tick one)</td></tr>
<tr><td>Draft manuscript</td><td></td><td>Submitted</td><td></td><td>In review</td><td></td><td>Accepted</td><td></td><td>Published</td><td>☑</td></tr>
<tr><td>Publication details (reference)</td><td colspan="9">Zhang, C., Guo, H., Jung, K., Harris, R. and Chang, W., 2018. Using self-tapping screw to reinforce dowel-type connection in a timber portal frame. Engineering Structures, Volume 178, Pages 656-664. DOI: 10.1016/j.engstruct.2018.10.066</td></tr>
<tr><td>Candidate's contribution to the paper (detailed, and also given as a percentage).</td><td colspan="9">The candidate contributed to/ considerably contributed to/predominantly executed the…

Formulation of ideas: 90%

I formulated the idea of this paper and discussed with my supervisor Dr Wen-Shao Chang for suggestions.

Design of methodology: 100%

I designed the methodology.

Experimental work: 90%

I discussed the set-up of experimental work with Dr Kiho Jung who gave useful suggestions. I conducted the experimental work in the lab at the University of Bath.

Presentation of data in journal format: 80%

I wrote the manuscript; Prof Richard Harris and Dr Hai-Bo Guo improved its quality. Dr Wen-Shao Chang also provided suggestions on the layout and demonstration of the results.</td></tr>
<tr><td>Statement from Candidate</td><td colspan="9">This paper reports on original research I conducted during the period of my Higher Degree by Research candidature.</td></tr>
<tr><td>Signed</td><td colspan="5">  </td><td>Date</td><td colspan="3">28/09/2018</td></tr>
</table>

<table>
<tr><td colspan="10">This declaration concerns the article entitled:</td></tr>
<tr><td colspan="10">Screw reinforcement on dowel-type moment-resisting connection with cracks.</td></tr>
<tr><td colspan="10">Publication status (tick one)</td></tr>
<tr><td>Draft manuscript</td><td></td><td>Submitted</td><td></td><td>In review</td><td>☑</td><td>Accepted</td><td></td><td>Published</td><td></td></tr>
<tr><td>Publication details (reference)</td><td colspan="9">Zhang, C., Guo, H., Jung, K., Harris, R. and Chang, W. Screw reinforcement on dowel-type moment-resisting connection with cracks. Submitted to Construction and Building Materials.</td></tr>
<tr><td>Candidate's contribution to the paper (detailed, and also given as a percentage).</td><td colspan="9">The candidate contributed to/ considerably contributed to/predominantly executed the…

Formulation of ideas: 90%

I formulated the idea of this paper and discussed with my supervisor Dr Wen-Shao Chang for suggestions.

Design of methodology: 90%

I designed the methodology and Dr Wen-Shao Change provided his suggestions.

Experimental work: 90%

I discussed the set-up of experimental work with Dr Kiho Jung and Dr Hai-Bo Guo who gave useful suggestions. I conducted the experimental work in the lab at the University of Bath.

Presentation of data in journal format: 80%

I wrote the manuscript; Prof Richard Harris improved its quality. Dr Wen-Shao Chang also provided suggestions on the calculation for the prediction method.</td></tr>
<tr><td>Statement from Candidate</td><td colspan="9">This paper reports on original research I conducted during the period of my Higher Degree by Research candidature.</td></tr>
<tr><td>Signed</td><td colspan="5">  </td><td>Date</td><td colspan="3">28/09/2018</td></tr>
</table>

<table>
<tr><td colspan="9">This declaration concerns the article entitled:</td></tr>
<tr><td colspan="9">Rope effect of self-tapping screw as reinforcement on dowel-type connections.</td></tr>
<tr><td colspan="9">Publication status (tick one)</td></tr>
<tr><td>Draft manuscript</td><td></td><td>Submitted</td><td></td><td>In review</td><td>☑</td><td>Accepted</td><td></td><td>Published</td><td></td></tr>
<tr><td>Publication details (reference)</td><td colspan="8">Zhang, C., Harris, R. and Chang, W. Rope effect of self-tapping screw as reinforcement on dowel-type connections. Submitted to Proceedings of the Institution of Civil Engineers – Construction Materials.</td></tr>
<tr><td>Candidate's contribution to the paper (detailed, and also given as a percentage).</td><td colspan="8">The candidate contributed to/ considerably contributed to/predominantly executed the…

Formulation of ideas: 90%

I formulated the idea of this paper and discussed with my supervisor Dr Wen-Shao Chang for suggestions.

Design of methodology: 100%

I designed the methodology.

Experimental work: 100%

I conducted the experimental work in the lab at the University of Bath.

Presentation of data in journal format: 80%

I wrote the manuscript; Prof Richard Harris and Dr Wen-Shao Chang improved its quality.</td></tr>
<tr><td>Statement from Candidate</td><td colspan="8">This paper reports on original research I conducted during the period of my Higher Degree by Research candidature.</td></tr>
<tr><td>Signed</td><td colspan="5"> 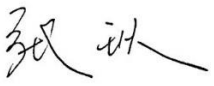 </td><td>Date</td><td colspan="2">28/09/2018</td></tr>
</table>

<table>
<tr><td colspan="10">This declaration concerns the article entitled:</td></tr>
<tr><td colspan="10">Strain distribution of self-tapping screw-reinforced dowel-type connections.</td></tr>
<tr><td colspan="10">Publication status (tick one)</td></tr>
<tr><td>Draft manuscript</td><td></td><td>Submitted</td><td></td><td>In review</td><td>☑</td><td>Accepted</td><td></td><td>Published</td><td></td></tr>
<tr><td>Publication details (reference)</td><td colspan="9">Zhang, C., Harris, R. and Chang, W. Strain distribution of self-tapping screw-reinforced dowel-type connections. Submitted to the Journal of Materials in Civil Engineering.</td></tr>
<tr><td>Candidate's contribution to the paper (detailed, and also given as a percentage).</td><td colspan="9">The candidate contributed to/ considerably contributed to/predominantly executed the…

Formulation of ideas: 90%

I formulated the idea of this paper and discussed with my supervisor Dr Wen-Shao Chang for suggestions.

Design of methodology: 100%

I designed the methodology.

Experimental work: 100%

I conducted the experimental work in the lab at the University of Bath.

Presentation of data in journal format: 80%

I wrote the manuscript, Prof Richard Harris and Dr Wen-Shao Chang improved its quality.</td></tr>
<tr><td>Statement from Candidate</td><td colspan="9">This paper reports on original research I conducted during the period of my Higher Degree by Research candidature.</td></tr>
<tr><td>Signed</td><td colspan="5">  </td><td>Date</td><td colspan="3">28/09/2018</td></tr>
</table>

<table>
<tr><td colspan="9">This declaration concerns the article entitled:</td></tr>
<tr><td colspan="9">Drive-in torque for self-tapping screws into timber.</td></tr>
<tr><td colspan="9">Publication status (tick one)</td></tr>
<tr><td>Draft manuscript</td><td></td><td>Submitted</td><td></td><td>In review</td><td>☑</td><td>Accepted</td><td></td><td>Published</td><td></td></tr>
<tr><td>Publication details (reference)</td><td colspan="8">Zhang, C., Jung, K., Harris, R. and Chang, W. Drive-in torque for self-tapping screws into timber. Submitted to Proceedings of the Institution of Civil Engineers - Construction Materials.</td></tr>
<tr><td>Candidate's contribution to the paper (detailed, and also given as a percentage).</td><td colspan="8">The candidate contributed to/ considerably contributed to/predominantly executed the…

Formulation of ideas: 90%

I formulated the idea of this paper and discussed with my supervisor Dr Wen-Shao Chang for suggestions.

Design of methodology: 100%

I designed the methodology.

Experimental work: 90%

I conducted the experimental work with Dr Kiho Jung in the lab at the University of Bath.

Presentation of data in journal format: 80%

I wrote the manuscript, Prof Richard Harris and Dr Wen-Shao Chang improved its quality.</td></tr>
<tr><td>Statement from Candidate</td><td colspan="8">This paper reports on original research I conducted during the period of my Higher Degree by Research candidature.</td></tr>
<tr><td>Signed</td><td colspan="5">  </td><td>Date</td><td colspan="2">28/09/2018</td></tr>
</table>

<table>
<tr><td colspan="9">This declaration concerns the article entitled:</td></tr>
<tr><td colspan="9">Self-tapping screws as reinforcement on single dowel connections with artificial cracks.</td></tr>
<tr><td colspan="9">Publication status (tick one)</td></tr>
<tr><td>Draft manuscript</td><td></td><td>Submitted</td><td></td><td>In review</td><td>☑</td><td>Accepted</td><td></td><td>Published</td><td></td></tr>
<tr><td>Publication details (reference)</td><td colspan="8">Zhang, C., Harris, R. and Chang, W. Self-tapping screws as reinforcement on single dowel connections with artificial cracks. Submitted to Proceedings of the Institution of Civil Engineers - Structures and Buildings.</td></tr>
<tr><td>Candidate's contribution to the paper (detailed, and also given as a percentage).</td><td colspan="8">The candidate contributed to/ considerably contributed to/predominantly executed the…

Formulation of ideas: 90%

I formulated the idea of this paper and discussed with my supervisor Dr Wen-Shao Chang for suggestions.

Design of methodology: 100%

I designed the methodology.

Experimental work: 100%

I conducted the experimental work in the lab at the University of Bath.

Presentation of data in journal format: 80%

I wrote the manuscript, Prof Richard Harris and Dr Wen-Shao Chang improved its quality.</td></tr>
<tr><td>Statement from Candidate</td><td colspan="8">This paper reports on original research I conducted during the period of my Higher Degree by Research candidature.</td></tr>
<tr><td>Signed</td><td colspan="5"> 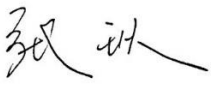 </td><td>Date</td><td colspan="2">28/09/2018</td></tr>
</table>